Synthesis and Properties of Oxepane Nucleosides, 2′-5′-linked RNAs, and Parallel-Stranded Duplexes

Maryam Habibian

Department of Chemistry

McGill University, Montréal

February 2017

A thesis submitted to McGill University in partial fulfillment of the requirements

of the degree of

Doctor of Philosophy

"Caminante, no hay camino;

Se hace camino al andar."

[Walker, there is no path;

The path is made by walking.]

Antonio Machado

1875-1939

Dedicated to my beloved Mom and Dad.

COPYRIGHT STATEMENT

ABSTRACT

Considerable attention has been directed towards chemically modified nucleic acid analogs, owing to their rising number of promising applications, ranging from nucleoside analogs as potent antiviral/anticancer agents, modified oligonucleotides for gene silencing purposes, diagnostic agents, functional genomics and target validation. Among various nucleic acid modifications, the work in this thesis is primarily focused on the design, synthesis, and characterization of ring-expanded oxepane nucleosides, 2′-5′ linkage modified siRNAs, and base modified parallel siRNAs. Structural and biological properties imparted by these modifications are investigated, with an emphasis on their structure, drug-like properties, and activity in cell based systems.

Our work on oxepane nucleosides describes the synthesis of a novel series of seven-membered ring nucleoside (oxepane) analogs as candidates for biological screening and gene silencing applications. Also, the conformational landscape and preferred ring-puckering of these analogs were investigated by means of NMR, X-ray crystallography, and quantum mechanical calculations. These analogs are valuable compounds for antiviral and anticancer applications, and build the grounds for designing novel sugar-expanded oligonucleotides as gene silencing therapeutics.

Our studies on the efficiency of 2'-5' linked siRNAs targeting firefly luciferase and P53 mRNAs with different positional variations of 2'-5' linkages showed that siRNAs with modified sense strands can retain their efficiency, while linkage modification in the AS strand compromised the siRNA activity. 2'-5' linked siRNAs were, also, found to abrogate the immunostimulatory response in comparison with their native siRNAs. Interactions of these siRNAs with the RNAi proteins was investigated, revealing that extensive 2'-5' modification of the AS strand is only

minimally affecting the siRNA phosphorylation by kinases, while it is detrimental to its hAGO2 loading. Further studies using molecular modelling and MD simulations suggested that extensive 2'-5' modification can largely affect the hAGO2-siRNA key interactions, arising from the structural changes in the RNA duplex induced by the linkage modification.

We introduced the “mixmer” strategy, as a novel approach in preparing active mixtures of chemically modified siRNAs with enhanced drug-like properties. siRNA libraries targeting firefly luciferase and P53 mRNAs were prepared with different positional variations of 2'-5' or 2'-5'/3'-5' (mixmer) modifications throughout the sense or AS strands. Screening these libraries against their corresponding mRNA targets showed that siRNAs with 2'-5' or 2'-5'/3'-5' mixmer modifications in the sense strand are as potent as native siRNAs. While 2'-5' modification in the AS strand was shown to be detrimental to the siRNA activity, the activity was compensated when 2′-5′ linkages were flanked with 3'-5' linkages in form of mixmer. Our preliminary studies show that the same results obtained with 2'-5'/3'-5' mixmers, can be also extended to siRNA mixmers prepared from mixtures of other modifications.

Finally, we report the synthesis and characterization of 2′-FRNA- and isoC- and isoG-nucleobase modified active parallel stranded siRNA hybrids at physiological pH. Our study revealed the benefits and challenges to the design of parallel stranded siRNAs, and explained the underlying rules to a successful parallel stranded siRNA design and synthesis. Mechanistic investigations using hAGO2 knockdown experiments confirmed that gene silencing by these parallel siRNAs was, indeed, happening through RNAi pathway. Our findings demonstrate that the helical conformation and groove dimensions of siRNAs are not critical determinants in activation of RNAi, and hence, introduce novel opportunities in designing a new class of potent parallel siRNAs as gene silencing therapeutics.

RÉSUMÉ

L'attention s'est portée sur les analogues d'acides nucléiques chimiquement modifiés à mesure que les applications prometteuses se sont accumulées, depuis les analogues de nucléosides comme puissants agents anticancéreux et antiviraux et les oligonucléotides modifiés comme silenceurs géniques jusqu'aux outils de diagnostic, de génomique fonctionnelle et de validation de cible. Parmi les nombreuses modifications d'acides nucléiques, nous avons choisi pour ce travail de thèse de nous concentrer principalement sur la conception, la synthèse et la caractérisation de nucléosides à sucre élargi de type oxépane et de siARNs contenant des liens 2′-5′ ou des bases modifiées et des brins appariés en parallèle. Nous avons étudié l'impact de ces modifications sur les propriétés structurelles et biologiques des nucléosides et des siARNs et, plus particulièrement, leurs propriétés thérapeutiques et leur activité en milieu cellulaire.

Nous décrivons en premier lieu la synthèse d'une nouvelle série d'analogues de nucléosides dont le sucre est constitué d'un cycle à 7 atomes de type oxépane en vue d'effectuer des tests de détection biologique et d'activité d'inhibition de l'expression génétique. Par ailleurs, des mesures menées par RMN, cristallographie à rayons X et par calculs de mécanique quantique ont permis de sonder l'espace conformationnel occupé par ces analogues ainsi que le plissage de leur sucre. Ils sont d'un intérêt certain comme anticancéreux et antiviraux et servent ainsi de fondation à la conception de nouveaux oligonucléotides à sucre étendu comme agents silenceurs de gènes.

Ensuite, nos études portées sur la capacité de siARNs contenant des liens 2′-5′ placés à différentes positions à cibler la luciférase de luciole et l'ARNm de la protéine p53 ont montré que les siARNs dont les modifications sont contenues dans le brin sens restent actifs, tandis que la modification chimique du brin antisens, au contraire, compromet leur efficacité. De plus, les

siARNs à liens 2′-5′ ne sont pas immunostimulants, contrairement aux siARNs originaux. L'étude des interactions entre ces siARNs et les protéines impliquées dans l'interférence à l'ARN (ARNi) a révélé qu'une modification profonde du brin antisens ne s'accompagne que d'une faible perturbation de la phosphorylation des siARNs par les kinases, mais qu'elle nuit à l'association (ou « chargement ») avec hAGO2. Ainsi étudiés par simulations de dynamique moléculaire et par modélisation moléculaire, les siARNs comprenant un nombre important de liens 2′-5′ perturbent fortement les interactions clé entre siARN et hAGO2, ce qui est dû à des changements structurels du duplex d'ARN induits par la modification du lien internucléosidique.

Nous avons alors introduit la stratégie dite de « mixmère » dans le but de préparer des mélanges actifs de siARNs chimiquement modifiés aux propriétés pharmacologiques améliorées. Nous avons préparé ainsi des banques de siARNs contenant des liens 2′-5′ à différentes positions ou des mixmères 2'-5'/3'-5' dans les brins sens et antisens et ciblant la luciférase de luciole ou les ARN messagers de p53. Le criblage de ces banques contre leurs cibles d'ARNm correspondant a montré que les siARNs 2′-5′ ou mixmères de 2'-5'/3'-5' dans le brin sens sont aussi actifs que les siARNs non-modifiés. Quoique la présence de modifications 2′-5′ dans le brin antisens s'accompagne d'une baisse de l'activité d'interférence du siARN, celle-ci peut être restaurée lorsque les liens 2′-5′ sont entourés de liens 3'-5' (forme mixmère). En outre, des études préliminaires ont montré que ces observations sont applicables à des siARNs mixmères comportant d'autres modifications.

Enfin, nous décrivons la synthèse et la caractérisation d'hybrides de siARNs appariés parallèlement à pH physiologique et contenant des bases modifiées isoC et isoG ainsi que des nucléosides modifiés 2′-F-ARN. Cette étude a mis en avant les avantages mais aussi les obstacles à la conception et la synthèse de siARNs à brins appariés en parallèle en en dessinant ses règles

sous-jacentes. Des expériences mécanistiques portées sur l'inhibition de l'expression de hAGO2 ont permis de confirmer que le silençage génique induit par des siARNs hybridés parallèlement provient bien, en effet, du mécanisme d'interférence à l'ARN. Nos résultats montrent ainsi que la conformation hélicoïdale et les dimensions des sillons des siARNs ne sont pas des facteurs cruciaux dans l'activation de l'ARNi et ouvrent ainsi de nouvelles approches vers la conception d'une classe originale de siARNs parallèles, puissants silenceurs de l'expression génétique.

ACKNOWLEDGMENT

There are numerous individuals I would like to acknowledge for helping me during my PhD studies at McGill University. First and foremost, I would like to express my sincere gratitude to my mentor and research supervisor, Dr. Masad Damha for his guidance, dedication, and support. He gave me the opportunity and freedom to shape who I am. It was through his guidance and constructive comments during every step of this journey that I developed the discipline and critical mindset to undertake scientific challenges. I am forever indebted to him for believing in me, supporting me, and always encouraging me to take a step further.

I am very grateful to all the people who made the progress of this research possible: Saúl, I have learnt a great deal from you, both in organic and oligonucleotide synthesis. Thank you, for answering all my questions patiently! You are a true friend and an amazing teacher. The Damha lab has been an amazing place to learn and share ideas. Adam, Dilip, Glen, Jory, Pascal, Ken, Nobu, Jovanka, Maryam, Fereshteh, Matt, Hala, Danielle, Elise, Dan, Logan, thank you all for offering me a hand with my research, for all the scientific (and non-scientific!) discussions, and for all the unforgettable moments of joy and laughter we shared. I would like to thank all the fantastic professors and staffs at the Chemistry department at McGill who helped me with my research and life in gradschool; in particular: Alex Wahba for running my always rushed! MS samples, Johans Fakhouri for running all the luciferase assays in this thesis, and Fred Morin for helping me with NMR experiments. Justin and Kai from Sleiman lab were always very kind in offering their help. Linda, Chantal, and Jennifer were extremely nice and helpful with all the administrative works. Thank you all! I am also very grateful to my committee members, Dr. Sleiman and Dr. Moitessier for their continuous guidance and support.

I had the opportunity for a few months to work in the lab of Dr. Pelletier at the Biochemistry department at McGill. I would like to thank Dr. Pelletier and Francis Robert for training me with the radiolabelling and AGO loading assays.

Some of the research presented in this thesis was done in collaboration with excellent researchers around the globe: Hari Krishna, Mayumi Takahashi, Regina Cencic, Matije Lucic, Carlos Gonzalez, Guillem Portella, Saúl Martínez-Montero, Zhijie Chua, and Keith Gagnon. My sincere gratitude goes to my collaborators for their hard work and never giving up on failing experiments. I have learned a great deal from them all. I also had the opportunity to supervise and work with Logan during his undergraduate project in our lab. I would like to thank him for his contributions to the parallel project in this thesis. Finally, I would like to sincerely thank Dr. Damha for proofreading and editing my thesis, and Jory for his help with the French translation of the abstract.

I am very grateful to all my friends and family who have never stopped supporting me. Nevertheless, my deepest appreciation goes to my dearest parents who have encouraged and supported me my entire life. My love and this thesis are dedicated to them.

PREFACE

Recognition of all the contributions made by our research collaborators to the work presented in this thesis are included here and within the thesis:

In Chapter 2, Saúl Martínez-Montero helped with some of the synthetic steps in the preparation of oxepane nucleosides. Zhijie Chua solved the crystal structure of the oxepane epoxide analog. The molecular modeling of oxepane analogs was performed by Guillem Portella.

In Chapters 3 and 4, Johans Fakhouri from Dr. Sleiman's lab conducted the firefly luciferase gene silencing experiments, and Regina Cencic from Dr. Pelletier's lab conducted the P53 gene silencing experiments. Mayumi Takahashi from Dr. Rossi's lab conducted the immunostimulation assays in PBMC cells. In Chapter 3, Hari Krishna from Dr. Pradeepkumar's research group performed the molecular modeling on 2′-5′-linked siRNAs loaded in hAGO2. In the same Chapter, Dr. Keith Gagnon performed the radiolabeling and hAGO2 loading experiments of 2′-5′-linked siRNAs.

In Chapter 5, Renilla reporter assay and AGO2 knockdown experiments were conducted by Matije Lucic from Dr. Hall's research group. 1D NMR experiment was performed by Dr. Carlos Gonzalez.

TABLE OF CONTENTS

LIST OF FIGURES

LIST OF TABLES

LIST OF SCHEMES

LIST OF ABBREVIATIONS

3′-UTR	3′-untranslated region
ETT	5-Ethylthio-tetrazole
ABB	AGO2 binding buffer
APS	Ammonium persulfate
AON	Antisense Oligonucleotide
AS	Antisense
ATP	Adenosine triphosphate
B/TB	Boat/Twist-Boat
CSD	Cambridge structural database
CD	Circular dichroism
CCND1	Cell-cycle regulator cyclin D1
C/TC	Chair/twist-chair
CCD	Charge-coupled device
CMV	Cytomegalovirus
COSY	Homonuclear correlation spectroscopy
DCA	Dichloroacetic acid
DCM	Dichloro Methane
DMTr	Dimethoxytrityl
dd H_2O	Distilled and deionized water
DMF	Dimethyl formamide
DMSO	Dimethyl Sulfoxide
DNA	Deoxyribo nucleic acid
DOTAP	(1,2-dioleoyl-3-trimethylammoniumpropane)

DS	Double stranded
ESI	Electron spray ionization
ELISA	Enzyme-linked immunosorbent assay
EMSA	Electrophoretic mobility shift assays
FANA	2′-Fluoroarabino nucleic acid
HEPES	4-(2-hydroxyethyl)-1-piperazineethanesulfonic acid
HSQC	Heteronuclear single quantum coherence
HRMS	High-resolution mass spectra
IFN-α	Interferon-α
IL-6	Interleukin-6
isoC	Isocytosine
isoG	Isoguanine
m.u.	Mass unit
*m*CPBA	Meta-Chloroperoxybenzoic acid
MD	Molecular dynamics
MDA5	Melanoma Differentiation-Associated protein 5
MeOD	Deuterated Methanol
TEMED	*N,N,N,N′* -Tetramethyl-ethylenediamine
NP	N3' phosphoramidate
NMR	Nucleic Magnetic Resonance
NOESY	Nuclear Overhauser effect spectroscopy
ON	Oligonucleotide
OTE	Off target effects
ONA	Oxepane Nucleic Acids
PACT	Protein activator of PKR

PDB	Protein database
PKR	Protein Kinase R
PNA	Peptide nucleic acids
PBMC	Peripherial blood mononuclear cell
PACE	Phosphonoacetate
PS	Phosphorothioate
PTEN	phosphatase and tensin homolog
Pre mRNA	Precursor mRNA
Pri miRNA	Primary miRNA
RNA	Ribo nucleic acid
RIG-1	Retinoic acid Inducible Gene-1
RISC	RNA-Induced Silencing Complex
RNP	Ribonucleoprotein
RMSD	Root mean square deviation
RT	Room Temperature
rWC	Reverse Watson Crick
S	Sense
SE	Sugar edge
siPools	siNRA pools
ETH Zurich	Swiss Federal Institute of Technology Zurich
PNK	T4 polynucleotide kinase
TCA	Trichloroacetic acid
TBDMS	*tert*-butyldimethylsilyl
THF	Tehtahydrofuran
TLC	Thin-layer chromatography

TLR	Toll like receptor
TRBP	Trans-activation response RNA-binding protein
TREAT-HF	Triethylamine trihydrofluoride
WC	Watson Crick

CHAPTER 1:INTRODUCTION

1.1 Nucleic acids as the building blocks of life

"Wir wollen nicht nur wissen wie die Natur ist (und wie ihre Vorgänge ablaufen), sondern wir wollen auch nach Möglichkeit das vielleicht utopisch und anmassend erscheinende Ziel erreichen, zu wissen, warum die Natur so und nicht anders ist.

[We not only want to know how nature is (and how her transactions are carried through), but we also want to reach, if possible, a goal which may seem utopian and presumptuous, namely, to know why nature is such and not otherwise.] Albert Einstein " [1]

Nucleic acids are the vital molecules that are fundamental for carrying the genetic material of life in all living cells. These building blocks are elegantly assembled by polymerase enzymes within the cells to yield two major forms of genetic material: Deoxyribonucleic Acid (DNA) and Ribonucleic Acid (RNA). It was the discovery of DNA as the carrier of the hereditary information that focused immediate attention on elucidation of its structure and biological function.[2]

Even though the primary structure of DNA building blocks was earlier known,[3-7] the three-dimensional DNA double helix structure was only discovered later in 1953 by James Watson and Francis Crick, with major scientific contributions from Rosalind Franklin and Maurice Wilkins. This model now could readily accommodate all previous experimental observations, as well as offering viable hypothesis on DNA replication derived from the Watson-Crick base paired complementary strand. Nobel prize in physiology or medicine in 1962 was awarded to Watson, Crick and Wilkins (unfortunately Franklin had passed away by this time, although her

contributions were unquestionably worthy of the prize) for participating in this significant scientific breakthrough.

Since the discovery of DNA double helix, DNA and RNA have been studied in exquisite details and their chemical and biological properties are firmly established, owing in part to the development of efficient and automated DNA and RNA synthesis.[8, 9] Due to their availability, synthetic nucleic acids and their analogues have vastly been utilized in medicine as therapeutics (gene silencing oligonucleotides, anticancer/antiviral agents), as molecular diagnostics for identifying disease related genes, as well as in basic research.[10-12]

This thesis focuses on developing nucleic acid analogues for therapeutic purposes, using either novel or commercially available synthetic building blocks.

1.2 Nucleic acid structure and function[13, 14]

1.2.1 Natural nucleotides and nucleosides

DNA and RNA are biopolymers consisting of building blocks, called nucleotides, that can reach in length to up to millions of units. An array of nucleotides is referred to as an oligonucleotide (ON). Each nucleotide consists of three components: a pentose sugar, a phosphate group, and a nitrogen containing heterocyclic base (nucleobase) (**Figure 1.1**). DNA is composed of 2'-deoxyribonucleotides, whereas RNA is composed of ribonucleotides. The major bases are monocyclic pyrimidines or bicyclic Purines: purines consist of Adenine (A) and Guanine (G) and are found in both DNA and RNA; pyrimidines consist of Cytosine (C), Thymine (T) and Uracil (U), with cytosine found in both DNA and RNA, and Thymine and Uracil found in DNA and RNA, respectively. Each nucleobase is connected to the anomeric carbon of the sugar unit (C1') through a β linkage to the N-1 nitrogen of pyrimidines and the N-9 nitrogen of purines.

Nucleotide units in oligonucleotides are connected to each other through a phosphodiester linkage, which connects the 5'-hydroxyl group of one nucleotide to the 3'-hydroxyl group of the next one (**Figure 1.1c**). By convention, single strands of DNA and RNA sequences are, written in a 5'-to-3' direction. This linear sequence constitutes the primary structure of nucleic acids.

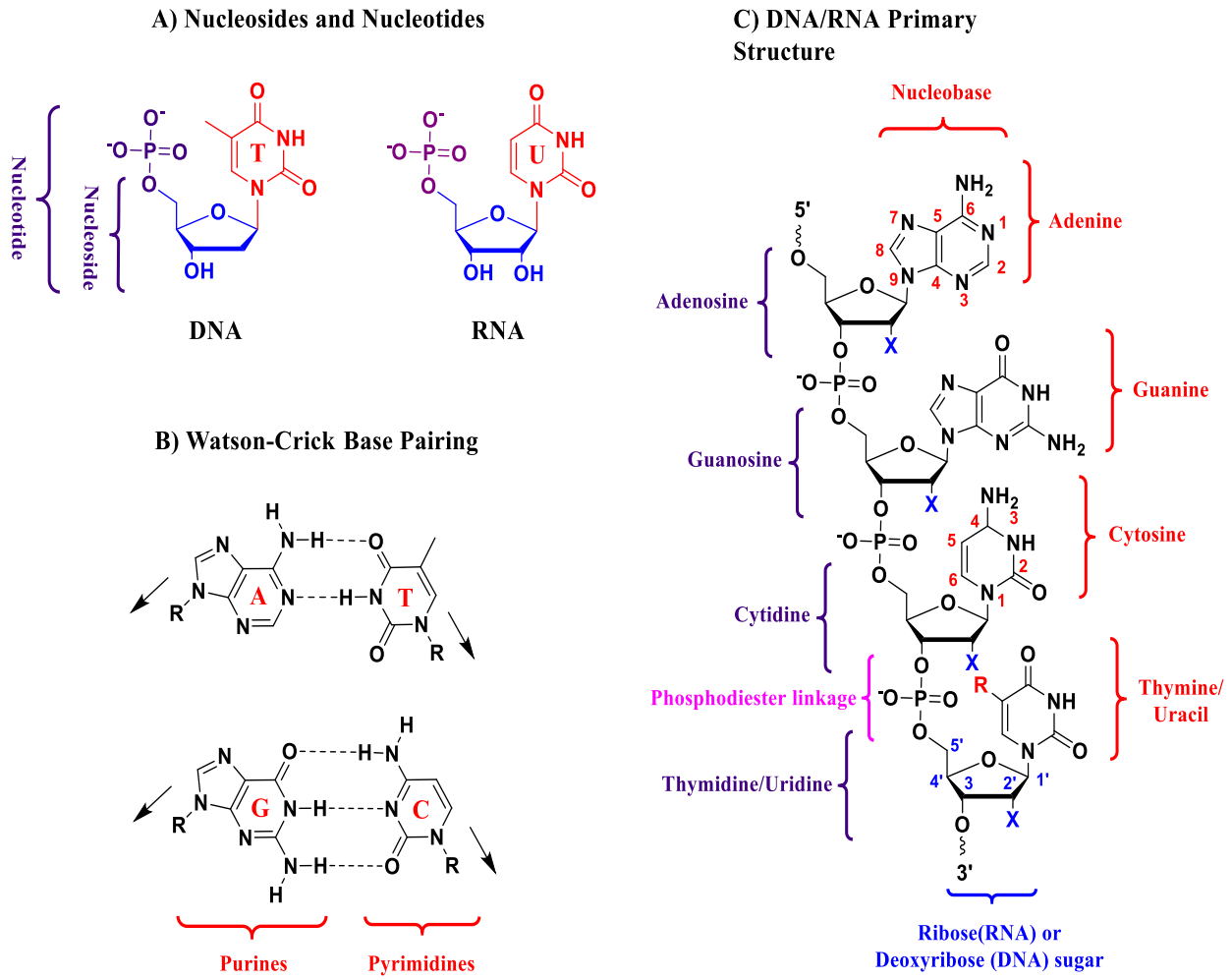

Figure 1.1 Structural components of nucleic acids. (A) Structure of nucleotides and nucleosides: nucleosides consist of a heterocyclic base and a ribose (RNA) or deoxyribose (DNA) sugar. Nucleotides are phosphate esters of nucleosides. (B) Watson-Crick base pairing relies on H-bonding interactions between appropriately positioned H-bond donors and acceptors of complementary purine and pyrimidine nucleobases. Arrows represent the cis geometry of the glycosidic bonds of the two strands relative to each other. (C) The primary structure of DNA and RNA nucleic acids, with X=H, OH and R=CH_3 ,H for DNA and RNA respectively.

1.2.2 Nucleoside conformation

Nucleoside sugar rings are twisted out of plane to adopt the most stable conformation with minimized ring strain and non-bonded interactions between their substituents. The sugar rings are free to explore a conformational space, which is described as sugar "puckering". By convention, the conformation of nucleoside sugar rings is numerically described using a phase angle value (P) shown diagrammatically in the "pseudorotational wheel" in **Figure 1.2**.[15]

Natural nucleosides generally adopt the North (*C3'-endo, C2'-exo*) or South (*C2'-endo, C3'-exo*) conformation. These conformation minima are in equilibrium with each other and while interconverting, pass through the East (*O4'-endo*) conformation (**Figure 1.2**).

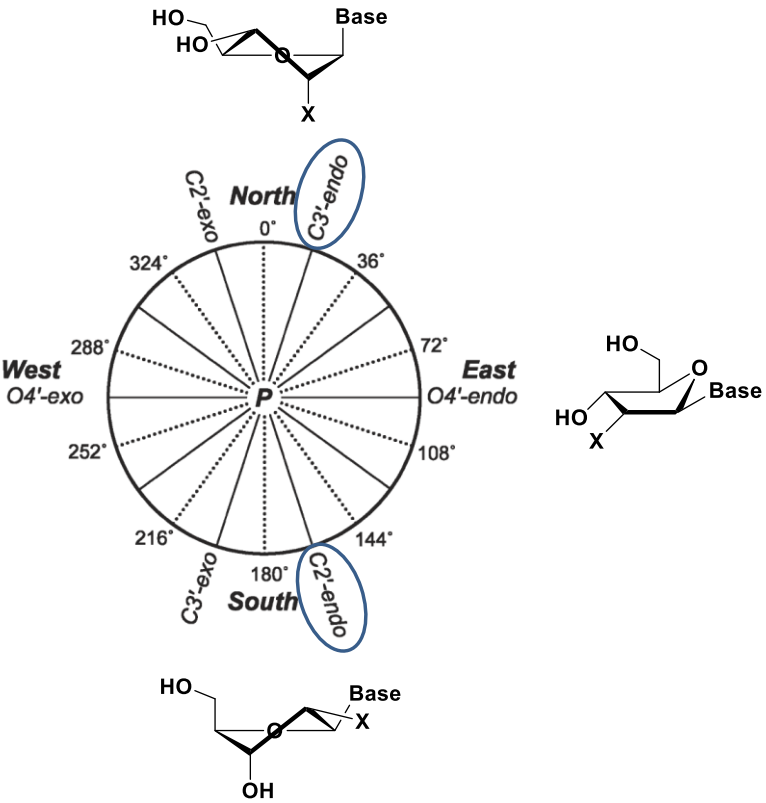

Figure 1.2 The psudorotational wheel and the corresponding sugar pucker notations adopted by nucleoside sugars. Areas circled in blue denote the most stable puckers of natural nucleosides: North or *C-3'endo* sugars are found in A-form RNAs and South or *C-2'endo* sugars are found in B-form DNAs.

While ribonucleosides have conformations almost evenly distributed in between North (51%) and South (49%), deoxyribonucleosides have a slight preference for the South (~65%) conformation.[16, 17] For most substituted furanose sugars a combination of factors such as steric, anomeric and gauche effects participate in shifting the conformation equilibrium towards one of the puckers, significantly populating a limited segment of the pseudorotational wheel.

1.2.3 The double helix

The double helix is composed of two right handed helical polynucleotide chains coiled around the same central axis. The two strands of the double helix are antiparallel, that is, their 5'-to-3' phosphodiester linkages run in opposite directions. The hydrophobic bases are inside the helix and are paired to each other via hydrogen bonding interactions, whereas the hydrophilic phosphate groups are located on the outside exposed to water. Earlier observations from Erwin Chargaff suggested that total amount of pyrimidine nucleotides (T+C) always equals the total amount of purine nucleotides (A+G). Furthermore, the amount of T always equals the amount of A, and the amount of C always equals the amount of G, but the amount of A+T is not necessarily equal to the amount of G+C.[18] G pairs with C, and A pairs with T, via three and two hydrogen bonds, respectively (**Figure 1.1b**). The Watson and Crick (WC) model of double helix is in full agreement with Chargaff's findings, and suggests how the genetic information can be subject to replication and transcription with fidelity and precision.

Our current understanding of the nucleic acid secondary structure has vastly progressed by means of structural techniques such as NMR and X-ray crystallography. It is now recognized that the structure, thermodynamic stability and dynamics of nucleic acid structures are governed by many factors that are beyond mere interstrand WC hydrogen bonds. For example, aromatic π-π base stacking of adjacent bases stabilize the duplex,[19-26] whereas electrostatic repulsion

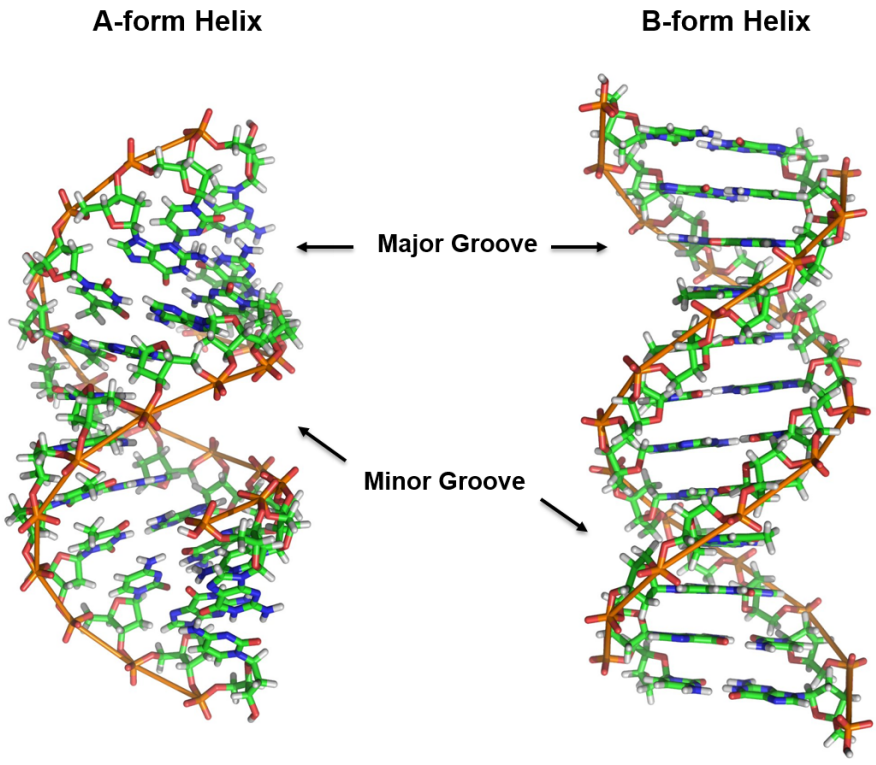

	A-form helix	B-form helix
Helix	Right handed	Right handed
Sugar pucker	*C2'-endo*	*C3'-endo*
Nucleotide/turn	11	10
Major groove depth	~13.5 Å	~8.8 Å
Major groove width	~2.7 Å	~11.7 Å
Minor groove depth	~2.8 Å	~7.5 Å
Minor groove width	~11 Å	~5.7 Å

Figure 1.3 Top: a comparison of the A-form and B-form helical structures in dsDNA. Bottom: some helical parameters of A-form and B-form duplexes[13].

between the negatively charged phosphates of the neighboring strands destabilize the duplex.[27] The final structure of a nucleic acid is the result of the balance among all these noncovalent interactions.[28-30] It has also been discovered that DNA can adopt a range of different helical structures, owing in part to its flexible sugar moieties and other factors, such as base sequence, ionic strength, binding by small molecules, etc.[31-36]

Inside the cells, duplex DNA is assumed to adopt a B-form helical structure. Double stranded (ds)-RNA, on the other hand, prefers an A-form helical structure. B-form helices have a wide major groove and a narrow minor groove, while A-form helices have a deep major groove and a wide minor groove (**Figure 1.3**). Differences in A-form and B-form helices are attributed to the divergence of sugar pucker at their nucleotide level; nucleotides in B-form ds-DNA are assumed to adopt a South sugar pucker, whereas in A-form ds-RNA they adopt a North sugar pucker.

1.3 Unconventional nucleic acid structures

1.3.1 Beyond the Watson-Crick base pairing

More than six decades of research performed in the field of nucleic acids has revolutionized our understanding of DNA and RNA structure and function. Beyond the original canonical W-C helix, there are many more structures that DNA and RNA can adopt. For example, a variety of noncanonical arrangements have been observed, such as i-motifs, G-quadruplexes, and parallel duplexes.[37-40] RNA, likewise, was found to have a variety of structures of its own.[41, 42]

The formation of nonstandard structures, in DNA or RNA, stems from the fact that nucleobases, and even the sugars, have multiple sites for H-bonding. Different RNA base pair systems can be categorized based on their hydrogen binding sites (The Watson Crick (WC) edge, the sugar edge, and the Hoogsteen or the "C-H" edge), as well as the relative orientation of the glycosidic bond

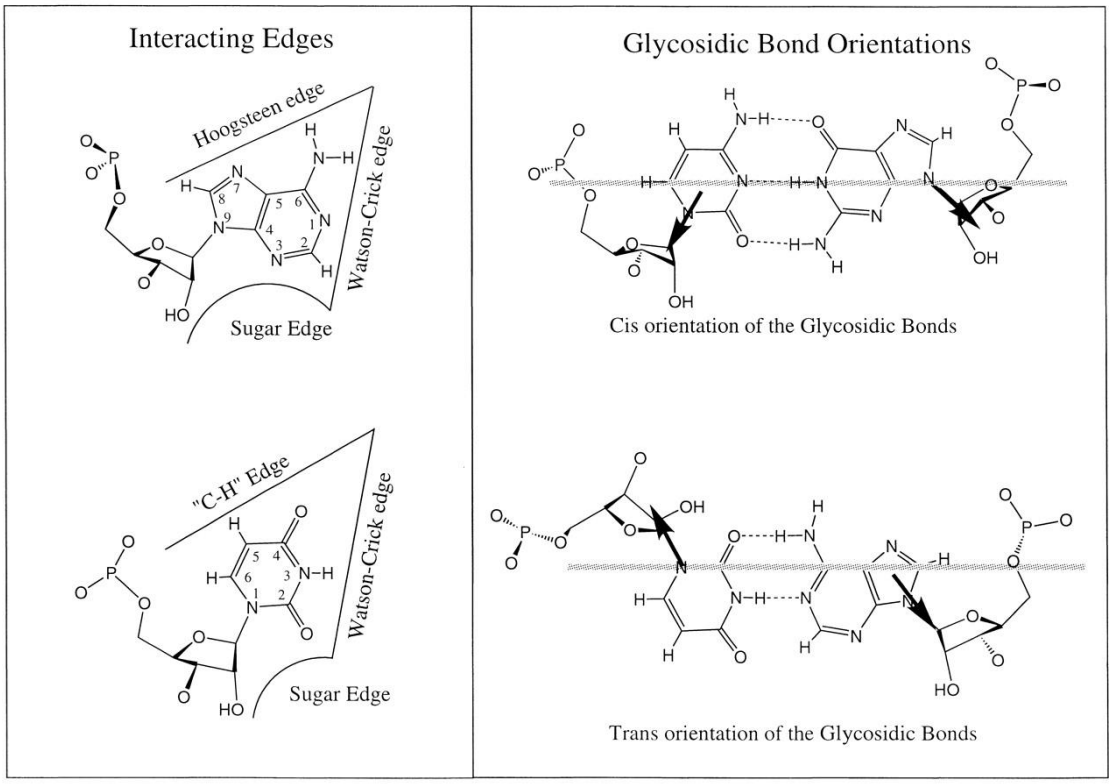

Figure 1.4 Identification of H-bonding edges and glycosidic bond orientations in RNA. Hydrogen bonding axis (axis of interaction) is shown in gray. Picture taken from reference [43].

to each other (**Figure 1.4**). While both the W-C and Hoogsteen edges involve the nucleobase in hydrogen bonding, the sugar edge involves the ribose group, where in the case of RNA only, is able to from hydrogen bonding via the 2'-hydroxyl group efficiently.[43]

As previously mentioned, the canonical hydrogen bonding motif in DNA and RNA is a WC to WC -edge interaction, with the glycosidic bond that is cis oriented relative to the axis of hydrogen bonding. However, nucleobases could hydrogen bond via either of their edges with each other, and with glycosidic bonds in cis or trans orientations relative to the axis of interaction. Different variety of hydrogen bond interactions depending on their bonding edges and the glycosidic bond orientation are listed in **Table 1.1**.

Some of these structures with unusual hydrogen bonding pattern include parallel duplexes,[44-46] triplexes,[47-50] G-quadruplexes,[51-53] and i-motifs[54, 55] (**Figure 1.5**). Unlike canonical duplexes that have their strands arranged in an antiparallel orientation, parallel stranded duplexes have both their strands arranged in a parallel orientation with regard to each other (both in 5' to 3' orientation) to construct the duplex. This noncanonical structure becomes feasible under unnatural chemical or environmental conditions. Parallel stranded duplexes will be discussed in more detail in Chapter 5 of this thesis.

Table 1.1 Different types of base pairs formed by natural bases defined by the relative orientation of the glycosidic bonds of the interacting bases and the edges they use.

Glycosidic bond orientation	Nucleobase interacting edge	Strand orientation
Cis	WC/WC	Antiparallel
Trans	WC/WC	Parallel
Cis	WC/Hoogsteen	Parallel
Trans	WC/Hoogsteen	Antiparallel
Cis	WC/sugar edge	Antiparallel
Trans	WC/sugar edge	Parallel
Cis	Hoogsteen/Hoogsteen	Antiparallel
Trans	Hoogsteen/Hoogsteen	Parallel
Cis	Hoogsteen/Sugar edge	Parallel
Trans	Hoogsteen/Sugar edge	Antiparallel
Cis	Sugar edge/Sugar edge	Antiparallel
Trans	Sugar edge/Sugar edge	Parallel

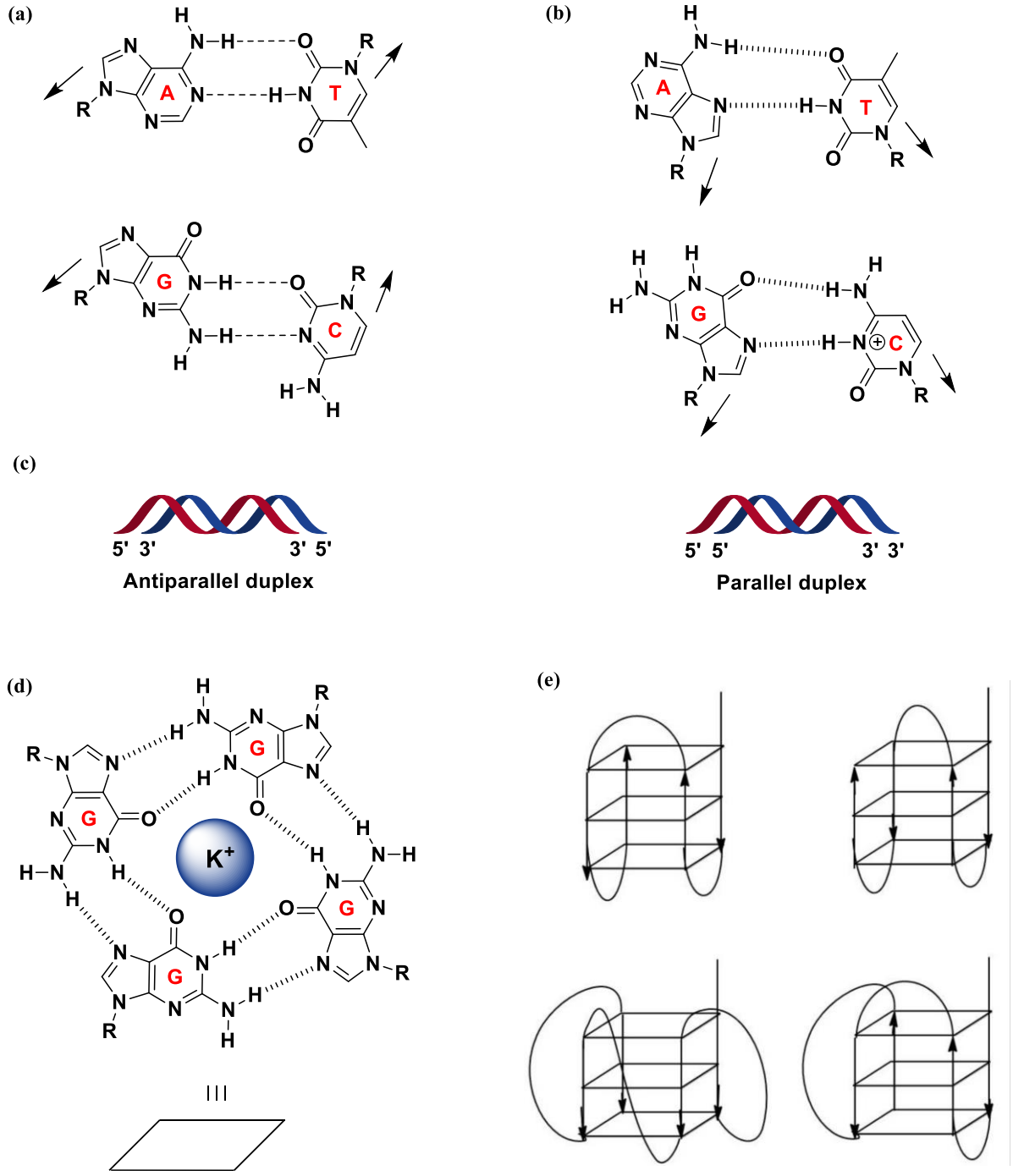

Figure 1.5 Representations of some common noncanonical hydrogen bonding schemes found in: (a) and (b) parallel duplexes and (d) G-quadruplexes. Schematic illustrations of antiparallel and parallel duplexes (c) and some variations of G-quadruplexes (e). The WC/reverse WC base pairing is shown with dashed bonds, and Hoogsteen/reverse Hoogsteen base pairing is shown with hashed bonds.

1.3.2 Beyond the 3'-5' linkage: 2'-5' linked RNAs

The structure of nucleic acids is not limited to the conventional 3'-5' linkage seen in DNA and RNA. In the contemporary world, the majority of phosphodiester linkages of RNA are 3'-5' linked. Yet, 2'-5' linkages still exist in the following cases: (I) lariat RNA introns contain both 3'-5' and 2'-5' linkages,[56-58] (II) 2'-5' oligomers of adenosine are formed by 2'-5' oligoadenylate synthase during the interferon antiviral response,[59, 60]; and (III) *in vitro* ligation of an RNA−DNA junction has been reported to generate a 2'-5' linkage in the DNA backbone.[61] Furthermore, "RNA world" hypothesis suggests that during the prebiotic era, when enzymes did not exist to govern the regiospecificity of RNA synthesis, the internucleotide linkage could form either through the 3'-OH or the 2'-OH group. As a result, during the nonenzymatic copying of an RNA template by primer extension, either the 2′ or the 3′ OH of the last nucleotide of the primer could attack the phosphate of the incoming activated monomer, generating either a 2′-5′- or a 3′-5′-linkage. The complementary strand would therefore have a mixture of 2′-5′- and 3′-5′-linkages (**Figure 1.6**).

RNA backbone heterogeneity was initially thought to disrupt the folding and subsequently the function of RNAs. This matter would have been a big issue especially with regard to the "RNA world" hypothesis. The RNA world theory, as described by evolutionary scientists, portrays an early stage in the evolution of life when RNA molecules did not only function in the transfer of genetic information, but also they served as the main functional polymer of biochemistry, involved in all aspects of life.[62, 63] As a result, the ability of RNA molecules to fold into defined three dimensional structures with exquisitely specific molecular recognition and catalytic properties becomes the conceptual basis to this theory.

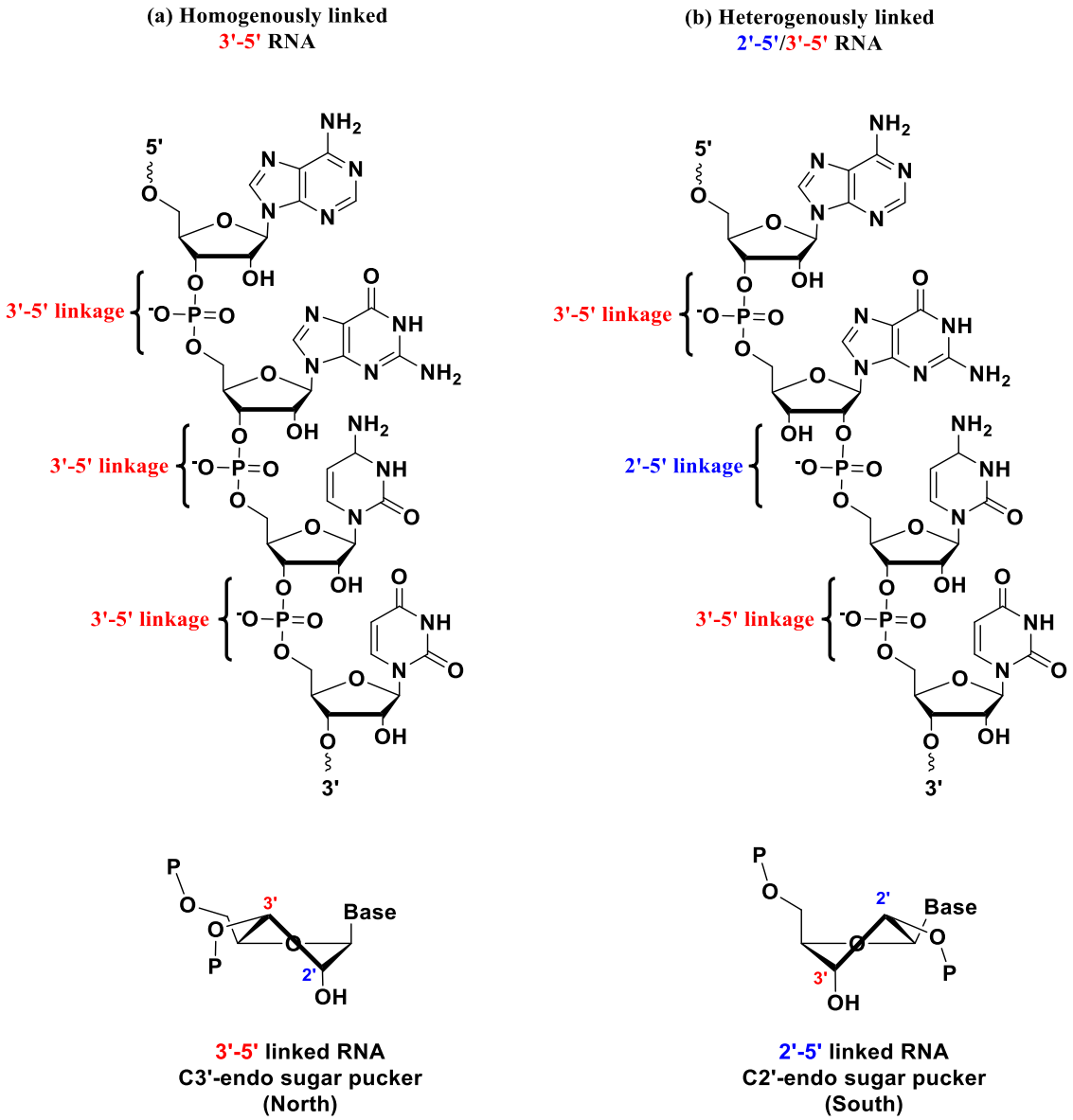

Figure 1.6 (a) Enzymatic synthesis of RNA results in completely uniformed 3'-5' phosphodiester linkage between nucleotides (homogenously linked 3'-5' RNA). (b) Prebiotically plausible synthesis of RNA, however, generates random distribution of 2'-5' and 3'5 linkages within an RNA strand (heterogeneously linked 2'-5'/3'-5' RNA). A heterogeneous RNA strand containing one 2'-5' linkage is shown here.

A central question in the origin-of-life field concerns the pathway from which the heterogeneously linked RNA synthesized under prebiotic conditions has retained its function to produce all forms of cellular life. Researchers have shown that homogeneous linkages (all 3′-5′

linkages) might not have been necessary for functional RNAs to retain their activity, as long as the heterogeneously linked RNAs (mixture of 3′-5′ and 2′-5′ linkages) could still fold into tertiary structures able to show reproducible function.[64] In a more recent work by Szostak and co-workers, it was shown that ribozymes (RNA with catalytic activity) containing up to 25% 2'-5' linkages randomly distributed along the oligonucleotide chain were able to retain the catalytic activity observed for the all-3'-5' ribozyme.[65] In another report by Wang and co-workers, incorporation of 2'-5' linkages in the DNA primer was investigated on the efficiency of RNA synthesis by RNA polymerase II.[66] They demonstrated that RNA polymerase II cannot tolerate and bypass linkage heterogeneity sites in the template, and would pause at 2′-5′ linkage sites. More investigation on the interactions of 2'-5' linked RNAs with modern day proteins will be more discussed in Chapter 3 of this thesis.

1.4 Cellular RNA[67]

The Central Dogma of biology describes the flow of genetic information in cells from duplex DNA, to messenger RNA (mRNA), to proteins. DNA as the genetic material is kept in the nucleus; hence RNA acts as a shuttle in between the nucleus and the cytoplasm transferring the blueprint for protein synthesis to ribosomes. This process happens in two main steps: transcription of DNA to RNA in the nucleus and translation of the RNA in to protein outside of the nucleus. The RNA transcript produced in the nucleus, called precursor mRNA (pre-mRNA), is later processed in the cytoplasm during splicing to form the mature messenger RNA (mRNA). During splicing, the non-coding (intron) regions are removed to join the coding (exon) regions producing the mature mRNA. The mRNA is subsequently processed (translated) by the ribosome into functional proteins, utilizing the amino acylated transfer RNA (tRNA) adaptor molecules to build the polypeptide chain.

Gene expression is an extremely controlled and regulated process in cells. Consequently, problems in the regulation of gene expression are associated with several diseases including cancer. Gene expression regulation can occur at different stages, i.e., transcription, post-transcription, translation, or post-translation. Chapters 3-5 of this thesis are mainly focused on designing nucleic acid probes to control gene expression at the post-transcriptional level, through mRNA degradation pathways.

1.5 Synthetic oligonucleotides as gene silencing therapeutics

A direct outcome of WC base pairing is that an oligonucleotide can be designed to bind specifically to a region of DNA or mRNA. This complementary oligonucleotide is called anti*sense* strand and the target DNA or mRNA is referred to as the *sense* strand. In 1978 Zamecnik and Stephenson showed that an oligodeoxynucleotide can bind to a specific nucleic acid sequence in the cell, and inhibit the translation of a viral mRNA into the protein.[68] This pioneering work demonstrated the potential of oligonucleotides for targeting any specific malfunctioning gene and silent its translation. Moreover, it paved the way for the discovery of several other hybridization-mediated techniques that are used to disrupt gene function in vivo. Synthetic oligonucleotides (ONs) and their chemically modified mimics are now routinely utilized in laboratories to study the roles and control the expression of therapeutically relevant genes in living systems. ONs are also under active investigation in the clinic, with four FDA-approved drugs for the treatment of cytomegalovirus (CMV) retinitis (Fomiversen; withdrawn from the market)[69], wet age-related macular degeneration (Macugen)[70], severe hypercholesterolaemia (Mipomersen)[71], and duchenne muscular dystrophy (Eteplirsen), and many others in final stages of clinical trials. In addition to antisense ONs (AONs),[72-74] several other classes of ONs are being developed for controlling gene expression, including small

interfering RNAs (siRNAs),[75] and microRNA-targeting ONs (anti-miRNAs and antagomirs),[76] aptamers,[77] DNA/RNAzymes,[78, 79] and immunostimulatory NAs[80]. Chapters 3, 4, and 5 of this thesis focus on the design, development, and mechanistic investigation of chemically modified siRNAs. Therefore, the remaining sections of this chapter will focus on RNA interference (RNAi) as mediated by siRNAs.

1.6 RNA interference (RNAi) mediated gene silencing: miRNA and siRNA

The observation that dsRNA sharing sequence with a cellular mRNA (Onc-22) can silence the expression of that gene in C. elegans led to the discovery of RNAi pathway.[74] Following this discovery, it was found that RNAi pathway could also be triggered in mammalian cells using 21nt-long dsRNA duplexes.[75] Nobel prize in physiology was awarded to Andrew Fire and Craig Mello in 2006 for this discovery. Through RNAi, cells can achieve post-transcriptional gene expression control by means of microRNA (miRNA) expression as illustrated in **Figure 1.7**.

Transcription of intergenic or intronic DNA regions[81] results in the formation of primary miRNA (pri-miRNA) hairpins in the nucleus. These hairpins are then processed by a protein called Drosha to form dsRNA duplexes featuring a hairpin loop with imperfect sequence complementarity, termed precursor miRNA (pre-miRNA). At this point, pre-miRNAs are exported out of the nucleus and further processed by Dicer, an endoribonuclease usually accompanied by an associated dsRNA binding protein, TRBP, to remove the loop and form the mature miRNA.[82-84]

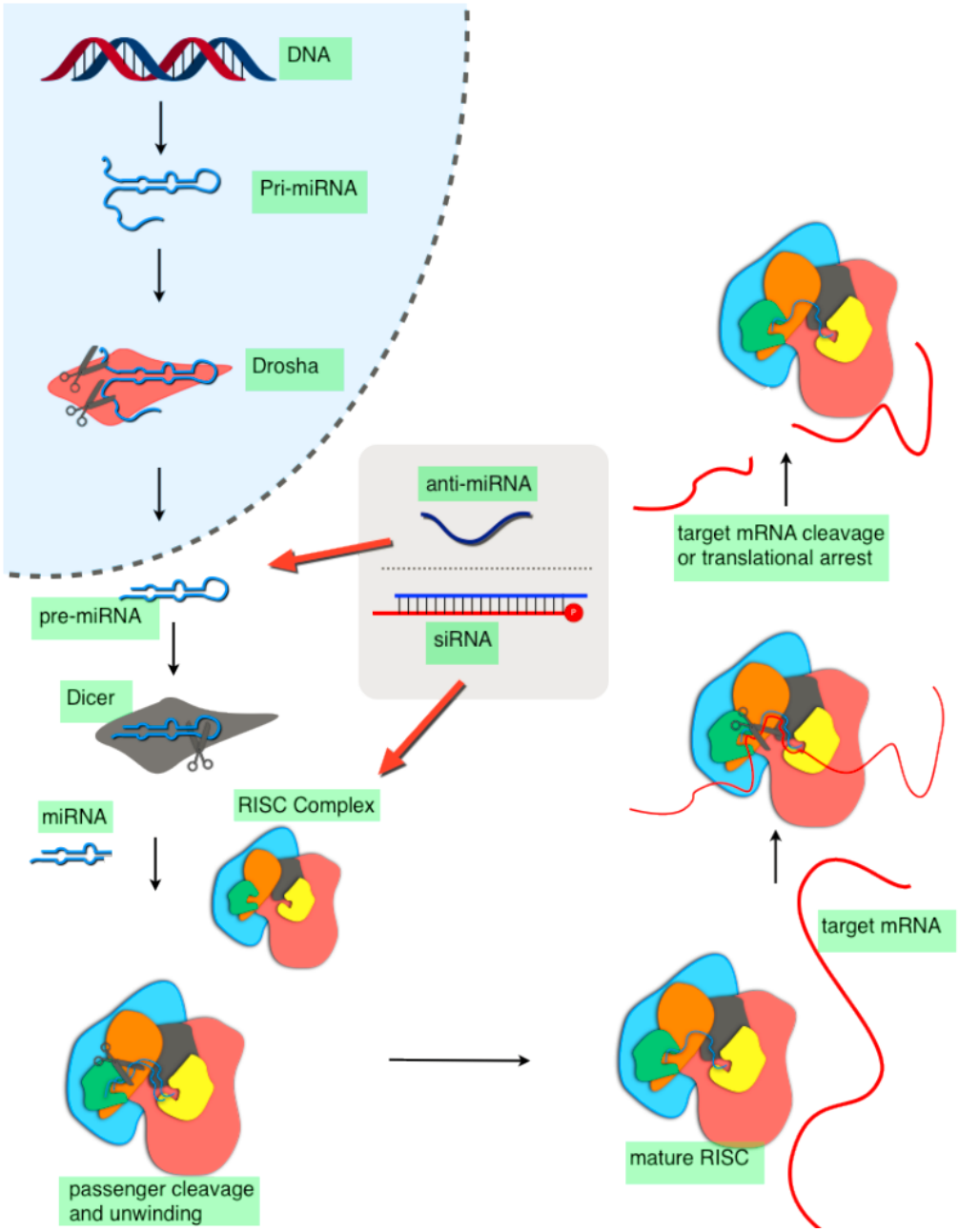

Figure 1.7 mRNA-targeting by miRNA and siRNA. miRNAs, once loaded into the RISC, are capable of recognizing and binding partially complementary mRNAs, especially those with sequence complementarity to the miRNA "seed region". As an outcome of this, gene expression decreases, adding an additional layer of post-transcriptional control over gene expression. Anti-miRNAs can target and inhibit miRNAs. Synthetic siRNAs, mimicking natural miRNAs, can be introduced into cells to make use of the cellular RISC machinery for mRNA gene silencing. Figure adapted from reference [85].

miRNAs are dsRNAs with imperfect complementarity that have 2nt-long 3′ overhangs. Once recognized, miRNAs are loaded into a complex of enzymes and proteins known as the RNA-Induced Silencing Complex (RISC). Phosphorylation of the 5' termini of the miRNA duplex is required for loading into RISC. One of the two 21-nt long miRNA strands called the "passenger strand" (or *sense* strand) is unwound and then discarded, whereas the remaining strand called the "guide strand" (or *antisense* (AS) strand) is selected and utilized in the mature RISC complex to continue the process. Finally, the mature RISC complex containing the guide strand, binds the mRNAs to inhibit their translation either via translational arrest or mRNA cleavage; the choice of which is determined by the extent of sequence complementarity between the miRNA guide strand and the mRNA target. Translational arrest happens when there is partial complementarity between the guide strand and mRNA, where mRNA recognition by RISC and mRNA cleavage results only when there is near full complementarity.[86] In most of the cases, miRNAs are only partially complementary to their mRNA targets, rendering translational arrest to be the more common outcome.

A necessary feature for miRNAs to trigger gene silencing is to have complete complementarity with the 3′ UTR of the mRNA. Binding occurs via a 7-nt "seed region" within the miRNA AS strand (nucleotide #2 to #8, from 5'-terminus) and the target mRNA.[86]

Short interfering RNAs (siRNAs) are chemically produced double-stranded RNAs, typically 21-24nt in length with 2nt 3′ overhangs. They are different from miRNAs in that the AS strand of siRNAs is designed to be fully complementary to their target mRNA. One of the two strands of the siRNA is loaded into RISC, while the other strand is cleaved and unwound from the AS strand and is sometimes discarded.[87, 88]

In flies, two other proteins (Dicer-2 and R2D2) interact with siRNAs to facilitate loading into RISC.[84, 89] However, in mammals, the mechanism by which RISC loading occurs is less understood; in some cases, Dicer is not required for siRNA loading.[89] In theory, either one of the siRNA strands could be picked as AS strand, especially since both 5' terminals are phosphorylated. Several studies suggest that "strand selection" is based on several factors including duplex thermodynamics, the presence of a 5' phosphate, and the base sequence at the 5' terminus of the strand. Duplex thermodynamics govern the strand selection by favoring the strand with the least tightly bound 5′ end as the AS strand.[90, 91] Also, the presence of a 5′ phosphate is critical for binding of the AS strand within RISC, so if one strand lacks the 5' phosphate group it will not be designated as the AS strand.[92] The 5' phosphate group can be added either synthetically, or enzymatically, using an endogenous kinase such as Clp1, and is essential to the correct loading orientation of the AS strand.[93]

Human cells encode a single Dicer enzyme that can associate with two different double-stranded RNA (dsRNA)-binding proteins, protein activator of PKR (protein kinase R) (PACT) and trans-activation response RNA-binding protein (TRBP). A model proposed by Doudna and co-workers highlights the role of these proteins in strand selection (**Figure 1.8**).[94] According to this model, dsRNA is first processed in a catalytic region of Dicer to form an siRNA or miRNA product. The dsRNA is then repositioned within Dicer to make contacts with its helicase domain. While TRBP (or PACT) interact with the dsRNA on its more stable end, Dicer interacts with the less stable end of the duplex, spatially orienting the duplex for a subsequent loading step in the Argonaute 2 (AGO2) protein. AGO2 protein is an endonuclease responsible for cleavage of the mRNA with catalytic turnover, and is made of four main domains: N-terminal, PAZ, MID, and PIWI (**Figure 1.9**).[95-97] During the AGO2 loading, TRBP (or PACT) proteins hand off the stable end of the

duplex to the PAZ domain of AGO2 (**Figure 1.8**). This model proposes a mechanism for AS strand selection based on siRNA duplex thermodynamic asymmetry, and is in agreement with previous observations that the siRNA strand with the least tightly bound 5′ end frequently becomes the AS strand.[90, 91]

As mentioned above, following the guide strand selection and binding to the mRNA, mRNA cleavage happens by AGO2. Argonaute family of proteins are responsible for the endonuclease function of the RISC complex. The Argonaute family in humans has four members: hAGO1, hAGO2, hAGO3, and hAGO4, from which only hAGO2 has endonuclease (slicer-type) activity, and is therefore the subject of many studies as the core catalytic component of the RNAi pathway.[95] MID domain of the hAGO2 is anchored to the 5' end of the AS strand, while the PAZ domain holds the 3' nucleotide of the AS strand (**Figure 1.9**), keeping the AS strand in the

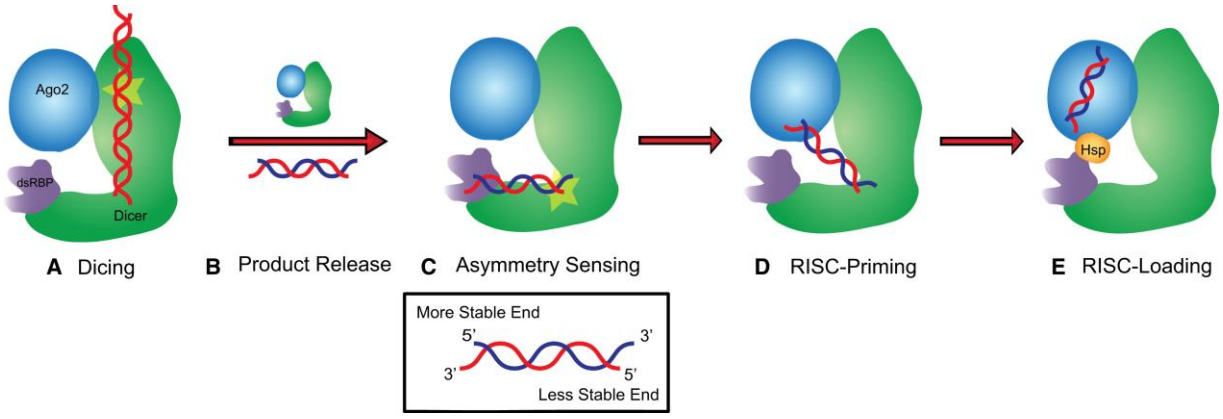

Figure 1.8 Model for dsRNA positioning by the human RISC-loading complex. (A) Human Dicer recognizes and orients dsRNA substrates along its catalytic domain, with the correct positioning in the active site, ready for cleavage. (B) Following the cleavage, the nascent siRNA product is released from Dicer to be repositioned. (C) Dicer and TRBP or PACT bind the siRNA, to position them along Dicer's helicase domain for asymmetry sensing. Dicer prefers to binds to the less stable end of the duplex, whereas the TRBP binds the more stable end, placing the 3′ end of the AS strand near the PAZ domain of AGO2 prior to RISC loading. (D) In a hypothetical RISC-priming step, the more stable end of the siRNA repositions to the Ago2 PAZ domain, leading to a transient intermediate in which the siRNA is coordinately bound by Dicer and AGO2. (E) Finally, the siRNA is loaded into AGO2 with the 3′ end of the AS strand bound to the PAZ domain and the 5′ end bound to the Mid domain of AGO2. The AS and sense strands are illustrated in red and blue, respectively. Figure adapted from the reference [94].

correct orientation.[98, 99] Upon binding of the 5' phosphate to the 5' binding pocket, the 5' nucleotide of the AS strand bends away from the rest of the AS strand seed region, and therefore, becomes unavailable to the upcoming mRNA for complementarity recognition and binding.[95, 98] Following that, the PIWI subdomain of hAGO2 uses the two magnesium ions to catalyze the cleavage of the target mRNA.[95, 100] This cleavage of either the siRNA passenger strand or the target mRNA occurs between the nucleotides paired to nucleotides 10 and 11 of the hAGO2 AS strand (from the 5′ end).[101-104]

It is yet not known what happens to the siRNA passenger strand after it is loaded into RISC. However, at least three different mechanisms have been proposed: [I] upon loading of the siRNA guide strand in the hAGO2, the passenger strand is cleaved by the PIWI subdomain and is released subsequently;[95] [II] in a process independent of passenger cleavage process (I), an ATP-dependent helicase unwinds and releases the passenger strand;[95] and [III] the passenger strand is cut by the hAGO2, eliciting the subsequent passenger strand degradation by C3PO (the third component promoter of RISC).[105] It has been observed that in most cases, chemical modifications at the cleavage site of the passenger strand can interfere with passenger strand cleavage, especially 2' modifications at the scissile nucleotide position.[88, 106, 107] However, RISC-mediated passenger strand cleavage results in the formation of a 3'-OH fragment as well as a 5'-phosphate fragment, which suggest that an available 2'-OH -to form the 2′-3′ cyclic phosphate as observed for some other nucleases- is not necessary.[107] In any case, it is clear that the RISC complex has an essential role in the RNAi pathway, and therefore, understanding and optimizing siRNA interactions with the RISC is of great importance to improve the potency of siRNA therapeutics.

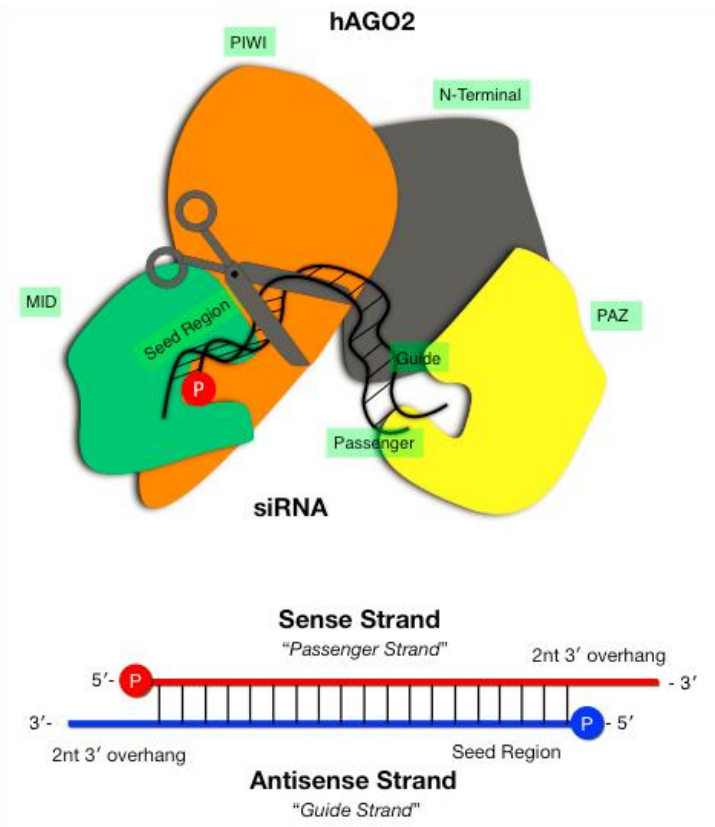

Figure 1.9 hAGO2 with an siRNA loaded in it. (top) A simplified diagram of AGO2 subunits interacting with an siRNA. (bottom) Classical siRNA structure; 21nt RNA duplex with 2 nucleotide overhangs on each 3′ end. The antisense strand ("guide" strand) is complementary to target mRNA. The sense strand ("passenger" strand) is complementary to the guide strand. The guide strand contains the seed region at the 5' end. Figure adapted from reference[85].

1.7 Chemical modifications of nucleic acids

Despite of the high potency exhibited by oligonucleotide therapeutics *in vitro*, there are many shortcomings that preclude the use of oligonucleotides *in vivo*: [1] their poor extracellular and intracellular stability; [2] low efficiency of intracellular delivery to target cells or tissues; and [3] the potential for "off-target" gene silencing, immunostimulation, and other side effects. A solution to overcome many of these shortcomings is the chemical modification of nucleic acids. The following sections will discuss in more details the challenges in the ON therapeutic field and how chemical modifications can help alleviate some of these issues.

1.7.1 Challenges in the oligonucleotide therapeutics field

Previous studies have demonstrated that unmodified nucleic acids, particularly RNA, have limited stability in biological media and are rapidly degraded by nucleases.[108] This, results in shortened duration of activity and delivery challenges for such molecules. Moreover, they have poor pharmacokinetic properties; they weakly bind to plasma proteins, are filtered by the kidneys and ultimately excreted in the urine rapidly after *in vivo* administration. Finally, highly negatively charged nature of oligonucleotides, prevents them from crossing the cell membrane and reaching the cytoplasm.[109] From a medicinal chemistry perspective, key attributes for enhancing the drug-like properties of oligonucleotides include enhancing binding affinity for the target RNA, enhancing stability against nuclease mediated metabolism, improving pharmacokinetic properties, and maintaining (or improving) the ability to elicit a functional gene silencing response.[85, 110, 111]

Fortunately, many of the obstacles hindering the progress of ON therapeutics have been overcome by development and incorporation of a vast array of ON chemical modifications. These nucleic acid analogues are often rationally designed to adjust many of the inherent properties of ONs, resulting in their improved nuclease stability, biological application, and potency without altering their sequence.[111]

A more challenging hurdle to overcome, however, has been the delivery of the ON therapeutics. Many approaches have been developed to achieve efficient cellular delivery of ON therapeutics, namely: covalent attachment of ONs to chemical or biologically relevant moieties, in order to facilitate their cellular update. Also, ONs can be attached to delivery vehicles in order to encapsulate and shield the ON from degradation, as well as facilitate their cellular uptake.[112-116] Another well-known side effect of treatment with ON therapeutics is the knockdown of

unintended genes known as Off Target Effects (OTEs). This side effect is more prominent with the use of siRNAs, but is also observed with AONs. Due to the hybridization-dependent nature of the ON therapeutics, OTEs happen when there is partial complementarity between the ON target and an mRNA other than the intended target.

In the case of siRNAs, OTEs can also happen when the passenger strand is selected to load in the RISC, instead of the guide strand. As a result, the RNAi machinery targets a completely different mRNA and results in unintended gene knockdown. Another possible pathway for OTEs is when siRNA acts as a miRNA. miRNAs recognize their target only based on seed region complementarity, and therefore, when an siRNA functions as a miRNA, there are many possible mRNAs sharing similar short stretch of nucleotides that can be targeted resulting in OTSs.[112, 117]

OTEs can be overcome by chemical modification of siRNAs passenger or guide strands. Chemical modification of passenger strand has been developed as a method to prevent the RISC from selecting siRNAs passenger strand as guide strand by mistake, as the RISC is not able to tolerate many chemical modifications in the guide strand. Nevertheless, some modifications have been shown to be accepted in the guide strand by the RISC, and this allowed for another approach through which modifications were introduced in the guide strand seed region in order to weaken the seed pairing with its complementary strand (passenger or mRNA). Seed region weakening can assist guide strand selection in two ways: (a) by introducing thermodynamic bias in the siRNA duplex rendering the 5' end of guide strand as the weaker end of the duplex and hence help the RISC in picking the correct strand as guide, and (b) by weakening the seed pairing with the binding mRNAs and therefore, differentially destabilize the guide strand with seed-only matched targets.[118-121] A recent work by Beal and co-workers demonstrates a new approach in reducing OTEs via a special base modification incorporated in the first 5' end

nucleotide of the guide strand. It is proposed that the selectivity of the hAGO2 for target mRNAs were tuned in this method via projection of the nucleobase substituent group in to the central cleft of the enzyme.[118]

Finally, another potential side effect that is associated with ON therapeutics is immunostimulation.[122-124] Different cellular immune receptors positioned in different cellular locations are able detect AONs and siRNAs, potentially leading to cytokine release and eventual changes in gene expression. The siRNA receptors include toll-like receptor 3 (TLR3) (dsRNA, cell surface and endosomal), TLR7 (ssRNA, endosomal), TLR8 (ssRNA, endosomal), RNA helicase enzymes Melanoma Differentiation-Associated protein 5 (MDA5) (cytoplasm), Retinoic acid Inducible Gene 1 (RIG-1) (cytoplasm), and PKR (cytoplasm).[112, 122, 124-127] In the case of AONs, they can be immunostimulatory upon recognition by TLR9 (endosomal) when the DNA sequence (as in AONs) contains unmodified 5'-CpG motif(s).[128, 129] Also, for siRNAs some immunostimulatory sequence motifs have been identified such as the 5'-UGUGUU[130] and 5'-GUCCUUCAA[131] motifs. Immunostimulatory response following an OT treatment is problematic as it can confuse experiments designed to measure gene silencing potencies of AONs and siRNAs. The non-specific innate immune responses triggered by siRNAs and AONs can cause changes in cellular gene expression levels, and therefore affect gene silencing data.[123, 124] Luckily, many of the chemical modifications of the ON therapeutics can significantly help the ONs go unrecognized and abrogate the immunostimulatory response, providing an effective means for avoiding these potential side effects.[124] More information on this topic is provided in Chapter 3 of this thesis.

1.7.2 Chemical modifications of oligonucleotides

As explained in previous sections, the development of chemically modified nucleic acids is crucial for the success of oligonucleotide-based therapies. Fortunately, much of the chemistries developed to design and synthesize nucleoside analogues as antiviral and anticancer agents have also be applied in the development of chemically modified oligonucleotides. This has provided nucleic acid chemists with diverse chemical modifications that upon incorporation into oligonucleotides can control and adjust many important oligonucleotide properties such as binding affinity for RNA targets, conformation, nuclease stability and immunostimulatory properties.

There are three main sites on oligonucleotides which are amenable for chemical modification: [I] Backbone modifications; [II] Sugar modifications; and [III] Nucleobase modifications. The following sections will briefly describe each category, focusing on the modifications used in this thesis.

[I] Backbone modifications:

The internucleotide phosphodiester linkages of nucleic acids are negatively charged at physiological pH (pKa~2).[85] If unmodified, endo- and exonucleases found in serum and within mammalian cells readily hydrolyze these phosphodiester linkages.[85] Chemical modification of these linkages have been extensively studied and there are many chemical strategies developed successfully to avoid such nuclease degradation.

Perhaps the most popular ON backbone modifications is the phosphorothioate (PS) linkage, where a sulphur atom substitutes for one nonbridging phosphate oxygen (**Figure 1.10**).[132-134] This modification imparts significant resistance to nuclease degradation, and can be readily

incorporated using standard solid-phase ON synthesis protocols.[135] PS modification is commonly used in AON,[135, 136] and have been utilized in FDA approved ON drugs, Formivirsen and Spinraza.[135] An important point about the PS linkage is that it introduces chirality to internucleotide linkages, and only one stereochemistry (*Sp* linkage) is highly resistant to nuclease-mediated cleavage.[137]

Although synthetically challenging, some strategies have been developed for diastereoselective synthesis of PS linkages.[138] However, PS-modified ON therapeutics are commonly synthesized as a diastereomeric mixture, with this justification that each strand will contain multiple resistant linkages which eventually enhances the overall stability of the population. PS linkages can improve pharmacokinetics of ON therapeutics by enhancing their affinity for binding with serum albumin and therefore improving circulation time.[136] siRNAs have been more sensitive toward accepting PS linkages. PS linkage incorporation into siRNAs have been successful with no significant loss of potency. However, this modification can reduce siRNA activity in some cases, such as PS modifications at the AGO2 cleavage site.[87, 112]

As discussed in previous sections, 2'-5' linkage modification, also, is another linkage modification with natural origins. Some research has been reported on the 2'-5' linked AON.[139] However, there is very limited study done on utilizing this modification in siRNAs. Positive traits such as nuclease stability gain, simplicity, affordability, and feasible synthesis motivated us to investigate 2'-5' linkage modification as an attractive candidate for siRNA therapeutics. Chapters 3 and 4 of this thesis will describe this modification in more detail.

Many other linkage modifications with interesting prospects have been developed, such as N3' phosphoramidate (NP),[140] phosphonoacetate (PACE),[141] morpholino phosphoramidates,[142] and peptide nucleic acids (PNA)[143] (**Figure 1.10**). More information on these ON backbone modifications can be found in the cited reviews.

[II] Nucleobase modifications:

Chemically modified nucleobases are useful modifications in ON analogue development that can be used to affect thermal stability, reduce immunostimulation, and affect siRNA OTEs. Modified nucleobases are mostly designed in order to enhance duplex stability while retaining the native base pairing recognition and hydrogen bonding. Some examples of modified nucleobases with such abilities are the 5-bromo-Ura and 5-iodo-Ura substitutes of Ura, as well as 2,6-

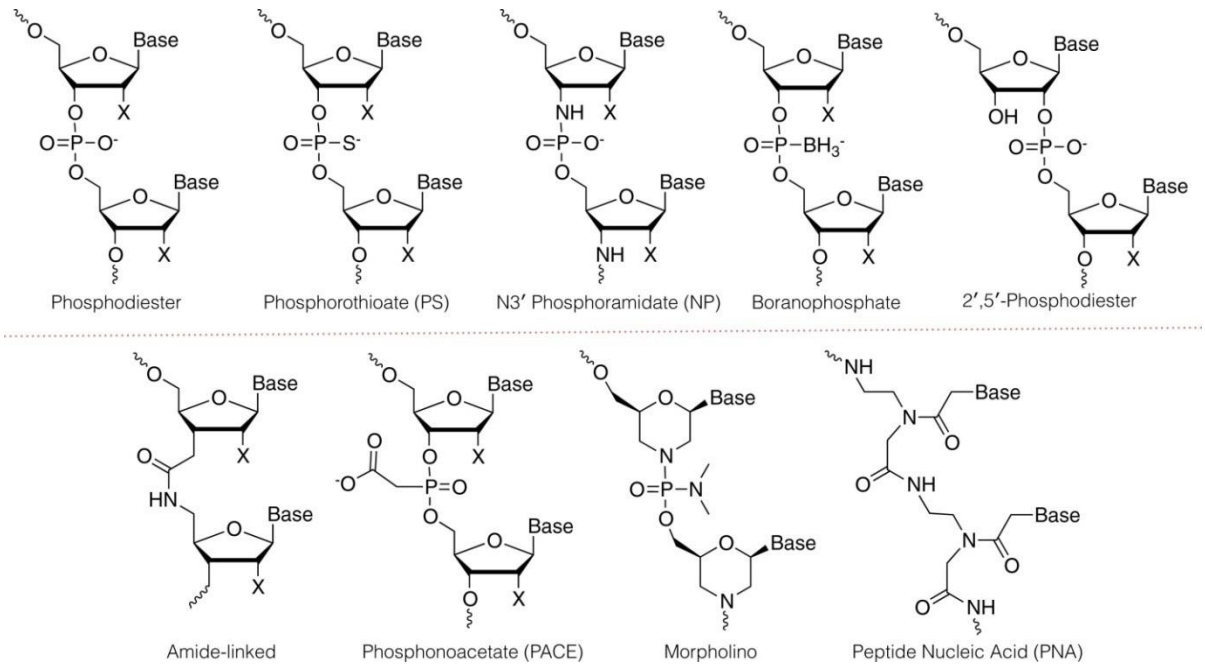

Figure 1.10 Selected chemical modifications of internucleotide backbone. Phosphodiester linkages form the backbone of natural DNA (X = H) and RNA (X=OH). Figure adapted from reference[85].

diaminopurine in place of Ade being used to stabilize A-U base pairs in ON duplexes.[112, 122, 144] Isocytosine (isoC) and isoguanine (isoG) base modifications, nucleobase isomers of cytosine and guanine, were developed as alternatives for standard genomic bases which are able to form the WC base pairing.[145-149] They were hypothesized to be a component of primitive nucleic acids early in the development of life, specially upon the discovery that they were recognized and incorporated in chain elongation by polymerase enzyme.[145] However, their diminished chemical stability would have been a setback to this hypothesis. IsoG is also a product of oxidative damage to DNA and has been shown to cause mutation, as it can also pair with thymine.[150] IsoG:C and isoC:G base pairs have been used to improve the hydrogen bonding and duplex stability in parallel oriented duplexes.[151, 152] Their twisted base structure is able restore all the three hydrogen bondings within isoG:C or isoC:G base pairs in the parallel mode, and hence stabilize the otherwise unstable parallel duplexes. Chapter 5 of this thesis will provide more details on iso base modifications.

A variety of modified nucleobases with minor-groove projections were designed which are able to abrogate the immunostimulatory responses to siRNAs and miRNA mimics, most likely by preventing interactions with TLR and PKR receptors.[153] In the case of AONs, immunostimulation responses to CpG motifs can be abrogated by replacing cytosine with 5-methylcytosine.[128] Nucleobase modifications can provide the means for probing duplex physical characteristics.[153] Intrinsically fluorescent modified nucleobases were found to be extremely useful in studying mechanistic aspects of ON therapeutics, owing to their ability to impart fluorescent properties to nucleic acids. A more comprehensive review on nucleobase modifications can be found here.[153, 154]

[III] Sugar modifications:

Tremendous research done in developing nucleic acids with chemically modified sugars has provided a vast library of nucleoside analogues that allow a remarkable level of diversity and control over nucleic acid properties. Chemical modifications of sugar component of nucleotides directly affect their puckering properties, which consequently affects duplex conformation, binding affinity of the ON towards their complementary strand, and eventually their interactions with proteins. Most nucleotide sugars analogues adopt conformations characterized on the pseudorotational wheel as either "North" (C3'-*endo*), or “South” (C2'-*endo*), passing through the “East” (O4'-*endo*) while transitioning between the north and south conformations. For a nucleotide analogue, to be considered DNA-like, it should adopt the “South” puckering in B-form dsDNA, whereas an RNA- like nucleotide analogue should adopt the “North” conformation in an A-form dsRNA. These structural analysis of nucleotide analogues can be particularly important when designing a chemically modified ON therapeutic, considering the sensitivity and tolerance of the cellular enzymes involved in the AON- or siRNA-mediated gene silencing. Some of sugar-modified nucleotide analogues are highlighted in **Figure 1.11** and will be described below.[85]

One of the most widely used nucleoside analogues is the 2'-*O*-Me modification. 2'-*O*-Me sugars adopt a North conformation, resembling RNA, and form A-form duplexes.[155, 156] As a result, these nucleotide analogues are very well suited for siRNA modification and are, indeed, very well tolerated by the RISC, even in the guide strand. Compared with DNA, 2'-*O*-Me shows increased binding affinity for RNA. It also highly increases nuclease stability, as well as reduced immunostimulatory properties, making it an attractive candidate for therapeutic agents. 2'-*O*-Me modification is used in the first FDA-approved aptamer, Macugen.[157]

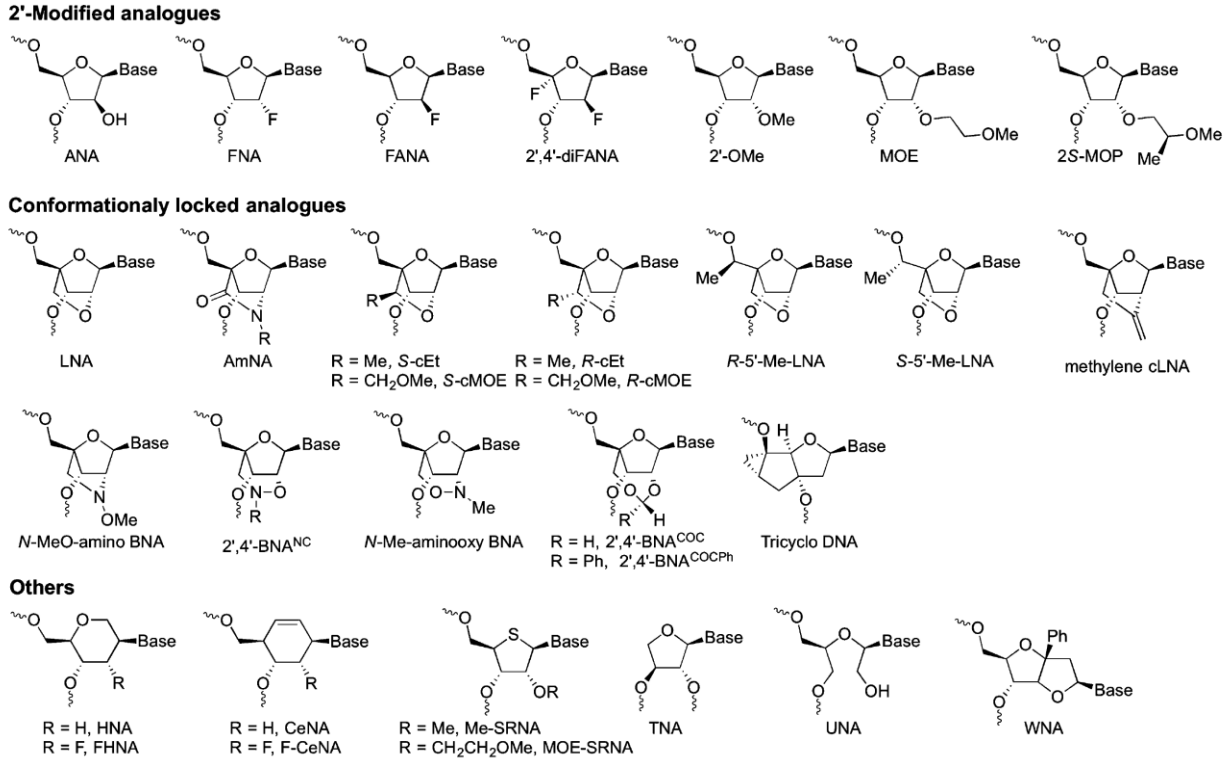

Figure 1.11 Selected chemical sugar-modified nucleoside analogues. Most of the nucleotide analogues involve modification of the 2' position of RNA. Other modifications include replacement of the ring oxygen with Sulphur; bridges between the C2' and C4' positions of sugar; modified C4' nucleotides, and replacement of furanose with bicyclic, tricyclic, or ring expanded analogues. Figure from reference[162].

2'F-RNA is a very good mimic of RNA, making it a versatile and well-tolerated chemical modification for many applications. Like 2'-*O*-Me RNA, 2'F-RNA also adopts a North pucker sugar conformation within an A-form duplex.[158, 159] This modification increases the binding affinity of the ON for target RNA[136] due to stronger hydrogen bonding originating from fluorine's electronegativity, as well as duplex conformational preorganization.[160] 2'F-RNA modification is very well tolerated in both passenger and guide strands in siRNA, making it an attractive siRNA modification.[112, 122] However, unlike the 2'-*O*-Me modification, it is more susceptible to nuclease-mediated degradation, with the exception of in pyrimidine-rich

sequences.[161] The 2'F-ribo modification is also used in the structure of the FDA approved aptamer, Macugen.[157]

While the majority of sugar modifications are focused on the 2' position, there are other analogue categories such as: modifications on the 4' position, analogues with altered ring oxygen, analogues with bicyclic sugar rings, etc. More information about these analogues can be found elsewhere.[111, 112]

Many valuable nucleoside analogues have been developed with expanded sugar scaffolds, extending the pool of available modified nucleosides for ON therapeutics beyond the 5-membered ring mimics of ribose. Some of these analogues including Morpholino nucleic acids (NA), cyclohexene nucleic acid (CeNA),[163, 164] altritol nucleic acid (ANA),[165, 166] oxepane NAs (ONA),[167] and hexitol NA (HNA)[166] modifications have been used in gene silencing experiments. CeNA was shown to bind RNA more tightly than a DNA strand, increasing serum stability, and activating RNase H.[164, 168] ANA is a stabilizing RNA-binding modification that favor A-form duplexs. Finally, Oxepane nucleic acids (ONA) are seven membered ring nucleotide analogues, which are nuclease resistant and can trigger RNase H.[167] An investigation to improve properties of the first generation of oxepane nucleic acids will be discussed in Chapter 2 of this thesis.

1.8 Solid phase synthesis of oligonucleotide

One of the most significant technical advancements in the field of nucleic acid research has been the discovery and development of automated solid phase synthesis of oligonucleotides. One of the first automated oligonucleotide synthesizer ("Gene Machine") was built by Dr. Kevin Ogilvie at McGill University in 1981.[169] Since then, oligonucleotides in any desired sequence and quantities sufficient for most scientific applications have been synthesized, enabling the drastic

progress of many biological sciences, as well as ON-based therapeutics. A typical solid phase synthesis cycle, utilizing the reagents and materials commonly applied to a regular oligonucleotide synthesis are illustrated in **Figure 1.12**.[170]

The building blocks of synthetic oligonucleotide synthesis are phosphoramidites. Phosphoramidite chemistry was first reported in 1981 by Serge Beaucage and Marvin Caruthers and has remained the commonly used ever since.[9] The structures of RNA and DNA phosphoramidite monomers are shown in **Figure 1.12**. RNA monomers are protected at the 2' hydroxyl position of the sugar with the *tert*-butyldimethylsilyl (TBDMS) group;[171] the 5' hydroxyl group of both DNA and RNA monomers is protected with the acid-labile dimethoxytrityl (DMTr) group; and the exocyclic amines of the A, G, and C nucleobases are protected as amides (T and U do not require base protection).[172, 173]

The 3' hydroxyl group in DNA and RNA monomers features a phosphorus (III) moiety, a 2-cyanoethyl, *N*,*N*-diisopropyl phosphoramidite group (**Figure 1.12**). A typical solid phase synthesis (**Figure 1.12**) starts with a derivatized solid support (usually CPG or polystyrene) and proceeds in the 3' to 5' direction. Different linkers can be used to connect the synthesized strand to the solid support; throughout this thesis, the commercially available UnyLinker solid support was employed.[172] The cycle starts with a detritylation step ("Deblock" step) using 3% trichloroacetic acid in dichloromethane to remove the DMTr protecting group and release the 5' hydroxyl group.

In the next step ("Coupling" step) a phosphoramidite monomer is activated with 5-ethylthiotetrazole and couples to 5' hydroxyl group to form a phosphite linkage. This step proceeds typically in 98.5% yield for RNA, and 99% for DNA. Next, a "Capping" step (acetic

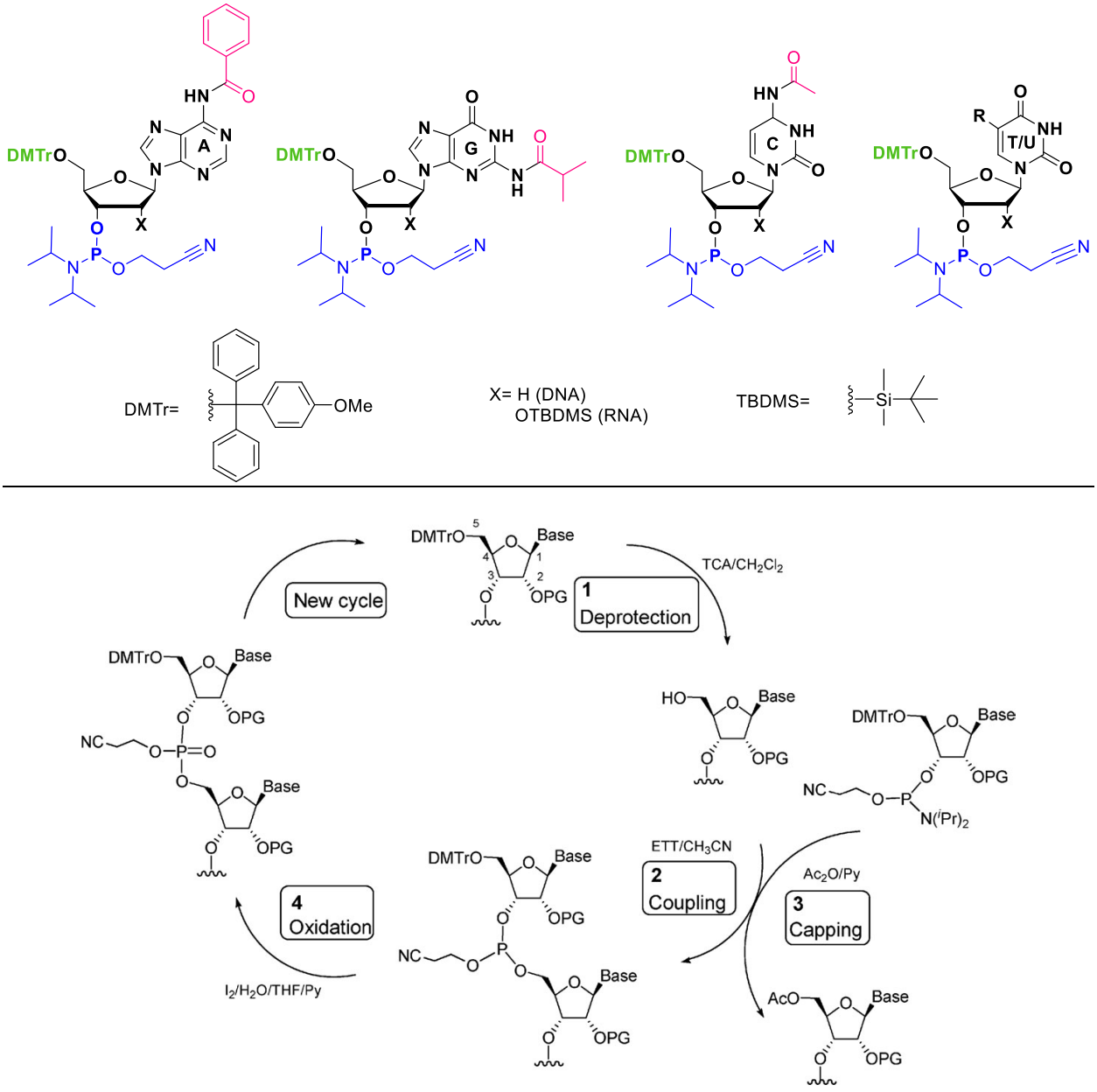

Figure 1.12 (Top) Phosphoramidite monomers used in the automated solid-phase synthesis of DNA and RNA oligonucleotides; (Bottom) A typical solid phase synthesis cycle for the synthesis of DNA or RNA. Picture adapted from [170]

anhydride/*N*-methylimidazole) is used to esterify (“cap”) any unreacted 5' hydroxyl groups, preventing these from undergoing chain extension in subsequent steps. The phosphite triester linkage formed is oxidized using a mixture of iodine and water in tetrahydrofuran to afford the more stable phosphotriester group. This cycle is repeated until the oligomer of desired length and base sequence is synthesized. Finally, the oligonucleotide is cleaved from the solid support, deprotected, purified and characterized.

1.9 Thesis objectives

The focus of this thesis revolves around development and mechanistic investigations of chemically modified nucleic acid therapeutics. Chapter 2 describes the synthesis of a novel series of seven-membered ring nucleoside (oxepane) analogues as candidates for biological screening and gene silencing applications. The conformational landscape and preferred ring-puckering of selected oxepane nucleosides are investigated by means of NMR, X-ray crystallography, and quantum mechanical calculations. These nucleoside analogues are valuable compounds for both antiviral applications and oligonucleotide modification purposes.

Chapter 3 examines the effect of 2'-5' linkage modification in siRNA efficiency and interactions of such siRNAs with the proteins involved in the RNAi pathway. siRNA libraries targeting two different mRNAs with different positional variations of 2'-5' linkages throughout the sense or antisense strands are prepared. Our results show that introduction of 2'-5' linkages can afford a potent class of modified siRNAs with diminished immunostimulatory response.

Chapter 4 introduces the novel topic of ON "mixmers" as an approach to attain potent chemically modified oligonucleotide mixtures, without screening and singling out the most active modification design within the mixture. The synthesis, characterization, and preliminary biological screening of mixmer siRNAs are presented.

Chapter 5 investigates the impact of several sugar and nucleobase modifications on the formation of parallel-stranded duplexes at neutral pH. This study expands previous studies in this laboratory on the synthesis of isoguanosine- and isocytidine- modified parallel stranded DNA:RNA hybrids as active siRNAs under physiological conditions. This study also reveals the benefits and challenges to the design of parallel stranded siRNAs and explains the underlying rules to make successful parallel stranded siRNAs. These results demonstrate that strand orientation is not a critical determinant in the recognition of siRNA triggers by the RISC complex.

1.10 References

1. Honegger, E., *Festschrift Prof. Dr. A. Stodola zum 70. Geburtstag, überreicht von seinen Freunden und Schülern*. Orell Füssli: Zürich, 1929.
2. Avery, O. T.; MacLeod, C. M.; McCarty, M., Studies on the chemical nature of the substance inducing transformation of pneumococcal types: Induction of transformation by a desoxyribonucleic acid fraction isolated from pneumococcus type III. *The Journal of Experimental Medicine* **1944,** *79*, 137-158.
3. Levene, P. A., The structure of yeast nucleic acid: IV. Ammonia hydrolysis. *Journal of Biological Chemistry* **1919,** *40*, 415-424.
4. Levene, P. A.; Tipson, R. S., The ring structure of thymidine. *Science* **1935,** *81*, 98.
5. Griffith, F., The Significance of Pneumococcal Types. *The Journal of Hygiene* **1928,** *27*, 113-159.
6. Hayes, D. H.; Michelson, A. M.; Todd, A. R., Nucleotides. Part XXX. Mononucleotides derived from deoxyadenosine and deoxyguanosine. *Journal of the Chemical Society (Resumed)* **1955**, 808-815.
7. Chargaff, E., Chemical specificity of nucleic acids and mechanism of their enzymatic degradation. *Experientia* **1950,** *6*, 201-9.
8. Usman, N.; Ogilvie, K. K.; Jiang, M. Y.; Cedergren, R. J., The automated chemical synthesis of long oligoribuncleotides using 2'-O-silylated ribonucleoside 3'-O-phosphoramidites on a controlled-pore glass support: synthesis of a 43-nucleotide sequence similar to the 3'-half molecule of an Escherichia coli formylmethionine tRNA. *J Am Chem Soc* **1987,** *109*, 7845-7854.
9. Beaucage, S. L.; Caruthers, M. H., Deoxynucleoside phosphoramidites—A new class of key intermediates for deoxypolynucleotide synthesis. *Tetrahedron Letters* **1981,** *22*, 1859-1862.
10. Goodchild, J., Therapeutic oligonucleotides. *Methods in molecular biology (Clifton, N.J.)* **2011,** *764*, 1-15.

11. O'Connor, L.; Glynn, B., Recent advances in the development of nucleic acid diagnostics. *Expert review of medical devices* **2010,** *7*, 529-39.
12. Cotton, R. G., Current methods of mutation detection. *Mutation research* **1993,** *285*, 125-44.
13. Chapter 2 DNA and RNA Structure. In *Nucleic Acids in Chemistry and Biology (3)*, The Royal Society of Chemistry2006; pp 13-76.
14. Chapter 3 Nucleosides and Nucleotides. In *Nucleic Acids in Chemistry and Biology (3)*, The Royal Society of Chemistry2006; pp 77-142.
15. Altona, C.; Sundaralingam, M., Conformational analysis of the sugar ring in nucleosides and nucleotides. New description using the concept of pseudorotation. *J Am Chem Soc* **1972,** *94*, 8205-8212.
16. Altona, C.; Sundaralingam, M., Conformational analysis of the sugar ring in nucleosides and nucleotides. Improved method for the interpretation of proton magnetic resonance coupling constants. *J Am Chem Soc* **1973,** *95*, 2333-2344.
17. Damha, M. J.; Ogilvie, K. K., Conformational properties of branched RNA fragments in aqueous solution. *Biochemistry* **1988,** *27*, 6403-6416.
18. Magasanik, B.; Vischer, E.; Doniger, R.; Elson, D.; Chargaff, E., THE SEPARATION AND ESTIMATION OF RIBONUCLEOTIDES IN MINUTE QUANTITIES. *Journal of Biological Chemistry* **1950,** *186*, 37-50.
19. Yakovchuk, P.; Protozanova, E.; Frank-Kamenetskii, M. D., Base-stacking and base-pairing contributions into thermal stability of the DNA double helix. *Nucleic Acids Research* **2006,** *34*, 564-574.
20. Maroun, R. C.; Olson, W. K., Base sequence effects in double-helical DNA. III. Average properties of curved dna. *Biopolymers* **1988,** *27*, 585-603.
21. Hunter, C. A., Sequence-dependent DNA structure. The role of base stacking interactions. *Journal of molecular biology* **1993,** *230*, 1025-54.
22. Lowe, M. J.; Schellman, J. A., Solvent effects on dinucleotide conformation. *Journal of molecular biology* **1972,** *65*, 91-109.
23. Guckian, K. M.; Schweitzer, B. A.; Ren, R. X. F.; Sheils, C. J.; Paris, P. L.; Tahmassebi, D. C.; Kool, E. T., Experimental Measurement of Aromatic Stacking Affinities in the Context of Duplex DNA. *J Am Chem Soc* **1996,** *118*, 8182-8183.
24. Guckian, K. M.; Schweitzer, B. A.; Ren, R. X. F.; Sheils, C. J.; Tahmassebi, D. C.; Kool, E. T., Factors Contributing to Aromatic Stacking in Water: Evaluation in the Context of DNA. *J Am Chem Soc* **2000,** *122*, 2213-2222.
25. Kool, E. T.; Morales, J. C.; Guckian, K. M., Mimicking the Structure and Function of DNA: Insights into DNA Stability and Replication. *Angewandte Chemie (International ed. in English)* **2000,** *39*, 990-1009.
26. Freier, S. M.; Sugimoto, N.; Sinclair, A.; Alkema, D.; Neilson, T.; Kierzek, R.; Caruthers, M. H.; Turner, D. H., Stability of XGCGCp, GCGCYp, and XGCGCYp helixes: an empirical estimate of the energetics of hydrogen bonds in nucleic acids. *Biochemistry* **1986,** *25*, 3214-9.
27. Manning, G. S., The molecular theory of polyelectrolyte solutions with applications to the electrostatic properties of polynucleotides. *Quarterly reviews of biophysics* **1978,** *11*, 179-246.
28. Kool, E. T., Preorganization of DNA: Design Principles for Improving Nucleic Acid Recognition by Synthetic Oligonucleotides. *Chemical reviews* **1997,** *97*, 1473-1488.

29. Kool, E. T., Hydrogen bonding, base stacking, and steric effects in dna replication. *Annual review of biophysics and biomolecular structure* **2001,** *30*, 1-22.
30. Sponer, J.; Leszczynski, J.; Hobza, P., Electronic properties, hydrogen bonding, stacking, and cation binding of DNA and RNA bases. *Biopolymers* **2001,** *61*, 3-31.
31. Arnott, S., The geometry of nucleic acids. *Progress in Biophysics and Molecular Biology* **1970,** *21*, 265-319.
32. Drew, H. R.; Wing, R. M.; Takano, T.; Broka, C.; Tanaka, S.; Itakura, K.; Dickerson, R. E., Structure of a B-DNA dodecamer: conformation and dynamics. *Proceedings of the National Academy of Sciences* **1981,** *78*, 2179-2183.
33. Ghosh, A.; Bansal, M., A glossary of DNA structures from A to Z. *Acta crystallographica. Section D, Biological crystallography* **2003,** *59*, 620-6.
34. Dervan, P., Design of sequence-specific DNA-binding molecules. *Science* **1986,** *232*, 464-471.
35. Zimmer, C.; Wahnert, U., Nonintercalating DNA-binding ligands: specificity of the interaction and their use as tools in biophysical, biochemical and biological investigations of the genetic material. *Prog Biophys Mol Biol* **1986,** *47*, 31-112.
36. Egli, M., Structural Aspects of Nucleic Acid Analogs and Antisense Oligonucleotides. *Angewandte Chemie International Edition in English* **1996,** *35*, 1894-1909.
37. Jissy, A. K.; Datta, A., Design and Applications of Noncanonical DNA Base Pairs. *The Journal of Physical Chemistry Letters* **2014,** *5*, 154-166.
38. Mooers, B. H.; Eichman, B. F.; Ho, P. S., The structures and relative stabilities of d(G x G) reverse Hoogsteen, d(G x T) reverse wobble, and d(G x C) reverse Watson-Crick base-pairs in DNA crystals. *Journal of molecular biology* **1997,** *269*, 796-810.
39. Carell, T.; Brandmayr, C.; Hienzsch, A.; Muller, M.; Pearson, D.; Reiter, V.; Thoma, I.; Thumbs, P.; Wagner, M., Structure and function of noncanonical nucleobases. *Angewandte Chemie (International ed. in English)* **2012,** *51*, 7110-31.
40. Chou, S. H.; Chin, K. H.; Wang, A. H., Unusual DNA duplex and hairpin motifs. *Nucleic Acids Res* **2003,** *31*, 2461-74.
41. Das, R.; Karanicolas, J.; Baker, D., Atomic accuracy in predicting and designing noncanonical RNA structure. *Nat Meth* **2010,** *7*, 291-294.
42. Moore, P. B., Structural motifs in RNA. *Annu Rev Biochem* **1999,** *68*, 287-300.
43. Leontis, N. B.; Stombaugh, J.; Westhof, E., The non-Watson-Crick base pairs and their associated isostericity matrices. *Nucleic Acids Res* **2002,** *30*, 3497-531.
44. van de Sande, J. H.; Ramsing, N. B.; Germann, M. W.; Elhorst, W.; Kalisch, B. W.; et al., Parallel Stranded DNA. *Science* **1988,** *241*, 551.
45. Pattabiraman, N., Can the double helix be parallel? *Biopolymers* **1986,** *25*, 1603-1606.
46. Ramsing, N. B.; Jovin, T. M., Parallel stranded duplex DNA. *Nucleic Acids Res* **1988,** *16*, 6659-76.
47. Frank-Kamenetskii, M. D.; Mirkin, S. M., Triplex DNA Structures. *Annual Review of Biochemistry* **1995,** *64*, 65-95.
48. Lavelle, L.; Fresco, J. R., UV spectroscopic identification and thermodynamic analysis of protonated third strand deoxycytidine residues at neutrality in the triplex d(C+-T)6:[d(A-G)6d(C−-T)6]; evidence for a proton switch. *Nucleic Acids Research* **1995,** *23*, 2692-2705.
49. Marfurt, J.; Parel, S. P.; Leumann, C. J., Strong, specific, monodentate G-C base pair recognition by N7-inosine derivatives in the pyrimidine.purine-pyrimidine triple-helical binding motif. *Nucleic Acids Res* **1997,** *25*, 1875-82.

50. Sun, J.-S.; Hélène, C., Oligonucleotide-directed triple-helix formation. *Current Opinion in Structural Biology* **1993,** *3*, 345-356.
51. Burge, S.; Parkinson, G. N.; Hazel, P.; Todd, A. K.; Neidle, S., Quadruplex DNA: sequence, topology and structure. *Nucleic Acids Research* **2006,** *34*, 5402-5415.
52. Phan, A. T., Human telomeric G-quadruplex: structures of DNA and RNA sequences. *The FEBS journal* **2010,** *277*, 1107-17.
53. Collie, G. W.; Parkinson, G. N., The application of DNA and RNA G-quadruplexes to therapeutic medicines. *Chemical Society reviews* **2011,** *40*, 5867-92.
54. Gueron, M.; Leroy, J. L., The i-motif in nucleic acids. *Curr Opin Struct Biol* **2000,** *10*, 326-31.
55. Volker, J.; Klump, H. H.; Breslauer, K. J., The energetics of i-DNA tetraplex structures formed intermolecularly by d(TC5) and intramolecularly by d[(C5T3)3C5]. *Biopolymers* **2007,** *86*, 136-47.
56. Will, C. L.; Luhrmann, R., Spliceosome structure and function. *Cold Spring Harbor perspectives in biology* **2011,** *3*.
57. Keller, W., The RNA lariat: a new ring to the splicing of mRNA precursors. *Cell* **1984,** *39*, 423-5.
58. Carlomagno, T.; Amata, I.; Codutti, L.; Falb, M.; Fohrer, J.; Masiewicz, P.; Simon, B., Structural principles of RNA catalysis in a 2'-5' lariat-forming ribozyme. *J Am Chem Soc* **2013,** *135*, 4403-11.
59. Hartmann, R.; Justesen, J.; Sarkar, S. N.; Sen, G. C.; Yee, V. C., Crystal structure of the 2'-specific and double-stranded RNA-activated interferon-induced antiviral protein 2'-5'-oligoadenylate synthetase. *Molecular cell* **2003,** *12*, 1173-85.
60. Hovanessian, A. G.; Justesen, J., The human 2'-5'oligoadenylate synthetase family: unique interferon-inducible enzymes catalyzing 2'-5' instead of 3'-5' phosphodiester bond formation. *Biochimie* **2007,** *89*, 779-88.
61. Vengrova, S.; Dalgaard, J. Z., The wild-type Schizosaccharomyces pombe mat1 imprint consists of two ribonucleotides. *EMBO reports* **2006,** *7*, 59-65.
62. Joyce, G. F., RNA evolution and the origins of life. *Nature* **1989,** *338*, 217-224.
63. Gilbert, W., Origin of life: The RNA world. *Nature* **1986,** *319*, 618-618.
64. Trevino, S. G.; Zhang, N.; Elenko, M. P.; Luptak, A.; Szostak, J. W., Evolution of functional nucleic acids in the presence of nonheritable backbone heterogeneity. *Proceedings of the National Academy of Sciences of the United States of America* **2011,** *108*, 13492-7.
65. Engelhart, A. E.; Powner, M. W.; Szostak, J. W., Functional RNAs exhibit tolerance for non-heritable 2′–5′ versus 3′–5′ backbone heterogeneity. *Nat Chem* **2013,** *5*, 390-394.
66. Xu, L.; Wang, W.; Zhang, L.; Chong, J.; Huang, X.; Wang, D., Impact of template backbone heterogeneity on RNA polymerase II transcription. *Nucleic Acids Res* **2015,** *43*, 2232-41.
67. Voet, D.; Voet, J. G., *Biochemistry*. Wiley2004.
68. Stephenson, M. L.; Zamecnik, P. C., Inhibition of Rous sarcoma viral RNA translation by a specific oligodeoxyribonucleotide. *Proceedings of the National Academy of Sciences of the United States of America* **1978,** *75*, 285-288.
69. Piascik, P., Fomiversen sodium approved to treat CMV retinitis. *Journal of the American Pharmaceutical Association (Washington,D.C. : 1996)* **1999,** *39*, 84-5.
70. Tobin, K. A., Macugen treatment for wet age-related macular degeneration. *Insight (American Society of Ophthalmic Registered Nurses)* **2006,** *31*, 11-4.

71. Raal, F. J.; Santos, R. D.; Blom, D. J.; Marais, A. D.; Charng, M. J.; Cromwell, W. C.; Lachmann, R. H.; Gaudet, D.; Tan, J. L.; Chasan-Taber, S.; Tribble, D. L.; Flaim, J. D.; Crooke, S. T., Mipomersen, an apolipoprotein B synthesis inhibitor, for lowering of LDL cholesterol concentrations in patients with homozygous familial hypercholesterolaemia: a randomised, double-blind, placebo-controlled trial. *Lancet (London, England)* **2010,** *375*, 998-1006.
72. Aartsma-Rus, A., *Exon skipping : methods and protocols*. Humana Press: New York, 2012.
73. Kole, R.; Krainer, A. R.; Altman, S., RNA therapeutics: beyond RNA interference and antisense oligonucleotides. *Nat Rev Drug Discov* **2012,** *11*, 125-40.
74. Fire, A.; Xu, S.; Montgomery, M. K.; Kostas, S. A.; Driver, S. E.; Mello, C. C., Potent and specific genetic interference by double-stranded RNA in Caenorhabditis elegans. *Nature* **1998,** *391*, 806-11.
75. Elbashir, S. M.; Harborth, J.; Lendeckel, W.; Yalcin, A.; Weber, K.; Tuschl, T., Duplexes of 21-nucleotide RNAs mediate RNA interference in cultured mammalian cells. *Nature* **2001,** *411*, 494-498.
76. Ambros, V., The evolution of our thinking about microRNAs. *Nature medicine* **2008,** *14*, 1036-40.
77. Keefe, A. D.; Pai, S.; Ellington, A., Aptamers as therapeutics. *Nat Rev Drug Discov* **2010,** *9*, 537-550.
78. Mulhbacher, J.; St-Pierre, P.; Lafontaine, D. A., Therapeutic applications of ribozymes and riboswitches. *Current opinion in pharmacology* **2010,** *10*, 551-6.
79. Chan, C. W.; Khachigian, L. M., DNAzymes and their therapeutic possibilities. *Internal medicine journal* **2009,** *39*, 249-51.
80. Barchet, W.; Wimmenauer, V.; Schlee, M.; Hartmann, G., Accessing the therapeutic potential of immunostimulatory nucleic acids. *Current opinion in immunology* **2008,** *20*, 389-95.
81. Duroux-Richard, I.; Presumey, J.; Courties, G.; Gay, S.; Gordeladze, J.; Jorgensen, C.; Kyburz, D.; Apparailly, F., MicroRNAs as new player in rheumatoid arthritis. *Joint, bone, spine : revue du rhumatisme* **2011,** *78*, 17-22.
82. Filipowicz, W.; Bhattacharyya, S. N.; Sonenberg, N., Mechanisms of post-transcriptional regulation by microRNAs: are the answers in sight? *Nature reviews. Genetics* **2008,** *9*, 102-14.
83. Lennox, K. A.; Behlke, M. A., Chemical modification and design of anti-miRNA oligonucleotides. *Gene therapy* **2011,** *18*, 1111-20.
84. Kawamata, T.; Tomari, Y., Making RISC. *Trends in biochemical sciences* **2010,** *35*, 368-76.
85. Deleavey, Glen F.; Damha, Masad J., Designing Chemically Modified Oligonucleotides for Targeted Gene Silencing. *Chemistry & Biology* **2012,** *19*, 937-954.
86. Humphreys, D. T.; Westman, B. J.; Martin, D. I. K.; Preiss, T., MicroRNAs control translation initiation by inhibiting eukaryotic initiation factor 4E/cap and poly(A) tail function. *Proceedings of the National Academy of Sciences of the United States of America* **2005,** *102*, 16961-16966.
87. Leuschner, P. J.; Ameres, S. L.; Kueng, S.; Martinez, J., Cleavage of the siRNA passenger strand during RISC assembly in human cells. *EMBO reports* **2006,** *7*, 314-20.
88. Matranga, C.; Tomari, Y.; Shin, C.; Bartel, D. P.; Zamore, P. D., Passenger-strand cleavage facilitates assembly of siRNA into Ago2-containing RNAi enzyme complexes. *Cell* **2005,** *123*, 607-20.

89. Betancur, J. G.; Tomari, Y., Dicer is dispensable for asymmetric RISC loading in mammals. *RNA (New York, N.Y.)* **2012,** *18*, 24-30.
90. Khvorova, A.; Reynolds, A.; Jayasena, S. D., Functional siRNAs and miRNAs Exhibit Strand Bias. *Cell* **2003,** *115*, 209-216.
91. Schwarz, D. S.; Hutvagner, G.; Du, T.; Xu, Z.; Aronin, N.; Zamore, P. D., Asymmetry in the assembly of the RNAi enzyme complex. *Cell* **2003,** *115*, 199-208.
92. Schwarz, D. S.; Hutvagner, G.; Haley, B.; Zamore, P. D., Evidence that siRNAs function as guides, not primers, in the Drosophila and human RNAi pathways. *Molecular cell* **2002,** *10*, 537-48.
93. Weitzer, S.; Martinez, J., The human RNA kinase hClp1 is active on 3' transfer RNA exons and short interfering RNAs. *Nature* **2007,** *447*, 222-6.
94. Noland, C. L.; Ma, E.; Doudna, J. A., siRNA repositioning for guide strand selection by human Dicer complexes. *Molecular cell* **2011,** *43*, 110-21.
95. Gaynor, J. W.; Campbell, B. J.; Cosstick, R., RNA interference: a chemist's perspective. *Chemical Society reviews* **2010,** *39*, 4169-84.
96. Gagnon, K. T.; Corey, D. R., Argonaute and the nuclear RNAs: new pathways for RNA-mediated control of gene expression. *Nucleic acid therapeutics* **2012,** *22*, 3-16.
97. Jinek, M.; Doudna, J. A., A three-dimensional view of the molecular machinery of RNA interference. *Nature* **2009,** *457*, 405-12.
98. Frank, F.; Sonenberg, N.; Nagar, B., Structural basis for 5'-nucleotide base-specific recognition of guide RNA by human AGO2. *Nature* **2010,** *465*, 818-22.
99. Ma, J. B.; Yuan, Y. R.; Meister, G.; Pei, Y.; Tuschl, T.; Patel, D. J., Structural basis for 5'-end-specific recognition of guide RNA by the A. fulgidus Piwi protein. *Nature* **2005,** *434*, 666-70.
100. Liu, J.; Carmell, M. A.; Rivas, F. V.; Marsden, C. G.; Thomson, J. M.; Song, J. J.; Hammond, S. M.; Joshua-Tor, L.; Hannon, G. J., Argonaute2 is the catalytic engine of mammalian RNAi. *Science* **2004,** *305*, 1437-41.
101. Kraynack, B. A.; Baker, B. F., Small interfering RNAs containing full 2′-O-methylribonucleotide-modified sense strands display Argonaute2/eIF2C2-dependent activity. *RNA (New York, N.Y.)* **2006,** *12*, 163-176.
102. Soutschek, J.; Akinc, A.; Bramlage, B.; Charisse, K.; Constien, R.; Donoghue, M.; Elbashir, S.; Geick, A.; Hadwiger, P.; Harborth, J.; John, M.; Kesavan, V.; Lavine, G.; Pandey, R. K.; Racie, T.; Rajeev, K. G.; Rohl, I.; Toudjarska, I.; Wang, G.; Wuschko, S.; Bumcrot, D.; Koteliansky, V.; Limmer, S.; Manoharan, M.; Vornlocher, H. P., Therapeutic silencing of an endogenous gene by systemic administration of modified siRNAs. *Nature* **2004,** *432*, 173-8.
103. Ui-Tei, K.; Naito, Y.; Zenno, S.; Nishi, K.; Yamato, K.; Takahashi, F.; Juni, A.; Saigo, K., Functional dissection of siRNA sequence by systematic DNA substitution: modified siRNA with a DNA seed arm is a powerful tool for mammalian gene silencing with significantly reduced off-target effect. *Nucleic Acids Research* **2008,** *36*, 2136-2151.
104. Judge, A. D.; Robbins, M.; Tavakoli, I.; Levi, J.; Hu, L.; Fronda, A.; Ambegia, E.; McClintock, K.; MacLachlan, I., Confirming the RNAi-mediated mechanism of action of siRNA-based cancer therapeutics in mice. *The Journal of clinical investigation* **2009,** *119*, 661-73.
105. Ye, X.; Huang, N.; Liu, Y.; Paroo, Z.; Huerta, C.; Li, P.; Chen, S.; Liu, Q.; Zhang, H., Structure of C3PO and mechanism of human RISC activation. *Nature structural & molecular biology* **2011,** *18*, 650-7.

106. Muhonen, P.; Tennila, T.; Azhayeva, E.; Parthasarathy, R. N.; Janckila, A. J.; Vaananen, H. K.; Azhayev, A.; Laitala-Leinonen, T., RNA interference tolerates 2'-fluoro modifications at the Argonaute2 cleavage site. *Chemistry & biodiversity* **2007,** *4*, 858-73.
107. Martinez, J.; Tuschl, T., RISC is a 5' phosphomonoester-producing RNA endonuclease. *Genes & development* **2004,** *18*, 975-80.
108. Watts, J. K.; Corey, D. R., Silencing disease genes in the laboratory and the clinic. *The Journal of Pathology* **2012,** *226*, 365-379.
109. Geary, R. S., Antisense oligonucleotide pharmacokinetics and metabolism. *Expert opinion on drug metabolism & toxicology* **2009,** *5*, 381-91.
110. Egli, M.; Flavell, A.; Pyle, A. M.; Wilson, W. D.; Haq, S. I.; Luisi, B.; Fisher, J.; Laughton, C.; Allen, S.; Engels, J.; Blackburn, G. M.; Gait, M. J.; Loakes, D.; Williams, D. M., - *Nucleic Acids in Chemistry and Biology*. p - i.
111. Wan, W. B.; Seth, P. P., The Medicinal Chemistry of Therapeutic Oligonucleotides. *Journal of Medicinal Chemistry* **2016**.
112. Deleavey, G. F.; Watts, J. K.; Damha, M. J., Chemical Modification of siRNA. In *Current protocols in nucleic acid chemistry*, John Wiley & Sons, Inc.2009.
113. Williford, J. M.; Wu, J.; Ren, Y.; Archang, M. M.; Leong, K. W.; Mao, H. Q., Recent advances in nanoparticle-mediated siRNA delivery. *Annual review of biomedical engineering* **2014,** *16*, 347-70.
114. Juliano, R. L.; Ming, X.; Nakagawa, O., The chemistry and biology of oligonucleotide conjugates. *Accounts of chemical research* **2012,** *45*, 1067-76.
115. Lonnberg, H., Solid-phase synthesis of oligonucleotide conjugates useful for delivery and targeting of potential nucleic acid therapeutics. *Bioconjugate chemistry* **2009,** *20*, 1065-94.
116. Manoharan, M., Oligonucleotide conjugates as potential antisense drugs with improved uptake, biodistribution, targeted delivery, and mechanism of action. *Antisense & nucleic acid drug development* **2002,** *12*, 103-28.
117. Jackson, A. L.; Burchard, J.; Schelter, J.; Chau, B. N.; Cleary, M.; Lim, L.; Linsley, P. S., Widespread siRNA "off-target" transcript silencing mediated by seed region sequence complementarity. *RNA (New York, N.Y.)* **2006,** *12*, 1179-87.
118. Suter, S. R.; Sheu-Gruttadauria, J.; Schirle, N. T.; Valenzuela, R.; Ball-Jones, A. A.; Onizuka, K.; MacRae, I. J.; Beal, P. A., Structure-Guided Control of siRNA Off-Target Effects. *J Am Chem Soc* **2016,** *138*, 8667-8669.
119. Lee, H. S.; Seok, H.; Lee, D. H.; Ham, J.; Lee, W.; Youm, E. M.; Yoo, J. S.; Lee, Y. S.; Jang, E. S.; Chi, S. W., Abasic pivot substitution harnesses target specificity of RNA interference. *Nature communications* **2015,** *6*, 10154.
120. Jackson, A. L.; Burchard, J.; Leake, D.; Reynolds, A.; Schelter, J.; Guo, J.; Johnson, J. M.; Lim, L.; Karpilow, J.; Nichols, K.; Marshall, W.; Khvorova, A.; Linsley, P. S., Position-specific chemical modification of siRNAs reduces "off-target" transcript silencing. *RNA (New York, N.Y.)* **2006,** *12*, 1197-205.
121. Vaish, N.; Chen, F.; Seth, S.; Fosnaugh, K.; Liu, Y.; Adami, R.; Brown, T.; Chen, Y.; Harvie, P.; Johns, R.; Severson, G.; Granger, B.; Charmley, P.; Houston, M.; Templin, M. V.; Polisky, B., Improved specificity of gene silencing by siRNAs containing unlocked nucleobase analogs. *Nucleic Acids Res* **2011,** *39*, 1823-32.
122. Watts, J. K.; Deleavey, G. F.; Damha, M. J., Chemically modified siRNA: tools and applications. *Drug Discovery Today* **2008,** *13*, 842-855.

123. Marques, J. T.; Williams, B. R. G., Activation of the mammalian immune system by siRNAs. *Nat Biotech* **2005,** *23*, 1399-1405.
124. Kleinman, M. E.; Yamada, K.; Takeda, A.; Chandrasekaran, V.; Nozaki, M.; Baffi, J. Z.; Albuquerque, R. J.; Yamasaki, S.; Itaya, M.; Pan, Y.; Appukuttan, B.; Gibbs, D.; Yang, Z.; Kariko, K.; Ambati, B. K.; Wilgus, T. A.; DiPietro, L. A.; Sakurai, E.; Zhang, K.; Smith, J. R.; Taylor, E. W.; Ambati, J., Sequence- and target-independent angiogenesis suppression by siRNA via TLR3. *Nature* **2008,** *452*, 591-7.
125. Whitehead, K. A.; Dahlman, J. E.; Langer, R. S.; Anderson, D. G., Silencing or stimulation? siRNA delivery and the immune system. *Annual review of chemical and biomolecular engineering* **2011,** *2*, 77-96.
126. Takeda, K.; Akira, S., Toll-like receptors in innate immunity. *International immunology* **2005,** *17*, 1-14.
127. Judge, A.; MacLachlan, I., Overcoming the innate immune response to small interfering RNA. *Human gene therapy* **2008,** *19*, 111-24.
128. Krieg, A. M., CpG still rocks! Update on an accidental drug. *Nucleic acid therapeutics* **2012,** *22*, 77-89.
129. Hemmi, H.; Takeuchi, O.; Kawai, T.; Kaisho, T.; Sato, S.; Sanjo, H.; Matsumoto, M.; Hoshino, K.; Wagner, H.; Takeda, K.; Akira, S., A Toll-like receptor recognizes bacterial DNA. *Nature* **2000,** *408*, 740-5.
130. Judge, A. D.; Sood, V.; Shaw, J. R.; Fang, D.; McClintock, K.; MacLachlan, I., Sequence-dependent stimulation of the mammalian innate immune response by synthetic siRNA. *Nat Biotech* **2005,** *23*, 457-462.
131. Hornung, V.; Guenthner-Biller, M.; Bourquin, C.; Ablasser, A.; Schlee, M.; Uematsu, S.; Noronha, A.; Manoharan, M.; Akira, S.; de Fougerolles, A.; Endres, S.; Hartmann, G., Sequence-specific potent induction of IFN-[alpha] by short interfering RNA in plasmacytoid dendritic cells through TLR7. *Nature medicine* **2005,** *11*, 263-270.
132. Eckstein, F., Nucleoside phosphorothioates. *Annu Rev Biochem* **1985,** *54*, 367-402.
133. Eckstein, F., A dinucleoside phosphorothioate. *Tetrahedron Letters* **1967,** *8*, 1157-1160.
134. Eckstein, F., Phosphorothioate oligodeoxynucleotides: what is their origin and what is unique about them? *Antisense & nucleic acid drug development* **2000,** *10*, 117-21.
135. Sanghvi, Y. S., A Status Update of Modified Oligonucleotides for Chemotherapeutics Applications. In *Current protocols in nucleic acid chemistry*, John Wiley & Sons, Inc.2001.
136. Bennett, C. F.; Swayze, E. E., RNA targeting therapeutics: molecular mechanisms of antisense oligonucleotides as a therapeutic platform. *Annual review of pharmacology and toxicology* **2010,** *50*, 259-93.
137. Eckstein, F., Developments in RNA chemistry, a personal view. *Biochimie* **2002,** *84*, 841-8.
138. Guga, P.; Stec, W. J., Synthesis of Phosphorothioate Oligonucleotides with Stereodefined Phosphorothioate Linkages. In *Current protocols in nucleic acid chemistry*, John Wiley & Sons, Inc.2001.
139. Torrence, P. F.; Maitra, R. K.; Lesiak, K.; Khamnei, S.; Zhou, A.; Silverman, R. H., Targeting RNA for degradation with a (2'-5')oligoadenylate-antisense chimera. *Proceedings of the National Academy of Sciences of the United States of America* **1993,** *90*, 1300-1304.
140. Gryaznov, S. M., Oligonucleotide n3'-->p5' phosphoramidates and thio-phoshoramidates as potential therapeutic agents. *Chemistry & biodiversity* **2010,** *7*, 477-93.

141. Sheehan, D.; Lunstad, B.; Yamada, C. M.; Stell, B. G.; Caruthers, M. H.; Dellinger, D. J., Biochemical properties of phosphonoacetate and thiophosphonoacetate oligodeoxyribonucleotides. *Nucleic Acids Res* **2003,** *31*, 4109-18.
142. Corey, D. R.; Abrams, J. M., Morpholino antisense oligonucleotides: tools for investigating vertebrate development. *Genome biology* **2001,** *2*, Reviews1015.
143. Demidov, V. V.; Potaman, V. N.; Frank-Kamenetskii, M. D.; Egholm, M.; Buchard, O.; Sonnichsen, S. H.; Nielsen, P. E., Stability of peptide nucleic acids in human serum and cellular extracts. *Biochemical pharmacology* **1994,** *48*, 1310-3.
144. Chiu, Y. L.; Rana, T. M., siRNA function in RNAi: a chemical modification analysis. *RNA (New York, N.Y.)* **2003,** *9*, 1034-48.
145. Switzer, C. Y.; Moroney, S. E.; Benner, S. A., Enzymic recognition of the base pair between isocytidine and isoguanosine. *Biochemistry* **1993,** *32*, 10489-10496.
146. Bain, J. D.; Switzer, C.; Chamberlin, R.; Bennert, S. A., Ribosome-mediated incorporation of a non-standard amino acid into a peptide through expansion of the genetic code. *Nature* **1992,** *356*, 537-539.
147. Tor, Y.; Dervan, P. B., Site-specific enzymic incorporation of an unnatural base, N6-(6-aminohexyl)isoguanosine, into RNA. *J Am Chem Soc* **1993,** *115*, 4461-4467.
148. Strobel, S. A.; Cech, T. R.; Usman, N.; Beigelman, L., The 2,6-Diaminopurine Riboside.cntdot.5-Methylisocytidine Wobble Base Pair: An Isoenergetic Substitution for the Study of G.cntdot.U Pairs in RNA. *Biochemistry* **1994,** *33*, 13824-13835.
149. Musier-Forsyth, K.; Shi, J. P.; Henderson, B.; Bald, R.; Fuerste, J. P.; Erdmann, V. A.; Schimmel, P., Base-analog-induced aminoacylation of an RNA helix by a tRNA synthetase. *J Am Chem Soc* **1995,** *117*, 7253-7254.
150. Kamiya, H.; Kasai, H., Mutations Induced by 2-Hydroxyadenine on a Shuttle Vector during Leading and Lagging Strand Syntheses in Mammalian Cells. *Biochemistry* **1997,** *36*, 11125-11130.
151. Yang, X. L.; Sugiyama, H.; Ikeda, S.; Saito, I.; Wang, A. H., Structural studies of a stable parallel-stranded DNA duplex incorporating isoguanine:cytosine and isocytosine:guanine basepairs by nuclear magnetic resonance spectroscopy. *Biophysical journal* **1998,** *75*, 1163-71.
152. Seela, F.; Wei, C., Oligonucleotides Containing Consecutive 2′-Deoxyisoguanosine Residues: Synthesis, duplexes with parallel chain orientation, and aggregation. *Helvetica Chimica Acta* **1997,** *80*, 73-85.
153. Peacock, H.; Kannan, A.; Beal, P. A.; Burrows, C. J., Chemical Modification of siRNA Bases To Probe and Enhance RNA Interference. *The Journal of Organic Chemistry* **2011,** *76*, 7295-7300.
154. Herdewijn, P., Heterocyclic modifications of oligonucleotides and antisense technology. *Antisense & nucleic acid drug development* **2000,** *10*, 297-310.
155. Kawai, G.; Yamamoto, Y.; Kamimura, T.; Masegi, T.; Sekine, M.; Hata, T.; Iimori, T.; Watanabe, T.; Miyazawa, T.; Yokoyama, S., Conformational rigidity of specific pyrimidine residues in tRNA arises from posttranscriptional modifications that enhance steric interaction between the base and the 2'-hydroxyl group. *Biochemistry* **1992,** *31*, 1040-1046.
156. Nishizaki, T.; Iwai, S.; Ohtsuka, E.; Nakamura, H., Solution structure of an RNA.2'-O-methylated RNA hybrid duplex containing an RNA.DNA hybrid segment at the center. *Biochemistry* **1997,** *36*, 2577-85.

157. Ng, E. W. M.; Shima, D. T.; Calias, P.; Cunningham, E. T.; Guyer, D. R.; Adamis, A. P., Pegaptanib, a targeted anti-VEGF aptamer for ocular vascular disease. *Nat Rev Drug Discov* **2006,** *5*, 123-132.
158. Ikeda, H.; Fernandez, R.; Wilk, A.; Barchi, J. J., Jr.; Huang, X.; Marquez, V. E., The effect of two antipodal fluorine-induced sugar puckers on the conformation and stability of the Dickerson-Drew dodecamer duplex [d(CGCGAATTCGCG)]2. *Nucleic Acids Res* **1998,** *26*, 2237-44.
159. Viazovkina, E.; Mangos, M. M.; Elzagheid, M. I.; Damha, M. J., Solid-Phase Synthesis of 2′-Deoxy-2′-fluoro- β-D-Oligoarabinonucleotides (2′F-ANA) and Their Phosphorothioate Derivatives. In *Current protocols in nucleic acid chemistry*, John Wiley & Sons, Inc.2001.
160. Pallan, P. S.; Greene, E. M.; Jicman, P. A.; Pandey, R. K.; Manoharan, M.; Rozners, E.; Egli, M., Unexpected origins of the enhanced pairing affinity of 2'-fluoro-modified RNA. *Nucleic Acids Res* **2011,** *39*, 3482-95.
161. Manoharan, M., 2'-carbohydrate modifications in antisense oligonucleotide therapy: importance of conformation, configuration and conjugation. *Biochimica et biophysica acta* **1999,** *1489*, 117-30.
162. Morihiro, K.; Kasahara, Y.; Obika, S., Biological applications of xeno nucleic acids. *Molecular bioSystems* **2017,** *13*, 235-245.
163. Nauwelaerts, K.; Fisher, M.; Froeyen, M.; Lescrinier, E.; Aerschot, A. V.; Xu, D.; DeLong, R.; Kang, H.; Juliano, R. L.; Herdewijn, P., Structural characterization and biological evaluation of small interfering RNAs containing cyclohexenyl nucleosides. *J Am Chem Soc* **2007,** *129*, 9340-8.
164. Verbeure, B.; Lescrinier, E.; Wang, J.; Herdewijn, P., RNase H mediated cleavage of RNA by cyclohexene nucleic acid (CeNA). *Nucleic Acids Res* **2001,** *29*, 4941-7.
165. Fisher, M.; Abramov, M.; Van Aerschot, A.; Xu, D.; Juliano, R. L.; Herdewijn, P., Inhibition of MDR1 expression with altritol-modified siRNAs. *Nucleic Acids Res* **2007,** *35*, 1064-74.
166. Fisher, M.; Abramov, M.; Van Aerschot, A.; Rozenski, J.; Dixit, V.; Juliano, R. L.; Herdewijn, P., Biological effects of hexitol and altritol-modified siRNAs targeting B-Raf. *European journal of pharmacology* **2009,** *606*, 38-44.
167. Sabatino, D.; Damha, M. J., Oxepane nucleic acids: Synthesis, characterization, and properties of oligonucleotides bearing a seven-membered carbohydrate ring. *J Am Chem Soc* **2007,** *129*, 8259-8270.
168. Wang, J.; Verbeure, B.; Luyten, I.; Lescrinier, E.; Froeyen, M.; Hendrix, C.; Rosemeyer, H.; Seela, F.; Van Aerschot, A.; Herdewijn, P., Cyclohexene Nucleic Acids (CeNA): Serum Stable Oligonucleotides that Activate RNase H and Increase Duplex Stability with Complementary RNA. *J Am Chem Soc* **2000,** *122*, 8595-8602.
169. Alvarado-Urbina, G.; Sathe, G. M.; Liu, W. C.; Gillen, M. F.; Duck, P. D.; Bender, R.; Ogilvie, K. K., Automated synthesis of gene fragments. *Science* **1981,** *214*, 270-4.
170. Somoza, A., Protecting groups for RNA synthesis: an increasing need for selective preparative methods. *Chemical Society reviews* **2008,** *37*, 2668-2675.
171. Ogilvie, K. K.; Schifman, A. L.; Penney, C. L., The synthesis of oligoribonucleotides. III. The use of silyl protecting groups in nucleoside and nucleotide chemistry. VIII. *Canadian Journal of Chemistry* **1979,** *57*, 2230-2238.

172. Damha, M. J.; Giannaris, P. A.; Zabarylo, S. V., An improved procedure for derivatization of controlled-pore glass beads for solid-phase oligonucleotide synthesis. *Nucleic Acids Research* **1990,** *18,* 3813-3821.
173. Pon, R. T.; Damha, M. J.; Ogilvie, K. K., Modification of guanine bases by nucleoside phosphoramidite reagents during the solid phase synthesis of oligonucleotides. *Nucleic Acids Research* **1985,** *13,* 6447-6465.

CHAPTER 2: SEVEN-MEMBERED RING NUCLEOSIDE ANALOGS: STEREOSELECTIVE SYNTHESIS AND STUDIES ON THEIR CONFORMATIONAL PROPERTIES

2.1 Overview

This chapter describes the synthesis of a novel series of seven-membered ring nucleosides, with emphasis on the structural characterization of intermediates and target molecules. The key step in the presented synthetic approach is a stereoselective synthesis of an epoxide which is used as a common synthetic intermediate to prepare functionalized oxepane nucleoside derivatives. We also study the conformational landscape and preferred ring-puckering of selected oxepane nucleosides by NMR, X-ray crystallography, and quantum mechanical calculations. The results of these studies will be presented in the following sections.

2.2 Introduction

Nucleoside analogues, as previously described in chapter 1, are extremely valuable compounds in medicinal chemistry.[1, 2] Modification in the furanose moiety and its impact on the conformation and biological activity of nucleosides have been studied extensively.[3, 4] However, due to their more challenging accessibility, ring expanded derivatives have been considerably less explored. Hexose- and hexitol-based nucleosides are the most studied among this class and were first described by the Eschenmoser[5, 6] and Herdewijn[7, 8] groups respectively. In the hexitol series (**1**), the flexible furanose ring is replaced with a more rigid six-membered hexitol sugar and the position of the nucleobase is moved from the anomeric carbon to the 3′-position (**Figure 2.1**). Nucleic acids derived from hexitol nucleosides have been proven useful for incorporation into gene silencing oligonucleotides, biotechnology, and synthetic biology applications.[9]

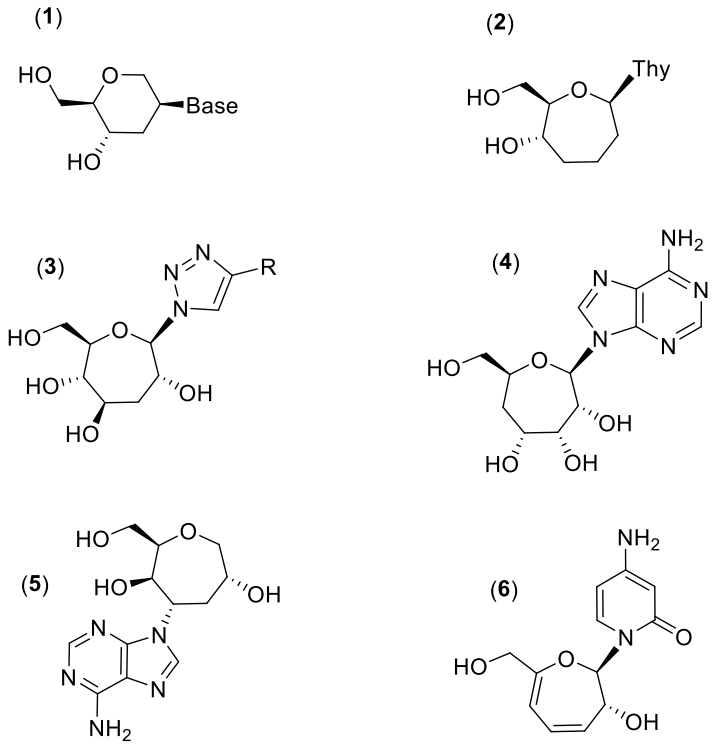

Figure 2.1 Expanding the nucleoside ring size, from five- membered, to 6-membered as in Hexitol (**1**)[7] andseven-membered as in first generation Oxepane (**2**)[10]. Other examples of nucleoside analogues previously reported in the literature (**3-6**).[11-14]

Seven-membered oxepane scaffolds are commonly found in natural products and biologically active molecules.[15-18] In the search for ring expanded DNA analogues, our lab recently reported the synthesis of the first generation of oxepane nucleoside (**Figure 2.1**), which was then incorporated into oligonucleotides, constructing Oxepane Nucleic Acids (ONA).[10] It was hypothesized that expanding the carbohydrate moiety of DNA to a seven-membered skeleton would provide conformationally more flexible sugars relative to the six-membered ring pyranose, thus better mimicking the conformation of natural 2′-deoxyribose. Indeed, ONA, like DNA oligonucleotides, represented a rare example of nuclease stable oligonucleotides based on a 7-membered sugar ring able to trigger, as natural DNA, the RNase H-mediated degradation of a complementary RNA strand.[10] Moreover, ONAs were able to bind to both DNA and RNA,

owing to the flexible nature of the oxepane sugar ring. Despite these unique properties, however, the low affinity towards RNA targets limits the use of first generation ONAs as gene silencing oligonucleotides. Following the work in our lab, a few more examples of oxepane nucleoside analogues (**Figure 2.1**) have been reported as potential glycosidase inhibitors (**3**),[11] antiviral agents (**4**[12] and **5**[13]), and unexpected byproducts of nucleoside syntheses (**6**).[14]

As part of our ongoing interest on the development of nucleosides with expanded sugar rings,[10, 19] we aimed to expand the library of novel oxepane-based nucleoside analogues as excellent candidates for biological screening and building blocks for gene silencing oligonucleotides.[20] Molecular modeling of the first generation oxepane nucleoside (**Figure 2.2**) suggested that even though this modification provides a more compact oligonucleotide structure that can, in principle, hybridize to DNA and, even more favorably, to the more compact C3'-*endo* geometry of RNA, some factors still limit its base-pairing potential with complementary DNA and RNA.[10] These limiting factors were anticipated as (a) the increased ring size of the oxepane ring, as observed with pyranose-based ONs,[21, 22] and (b) the relative orientation of the glycosidic bond (C1'-N1) with respect to the C5'-OH bond (**Figure 2.2**).[23]

To overcome the limitations faced with the first generation ONAs as gene silencing oligonucleotides, we focused our attention on the synthesis of novel nucleoside oxepane monomers that will allow placement of the phosphodiester backbone to positions C3' and C4'. This would, in principle, yield ONAs that closer mimic the natural DNA and RNA structures. As an alternative approach, we became also interested in synthesizing fluorinated derivatives of oxepane nucleosides, prompted by the conformational changes and stabilizing effects provided by 2'-FRNA and 2′-Fluoroarabino nucleic acid (FANA) in DNA:RNA and RNA:RNA duplexes.

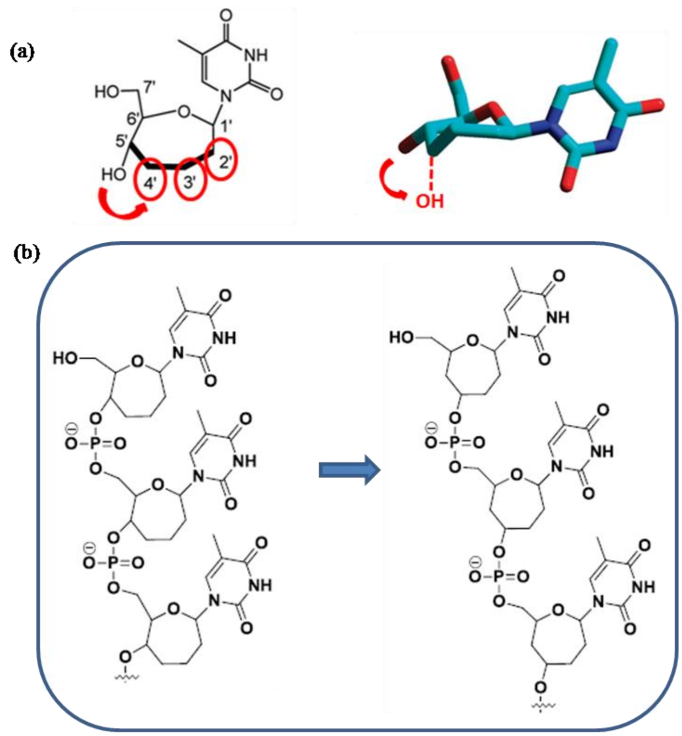

Figure 2.2 (a) Structure and conformation of first generation oxpeane nucleoside[10] (a) and oligonucleotide (b), and our strategy to move the phosphodiester linkage from 5' position closer to the glycosidic bond at the 1' position (4' position shown here, as an example).

The following sections describe our synthetic approach towards creating a common and versatile chiral synthetic intermediate used to generate more structurally diverse oxepane nucleosides. The conformation of some of the synthesized key analogues were assessed using X-ray crystallography, NMR, and theoretical (classical and quantum mechanical) calculations.

2.3 Synthesis and characterization of oxepane nucleosides

An efficient 5-step synthesis of oxepene **7** (**Scheme 2.1**) was previously described by David Sabatino, from our laboratory,[10] starting from commercially available tri-*O*-acetyl-D-glucal, and adapting the ring expansion strategy described by Hoberg *et al.*[24] The attractiveness of **7** is that its alkene functionality can be manipulated for the introduction of different functional groups in

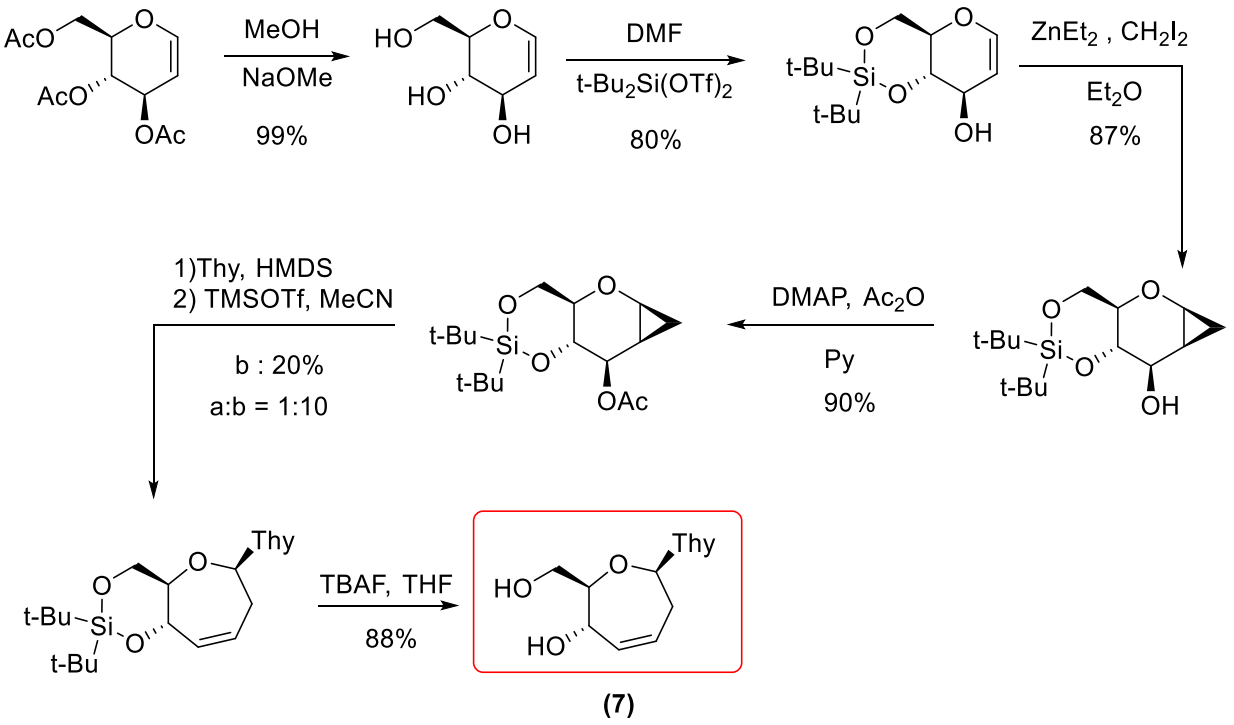

Scheme 2.1 Synthesis of oxepene precursor **(7)** by ring expansion method[10].

the seven-membered ring. For example, the access to a new series of functionalized oxepane nucleoside monomers was devised from an asymmetric epoxidation of **7**, enabling the diastereoselective installation of new stereocenters. Thus, we first focused on finding the best conditions for the stereoselective epoxidation of **7**.

2.3.1 Stereoselective synthesis of oxepane nucleoside (8)

We attempted to take advantage of the allylic alcohol to perform an asymmetric epoxidation. Thus, the silyl bridge of **7** was cleaved, before subjecting it to epoxidation with $VO(acac)_2$.[25] Under the experimental conditions, we observed rapid decomposition of the starting material. Classical oxidation of **7** with *m*CPBA in DCM was performed following a previously reported method,[26] affording a 2:1 α:β diastereomeric mixture of the epoxide in 50% yield. The two

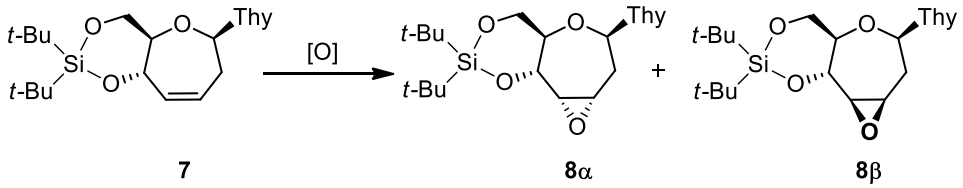

Figure 2.3 Stereoselective synthesis of oxepane nucleoside **(8)**.

isomers showed very similar polarity (TLC, $\Delta R_f < 0.1$) making it difficult to separate them by silica gel column chromatography (**Table 2.1**, Entry 1).

Next, we turned towards using a chiral catalyst to induce stereoselectivity. Jacobsen catalyst is an attractive candidate due to its ability to catalyze stereoselective epoxidations of unfunctionalized olefins.[27] When **7** was treated with 5 mol% (*S*,*S*) Jacobsen catalyst in a NaOCl/CH_2Cl_2 biphasic system, and in the presence of pyridine *N*-oxide, a 1:1.7 α:β diastereomeric mixture was obtained (**Table 2.1**, Entry 2). A significant improvement in stereoselectivity (d.e. 87%) was observed when the same reaction was carried out with the (*R*,*R*) Jacobsen catalyst (Sigma Aldrich; CAS# 138124-32-0) under the same conditions (**Table 2.1**, Entry 3). The reaction proceeded in better yields (58%) by increasing the catalyst loading to 10 mol% without any decrease in

Table 2.1 Epoxidation of protected oxepene 1 under different conditions.

entry	epoxidation reagent	cat. (mol %)	yield (%)	8α:8β[f]	de (%)
1[a]	*m*CPBA	-	50[d]	2:1	33
2[b]	(*S*,*S*) Jacobsen cat.	5	36[d]	1:1.7	26
3[b]	(*R*,*R*) Jacobsen cat.	5	34[e]	14:1	87
4[c]	(*R*,*R*) Jacobsen cat.	10	58[e]	14:1	87

Reaction conditions: [a]THF, 40 ° C, [b,c]NaOCl, DCM, 4-Phenyl Pyridine *N*-oxide ([b]20 mol %, [c]40 mol %), rt; [d]Crude epoxide yield (α + β); [e]Isolated yields for **8α**; [f]Ratio calculated by NMR in the isolated crude mixture.

stereoselectivity (**Table 2.1**, Entry 4). Traces of **8β** were removed by flash column chromatography. It is noteworthy that at this stage, the configuration of the epoxide ring was ambiguous as the NOESY NMR spectra did not show the expected key correlations. However, as will be explained in the following sections, subsequent formation of the anhydro oxepane **12** from **8α** (**Scheme 2.2**) allowed the assignment of stereochemistry at C3′-C4′.

2.3.2 Regio/stereoselective synthesis of trihydroxy oxepane nucleoside (10)

With the nucleoside **8α** in hand, the oxepane scaffold was then ready for diversification via epoxide opening to generate functionalized oxepane nucleosides. The reaction of **8α** with 10 equivalents of $LiEt_3BH$ at 0 ºC resulted in a completely stereo- and regioselective conversion to **9** in 36% yield, together with unreacted starting material (**Figure 2.4**). Additional equivalents of $LiEt_3BH$ did not increase the yield of the reaction and resulted in formation of base reduction products. Regioselective opening of epoxide **8α** can be explained by the possible coordination of $LiEt_3BH$ to the nucleobase and directing the attack of hydride to the proximal and less hindered C3′ position. Cleavage of the silyl protecting group afforded nucleoside **10** in 87% yield.

The structure of **9** was confirmed by COSY NMR in MeOD (**Figure 2.5**). The protons at C2' were easily assigned by $^3J_{HH}$ COSY correlations with the 1' proton. There were 2 protons (other than the H1') correlating with the 2' protons, indicating that the 3' position is a methylene (CH_2). It was inferred that the hydroxyl group is therefore, placed on the 4' position. Indeed, the 3'

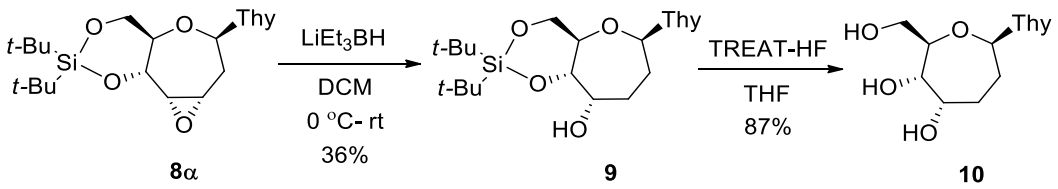

Figure 2.4 Regio/stereoselective synthesis of trihydroxy oxepane nucleoside **10**.

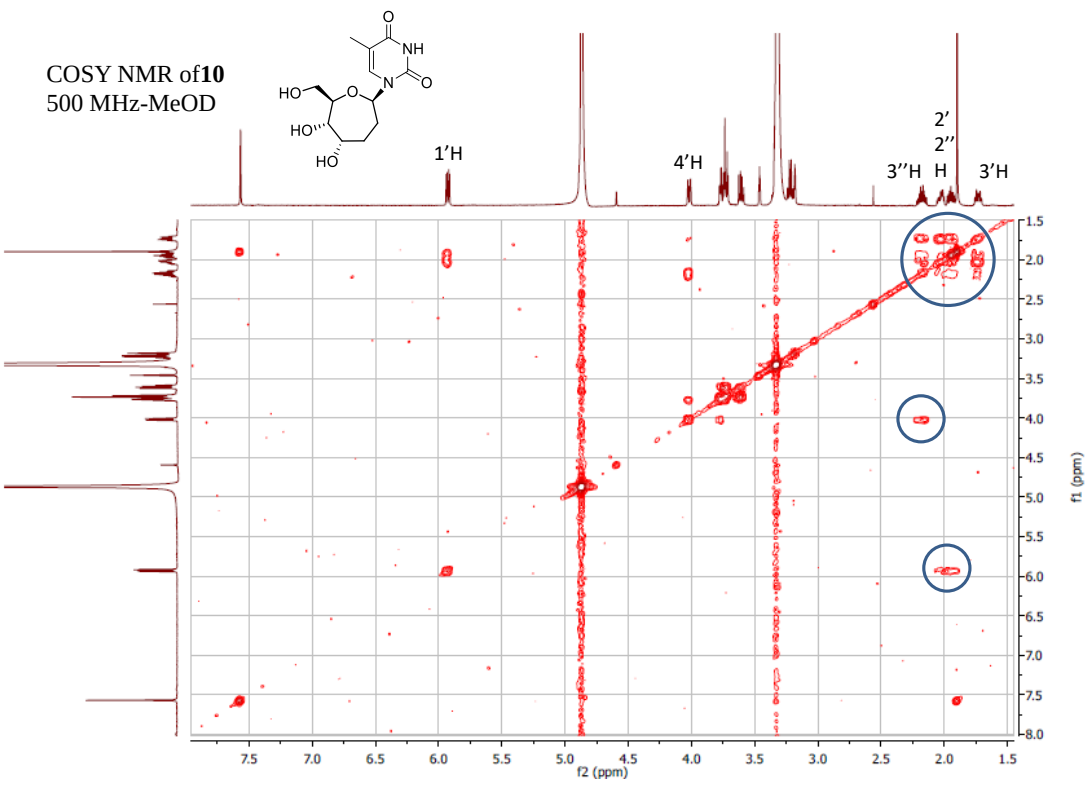

Figure 2.5 Regiochemistry of oxepane nucleoside **10** was assigned using the key $^{3}J_{HH}$ COSY correlations between 1', 2' and 2", 3' and 3", and 4' (circled).

protons were only correlating with one other proton, which was assigned as the 4' proton. The stereochemistry of the produced 4'OH was inferred to be (alpha), as in the starting material **8α**, since opening of the epoxide does not affect the stereochemistry at C4′.

2.3.3 Synthesis of azido oxepane nucleosides (13 and 14)

To further explore the scope of our strategy to synthesize structurally diverse oxepane nucleosides, diastereomerically pure **8α** was desilylated with triethylamine trihydrofluoride (TREAT-HF) in 90% yield to afford epoxide **11** that was then reacted with NaN_3 in DMF at 100 ºC and in the presence of 15-crown-5 (**Scheme 2.2**). Unlike the hydride reduction described above for protected nucleoside **8α**, the azidation reaction of **11** resulted in a 1:2.3 mixture of **13**

and **14** in 70% combined yield. The regioselectivity and yield of this step dropped significantly when azidation was carried out on **8α** instead. The position of the azide group in both **13** and **14** regioisomers was determined by a combination of COSY NMR experiments (solvent DMSO-d_6) which showed a correlation of the produced hydroxyl protons to their corresponding sugar C-H position, and (**Figure 2.6** and **Figure 2.7**).

The configuration at C3' (compound **14**) and C4' (compound **13**) was assessed by NOESY experiments. A clear correlation between H6 of the nucleobase and H3′ was observed for compound **14**, suggesting the β configuration of H3′ (**Scheme 2.2** and **Figure 2.7**). In the case of regioisomer **13**, a rather faint correlation between H4′ and H6 confirmed a *cis* relative orientation between the thymine and H4′. A stronger correlation, in this compound, was seen between H3' and H2'α, which was in agreement with our proposed structure for regioisomer **13** (**Scheme 2.2** and **Figure 2.6**).

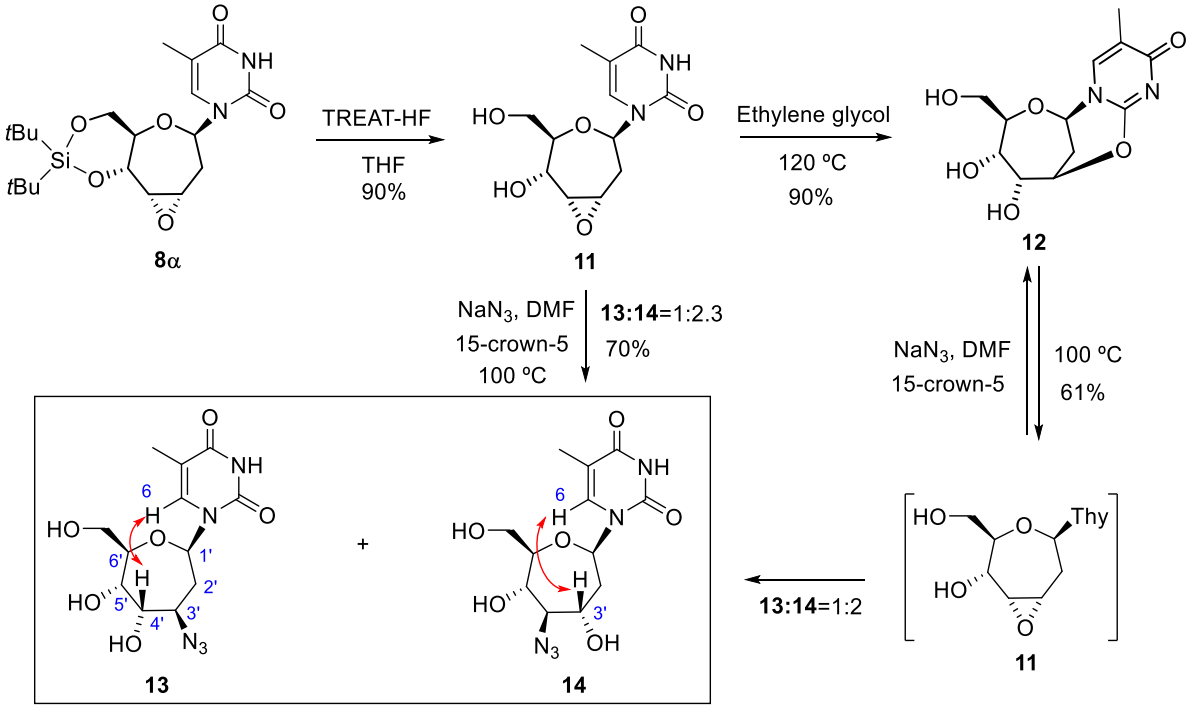

Scheme 2.2 Synthesis of azido (**13, 14**) and anhydro (**12**) oxepane nucleosides. Key NOE correlations in **13** and **14** are represented with red arrows.

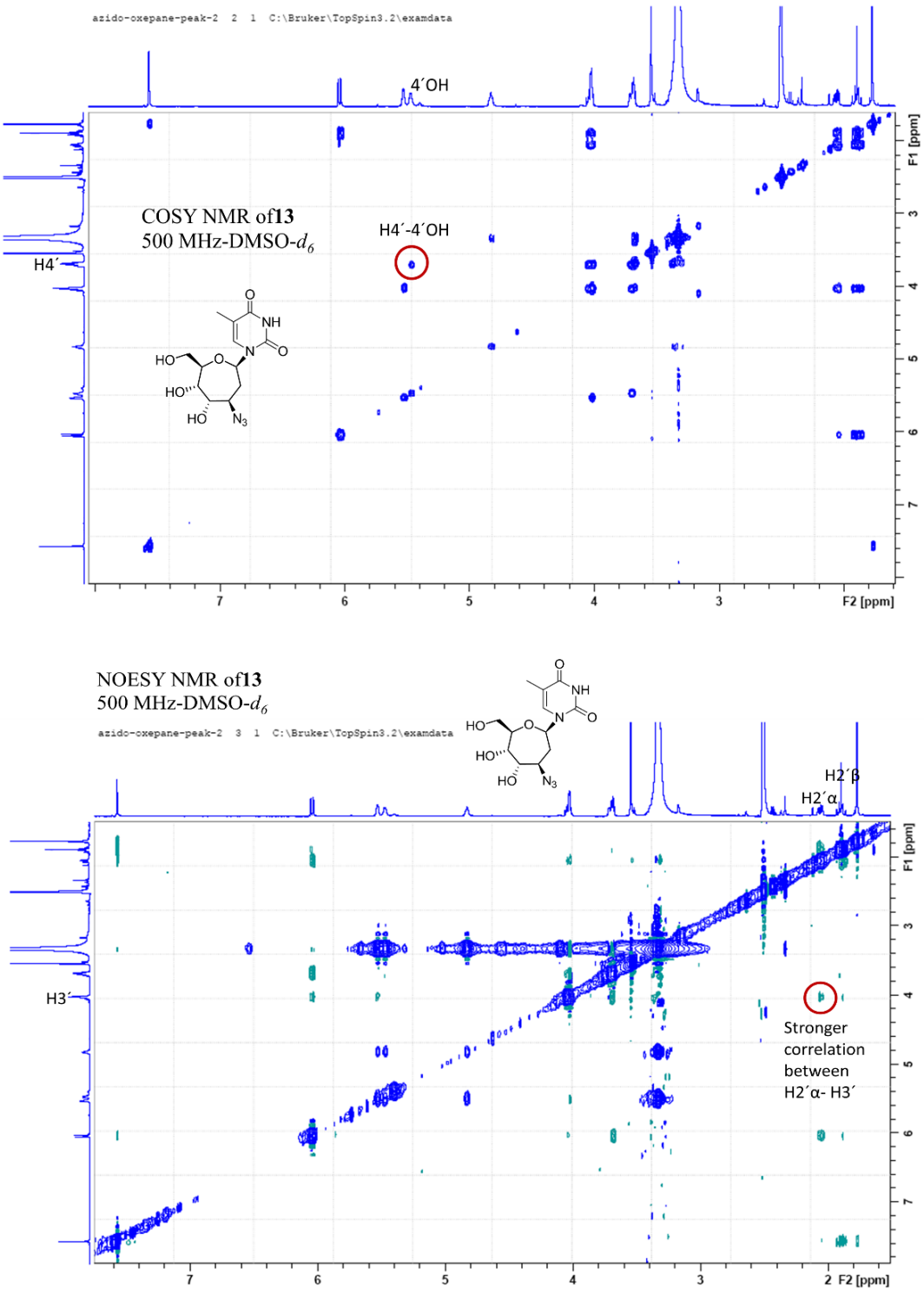

Figure 2.6 2D COSY and NOESY NMR experiments were performed in DMSO-d_6 to assess the structure of nucleoside analogue **13**. Key cross peaks are circled.

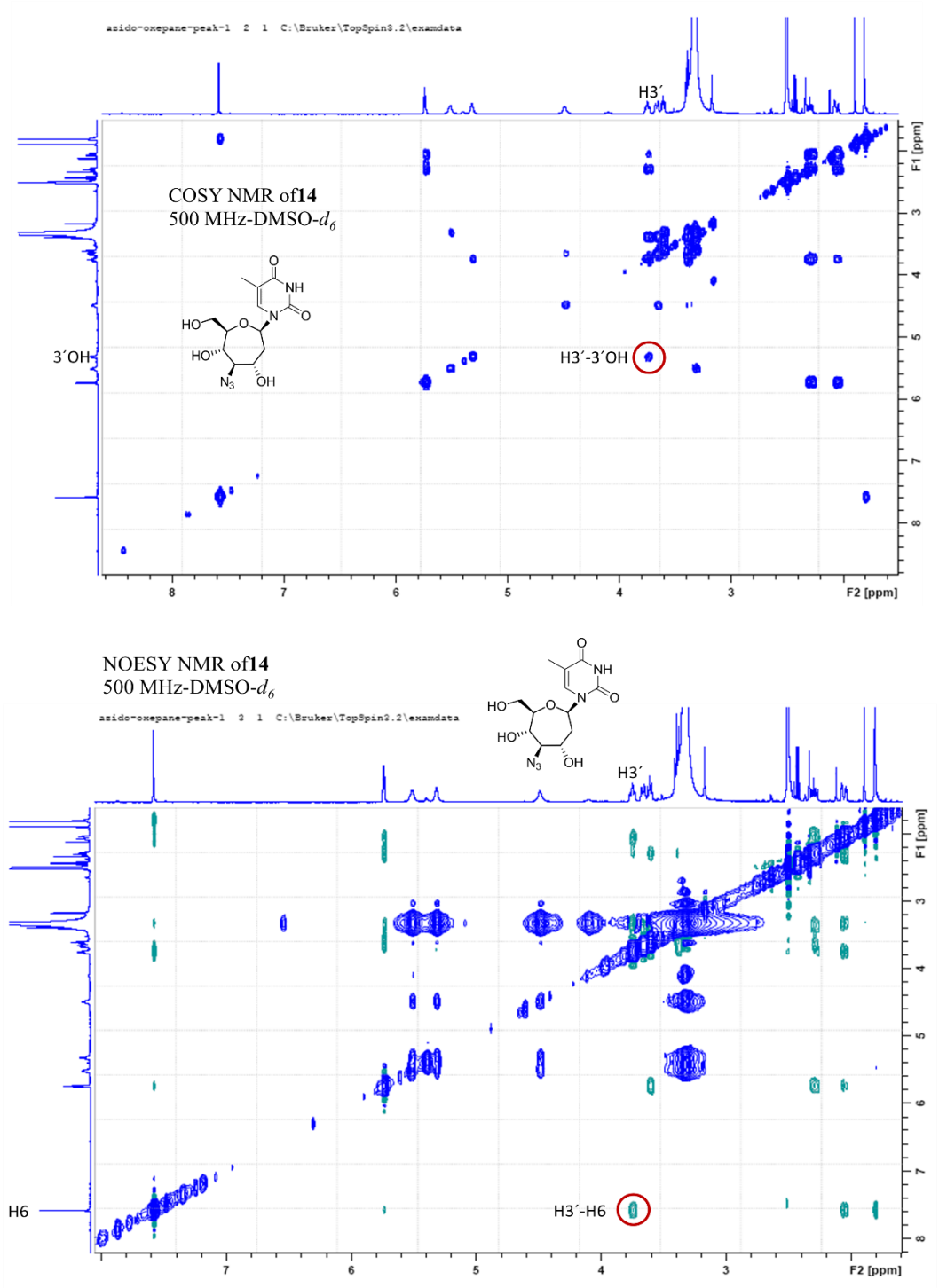

Figure 2.7 COSY and NOESY NMR experiments were performed in DMSO-d_6 to assess the structure of nucleoside analogue **14**. Key cross peaks are circled.

2.3.4 Attempted synthesis of fluorinated oxepane nucleosides. (12)

Based on our long-term interest in fluorinated nuclosides in our lab, we also took interest in fluorinated oxepanes, hoping that fluorination can have a positive influence on the sugar conformation (i.e. better ONA duplex binding properties).

Reaction of epoxide **11** with NaF/KHF_2 in ethylene glycol at 120 ºC did not produce the desired C3′/C4′-fluorinated nucleosides; instead, it afforded anhydro nucleoside **12** in high yield (**Scheme 2.2**). When **11** was heated in the absence of the fluoride salts, it afforded, again, the anhydro nucleoside **12** in the same yield, suggesting that NaF/KHF_2 has no role in this transformation. The identity, stereochemistry, and conformation of anhydro nucleoside **12** were unambiguously assigned by single crystal X-ray diffraction (**Figure 2.8**). Within the bicyclic structure, the oxepane ring adopts a chair-like conformation in which the hydroxymethyl group and 5′-OH are equatorial, while the thymine base and the 4′-OH group are pseudoaxial (**Figure 2.8**). Next, we attempted to open the anhydro compound directly with HF-py (obtained commercially from Sigma-Aldrich). To our surprise, we consistently obtained the corresponding chlorinated nucleoside **15** (80-85 % yield). Clearly the HF solution was contaminated with a

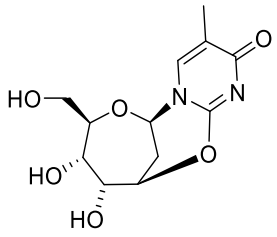

12

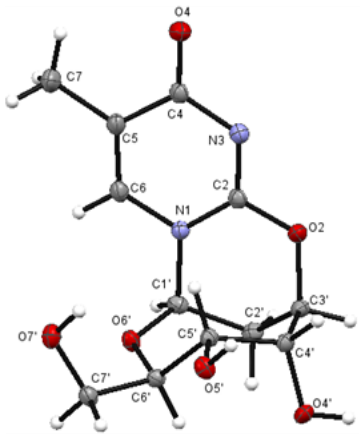

Figure 2.8 Crystal structure of nucleoside **12**.

chloride source (likely HCl-py). Despite our attempts to obtain higher purity HF-py from other commercial providers (Alfa Aesar, Sigma Aldrich, and Acros Organics) we were, still, unable to obtain the desired fluorinated nucleoside from **12**, and, instead, obtained the chlorinated nucleoside **15**. It is noteworthy that ^{1}HNMR tracking of our fluorination trials showed evidence for formation of small traces of a fluorinated product (<10%). Future work on this project is focused on investigating alternative fluorination methods in order to obtain fluorinated oxepane nucleosides.

2.3.5 Stereoselective synthesis of chloro oxepane nucleoside (15)

Given the above, and the recent discovery of chlorinated nucleoside analogues with promising biological activity, [28, 29] we next turned our attention to the direct chlorine functionalization of compound **12**, this time using HCl-py as the chloride source (Sigma Aldrich). Reaction of **12** with HCl-Py in DMF (23 °C, 12 hrs) provided the same chlorinated nucleoside analogues **15** with complete stereoselectivity in 88% yield (**Figure 2.9**). This product was identical to the one obtained during the attempted fluorination, and its structure was corroborated via COSY and NOESY NMR experiments.

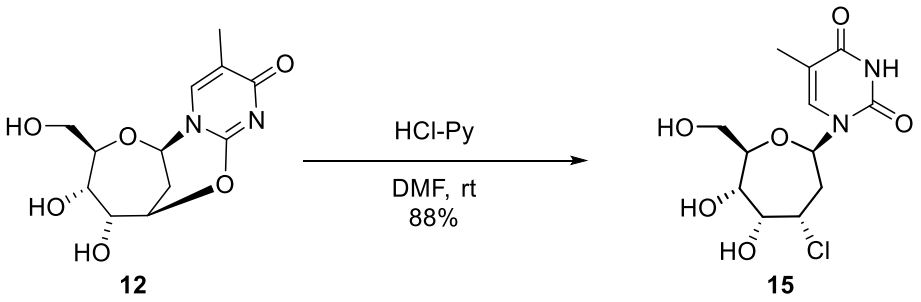

Figure 2.9 Synthesis of chloro oxepane nucleoside **15**.

2.3.6 Mechanistic studies regarding the synthesis of azide oxepane nucleosides (13 and 14)

Given the success with the regio- and stereo- selective synthesis of chloro oxepane **15** via opening of the anhydro ring, direct azidation of anhydro oxepane **12** was attempted (**Scheme 2.2**). Interestingly, this reaction produced a regioisomeric mixture of **13** and **14**, in a ratio similar to that observed during the azidation of epoxide **11**. As previously reported for furanose nucleosides,[30] we hypothesize that anhydo **12** equilibrates to epoxide **11** under these conditions, and that **11** is the direct precursor of **13** and **14** (**Scheme 2.2**). To further study the mechanism of this reaction, **12** was dissolved in DMF-d_6 in the absence of NaN_3 and crown ether, to see whether **12** would equilibrate to a mixture of **11** + **12**. After heating for 3 h at 100 °C in an NMR tube, no changes were observed in the ^{1}H-NMR spectrum (5% detection limit), suggesting that if present under the azidation conditions, the epoxide reacts rapidly to give **13** and **14**.

2.4 Conformational analysis of oxepane nucleosides 10 and 11

With this set of oxepane nucleosides in hand, we next studied the conformations of nucleosides **10** and **11** in collaboration with Dr. Guillem Portella (Cambridge University, UK).

The ring pucker of seven-membered ring systems can be described as a combination of boat/twist-boat (B/TB) and chair/twist-chair (C/TC) pseudorotational spaces.[31, 32] This was first assessed by molecular dynamics simulations coupled to a metadynamics enhanced sampling scheme[33] (details in experimental section). The most stable conformations were further minimized using quantum mechanical density functional theory calculations at the M062x/6-31+G(d,p) level using parameters of MeOH as a solvent (details in experimental section). The lowest energy states for epoxide **11** corresponded to a chair-like conformation, in which all the substituents assume a pseudo-equatorial disposition to alleviate steric interactions (**Figure 2.10a**). The differences in stability amongst the lowest energy states are due to small variations

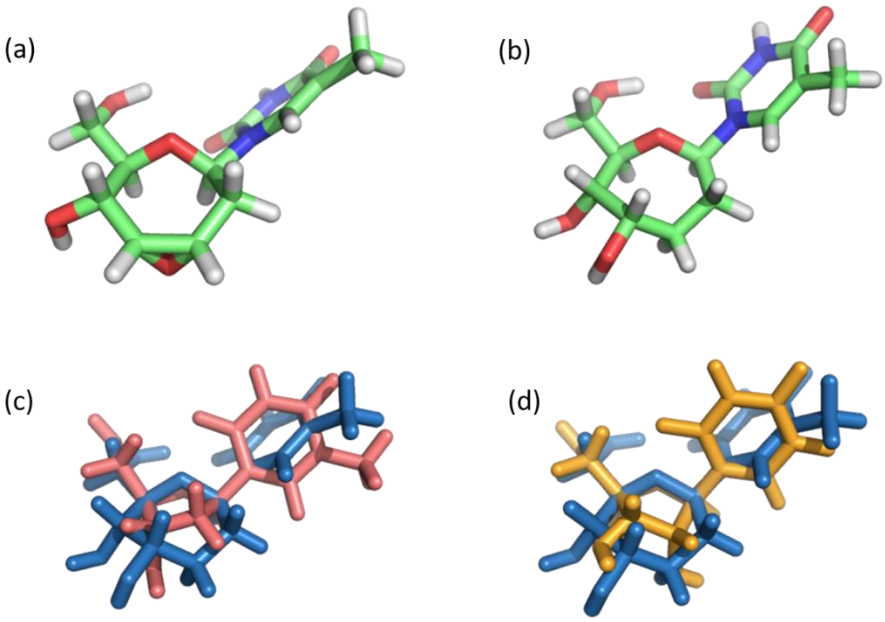

Figure 2.10 Lowest energy conformations of (a) **11** and (b) **10**. Derivative **10** is a mixture of boat and twisted boat conformations, and **11** is found exclusively in the chair conformation. Supersposition of **10** (blue) with (c) C2′-endo thymidine (red) and (d) C3′-endo uridine (orange).

in the orientation of the thymine and hydroxymethyl substituents, meanwhile the sugar pucker remains almost invariable. The lowest energy states for the alcohol derivative **10** are mixtures of twisted-chair and boat conformations (~65% and ~35% respectively) (**Figure 2.10b**). The main differences among low energy states are also in this case due to small variations in the orientation of the substituents causing very minor variations in the sugar conformation (more information in the experimental section).

Finally, to assess the validity of the calculated structures, $^{3}J_{HH}$ values from ^{1}H-NMR coupling constant analysis in MeOH-d_4 of **10** and **11** were compared to theoretical $^{3}J_{HH}$ values estimated from the computed low energy conformers (**Table 2.2**, details in experimental section). For **11**, there was sufficient spectral resolution of all the resonances so that coupling constants could be easily extracted from the spectra. In the case of **10**, the multiplets of the H2′ and H3′ resonances prevented the extraction of the coupling constants between these protons.

In general, there was good correspondence between calculated and observed $^3J_{HH}$, supporting the accuracy of the conformations provided by computation. The H1′ splitting pattern in both **10** and **11** are consistent with the pseudo-equatorial orientation of the pyrimidine base. **Figure 2.10 c** and **d** compare the three-dimensional structure of compound **10** to the natural nucleosides (dT and rU), by superposition of the structures. When the bases are aligned, the pseudoequatorial C4′-OH bond in **10** superimposes rather well with the pseudoequatorial C3′-OH bond of uridine (shown in the favoured C3′-endo conformation), suggesting that 4′,6′-linked oligomers of **10** may conform to the structure of natural nucleic acids (*e.g.*, RNA).

Table 2.2 Calculated and experimental $^3J_{H,H}$ coupling constants (±0.2 Hz) for **10** and **11**

coupling constant	calcd **10**[a]	exptl **10**[b]	calcd **11**[a]	exptl **11**[b]
$^3J_{1',2'}$	11.0	10.0	10.1	10.5
$^3J_{1',2''}$	2.3	3.4	0.7	2.4
$^3J_{2',3'}$	1.7	-	0.3	0
$^3J_{2'',3'}$	12.3	-	5.7	4.5
$^3J_{2',3''}$	6.0	-	NA	NA
$^3J_{2'',3''}$	2.5	-	NA	NA
$^3J_{3'',4'}$	1.0	2.0	NA	NA
$^3J_{3',4'}$	9.9	9.8	4.0	4.7
$^3J_{4',5'}$	4.2	2.5	0.6	0
$^3J_{5',6'}$	7.9	5.7	9.1	9.6

[a] Values calculated using GIAO/B3LYP/*aug*-cc-pVDZ methodology on optimized structures, averaged based on their Boltzmann population. [b] Observed coupling constants from ^{1}H-NMR experiments in MeOH-d_4.

2.5 Conclusion and future work

In summary, several novel oxepane nucleosides were prepared from a diastereomerically pure epoxide, as a common intermediate. This epoxide (compound **11**) was obtained by a stereoselective oxidation of alkene **7**. Stereo- and regioselective addition of hydride to epoxide **11** afforded trihydroxy oxepane **10**. Azidation of epoxide **11** results in formation of azido oxepanes **13** and **14**. These nucleosides were also accessed by reaction of Anhydro nucleoside **12** and sodium azide, which we hypothesize it proceeds via the epoxide derivative, *i.e.*, **12** → **11** → (**13**+**14**). Finally, chlorination of anhydro **12** results in the formation of regio- and stereo- pure chloro oxepane **15**. Computational and NMR studies suggest that **10** and **11** adopt a chair conformation with the pyrimidine base adopting a pseudo-equatorial orientation. We expect this new series of ring expanded nucleic acid analogs to be useful as building blocks for new functional genetic systems and gene silencing oligonucleotides. Current work in our group focuses on synthesizing these and other oxepane analogs more efficiently, and in larger quantities for incorporation into oligonucleotides.

2.6 Experimental methods

2.6.1 General remarks

When needed, reactions were carried out in over-dried glassware and under argon atmosphere. All reagents were of highest commercial purity and were purchased from Sigma-Aldrich and used without further purification. Jacobsen epoxidation catalysts were purchased from Strem Chemicals and stored under argon atmosphere. Sodium hypochlorite solution (14.5% available chlorine) was purchased from Alfa Aesar. Solvents were dried with standard procedures prior to use. Thin-layer chromatography (TLC) was performed to monitor reactions and visualized with a solution of 10% H_2SO_4 in MeOH and/or UV light. Flash chromatography was performed with

silica gel 60 (40−63μm). Spectroscopic ^{1}H and ^{13}C NMR, MS, and/or analytical data were obtained using chromatographically homogeneous samples. ^{1}H and ^{13}C NMRs were obtained using 400, 500 and 800 MHz instruments for ^{1}H and 125 MHz for ^{13}C. The same spectrometers were used for the acquisition of $^{1}H–^{1}H$ homonuclear (COSY and NOESY) and ^{1}H-^{13}C heteronuclear (HSQC) correlations. High-resolution mass spectra (HRMS) were recorded on a mass spectrometer under electron spray ionization (ESI) conditions.

2.6.2 Synthesis of oxepene precursor (7)

Compound **7** and the corresponding deprotected analogue were prepared according to a previously reported literature procedure in 5 steps.[10]

2.6.3 Synthesis of 1- [(5S,6R)-2,3,4-trideoxy-5-hydroxy-7-hydroxymethyl)-β-oxepanyl] thymine (8α).

A solution of **7** (239 mg, 0.585 mmol) and 4-phenylpyridine *N*-oxide (20.0 mg, 20 mol%) in CH_2Cl_2 (4 mL) was cooled down to 0° C in an ice bath, before the (*R*,*R*)-Jacobsen's catalyst (37.2 mg, 10 mol%) was added. Buffered bleach solution was prepared in a different flask by adding a solution of 0.05 M Na_2HPO_4 (2.5 mL) to 6.25 mL of the sodium hypochlorite solution. The pH of the resulted solution was adjusted to pH 11.3 by addition of a 1M NaOH solution. 5 ml of the bleach buffer was cooled down in an ice bath and was added to the cooled solution in the first flask. The biphasic solution was vigorously shaked for 48 h at room temperature. After completion of the reaction, EtOA (20 mL) was added to the reaction and the organic phase was separated and evaporated to dryness. The obtained solid was filtered over a small bed of silica gel using 50% MeOH/ CH_2Cl_2 as eluent to remove the catalyst. Fractions containing the product were collected, solvents were evaporated and the resulting residue was purified by column

chromatography (1% MeOH/ DCM) to afford **8α** (pure α-anomer: 99.4 mg, 58%) as a white foam. R_f (5% MeOH/ CH_2Cl_2): 0.37

^{1}H NMR (CD_3OD, 500 MHz) δ 7.44 (d, 1H, H6, *J*= 1.0),5.75 (dd, 1H, H1′, *J*= 2.0, *J*= 11.0),4.33 (d, 1H, H5′, *J*= 9.0),4.05 (dd, 1H, H7″, *J*= 10.5, *J*= 5.5), 3.79 (t, 1H, H7′, *J* = 10.5), 3.72 (m, 1H,H6′), 3.40 (d, 1H, H4′, *J* = 4.5), 3.36 (t, 1H, H3′, *J* = 4.5), 2.54 (dd, 1H, H2′, *J* = 11.0, *J* = 15.2), 2.43 (ddd, 1H, H2″, *J* = 1.5, *J* = 5.0, *J* = 15.2), 1.86 (s, 3H, CH_3), 1.06 (s, 9H, ^{t}Bu), 1.02 (s, 9H, ^{t}Bu).**^{13}C NMR** (CD_3OD, 125 MHz)δ164.8,150.6,136.2, 110.5, 81.8, 75.9, 73.1, 66.1, 60.6, 52.0, 32.8, 26.5 (3C), 26.1 (3C), 22.1, 19.6, 10.9.**HRMS**: *m/z* [M+Na] calculated for $C_{20}H_{32}N_2NaO_6Si$: 447.1922. Found: 447.1914.

Other spectroscopic information provided: COSY and NOESY NMR in $CDCl_3$.

2.6.4 Epoxidation procedure using *m*CPBA.

7 (167 mg, 0.409 mmol) in THF (2ml) was dissolved in 2 ml of THF, before *m*CPBA (77%, 137.5 mg, 0.6136 mmol) was added to it. Reaction was warmed up to 40° C and allowed to stir for 8 hours. Reaction was followed by TLC and stopped by evaporating the THF and purifying the residue with column chromatography (1-5%MeOH/ DCM) to afford an inseparable mixture of **8α** and **8β** (α/β= 2/1, total yield: 86.8 mg, 50%) as a white foam. R_f (10% MeOH/ CH_2Cl_2): 0.53

2.6.5 1-[(4S,5R,6R)-2,3-dideoxy-4-hydroxy-5,7-di-tert-butylsilanediyl)-β-oxepanyl] thymine (9)

Compound **8α** (62.5 mg, 0.147 mmol) was coevaporated with pyridine and kept under vacuum overnight prior to reaction. Solution of **8α** in anhydrous THF (5 mL) at 0° C was treated with 1 M solution of $LiEt_3BH$ (1.4 mL, 1.4 mmol) in THF under argon atmosphere. The reaction

mixture was stirred for 17 hours at room temperature. After completion, the reaction was quenched by addition of 5% acetic acid solution (2.34 mL), followed by purging the flask with argon for 30 minutes. THF was evaporated under vacuum and the obtained residue was directly purified by column chromatography to obtain **9** (22.6 mg, 36%) as a white solid. R_f (5% MeOH/ CH_2Cl_2): 0.34.

H NMR ($CDCl_3$, 500 MHz) δ 8.18 (bs, 1H, NH), 7.12 (s, 1H, H6), 5.96 (t, 1H, H1′, J= 6.1), 4.12 (m, 1H, H4′), 3.82 (m, 1H, H6′), 3.78 (m, 3H, H5′,H7′, H7″), 2.65 (bs, 1H, H4′-OH), 2.48 (m, 1H, H2′), 2.06 (m, 1H, H3′), 1.90 (s, 3H, CH_3), 1.74 (m, 2H, H2″, H3″), 1.02 (s, 9H, ^{t}Bu), 0.98 (s, 9H, ^{t}Bu). **HRMS:***m/z* [M+Na] calculated for $C_{20}H_{34}N_2NaO_6Si$: 449.2078. Found: 449.2067.

Other spectroscopic information provided: COSY NMR in $CDCl_3$ (showing the 4´OH connectivity), ^{1}H NMR in MeOD.

2.6.6 1- [(4S,5R,6R)-(2,3-dideoxy -4,5-dihydroxy-6-hydroxymethyl)-β-oxepanyl] thymine (10)

Compound **9** (22.6 mg, 0.053 mmol) was coevaporated with pyridine and kept under vacuum overnight prior to the reaction. The solution of **9** in anhydrous THF (2 mL) was then treated with TREAT-HF solution (20.1 μL, 0.122 mmol) at room temperature and was left for stirring for 8 hours under argon atmosphere. After completion, the reaction was quenched by addition of 10 μL of Milli-Q water.The mixture was evaporated under vacuum and the obtained residue was purified by column chromatography (2-8% MeOH/ CH_2Cl_2) to afford **10** (13.2 mg, 87%) as a white solid. R_f (15% MeOH/ CH_2Cl_2): 0.18.

^{1}H NMR (CD_3OD, 500 MHz) δ 7.56 (d, 1H, H6, J= 1.1), 5.93 (dd, 1H, H1′, $J_{1',2''}$= 3.4, $J_{1',2''}$= 10.0), 4.02 (dt,1H, H4′, $J_{4',3'}$= 9.8, $J_{4',3''}$= 2.0, $J_{4',5''}$= 2.5),3.71-3-78 (m, 3H, H5′, H6′, H7″), 3.61

(dd, 1H, H7′, $J_{7',7''}$= 12.5, $J_{7',6'}$ = 7.2), 2.17 (m, 1H, H3′), 2.03 (m, 1H, H2′), 1.94 (m, 1H, H2″), 1.90 (s, 3H, CH_3), 1.73 (m, 1H, H3″). **^{13}C NMR** (CD_3OD, 125 MHz) δ150.7, 136.7, 109.8, 84.9, 83.8, 74.1, 71.4, 63.1, 30.5, 25.7, 10.9. **HRMS:** *m/z* [M+Na] calculated for $C_{12}H_{18}N_2NaO_6$: 309.1057. Found: 309.1061.

Other spectroscopic information provided: COSY NMR in MeOD, HSQC, and NOESY NMR in DMSO-d_6.

2.6.7 1- [(3R,4S,5R,6R)-2-deoxy-3,4-epoxy- 5-hydroxy-6-hydroxylmethyl)-β-oxepanyl] thymine (11)

Compound **8α** (132 mg, 0.310 mmol) was coevaporated with pyridine and kept under vacuum overnight prior to the reaction. The solution of **8α**in anhydrous THF (3 mL) was then treated with TREAT-HF solution (56 μL, 0.342 mmol) at room temperature and the mixture was allowed to react for 3 hours under argon atmosphere. After completion, the reaction was quenched with 20 μL of Milli-Q water, the mixture was evaporated under vacuum and the obtained residue was purified by column chromatography (2-8% MeOH/ CH_2Cl_2) to afford **11** (79 mg, 90%) as a white solid. R_f (10% MeOH/ CH_2Cl_2): 0.24.

^{1}H NMR (CD_3OD, 500 MHz) δ 7.53 (d, 1H, H6, *J*= 1.0), 5.70 (dd, 1H, H1′, $J_{1',2''}$= 2.5, $J_{1',2''}$= 10.5), 3.98 (d, 1H, H5′, $J_{5',6'}$= 9.7), 3.83 (dd, 1H, H7′, $J_{6',7'}$= 2.3, $J_{7',7''}$ = 11.9), 3.63 (dd, 1H, H7″, $J_{7',7''}$= 11.9, $J_{7'',6'}$ = 5.7), 3.52 (ddd, 1H, H6′, $J_{6',7'}$ = 2.4, $J_{6',7''}$= 11.9, $J_{6',5'}$ = 9.6), 3.35 (d, 1H, H4′, $J_{4',3'}$ = 4.7), 3.33 (t, 1H, H3′, $J_{3',4'}$ = 4.5, $J_{3',2'}$ = 4.5), 2.48 (dd, 1H, H2″, $J_{2'',1'}$= 10.5, $J_{2'',2'}$= 14.7), 2.44 (ddd, 1H, H2′, $J_{1',2'}$= 2.5, $J_{2',3'}$= 4.5, $J_{2',2''}$= 14.9),1.90 (s, 3H, CH_3).**^{13}C NMR** (CD_3OD, 125 MHz) δ 165.0 (Base CO), 150.5 (Base CO), 136.7 (C6), 110.1 (C5), 82.0 (C1′), 80.3 (C6′), 68.3

(C5′), 62.4 (C7′), 60.7 (C4′), 52.8 (C3′), 33.4 (C2′), 10.9 (C5-CH_3). **HRMS:** *m/z* [M+Na] calculated for $C_{12}H_{16}N_2NaO_6$: 307.0901. Found: 307.0893.

Other spectroscopic information provided: COSY, NOESY, and HSQC NMR

2.6.8 1-[(3R,4S, 5R, 6R)- (1,3-anhydro- 3- deoxy- 4,5-dihydroxy- 6-hydroxymethyl) -β-oxepanyl] thymine (12)

Compound **11** (41 mg, 0.144 mmol) was dissolved in dry ethylene glycol (1.5 ml) and was then heated to 120 °C for 2 hours. Reaction was monitored by TLC and was stopped when all the starting material had reacted. Ethylene glycol was coevaporated with toluene and the resulting residue was purified by column chromatography (5-10% MeOH/ CH_2Cl_2) to yield pure **12** as a white solid (39 mg, 0.137 mmol, 95%). R_f (20% MeOH/ CH_2Cl_2): 0.18.

^{1}H NMR (CD_3OD, 500 MHz) δ 7.54 (d, 1H, H6, J= 1.0), 5.64 (d, 1H, H1′, $J_{1',2'}$= 3.0), 4.79 (dd, 1H, H3′, $J_{3',4'}$= 4.5, $J_{2',3'}$= 5.5), 4.19 (ddd, 1H, H6′, $J_{6',7'}$= 2.5, $J_{6',7''}$= 6.0, $J_{6',5'}$= 8.5), 4.17 (dd, 1H, H4′, $J_{4',5'}$ = 2, $J_{3',4'}$ = 4), 3.81 (dd, 1H, H7′, $J_{6',7'}$ = 3.0, $J_{7',7''}$= 12.0), 3.71 (dd, 1H, H7″, $J_{7'',6'}$ = 6.0, $J_{7',7''}$= 11.5), 3.54 (dd, 1H, H5′, $J_{5',4'}$ = 2.5, $J_{5',6'}$ = 8.5), 2.93 (d, 1H, H2″, $J_{2'',1'}$= 15.0), 2.56 (ddd, 1H, H2′, $J_{1',2'}$= 4, $J_{2',3'}$= 6, $J_{2',2''}$= 15.0), 1.96 (s, 3H, CH_3).**^{13}C NMR** (CD_3OD, 125 MHz) δ 173.1, 153.7, 138.9, 118.5, 82.4, 74.8, 74.7, 70.7, 69.3, 62.3, 21.6, 11.8.**HRMS:** *m/z* [M+Na] calculated for $C_{12}H_{16}N_2NaO_6$: 307.0901. Found: 307.0887.

Other spectroscopic information provided: COSY NMR and crystal structure

2.6.9 General procedure for azidation of anhydro oxepane 12

A mixture of **12** (13 mg, 0.0457 mmol), NaN_3 (10 mg, 0.1373 mmol), and 15-crown-5 (30.2 mg, 0.1373 mmol) in DMF (2 mL) was heated to 100 °C for 3 hours. After completion, DMF was evaporated under vacuum and the crude was purified by column chromatography (2-6% MeOH/

CH_2Cl_2) to give an inseparable mixture of **13** and **14** (**13**/**14** = 1/2 , total of 9.2 mg, 0.028 mmol, yield: 61%, R_f (20% MeOH/ CH_2Cl_2): 0.70).This mixture was further purified by reverse phase HPLC (Hamilton PRP-1, 10µm-100 Å-10x250 mm. Eluent conditions: A: ACN, B: H_2O, gradient: 0-50% ACN in 36 minutes) to obtain pure **13** (Rt: 25.5) and **14** (Rt: 22.7) as white solids.

2.6.10 1-[(3R,4S,5R,6R)-(3-azido-2,3-dideoxy-4,5-dihydroxy-6-hydroxymethyl)-β-oxepanyl] thymine (13)

^{1}H NMR (DMSO-d_6, 500 MHz) δ 7.57 (d, 1H, H6, J= 1.1), 6.04 (dd, 1H, H1′, $J_{1',2'}$= 1.1, $J_{1',2''}$= 10.8), 5.53 (d, 1H, 5′OH, $J_{5',OH}$= 3.9), 5.47 (d, 1H, 4′OH, $J_{4',OH}$= 4.5), 4.82 (bs, 1H, 7′OH), 4.03 (m, 2H, H3′, H5′), 3.69 (m, 2H, H4′, H6′), 3.20-3.45 (H7′and H7′′covered under the H_2O peak), 2.06 (ddd, 1H, H2′, $J_{1',2'}$= 1.2, $J_{2',3'}$= 6.1, $J_{2',2''}$= 13.1), 1.88 (m, 1H, H2′′, $J_{1',2''}$=10.9), 1.77 (s, 3H, CH_3).**^{13}C NMR** (DMSO-d_6, 125 MHz) δ168.3 (Base CO), 164.1 (Base CO), 136.7 (C6), 109.8 (C5), 83.7 (C4′), 78.7 (C1′), 75.3 (C5′), 73.8 (C6′), 62.4 (C7′), 60.2 (C3′), 39.3 (C2′), 12.4 (C5-CH_3).**HRMS:***m/z* [M+Na] calculated for $C_{12}H_{17}N_5NaO_6$: 350.1071. Found: 350.1072.

Other spectroscopic information provided: COSY, NOESY and HSQC NMR.

2.6.11 1-[(3S,4R,5R,6R)-(4-azido-2,4-dideoxy-3,5-dihydroxy-6-hydroxymethyl)-β-oxepanyl] thymine (14)

^{1}H NMR (DMSO-d_6, 500 MHz) δ 7.58 (d, 1H, H6, J= 1.2), 5.74 (dd, 1H, H1′, $J_{1',2''}$= 4.1, $J_{1',2'}$= 5.2), 5.49 (d, 1H, 5′OH, $J_{5',OH}$= 6.4), 5.30 (d, 1H, 3′OH, $J_{3',OH}$= 4.8), 4.47 (t, 1H, 7′OH, $J_{7',OH}$ = 6.2), 3.74 (m, 1H, H3′), 3.66 (ddd, 1H, H7′, $J_{7',6'}$ = 2.6, $J_{7',OH}$= 6.8, , $J_{7',7''}$ = 11.9), 3.60 (ddd, 1H, H6′, $J_{6',7'}$ = 2.4, J= 6.6, J = 9.2), 3.35-3.41 (m, 2H, H7′′, H4′), 3.30-3.33 (H5′ partly covered

under the H_2O peak), 2.30 (ddd, 1H, H2′, $J_{1',2'}$= 5.4, $J_{2',3'}$= 9.8, $J_{2',2''}$= 15.2), 2.06 (ddd, 1H, H2″, $J_{2'',3'}$= 2.7, $J_{1',2''}$= 4.1, $J_{2',2''}$= 15.4), 1.81 (s, 3H, CH_3).**^{13}C NMR** (DMSO-d_6, 125 MHz) δ164.2 (Base CO), 150.5 (Base CO), 136.8 (C6), 109.3 (C5), 80.8 (C1′), 79.4 (C6′), 75.3 (C4′), 71.8 (C5′), 66.2 (C3′), 62.4 (C7′), 39.2 (C2′), 12.5 (C5-CH_3).**HRMS:***m/z* [M+Na] calculated for $C_{12}H_{17}N_5NaO_6$: 350.1071. Found: 350.1070.

Other spectroscopic information provided: COSY, NOESY and HSQC NMR.

2.6.12 General procedure for azidation of epoxide oxepane 11

The azidation reaction was also performed in epoxide **11** following the same reaction and work up conditions as mentioned above for the azidation of anhydrooxepane**12**. A mixture of **11** (18 mg, 0.0632 mmol), NaN_3 (13.8 mg, 0.1896 mmol), and 15-crown-5 (41.40 mg, 0.1896 mmol) in DMF (2 mL) was heated to 100° C for 3 hours. After completion, DMF was evaporated under vacuum at 100° C and the crude was purified by column chromatography (2-6% MeOH/ CH_2Cl_2) to give an inseparable mixture of **13** and **14**. This mixture was further purified by reverse phase HPLC (Hamilton PRP-1, 10μm-100 Å-10x250 mm. Eluent conditions: A: ACN, B: H_2O, gradient: 0-50% ACN in 36 minutes) to obtain pure **13** (Rt: 25.5) and **14** (Rt: 22.7) as white solids. R_f (20% MeOH/ CH_2Cl_2): 0.70. Structure and ratio of the obtained products were confirmed by ^{1}HNMR of the isolated product mixture (**13**/**14** = 1/2.3, total of 11 mg, 0.033 mmol, yield: 70%).

2.6.13 1-[(3S,4S,5R,6R)-(3-chloro-2,3-dideoxy-4,5-dihydroxy-6-hydroxymethyl)-β-oxepanyl] thymine (15)

Compound **12** (23 mg, 0.081 mmol) was coevaporated with dry pyridine and kept under vacuum overnight prior to reaction. A solution of **12** in anhydrous DMF (2 mL) was then treated with HCl-Py (113 mg, 0.975 mmol). The mixture was stirred overnight at room temperature under argon atmosphere. After reaction completion, DMF was evaporated under vacuum at 60° C and the crude was purified by column chromatography (2-5% MeOH/ CH_2Cl_2) to give **15** as a white solid (22.8 mg, 0.071 mmol, 88%).R_f (20% MeOH/ CH_2Cl_2): 0.76.

^{1}H NMR (DMSO-d_6, 500 MHz) δ11.24(bs, 1H, NH), 7.58 (d, 1H, H6, J= 1.1), 5.98 (dd, 1H, H1′, J = 6.1, J= 9.3), 5.77 (d, 1H, 5′OH, J= 4.9), 5.01 (d, 1H, 4′OH, J = 6.7), 4.51 (t, 1H, 7′OH, J = 5.8), 4.41 (dd, H, H3′, J= 7.1, J= 9.7), 4.10 (m, 1H, H5′), 3.55 (m, H7′), 3.27-3.40 (m, 3H, H4′, H6′, H7′′), 2.43 (m, 1H, H2′′), 2.26(m, 1H, H2′), 1.76 (s, 3H, CH_3).**^{13}C NMR** (DMSO-d_6, 125 MHz) δ165.1,150.4, 136.8, 110.3, 83.0, 82.8, 72.1, 71.1, 62.4, 60.8, 38.9, 10.9.**HR ESIMS:** *m/z* [M+Na] calculated for $C_{12}H_{17}ClN_2NaO_6$: 343.0667. Found: 343.0662.

Other spectroscopic information provided: COSY and NOESY NMR in DMSO-d_6,^{1}HNMR and COSY NMR in MeOD

2.6.14 Computational methods

The exploration of the torsional landscape of derivatives **10** and **11** was carried out using classical molecular dynamics (MD) simulations, and the most stable conformations were then energy minimized using quantum mechanical calculations. During the MD simulations, we enhanced the sampling of sugar conformations using Bias-exchange Metadynamics (BE-Metd), [34, 35] using 8 replicas (200 ns each) of the simulation system in parallel. In these calculations, we

subjected dihedral angles d1, d2 and d3 of the seven membered rings (**Figure 2.11**) to a time-dependent biasing potential to speed up conformational barrier crossing at room-temperature,

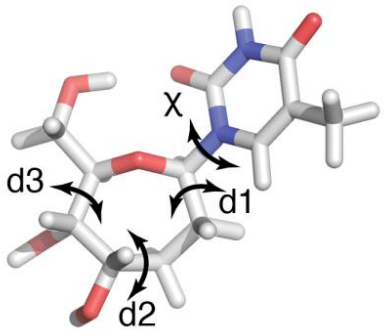

Figure 2.11 Schematic illustration of dihedrals angles that were subject a biasing potential during our Bias-Exchange Metadynamics simulations (d1, d2, d3), and those that were used as restraints during our quantum mechanical geometry optimization (d1, d2, d3 and χ).

while still generating a canonical ensemble. Each dihedral was biased in a different replica of the system, and we included five additional non-biased replicas. In each biased replica, the dihedral under consideration was biased with a time-dependent Gaussian potential deposited every 1 ps, with Gaussian width of $\sigma = 0.1$ and height of $h = 0.15$ and a tempered bias equal to 8. An exchange step between pairs of replicas, biased or not, was attempted every 2 ps using a Metropolis acceptance criteria.

The initial structures for derivatives **10** and **11** were prepared with the help of Avogadro molecular editor[36] starting from canonical coordinates of deoxyribosyl thymine available from Amber LEAP program.[37] Each derivative was immersed in a previously equilibrated water octahedral box such that the box boundaries were positioned at least 2 nm away from the nucleoside atoms. We used Amber's GAFF forcefield[38] to describe the intramolecular and intermolecular interactions of each derivative and the SPC/E[39] model to describe the water molecules. The set of fractional single-point charges was refined from quantum mechanical calculations at the HF/6-31G* level using RESP electrostatic fitting.[40] The classical simulations were carried out using the Gromacs-4.6 software,[41] with periodic boundary conditions and the

particle mesh Ewald method[42] for the long-range electrostatics, using a cut-off of 1.0 nm for the short-range repulsive and attractive dispersion interactions, which were modeled via a Lennard-Jones potential. We used constraints[43] on the bond lengths and angles of water molecules, as well as for the bond lengths of the derivatives,[44] allowing a time step of 2 fs for the integration of Newton equations of motion. The temperature was held constant at 300 K using Parrinello's thermostat.[45] We used accepted structures in the 8 replicas to perform a structural clustering and extract the most probable conformations, i.e. those with the lowest free energy. We reweighted (un-biased) the structures that were generated in the biased replicas using a weighted histogram method. The structural clustering was performed using a single-linkage algorithm using the root mean square deviation (RMSD) between ring atoms as a distance metric with a cutoff of 0.15 nm. We used a representative structure (a cluster centroid) of the 25th most populated clusters as initial structures for subsequent quantum mechanical calculations, i.e. geometry optimization and proton-proton J-coupling calculations (only data on structures with a theoretical weight above 0.5% in the total ensemble are reported here).

Quantum mechanical geometry optimizations were performed at the M062x/6-31+G(d,p) level restraining the dihedrals d1, d2 and d3, and the χ angle linking the sugar ring with the thymine substituent to the values obtained from the representative structures obtained from the lowest free energy conformations (**Figure 2.11**). The effect of the solvent (methanol) was included by means of a continuum solvation model SMD.[46] The calculation of proton-proton NMR J-couplings were performed on the lowest energy structures (threshold of 6 kJ/mol from global minima) using the GIAO/B3LYP/*aug*-cc-pVDZ methodology[47-50] (along with methanol solvation via SMD continuum model).[51] Prior to the NMR calculation with GIAO method the structures were re-optimized using the B3LYP/*aug*-cc-pVDZ level of theory.

lowest-free energy structures obtained from our BE-MetD simulations, in increasing order of energy and referenced to the lowest energy state for **10** and **11**. For each structure, the seudorotation parameters and their percentages are given.

Table 2.3 Results of the constrained quantum mechanical geometry optimization for the lowest free energy conformations obtained from our BE-Metd simulations for derivative **11**. Along with the relative energy, referenced to the lowest energy conformation, we give their Boltzmann weight (normalized using the lowest 25 energies) the pairs of puckering amplitudes and pseudorotation angles (q_2, φ_2) and (q_3, φ_3), which define the pseudorotation state of the ring, as well as the percentage of each amplitude.

Structure	Energy (kJ/mol)	Botlzmann weight	q_2	φ_2	% q_2	q_3	φ_3	% q_3
1	0	0.649	0.006	53.33	0.68	0.068	175.68	99.32
2	2.514	0.235	0.019	17.55	7.31	0.068	179.43	92.69
3	6.383	0.049	0.026	5.32	12.63	0.069	182.27	87.37
4	6.865	0.041	0.015	55.60	4.66	0.066	172.46	95.34
5	10.195	0.011	0.015	2.71	4.22	0.07	185.35	95.78
6	11.105	0.007	0.079	230.98	84.28	0.034	237.15	15.72
7	12.015	0.005	0.032	16.37	17.92	0.067	179.03	82.08

Table 2.4 Results of the constrained quantum mechanical geometry optimization for the lowest free energy conformations obtained from our BE-Metd simulations for derivative **10**. Along with the relative energy, referenced to the lowest energy conformation, we give their Boltzmann weight (normalized using the lowest 25 energies) and the pairs of puckering amplitudes and pseudorotation angles (q_2, φ_2) and (q_3, φ_3), which define the pseudorotation state of the ring, as well as the percentage of each amplitude.

Structure	Energy (kJ/mol)	Botlzmann weight	q_2	φ_2	% q_2	q_3	φ_3	% q_3
1	0	0.170	0.05	239.91	34.87	0.068	140.32	65.13
2	0.027	0.168	0.051	234.95	36.16	0.068	137.78	63.84
3	0.857	0.120	0.049	243.30	33.82	0.068	142.09	66.18
4	0.89	0.119	0.05	227.82	35.4	0.068	134.87	64.6
5	1.8	0.082	0.051	231.29	35.84	0.068	136.19	64.16
6	1.978	0.077	0.048	246.32	33.48	0.068	143.46	66.52
7	2.29	0.068	0.048	247.11	33.27	0.068	143.74	66.73
8	2.948	0.052	0.048	248.42	33.21	0.068	144.40	66.79
9	3.563	0.040	0.044	214.26	29.85	0.068	132.39	70.15
10	4.134	0.032	0.048	187.51	33.82	0.067	125.67	66.18
11	5.237	0.021	0.049	250.89	33.84	0.068	145.44	66.16
12	6.197	0.014	0.055	240.85	41	0.065	141.09	59
13	6.372	0.013	0.045	217.71	30.18	0.068	133.46	69.82
14	6.774	0.011	0.05	176.07	36.58	0.066	122.72	63.42
15	7.998	0.007	0.053	244.29	39.91	0.066	142.90	60.09

2.6.15 Crystallographic information

The Crystals of nucleoside **12** were mounted with Mitegen mounts using Paratone-N from Hampton Research. Single-crystal X-ray diffraction experiments were carried out with a BRUKER APEX-II Charge-coupled device (CCD) diffractometer using graphite-monochromated $Mo_{K\alpha}$ radiation (λ = 0.71073 Å) and KRYOFLEX for low temperature experiments. SAINT[52] was used for integration of the intensity reflections and scaling and

SADABS[53] for absorption correction. Patterson maps were used to generate the initial solutions. Non-hydrogen atoms were located by difference Fourier maps and final solution refinements were solved by full-matrix least-squares method on F^2 of all data, using SHELXTL[52] software. The hydrogen atoms were placed in calculated positions, except for the protons of the methanol solvent which were located from difference maps. The crystal structure was solved in the chiral space group $P2_12_12_1$ with the Flack parameter of 0.2.[54] Crystals of compound **12** were obtained from slow evaporation of CD_3OD at room temperature. The crystallographic data for **12** has been deposited at the Cambridge structural database (CSD) under the deposition number 1431967.

2.7 References

1. Sofia, M. J., Chapter Fifteen - Nucleosides and Nucleotides for the Treatment of Viral Diseases. In *Annual Reports in Medicinal Chemistry*, Manoj, C. D., Ed. Academic Press2014; Vol. Volume 49, pp 221-247.
2. Parker, W. B., Enzymology of Purine and Pyrimidine Antimetabolites Used in the Treatment of Cancer. *Chemical Reviews* **2009,** *109*, 2880-2893.
3. Marquez, V. E.; Ben-Kasus, T.; Barchi, J. J.; Green, K. M.; Nicklaus, M. C.; Agbaria, R., Experimental and Structural Evidence that Herpes 1 Kinase and Cellular DNA Polymerase(s) Discriminate on the Basis of Sugar Pucker. *J Am Chem Soc* **2004,** *126*, 543-549.
4. Marquez, V. E.; Ezzitouni, A.; Russ, P.; Siddiqui, M. A.; Ford, H.; Feldman, R. J.; Mitsuya, H.; George, C.; Barchi, J. J., HIV-1 Reverse Transcriptase Can Discriminate between Two Conformationally Locked Carbocyclic AZT Triphosphate Analogues. *J Am Chem Soc* **1998,** *120*, 2780-2789.
5. Pitsch, S.; Wendeborn, S.; Jaun, B.; Eschenmoser, A., Why Pentose- and Not Hexose-Nucleic Acids??. Part VII. Pyranosyl-RNA ('p-RNA'). Preliminary communication. *Helvetica Chimica Acta* **1993,** *76*, 2161-2183.
6. Eschenmoser, A.; Dobler, M., Warum Pentose- und nicht Hexose-Nucleinsäuren?? Teil I. Einleitung und Problemstellung, Konformationsanalyse für Oligonucleotid-Ketten aus 2′,3′-Dideoxyglucopyranosyl-Bausteinen ('Homo-DNS') sowie Betrachtungen zur Konformation von A- und B-DNS. *Helvetica Chimica Acta* **1992,** *75*, 218-259.
7. Verheggen, I.; Van Aerschot, A.; Toppet, S.; Snoeck, R.; Janssen, G.; Balzarini, J.; De Clercq, E.; Herdewijn, P., Synthesis and antiherpes virus activity of 1,5-anhydrohexitol nucleosides. *Journal of Medicinal Chemistry* **1993,** *36*, 2033-2040.
8. Aerschot Van, A.; Verheggen, I.; Hendrix, C.; Herdewijn, P., 1,5-Anhydrohexitol Nucleic Acids, a New Promising Antisense Construct. *Angewandte Chemie International Edition in English* **1995,** *34*, 1338-1339.

9. Taylor, A. I.; Pinheiro, V. B.; Smola, M. J.; Morgunov, A. S.; Peak-Chew, S.; Cozens, C.; Weeks, K. M.; Herdewijn, P.; Holliger, P., Catalysts from synthetic genetic polymers. *Nature* **2015,** *518*, 427-430.
10. Sabatino, D.; Damha, M. J., Oxepane nucleic acids: Synthesis, characterization, and properties of oligonucleotides bearing a seven-membered carbohydrate ring. *J Am Chem Soc* **2007,** *129*, 8259-8270.
11. Castro, S.; Cherney, E. C.; Snyder, N. L.; Peczuh, M. W., Synthesis of substituted septanosyl-1,2,3-triazoles. *Carbohydrate Research* **2007,** *342*, 1366-1372.
12. Sizun, G.; Dukhan, D.; Griffon, J.-F.; Griffe, L.; Meillon, J.-C.; Leroy, F.; Storer, R.; Sommadossi, J.-P.; Gosselin, G., Synthesis of the first example of a nucleoside analogue bearing a 5′-deoxy-β-d-allo-septanose as a seven-membered ring sugar moiety. *Carbohydrate Research* **2009,** *344*, 448-453.
13. Tripathi, S.; Roy, B. G.; Drew, M. G. B.; Achari, B.; Mandal, S. B., Synthesis of Oxepane Ring Containing Monocyclic, Conformationally Restricted Bicyclic and Spirocyclic Nucleosides from d-Glucose: A Cycloaddition Approach. *The Journal of Organic Chemistry* **2007,** *72*, 7427-7430.
14. Nomura, M.; Endo, K.; Shuto, S.; Matsuda, A., Nucleosides and nucleotides. 191: Ring expansion reaction of 1-[2,3,5-tri-o-TBS-4α-formyl-β-D-ribo-pentofuranosyl]uracil by treating with (methylene)triphenylphosphorane to give a new nucleoside containing dihydrooxepine ring at the sugar moiety. *Tetrahedron* **1999,** *55*, 14847-14854.
15. Kanojia, R. M.; Wachter, M. P.; Levine, S. D.; Adams, R. E.; Chen, R.; Chin, E.; Cotter, M. L.; Hirsch, A. F.; Huettemann, R., Isolation and structural elucidation of zoapatanol and montanol, novel oxepane diterpenoids from the Mexican plant zoapatle (Montanoa tomentosa). *The Journal of Organic Chemistry* **1982,** *47*, 1310-1319.
16. Basu, S.; Ellinger, B.; Rizzo, S.; Deraeve, C.; Schürmann, M.; Preut, H.; Arndt, H.-D.; Waldmann, H., Biology-oriented synthesis of a natural-product inspired oxepane collection yields a small-molecule activator of the Wnt-pathway. *Proceedings of the National Academy of Sciences* **2011,** *108*, 6805-6810.
17. Berger, D.; Overman, L. E.; Renhowe, P. A., Enantioselective total synthesis of (+)-isolaurepinnacin. *J Am Chem Soc* **1993,** *115*, 9305-9306.
18. Basu, S.; Waldmann, H., Polymer supported synthesis of a natural product-inspired oxepane library. *Bioorganic & Medicinal Chemistry* **2014,** *22*, 4430-4444.
19. Abou Assi, H.; Martínez-Montero, S.; Dixit, D. M.; Chua, Z.; Bohle, D. S.; Damha, M. J., Synthesis, Structure, and Conformational Analysis of Nucleoside Analogues Comprising Six-Membered 1,3-Oxathiane Sugar Rings. *European Journal of Organic Chemistry* **2015,** *2015*, 1945-1953.
20. Deleavey, Glen F.; Damha, Masad J., Designing Chemically Modified Oligonucleotides for Targeted Gene Silencing. *Chemistry & Biology* **2012,** *19*, 937-954.
21. Kerremans, L.; Schepers, G.; Rozenski, J.; Busson, R.; Van Aerschot, A.; Herdewijn, P., Hybridization between "Six-Membered" Nucleic Acids: RNA as a Universal Information System. *Organic Letters* **2001,** *3*, 4129-4132.
22. Eschenmoser, A., Chemical etiology of nucleic acid structure. *Science* **1999,** *284*, 2118-24.
23. Premraj, B. J.; Raja, S.; Yathindra, N., Structural basis for the unusual properties of 2′,5′ nucleic acids and their complexes with RNA and DNA. *Biophysical Chemistry* **2002,** *95*, 253-272.

24. Hoberg, J. O., Formation of Seven-Membered Oxacycles through Ring Expansion of Cyclopropanated Carbohydrates. *The Journal of Organic Chemistry* **1997,** *62*, 6615-6618.
25. Itoh, T.; Jitsukawa, K.; Kaneda, K.; Teranishi, S., Vanadium-catalyzed epoxidation of cyclic allylic alcohols. Stereoselectivity and stereocontrol mechanism. *J Am Chem Soc* **1979,** *101*, 159-169.
26. Sabatino, D., Expanding the size and shape of nucleic acids : studies on branched and heptose based nucleic acids. **2007**.
27. Zhang, W.; Loebach, J. L.; Wilson, S. R.; Jacobsen, E. N., Enantioselective epoxidation of unfunctionalized olefins catalyzed by salen manganese complexes. *J Am Chem Soc* **1990,** *112*, 2801-2803.
28. Srivastav, N. C.; Shakya, N.; Mak, M.; Liang, C.; Tyrrell, D. L. J.; Agrawal, B.; Kumar, R., Synthesis and in vitro antiviral activities of 3′-fluoro (or chloro) and 2′,3′-difluoro 2′,3′-dideoxynucleoside analogs against hepatitis B and C viruses. *Bioorganic & Medicinal Chemistry* **2010,** *18*, 7542-7547.
29. Srivastav, N. C.; Shakya, N.; Bhavanam, S.; Agrawal, A.; Tse, C.; Desroches, N.; Kunimoto, D. Y.; Kumar, R., Antimycobacterial activities of 5-alkyl (or halo)-3′-substituted pyrimidine nucleoside analogs. *Bioorganic & Medicinal Chemistry Letters* **2012,** *22*, 1091-1094.
30. Al-Masoudi, N. A.; Pfleiderer, W., Synthesis and reactions of 1-(5-azido-5-deoxy-3-O-p toluenesulfonyl-β-d-xylofuranosyl) derivatives of 5-alkyl- and 5-halo-pyrimidines. *Carbohydrate Research* **1995,** *275*, 95-105.
31. Jahn, M. K.; Dewald, D. A.; Vallejo-López, M.; Cocinero, E. J.; Lesarri, A.; Zou, W.; Cremer, D.; Grabow, J.-U., Pseudorotational Landscape of Seven-Membered Rings: The Most Stable Chair and Twist-Boat Conformers of ε-Caprolactone. *Chemistry – A European Journal* **2014,** *20*, 14084-14089.
32. DeMatteo, M. P.; Snyder, N. L.; Morton, M.; Baldisseri, D. M.; Hadad, C. M.; Peczuh, M. W., Septanose Carbohydrates: Synthesis and Conformational Studies of Methyl α-d-glycero-d-Idoseptanoside and Methyl β-d-glycero-d-Guloseptanoside. *The Journal of Organic Chemistry* **2005,** *70*, 24-38.
33. Zheng, S.; Pfaendtner, J., Enhanced sampling of chemical and biochemical reactions with metadynamics. *Molecular Simulation* **2015,** *41*, 55-72.
34. Piana, S.; Laio, A., A bias-exchange approach to protein folding. *J. Phys. Chem. B* **2007,** *111*, 4553-9.
35. Laio, A.; Parrinello, M., Escaping free-energy minima. *Proc. Natl. Acad. Sci. U. S. A.* **2002,** *99*, 12562-12566.
36. Hanwell, M. D.; Curtis, D. E.; Lonie, D. C.; Vandermeersch, T.; Zurek, E.; Hutchison, G. R., Avogadro: an advanced semantic chemical editor, visualization, and analysis platform. *Journal of cheminformatics* **2012,** *4*, 17.
37. Case, D. A.; Cheatham, T. E.; Darden, T.; Gohlke, H.; Luo, R.; Merz, K. M.; Onufriev, A.; Simmerling, C.; Wang, B.; Woods, R. J., The AMBER biomolecular simulation programs. *J. Comput. Chem.* **2005,** *26*, 1668-1688.
38. Wang, J.; Wolf, R. M.; Caldwell, J. W.; Kollman, P. A.; Case, D. A., Development and testing of a general amber force field. *J. Comput. Chem.* **2004,** *25*, 1157-74.
39. Berendsen, H. J. C.; Grigera, J. R.; Straatsma, T. P., The missing term in effective pair potentials. *J. Phys. Chem.* **1987,** *91*, 6269-6271.

40. Cieplak, P.; Cornell, W. D.; Bayly, C.; Kollman, P. A., Application of the multimolecule and multiconformational RESP methodology to biopolymers: Charge derivation for DNA, RNA, and proteins. *J. Comput. Chem.* **1995,** *16*, 1357-1377.
41. Hess, B.; Kutzner, C.; van der Spoel, D.; Lindahl, E., GROMACS 4: Algorithms for Highly Efficient, Load-Balanced, and Scalable Molecular Simulation. *J. Chem. Theory Comput.* **2008,** *4*, 435-447.
42. Darden, T.; York, D.; Pedersen, L., Particle mesh Ewald: an Nlog(N) method for Ewald sums in large systems. *J. Chem. Phys.* **1993,** *98*, 10089-10092.
43. Miyamoto, S.; Kollman, P. A., SETTLE: An Analytical Version of the SHAKE and RATTLE Algorithms for Rigid Water Models. *J. Comput. Chem.* **1992,** *13*, 952-962.
44. Hess, B., P-LINCS: A Parallel Linear Constraint Solver for Molecular Simulation. *J. Chem. Theory Comput.* **2008,** *4*, 116-122.
45. Bussi, G.; Donadio, D.; Parrinello, M., Canonical sampling through velocity rescaling. *J. Chem. Phys.* **2007,** *126*, 014101.
46. Marenich, A. V.; Cramer, C. J.; Truhlar, D. G., Universal Solvation Model Based on Solute Electron Density and on a Continuum Model of the Solvent Defined by the Bulk Dielectric Constant and Atomic Surface Tensions. *The Journal of Physical Chemistry B* **2009,** *113*, 6378-6396.
47. Ditchfield, R., Self-consistent perturbation theory of diamagnetism. *Mol. Phys.* **1974,** *27*, 789-807.
48. Wolinski, K.; Hinton, J. F.; Pulay, P., Efficient implementation of the gauge-independent atomic orbital method for NMR chemical shift calculations. *J. Am. Chem. Soc.* **1990,** *112*, 8251-8260.
49. Becke, A. D., Density-functional thermochemistry. III. The role of exact exchange. *The Journal of Chemical Physics* **1993,** *98*, 5648-5652.
50. Dunning, T. H., Gaussian basis sets for use in correlated molecular calculations. I. The atoms boron through neon and hydrogen. *The Journal of Chemical Physics* **1989,** *90*, 1007-1023.
51. Jain, R.; Bally, T.; Rablen, P. R., Calculating Accurate Proton Chemical Shifts of Organic Molecules with Density Functional Methods and Modest Basis Sets. *The Journal of Organic Chemistry* **2009,** *74*, 4017-4023.
52. Sheldrick, G., A short history of SHELX. *Acta Crystallographica Section A* **2008,** *64*, 112-122.
53. Sheldrick, G. M. University of Göttingen: Germany, 1996.
54. Flack, H., On enantiomorph-polarity estimation. *Acta Crystallographica Section A* **1983,** *39*, 876-881.

CHAPTER 3: EFFECT OF 2'-5' LINKAGE MODIFICATION ON RNA INTERFERENCE EFFICIENCY

3.1 Overview

This chapter focuses on the effect of the 2'-5' linkage modification on siRNA efficiency and interactions of such siRNAs with the proteins involved in the RNAi pathway. siRNA libraries targeting firefly luciferase and P53 mRNAs were prepared with different positional variations of 2'-5' linkages throughout the sense or antisense strands of the duplexes. Screening of these libraries against their corresponding mRNA targets showed that 2'-5' linkages are tolerated in the sense strand and, to some extent, the antisense strand of siRNAs. Furthermore, 2'-5' modified siRNAs were found to be less immunostimulatory than unmodified siRNAs. To study the effect of 2'-5' modified siRNAs on their interactions with the RNAi pathway proteins, a selection of these siRNAs were enzymatically phosphorylated, and their loading into the hAGO2 protein were investigated by gel shift assays. Extensive 2'-5' modification of the antisense strand minimally affected phosphorylation of the siRNA by kinases, however, it was found to affect loading of the siRNA into hAGO2. Molecular modelling and MD simulations of the 2'-5' modified siRNAs in the active site of hAGO2, also, suggested that the presence of too many 2'-5' linkages affects hAGO2-siRNA key interactions via structural changes in the RNA duplex. Nevertheless, our results show that 2'-5' modified siRNAs can afford a potent class of modified siRNAs with diminished immunostimulatory response.

3.2 Introduction

RNA, as explained in Chapter 1, has been proposed to play a key role in the early evolution of primitive life before DNA and proteins were evolved.[1] However, nonenzymatic RNA replication

in early life would have, quite likely, led to a mixture of 2'-5' and 3'-5' linkages.[2] Recent research has demonstrated that RNA with mixed 2'-5'/3'-5' backbone can fold into defined three-dimensional structures that retain molecular recognition and catalytic properties. Szostak and co-workers recently reported that hammerhead rybozymes containing up to 25% randomly distributed 2'-5' linkages are still able to retain their catalytic activity.[3] However, a study by Wang and co-workers investigating the effect of 2'-5' linkages on the efficiency of RNA synthesis by RNA polymerase II demonstrated that this protein cannot bypass this linkage modification sites in a DNA template, pausing at the 2′-5′ linkage site.[4]

While structures of a homogeneously 2'-5' -linked RNA duplex[5-11] and 2'-5'-linked dinucleotides[12] are known, high resolution crystallographic data on mixed-backbone RNA duplexes has been reported only recently.[13] These duplexes share the same global structure as the native duplex, suggesting that RNA backbone can accommodate perturbations caused by a few 2'-5' linkages. These crystallographic studies, along with accompanying molecular dynamics simulations, provided structural insights into the RNA duplex parameters, as well as nucleotide puckering changes upon linkage modification.[13] In contrast to RNA, the 2'-5' linked RNA adopts the C2'-endo ("South") sugar conformation, yet 2'-5'-RNA:RNA duplexes adopt an A-form structure, affording duplexes with good thermal stability, albeit less stable in comparison with the native RNA:RNA duplex.[8, 14,15].

For the past several years, our lab has been interested in studying the structure and function of 2'-5' linked RNAs. Giannaris and Damha reported that 2'-5' linked RNAs can bind to complementary RNA, but only weakly (if at all) to complementary single stranded DNA.[16] Further studies in our laboratory by Wasner *et al*. demonstrated that RNA:2′-5′-RNA duplexes structures resemble more closely the structure of the RNA:DNA hybrids, which adopt an A-like

character. The melting temperature comparison of the backbone-modified duplexes with that of the unmodified duplexes revealed the order of thermal stability as RNA:RNA > DNA:DNA ≈ RNA:DNA > RNA:2′-5′-RNA > 2′-5′-RNA:2′-5′-RNA ≫ DNA:2′-5′-RNA. Also, RNA:2′-5′-RNA duplexes were found to inhibit the RNase H-mediated cleavage of a natural DNA:RNA substrate, even though they were not substrates of this enzyme.[14]

In line with our previous studies, we became interested in investigating the effect of the 2'-5' modification on siRNA efficiency, and interactions of such siRNAs with the proteins involved in the RNAi pathway. As described below, our findings fully support the notion that mixed 2'-5'/3'-5' linkages in RNA could have been an important alternative functional backbone during early evolution.

3.3 2'-5'-Linkages in gene silencing oligonucleotides

As discussed in Chapter 1, 2'-5'-RNA is an attractive candidate for ON therapeutics due to its nuclease stability, simplicity, affordable monomers, and feasible synthesis. In fact, the required 2'-phosphoramidites are produced from byproducts obtained in the synthesis of the more common RNA 3'-phosphoramidite monomers. Furthermore, as for RNA, solid-phase synthesis of 2'-5'-RNA proceeds with high efficiency employing nearly identical conditions during growth of the oligonucleotide chain.[14, 16-18] 2'-5'-DNAs and 2'-5'-RNAs were both found to be resistant towards enzymatic hydrolysis by cellular and serum exonucleases and intracellular endonucleases, suggesting that this linkage can confer adequate stability *in vivo*.[16, 19-21] Finally, mixed backbone (2'-5'/3'-5') DNA showed less nonspecific binding to plasma and cellular proteins in comparison to 3'-5' linked phosphorothioate oligonucleotides.[21] This result suggests that 2'-5'-oligonucleotides may produce less side-effects, compared to 3'-5'-oligonucleotides,[21]

and make the 2'-5' linkage a very attractive modification to employ in ON drug candidates, specifically in siRNAs.

Extensive research has been reported on the 2'-5' linked AON.[22] However, there is only one report by Ionis Pharmaceuticals on utilizing this modification in siRNAs.[23] In this study, siRNAs duplexes with fully modified 2'-5'-RNA sense or antisense strands were designed to target the coding region of human phosphatase and tensin homolog (PTEN) mRNA (**Figure 3.1**). The 2'-5' linkage was found to be tolerated in the sense strand, showing moderate activity in reducing the message in cultured human cells, whereas it appeared to be less tolerated in the antisense strand. Based on these results, they concluded that 2'-5' linkage modification could be a useful as a "sense-only" modification for siRNA therapeutics.

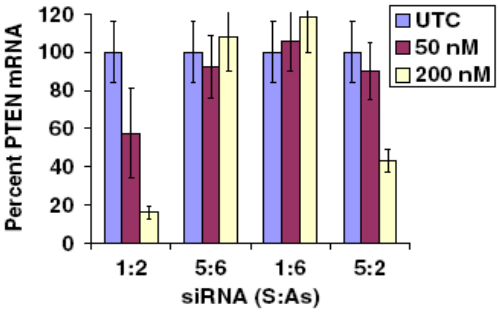

1:2	S	5' r(CAAAUCCAGAGGCUAGCAG) TT 3'
	As	3' TT r(GUUUAGGUCUCCGAUCGUC) 5'
5:6	S	5' r(*CAAAUCCAGAGGCUAGCAG*) TT 2'
	As	2' TT r(*GUUUAGGUCUCCGAUCGUC*) 5'
1:6	S	5' r(CAAAUCCAGAGGCUAGCAG) TT 3'
	As	2' TT r(*GTTTAGGTCTCCGATCGTC*) 5'
5:2	S	5' r(*CAAAUCCAGAGGCUAGCAG*) TT 2'
	As	3' TT r(GUUUAGGUCUCCGAUCGUC) 5'

Figure 4. Reduction of endogenous PTEN mRNA in HeLa cells by 2′,5′-RNA/3′,5′-RNA duplexes; S, sense strand; As, antisense strand; 2′,5′-linked residues in underline italics; TT overhangs with 3′,5′-linkages.

Figure 3.1 Reported results by Ionis Pharmaceuticals on 2'-5' modified siRNAs.[23] Reduction of endogenous PTEN mRNA in HeLa cells by 2'-5'-RNA/3'-5'-RNA duplexes is presented; S, sense strand; As, antisense strand;2'-5'-linked residues in underline italics; TT overhangs with 3'-5'-linkages. Sample 5:2 with full sense strand modification (circled in red) showed moderate gene silencing activity against PTEN mRNA. Figure from reference [23]

3.4 Project design and objectives

While the presented work by Ionis pharmaceuticals was intriguing, it was only limited to study the 2'-5' modified siRNAs targeting one mRNA sequence. Furthermore, in this study, only siRNAs with *fully* modified sense or antisense strands were tested, raising the question of whether siRNA with *partially* modified antisense strands could retain high gene silencing as unmodified siRNAs. To answer this question, we designed and synthesized siRNA libraries targeting two mRNA sequences (firefly luciferase and P53 mRNA targets) with different positional variations of 2'-5' linkages throughout the sense or antisense strands. We started these studies with a simple modification design: dividing each of the 21-nt sense and antisense strands into three sections each comprising a 7-nt segment (5'-end, central, 3'-end). Consecutive 2'-5' linkages were placed on each of these segments, while keeping the rest of the RNA strand unmodified (**Figure 3.2**). Screening of these libraries would reveal if modification of any specific positions on the siRNAs sense or antisense strands can result in better gene knock down activity.

We also wished to perform more in depth screening by incorporating the 2'-5' modification at every possible position within the AS strand. This strategy would reveal possible active

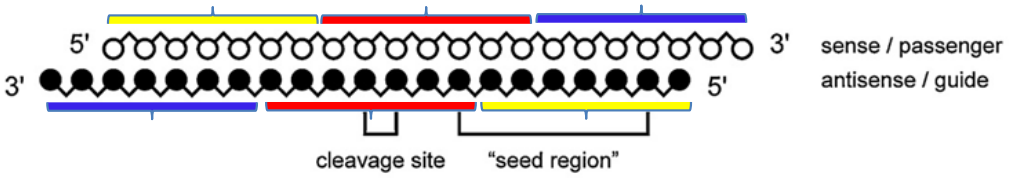

Figure 3.2 Schematic presentation of siRNA modification design: different positional variations of 2'-5' linkages throughout the sense or antisense strands of an siRNA are represented with yellow (5'-end strand modification), Red (central strand modification), and blue (3'-end strand modification).

modification patterns within an inactive larger segment of modification, as well as the tolerance of the antisense strand towards the number of 2'-5' linkages within a smaller segment of the AS strand.

Finally, we aimed to study the structural effects of 2'-5' linkage on the interactions of these modified siRNAs with enzymes involved in the RNAi pathway, such as kinases and hAGO2. This study focused on siRNAs with a modified AS strand with the aim to assess the tolerance limit of the RISC for 2'-5' linkages.

3.5 Targeting firefly luciferase by 2'-5'-linked siRNAs

Luciferase-based reporter gene assays are widely used as they allow for rapid library screening and evaluation of gene knockdown. In this assay, cells are modified to express the firefly luciferase mRNA. The level of luciferase protein can be quickly quantified using commercially available kits and through the addition of luciferin, a substrate of luciferase. Hence, luciferin is oxidized to produce oxyluciferin and bioluminescence (and hence luciferase activity) can be quantified using a luminometer. With the proper controls, this luciferase assay is a fast and efficient way for comparing the knockdown potency of a large number of siRNAs.

Our first siRNA library was synthesized based on targeting firefly luciferase mRNA and its sequences are shown in **Table 3.1**. All luciferase assays in this thesis were conducted by Dr. Johans Fakhouri from the Sleiman research group of our Chemistry Department.

Firefly luciferase levels following treatment with chemically modified siRNAs at a range of concentrations are shown in **Figure 3.3**. All siRNAs modified in the sense strand (Luc S1, S2, S3) were highly potent with IC_{50} values within the same range as the unmodified siRNA control duplex (**Figure 3.3**). Duplexes Luc- S1, -S2 and -S3 all showed higher activity than Luc-S7, the

siRNA with full sense strand modification, indicating that a few 2'-5' modifications in the sense strand can result in highly efficient mRNA knockdown.

None of the siRNAs with antisense modifications (Luc- AS4, -AS5, -AS6, AS8) showed any significant activity. For these duplexes, inhibition of luciferase activity (by ca. 20-30%) was only observed in the 20-100 nM range. This was in agreement with the previous findings by Ionis Pharmaceuticals that 2'-5' linkages are not well tolerated in the antisense strand of siRNAs, but also show that even a smaller number of 2'-5' linkages (up to 33%) results in inactive siRNAs. As expected, 2'-5' modification was destabilizing to the siRNA duplex (T_m values of duplexes are shown in **Table 3.1**).

Comparing the T_m values of Luc-S3 versus Luc-AS4 (and Luc-S1 vs Luc-S3) suggests that the 2'-5' modification has a larger impact on duplex stability when it is located within a GC-rich segment, rather than an AU-rich segments. The same pattern is seen in Luc-S1 (T_m: 55.5 °C) and Luc-AS6 (T_m: 60.0 °C) siRNAs, both with modifications located on nucleotides involved in base pairing, at the 5'-end of the sense and antisense respectively. This suggests that the 2'-5' linkage can affect RNA duplex stability by disrupting base pairing interactions. Molecular dynamics experiments described in Section 3.10 of this chapter are in agreement with this hypothesis.

Table 3.1 siRNAs targeting firefly luciferase mRNA, modified with 2'-5' linkages at various positions of sense or antisense strands. Sequences and thermal denaturation values of these siRNAs are shown below. Legend: 2'-5' linked RNA, 3'-5' linked RNA.

Sample		Sequence	T_m value (°C)	IC_{50} (nM)
Luc S1	(S) (AS)	5'- GCUUGAA GUCUUUA AUUAAUU -3' 3'- GGCGAAC UUCAGAA AUUAAUU -5'	55.5	13
Luc S2	(S) (AS)	5'- GCUUGAA GUCUUUA AUUAAUU -3' 3'- GGCGAAC UUCAGAA AUUAAUU -5'	55.2	2.2
Luc S3	(S) (AS)	5'- GCUUGAA GUCUUUA AUUAAUU-3' 3'- GGCGAAC UUCAGAA AUUAAUU -5'	60.1	20
Luc AS4	(S) (AS)	5'- GCUUGAA GUCUUUA AUUAAUU -3' 3'-GGCGAAC UUCAGAA AUUAAUU -5'	53.9	>400
Luc AS5	(S) (AS)	5'- GCUUGAA GUCUUUA AUUAAUU -3' 3'- GGCGAAC UUCAGAA AUUAAUU -5'	53.1	>400
Luc AS6	(S) (AS)	5'- GCUUGAA GUCUUUA AUUAAUU -3' 3'- GGCGAAC UUCAGAA AUUAAUU-5'	60.0	>400
Luc S7	(S) (AS)	5'- GCUUGAA GUCUUUA AUUAAUU -3' 3'- GGCGAAC UUCAGAA AUUAAUU -5'	45.0	71
Luc AS8	(S) (AS)	5'- GCUUGAA GUCUUUA AUUAAUU -3' 3'- GGCGAAC UUCAGAA AUUAAUU-5'	40.0	265
Luc-ctrl	(S) (AS)	5'- GCUUGAA GUCUUUA AUUAAUU -3' 3'- GGCGAAC UUCAGAA AUUAAUU-5'	65.0	10

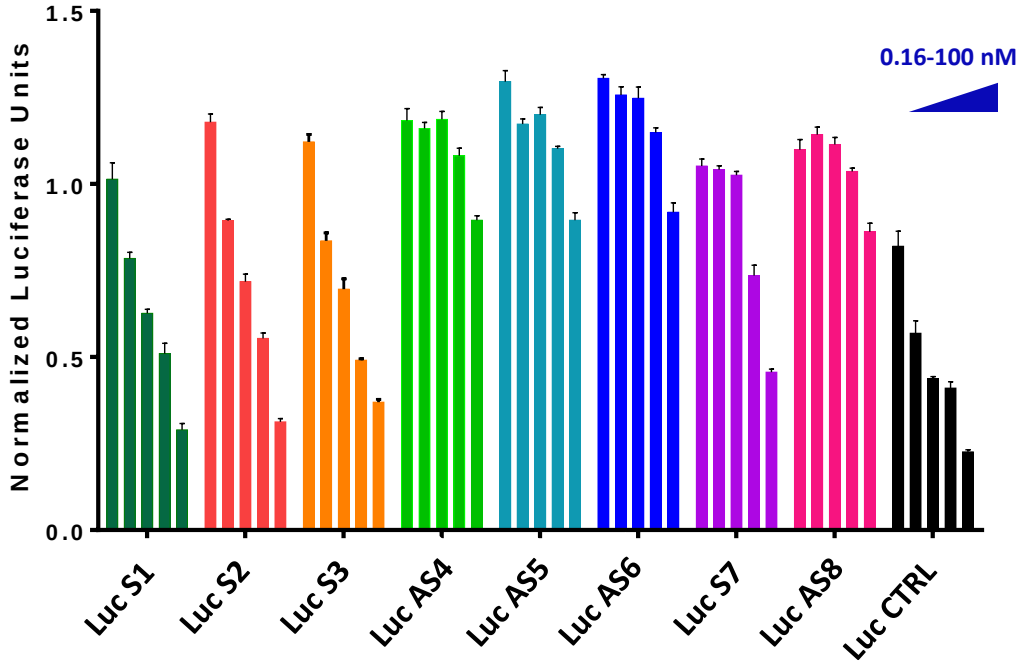

Figure 3.3 Assay demonstrating activity of 2'-5' modified siRNAs (n=2) at a range of 0.16, 0.8, 4, 20, 100 nM siRNA concentrations; Firefly luciferase levels were normalized to total cellular protein and luciferase counts of cells treated with a scrambled non-targeting siRNA.

3.5.1 Chemical phosphorylation of 2'-5'-modified AS strands

It is well known that cellular kinases may not be effective at phosphorylating modified nucleotides placed at the 5'-terminal of the antisense strands. Since 5'-phosphate is required for RISC loading (via binding to AGO2's MID domain), a common practice is to chemically phosphorylate the 5'-modified antisense strands of the siRNAs prior to testing.[24]

To investigate the reasons behind inactivity of the siRNAs with 2'-5'-modified antisense strands, the AS strands of siRNAs Luc-AS4, -AS5, -AS6, -AS8, and the control duplex were 5'-phosphorylated, then annealed to their complementary sense strand and again tested in the luciferase assay (**Figure 3.4**). Chemical phosphorylation of antisense strand turned out to not enhance the RNAi activity of 2'-5'-linked siRNAs, as none of the chemically phosphorylated siRNAs could exhibit gene silencing activity. This finding form the basis of further mechanistic assessments that will be described in in section 3.9 of this chapter.

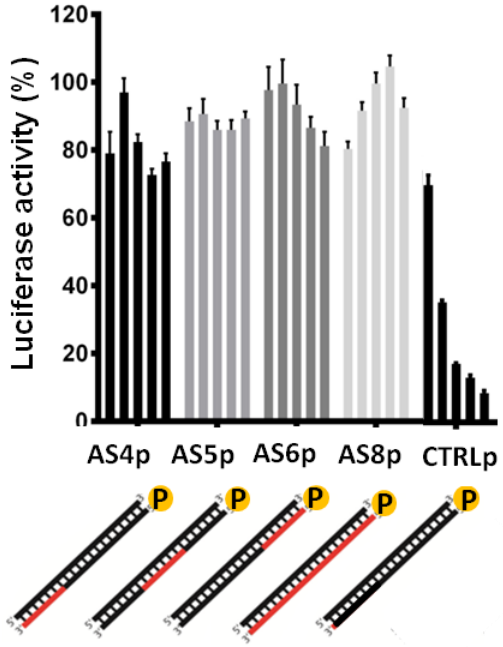

Figure 3.4 Assay demonstrating the activity of siRNAs AS4p, AS5p, AS6p, AS8p, and unmodified CTRL (control) with 2'-5' modification on their AS strand targeting firefly luciferase mRNA. All the antisense strands are 5'- phosphorylated chemically to bypass enzymatic phosphorylation by kinase. The red segments in the duplex illustrations represent the position of the 2'-5' modification within the antisense strand. "P" represents the 5'-PO group.

3.6 Targeting P53 mRNA by 2'-5'-modified siRNAs

When a potent siRNA design is found, the reproducibility of such siRNA needs to be tested against at least another (and preferentially many) different mRNA sequence(s). This ensures that the design can be universally applied to any target. Since we found that siRNAs targeting firefly luciferase were active when placing the 2'-5' modification in the sense strand, and inactive when modified in the antisense strand, we applied the same modification pattern within siRNAs targeting P53 mRNA.

The Trp53 tumor suppressor gene regulates cell division by coding p53, a protein that keeps cells from growing and dividing in an uncontrolled way. P53 also promotes cell death in response to hyperproliferative signals.[25] A "p53 knockdown assay" utilizes cells that have been transformed to overexpress Trp53. Given the high level of p53 protein they produce, these cells are constantly dying. Thus, the outcome of a successful p53 mRNA knockdown via RNAi, is that cells would now growth normally and rapidly. For this system, western blot assays are not precise enough to quantitate p53 protein levels,[26] hence we employed a luciferase reporter gene, containing a cloned target site for P53 siRNA.

The gene coding for the target mRNA is cloned upstream of a luciferase gene in an expression vector and then introduced into the cell, along with the siRNA targeting the mRNA.[27, 28] Since the target mRNA gene is fused to the luciferase reporter gene, the luciferase activity detected is directly correlated to the mRNA activity, and hence, is a measure of siRNA potency. All the Trp53-luciferase reporter assays described below were conducted by Dr. Regina Cencic from the Pelletier research group in the department of Biochemistry at McGill University.

3.6.1 P53 mRNA knockdown by 2'-5'-modified siRNAs

A library of siRNAs targeting P53 mRNA were synthesized (**Table 3.2**) following the same modification design utilized in the luciferase assays (Section 3.5). Renilla luciferase levels were measured relative to the unmodified renilla reporter, following treatment with chemically modified siRNAs at a range of concentrations (**Figure 3.5**).

While siRNAs modified in different positions of the sense strand showed high potencies comparable to the unmodified control, the siRNAs modified in the antisense strand either completely lost activity (p53-AS4) or showed diminished potencies (P53-AS5 and AS6). These results are in full agreement with our earlier findings with 2'-5' modified siRNAs targeting firefly luciferase. However, the decrease in activity induced by 2'-5' linkages in the AS strand seems to

Table 3.2 siRNAs targeting P53 mRNA, modified with 2'-5' linkages at various positions of sense or antisense strands. Sequences and thermal denaturation values of these siRNAs are shown below. Legend: 2'-5' linked RNA, 3'-5' linked RNA

Sample		Sequence	T_m value (°C)
P53-S1	(S)	3'-CCAAUGU GUACAUG AACAUCA-5'	64.0
	(AS)	5'-UUACACA UGUACUU GUAGUGG-3'	
P53-S2	(S)	3'-CCAAUGU GUACAUG AACAUCA-5'	57.3
	(AS)	5'-UUACACA UGUACUU GUAGUGG-3'	
P53-S3	(S)	3'-CCAAUGU GUACAUG AACAUCA-5'	59.5
	(AS)	5'-UUACACA UGUACUU GUAGUGG-3'	
P53-AS4	(S)	3'-CCAAUGU GUACAUG AACAUCA-5'	61.6
	(AS)	5'-UUACACAUGUACUU GUAGUGG-3'	
P53-AS5	(S)	3'-CCAAUGU GUACAUG AACAUCA-5'	59.8
	(AS)	5'-UUACACA UGUACUUGUAGUGG-3'	
P53-AS6	(S)	3'-CCAAUGU GUACAUG AACAUCA-5'	63.9
	(AS)	5'-UUACACA UGUACUU GUAGUGG-3'	
P53-ctrl	(S)	3'-CCAAUGU GUACAUG AACAUCA-5'	69.7
	(AS)	5'-UUACACA UGUACUU GUAGUGG-3'	

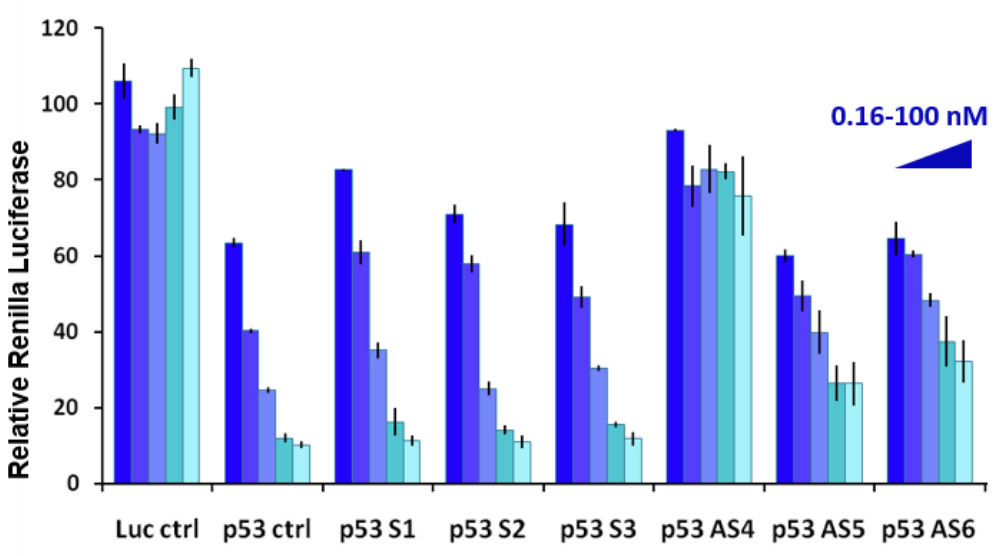

Figure 3.5 Renilla reporter assay demonstrating activity of 2'-5' modified siRNAs targeting P53 mRNA (n=2) at a range of 0.16, 0.8, 4, 20, 100 nM siRNA concentrations.

be sequence dependent. This was concluded based on the fact that, unlike AS modified siRNAs targeting luciferase, siRNAs p53-AS5 and -AS6 retained some activity (**Figure 3.5**). Predictably, among antisense modified siRNAs targeting p53, the most inactive siRNA was P53-AS4, which had the modification in the seed region, which is highly sensitive to modifications.

Similar to luciferase targeting siRNAs, no correlation was observed between activity and duplex thermal stability (T_m). Of note, the P53 target sequence, unlike the luciferase sequence, had a more homogenous distribution of the GC nucleotides across the siRNA duplex. Consequently, obvious correlations could not be observed between base sequence and duplex stability.

3.7 Immunostimulatory effect of 2'-5'-modified siRNAs

As previously explained in Chapter 1, chemical modification of siRNAs has proven to be helpful in lowering the immunostimulatory effect induced by ON drug candidates. For example, unmodified siRNA treatment can lead to a strong interferon-α (IFN-α) responses in human peripherial blood mononuclear cells (PBMCs).[29, 30] To investigate whether 2'-5' modified siRNAs are able to reduce the nonspecific immunostimulatory activity, an immune response assay on PBMC cells treated with unmodified or modified siRNAs was performed by Dr. Mayumi Takahashi (Dr. John Rossi lab) at the Beckman Research Institute at City of Hope.

siRNAs used in this study are listed in **Table 3.3**. PBMC cells were transfected with unmodified or modified siRNAs (**Figure 3.6**) using 1,2-dioleoyl-3-trimethylammoniumpropane (DOTAP), as the transfecting reagent. IFN-α and IL6 production levels were measured 24 hours later by an

Table 3.3 Sequences of single stranded RNAs and siRNAs modified with 2'-5' linkages targeting 728UU gene. Legend: 2'-5' linked RNA, 3'-5' linked RNA. The highlighted UGUGU sequence was reported to be the highly immunostimulatory motif and is incorporated in the sense strand of the siRNA targeting 728UU.

Sample	Sequence
728UU ctrl	5'- AAAUCGCUGAUUUGUGUAGUU-3' 3'-UUUUUAGCGACUAAACACAUC-5'
728UU-25S	5'-AAAUCGCUGAUUUGUGUAGUU-3' 3'-UUUUUAGCGACUAAACACAUC-5'
728UU-25AS	5'-AAAUCGCUGAUUUGUGUAGUU-3' 3'-UUUUUAGCGACUAAACACAUC-5'
RNA-S	5'-AAAUCGCUGAUUUGUGUAGUU-3'
RNA-AS	3'-UUUUUAGCGACUAAACACAUC-5'
2'5'-S	5'-AAAUCGCUGAUUUGUGUAGUU-3'
2'5'-AS	3'-UUUUUAGCGACUAAACACAUC-5'

enzyme-linked immunosorbent assay (ELISA). This experiment was initially performed on siRNAs previously tested in the P53 knockdown assays. However, the IFN and IL6 levels observed upon siRNA treatment were not high enough for a valid comparison between modified and unmodified samples. To overcome this, we selected an siRNA sequence previously reported to have strong immunostimulatory activity in PBMCs (728UU).[29] The high immune response detected with this sequence was reported to be due to a "UGUGU" pentanucleotide sequence embedded in sense RNA strand. Hence, we aimed to investigate whether the corresponding siRNAs with a 2'-5'-linked UGUGU segment would exert the same immune response (**Figure 3.6**).

The data obtained suggest that PBMCs treated with the unmodified control siRNAs (728UU ctrl) and single stranded RNA controls (RNA-S and RNA-AS) led to a significant increase in IFN

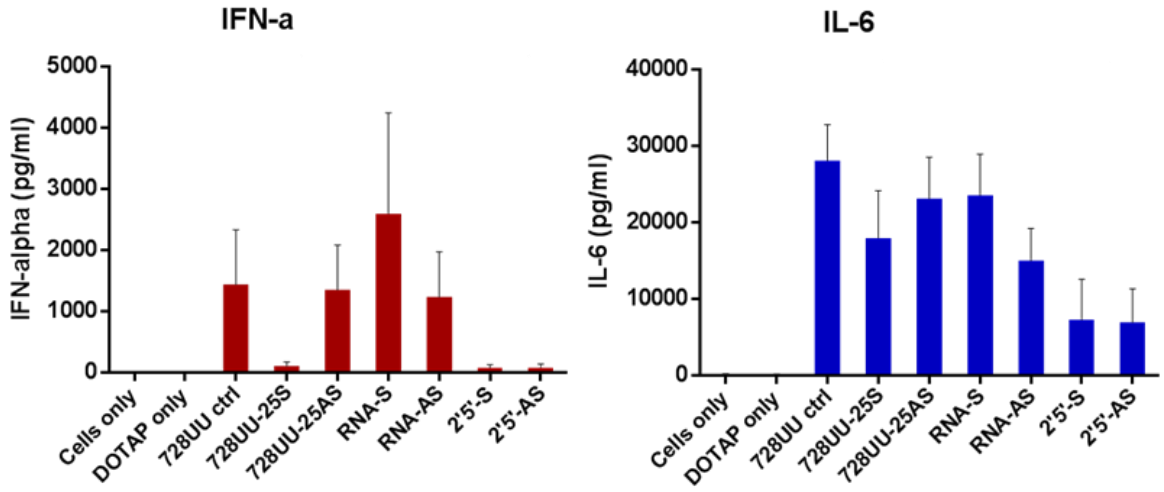

Figure 3.6 Comparison of immunostimulation prior to treatment with the siRNAs targeting 728UU. IFN levels were measured in PBMC cells 24 hours after siRNAs were transfected in duplicate using DOTAP. IFN-α levels (left graph) and IL-6 levels (right graph) in response to unmodified control siRNAs (728UU ctrl) and control single stranded RNAs (RNA-S and RNA-AS), is compared to 2'-5'- modified siRNAs (728UU-25S and 728UU-25AS) and single stranded 2'-5' RNAs (2'-5'-S and 2'-5'-AS). Cells only was the negative control with no reagents. DOTAP only treatment was transfection without siRNA. Data were collected in duplicate for each of six donors. Bars indicate standard deviation.

production compared to the mock treatments (i.e., cells with either no treatment or cells exposed only to DOTAP) (**Figure 3.6**).

Modification of the AS strand of 728UU siRNA (728UU-25AS), or within the UGUGU segment located in the sense strand (728UU-25S), all lowered IFN levels. However, IFN levels induced by 728UU-25S was significantly lower, in comparison with 728UU-25AS, suggesting that direct modification of UGUGU motif has a more pronounced effect on abrogating the immune response. Interestingly, the unmodified RNA single strands (RNA-S and RNA-AS) were immunostimulatory, in contrast to the corresponding 2'-5'-modified single strands (2'-5'-S and 2'-5'-AS). This result suggests that, independent of base sequence, incorporation of 2'-5' linkages abrogate the immunostimulatory profile of single stranded ONs. Induction of IL6 by siRNAs followed the same general trend, although reduction in IL6 levels by treatment with modified siRNAs were not as significant (**Figure 3.6**).

In summary, these results demonstrate that the immunostimulatory effect of siRNAs can be abrogated by incorporation of 2'-5' linkages within their sequence. The effect was more profound when the 2'-5' linkages were placed within the immunostimulatory motif, indicating that the degree by which the 2'-5' modification can reduce immunostimulation is somewhat sequence dependent.

3.8 Positional screening of 2'-5' linkage in siRNAs with modified AS strand

Previously, we demonstrated that incorporation of even up to 33% 2'-5' linkages in siRNA's AS strand resulted in loss of RNAi activity. The 2'-5' modification was found to be most detrimental when placed in the seed region of the duplex. The results of our study showing that 2'-5' linkage in an siRNA can decrease the immune response, encouraged us to investigate the tolerance of antisense strand for this modification in more detail. Specifically, we wondered if single and/or multiple substitution effects in the antisense strand are position-dependent. Towards these goals, we focused on a library of siRNAs targeting firefly luciferase containing all possible 2'-5' substitutions within the AS strand UUAAUU segment, located at the 5'-end of the AS strand. These nucleotides fall in the siRNA seed region, which is known to be very sensitive to chemical modifications, and so, its interaction with AGO2 has been studied in depth.[31-37]

To build the siRNAs with all possible modification patterns at this region, a library of (2)^6 = 64 oligonucleotide strands were synthesized as AS strands (we will refer to this library in this thesis as the "64-member library"; **Table 3.4**). Strands synthesized had a range of zero to six 2'-5' linkages statistically distributed along the 6-nt segment and annealed to the complementary sense strand for luciferase assay screening.

The initial screening was performed at one siRNA concentration (20 nM). The efficiency of these siRNAs in knocking down the firefly luciferase mRNA is arranged based on their potency from the most active (#1) to the least active (#56) siRNA (**Figure 3.7**).

Table 3.4 siRNA antisense strands modified with 2'-5'linkages at six nucleotides at the 5' terminal. Modified region is underlined. 3'-5' linked RNA, 2'-5' linked RNA (lowercase), RNA (unmodified region). Sense strand sequence is5'- GCUUGAAGUCUUUAAUUAAUU -3'.

1	5'- UUAAUUAAAGACUUCAAGCGG -3'	33	5'- uUAAUUAAAGACUUCAAGCGG -3'
2	5'- UUAAUuAAAGACUUCAAGCGG -3'	34	5'- uUAAUuAAAGACUUCAAGCGG -3'
3	5'- UUAAuUAAAGACUUCAAGCGG -3'	35	5'- uUAAuUAAAGACUUCAAGCGG -3'
4	5'- UUAAuuAAAGACUUCAAGCGG -3'	36	5'- uUAAuuAAAGACUUCAAGCGG -3'
5	5'- UUAaUUAAAGACUUCAAGCGG -3'	37	5'- uUAaUUAAAGACUUCAAGCGG -3'
6	5'- UUAaUuAAAGACUUCAAGCGG -3'	38	5'- uUAaUuAAAGACUUCAAGCGG -3'
7	5'- UUAauUAAAGACUUCAAGCGG -3'	39	5'- uUAauUAAAGACUUCAAGCGG -3'
8	5'- UUAauuAAAGACUUCAAGCGG -3'	40	5'- uUAauuAAAGACUUCAAGCGG -3'
9	5'- UUaAUUAAAGACUUCAAGCGG -3'	41	5'- uUaAUUAAAGACUUCAAGCGG -3'
10	5'- UUaAUuAAAGACUUCAAGCGG -3'	42	5'- uUaAUuAAAGACUUCAAGCGG -3'
11	5'- UUaAuUAAAGACUUCAAGCGG -3'	43	5'- uUaAuUAAAGACUUCAAGCGG -3'
12	5'- UUaAuuAAAGACUUCAAGCGG -3'	44	5'- uUaAuuAAAGACUUCAAGCGG -3'
13	5'- UUaaUUAAAGACUUCAAGCGG -3'	45	5'- uUaaUUAAAGACUUCAAGCGG -3'
14	5'- UUaaUuAAAGACUUCAAGCGG -3'	46	5'- uUaaUuAAAGACUUCAAGCGG -3'
15	5'- UUaauUAAAGACUUCAAGCGG -3'	47	5'- uUaauUAAAGACUUCAAGCGG -3'
16	5'- UUaauuAAAGACUUCAAGCGG -3'	48	5'- uUaauuAAAGACUUCAAGCGG -3'
17	5'- UuAAUUAAAGACUUCAAGCGG -3'	49	5'- uuAAUUAAAGACUUCAAGCGG -3'
18	5'- UuAAUuAAAGACUUCAAGCGG -3'	50	5'- uuAAUuAAAGACUUCAAGCGG -3'
19	5'- UuAAuUAAAGACUUCAAGCGG -3'	51	5'- uuAAuUAAAGACUUCAAGCGG -3'
20	5'- UuAAuuAAAGACUUCAAGCGG -3'	52	5'- uuAAuuAAAGACUUCAAGCGG -3'
21	5'- UuAaUUAAAGACUUCAAGCGG -3'	53	5'- uuAaUUAAAGACUUCAAGCGG -3'
22	5'- UuAaUuAAAGACUUCAAGCGG -3'	54	5'- uuAaUuAAAGACUUCAAGCGG -3'
23	5'- UuAauUAAAGACUUCAAGCGG -3'	55	5'- uuAauUAAAGACUUCAAGCGG -3'
24	5'- UuAauuAAAGACUUCAAGCGG -3'	56	5'- uuAauuAAAGACUUCAAGCGG -3'
25	5'- UuaAUUAAAGACUUCAAGCGG -3'	57	5'- uuaAUUAAAGACUUCAAGCGG -3'
26	5'- UuaAUuAAAGACUUCAAGCGG -3'	58	5'- uuaAUuAAAGACUUCAAGCGG -3'
27	5'- UuaAuUAAAGACUUCAAGCGG -3'	59	5'- uuaAuUAAAGACUUCAAGCGG -3'
28	5'- UuaAuuAAAGACUUCAAGCGG -3'	60	5'- uuaAuuAAAGACUUCAAGCGG -3'
29	5'- UuaaUUAAAGACUUCAAGCGG -3'	61	5'- uuaaUUAAAGACUUCAAGCGG -3'
30	5'- UuaaUuAAAGACUUCAAGCGG -3'	62	5'- uuaaUuAAAGACUUCAAGCGG -3'
31	5'- UuaauUAAAGACUUCAAGCGG -3'	63	5'- uuaauUAAAGACUUCAAGCGG -3'
32	5'- UuaauuAAAGACUUCAAGCGG -3'	64	5'- uuaauuAAAGACUUCAAGCGG -3'

As expected, the most active siRNA among all members was the unmodified siRNA. Next, we analyzed the siRNA activity of siRNAs having the same number of modifications. Each group of siRNAs containing the same number of modifications can have multiple possible arrangements, depicted as color-coded subsets in **Figure 3.7**.

This analysis revealed some interesting patterns particularly for the subgroups containing two or more linkage modifications: (i) The number of modification in each siRNA is not the only factor governing the siRNA activity. For instance, siRNA #61 with four modifications is much more active than many of the siRNAs with three modifications, suggesting that modification pattern plays a role in the siRNA activity. (ii)The most active siRNAs have a consecutive arrangement of 2'-5' linkages, whereas the least active siRNAs have alternating 2'-5' and 3'-5' linkages. This pattern was observed among all subsets, with siRNAs #7 and #11 (2 modifications subset), #8 and #38 (3 modifications subset), and#61 and #54 (3 modifications subset) as the most and the least active samples, respectively.

While the reasons behind this pattern dependence among 2'-5' siRNAs is unknown, it is interesting to note that a recent study by Szostak and co-workers[13] suggests that 2'-5' linkages that are flanked with 3'-5' RNA nucleotides show less perturbation in the duplex parameters, due to the flexibility induced by the flanking 3'-5'-linked RNA nucleotides. However, we found that such alternating arrangement in siRNA lead to less active duplexes, suggesting the local structural changes induced by certain 2′-5′ patterns affect activity. Interestingly, previous studies from our group[16] comparing the stability changes in $(rA)_{10}$: $(rU)_{10}$ duplexes which differ only in the arrangement of their 2'-5' linkages (alternating vs. consecutive), exhibited significantly different stability patterns: duplexes with consecutive 2'-5' linkages, appeared to destabilize the helix less than duplexes with alternating 2′-5′ arrangements.

However, in the series of decamer duplexes with mixed base sequence, the composition of the nucleotides being connected via a 2′-5′ linkage was more influential, than the arrangement of the 2′-5′ linkages. For instance, substitution of 2',5' linkages between uridines was more destabilizing relative to substitutions between adenosines.[16] Clearly, the degree which an siRNA duplex is destabilized by 2',5' linkages largely depends on both the sequence and arrangement of the linkage modifications.

We hypothesize that alternating 2'-5' linkages disturb the duplex structure to a larger extent than the consecutive 2'-5' linkages, by virtue of the larger region being perturbed by alternating linkages. Any firm conclusions correlating siRNA potency and structure will require detailed structural investigation of siRNA duplexes bound to AGO2. We try to address this issue in Section 3.10 of this Chapter.

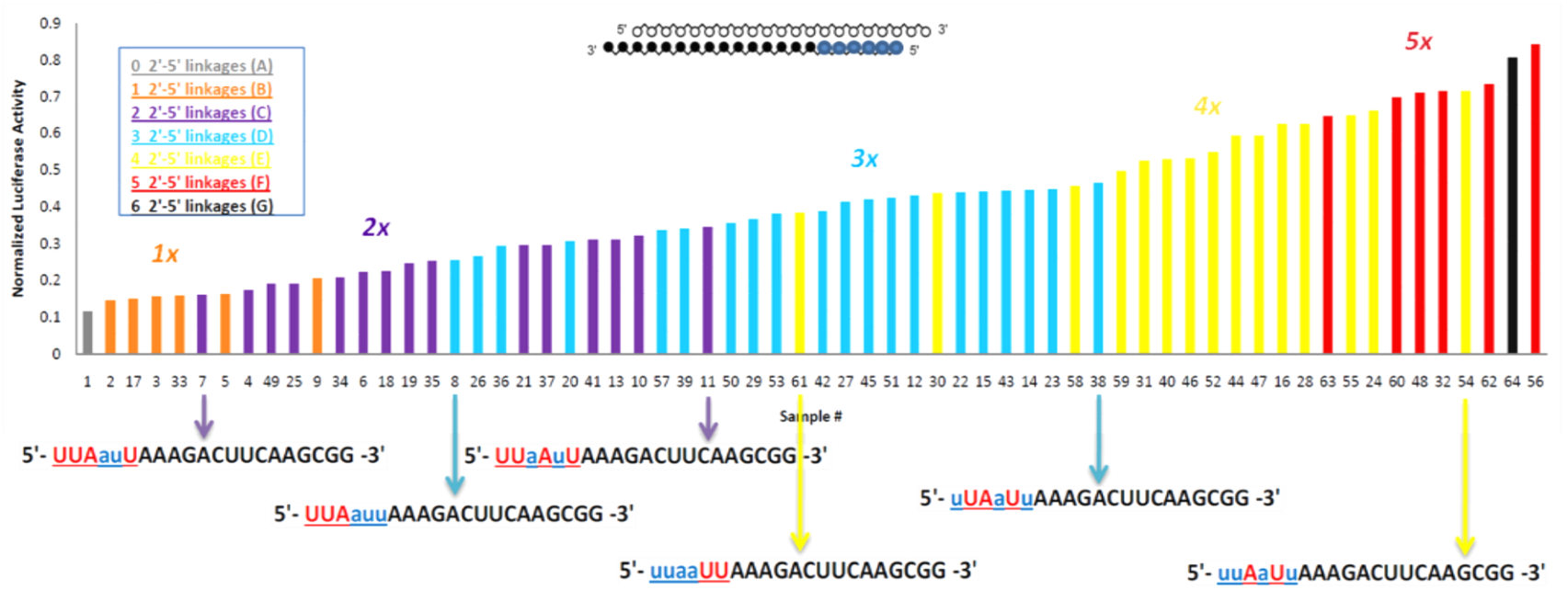

Figure 3.7 Positional screening of 2'-5' linked siRNAs targeting firefly luciferase. siRNAs are modified on the six nucleotides on the 5'-terminal of AS strand and are represented by the number corresponding to their AS strand shown in **Figure 3.4**. siRNAs luciferase activity is normalized to the negative control. siRNAs are arranged from the most active siRNA (#1) to the least active siRNA (# 56) The AS strand in these siRNAs has between zero to six 2'-5' linkages statistically distributed among the six nucleotides. Each color represents a group of siRNAs with the same number of modifications. Within each group, the modification pattern corresponding to the AS strand of the most and least active siRNAs areshown with an arrow underneath the graph. Sense strand of these siRNAs is omitted for clarity.

3.9 Mechanistic investigations: 2'-5' linkage modification in the siRNAs AS strand

Following our positional screening of 2'-5' AS-modified siRNAs, we became interested in gaining more mechanistic understanding on the underlying factors governing the acceptance of 2'-5' modification in the AS strand. The studies, thus far, have suggested that 5′-phosphorylation of the AS is likely not rate limiting, although this remained to be verified. It was also conceivable that efficiency of siRNA loading into hAGO2 was compromised by modification of the AS strand. Hence, both in vitro phosphorylation assay and an hAGO2 loading assay were set up. 2'-5' modified siRNAs (#49 and #64), as well as the unmodified control siRNA targeting firefly luciferase from the previously synthesized 64 library (**Table 3.4**) were chosen as model duplexes in this study.

3.9.1 Interactions of 2'-5'-linked siRNAs with kinase

Enzymatic phosphorylation normally results in the phosphorylation of both 5' terminals in an siRNA. However, since we were specifically interested in the ability of the kinase to phosphorylate the AS strands modified on the seed region, we performed the labelling assay only on the modified AS single strand, rather than their corresponding siRNA duplexes (**Figure 3.8**). During a phosphorylation assay, kinase enzyme incorporates a radiolabeled phosphate group from radioactive [γ-^{32}P] ATP into the 5'-OH of the oligonucleotide strand. The measurement of the amount of radioactivity incorporated into an RNA substrate, after RNA purification to remove the excess [γ-^{32}P] ATP, allows a comparison of the enzyme activity in between different samples. Our kinase assays revealed that an RNA strands modified at their 5' terminal with two 2'-5' linkages (AS-49) is efficiently recognized as substrate by the kinase, as it underwent 5' phosphorylation very efficiently. The efficiency of phosphorylation decreased slightly for AS-64,

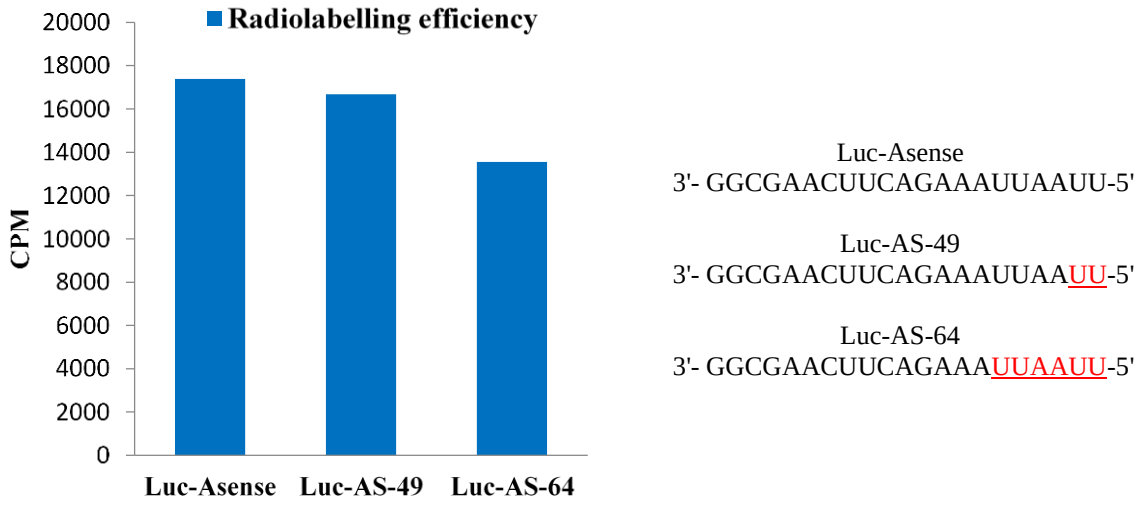

Figure 3.8 Kinase efficiency in radiolabelling 2'-5' linked RNAs. 2'-5' linked RNAs (Luc-AS-49 and Luc-AS-64) are substrates of kinase. However, they undergo 5'-phosphorylation less efficiently in comparison with unmodified RNA. Legend: 3'-5' linked RNA, 2'-5' linked RNA.

with six 2'-5' linkages (**Figure 3.8**), and significantly more so for a fully 2'-5' linked RNA strand (data not shown).

These findings ruled out 5′-phosphorylation as the cause for the poor activity observed for AS-modified siRNAs, and led us to look at subsequent steps, specifically at loading of siRNA into hAGO2, a key component of RISC.

3.9.2 Interactions of 2'-5'-linked siRNAs with hAGO2

We hypothesized that extensive AS strand modification in these siRNAs is detrimental to their optimal loading (or positioning) into RISC, therefore diminishing or abolishing gene silencing activity. It, also, occurred to us that extensive 2'-5' modification can be exploited to direct RISC to load and position the other strand for mRNA targeting. For example, introducing 2′-5′ modification in the sense strand may favour selection of the other (AS) strand for gene silencing. To test these hypotheses, 2'-5' modified ssRNA and siRNAs targeting firefly luciferase were 5'-radiolabelled by kinase enzyme, incubated with hAGO2 protein, and the resulting complex(es)

were analyzed by EMSA (electrophoretic mobility shift assays). The 2'-5'-RNA:RNA duplexes tested are shown in **Figure 3.9**. One duplex (RNA:2'-5'p) contains a single ^{32}P-label placed on the fully modified 2'-5'-RNA strand, whereas the other contains the label in both strands (pRNA:2'-5' p). A labeled single stranded 2'-5' –RNA (2'-5'p) was used as control. Loading occurs by anchoring the 5'-phosphate into the MID domain of hAGO2.

The results of this experiment are shown in **Figure 3.9**. When both siRNA strands were phosphorylated (pRNA:2'-5'p), a new, slow moving band appeared consistent with formation of a ribonucleoprotein complex (**Figure 3.9**). In contrast, neither the single strand (2'-5'p), nor the singly labeled duplex (RNA:2'-5'p) loaded into hAGO2 (no appearance of slower moving bands; **Figure 3.9**), suggesting that hAGO2 cannot bind the 5'-phosphate of a 2′-5′-RNA strand. The fact that only pRNA:2'-5'p loaded suggest that binding occurs via the terminal phosphate of the 3'-5' -RNA strand. That is, full modification of one strand favours anchoring the siRNA via the

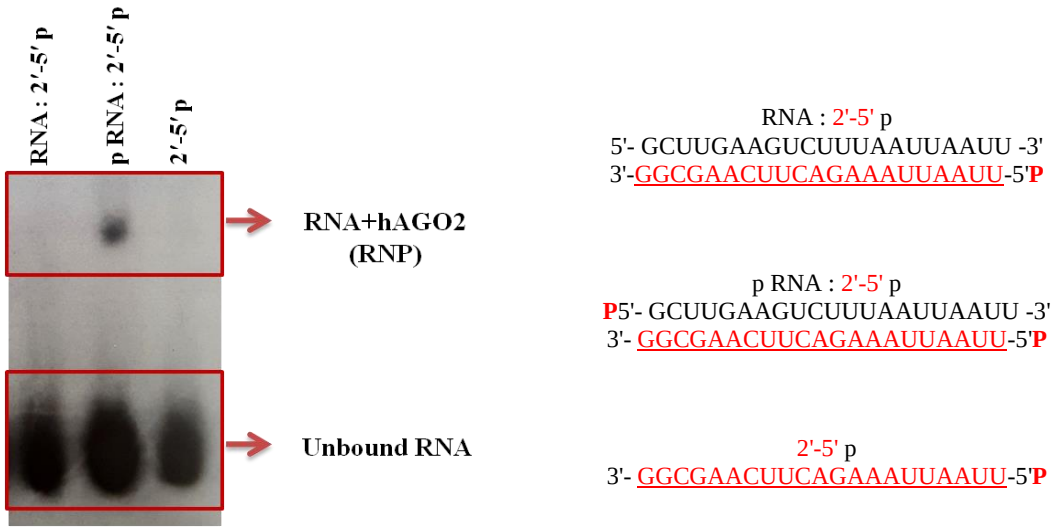

Figure 3.9 EMSA profile of modified siRNA duplexes (RNA:2'-5'p and pRNA:2'-5'p) and single strands (2'-5'p) targeting firefly luciferase and recombinant human AGO2. Among them, only pRNA:2'-5'p was loaded into RISC. Experimental details are provided in the experimental section. Legend: 3'-5' linked RNA, 2'-5' linked RNA.

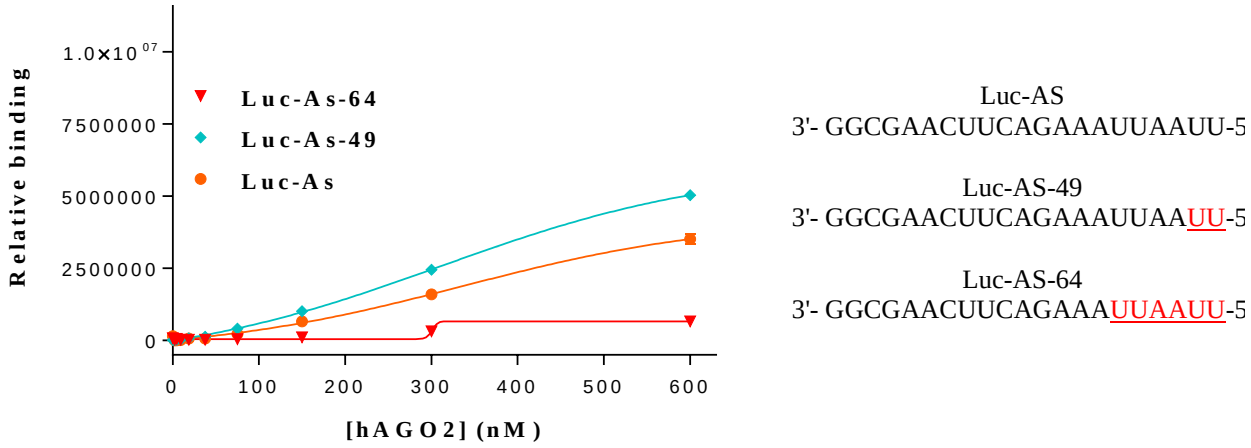

Figure 3.10 Titration profiles of 2'-5' modified ssRNAs (Luc-AS-49 and Luc-AS-64) as well as the unmodified ssRNA with increasing concentrations of recombinant human AGO2. The experiment was carried out using the dot-blot instrument. Legend: 3'-5' linked RNA, 2'-5' linked RNA.

other strand. The implications of this is that positioning of the right (AS) strand can be enhanced by introducing a significant number of 2'-5' linkages in the sense strand.

Next, we decided to measure the binding affinity of a selected number of partially 2'-5' modified ssRNAs (Luc -49 and -64) as well as the unmodified control RNA (Luc-AS). After radiolabelling, these samples were titrated by increasing concentrations of hAGO2 in order to quantitate their relative binding affinity to hAGO2 (**Figure 3.10**). Our preliminary results show that binding affinity of 2'-5' modified RNAs drastically decrease upon modification of six nucleotides at the 5' terminal (Luc-AS-64). Interestingly, Luc-AS-49 with the last two 5'-terminal nucleotides showed higher binding affinity to hAGO2 in comparison with the unmodified RNA (Luc-AS). Thus, the preferential bias to load one strand over the other appears to be dependent on the extent of modification. We are currently performing more detailed investigations into the binding affinity of 2'-5' modified RNAs with hAGO2.

3.10 Molecular modelling and MD studies of 2′-5' – linked siRNAs – hAGO2 complexes

Our next step was to investigate the effect of 2'-5' modification on the interactions of the antisense-modified siRNA and hAGO2. We had previously shown with our 64-member library that increasing the number of linkage modifications has generally an inverse effect on the siRNA potency. Also, our preliminary hAGO2 loading experiments suggested that this effect is possibly due to interruptions in the loading of the modified AS strand in the active site of hAGO2. Various siRNA modifications have been reported to affect RNAi activity, particularly when placed at the seed region (nucleotides 2-8 from 5' terminal of AS).[38-40] While 2'-FRNA and 2'-OMe modifications are generally tolerated at all positions in the AS strand, other modifications are shown to be tolerated only at specific positions in the AS strand. For instance, siRNAs containing 2'-*O*-benzyl (2'-OB) modification in the AS strand at positions g5, g8, g15, and g19 show enhanced RNAi activity in comparison to the unmodified siRNA control. The same modification, however, is detrimental to the RNAi activity when placed at position g2 of the AS strand.

The following sections show our investigation into the hAGO2 binding and positional effect of 2'-5' modification in the siRNA seed region using molecular dynamic (MD) simulations. These studies were performed in collaboration with Dr. Hari Krishna at the research group of Dr. P.I. Pradeepkumar at the Indian Institute of Technology.

3.10.1 MD simulations of 2'-5'-linked siRNAs (49) and (54) and hAGO2

MD studies were carried out on unmodified, as well as two previously tested modified siRNAs (#49 and #54), targeting firefly luciferase. MD simulations were performed using GPU

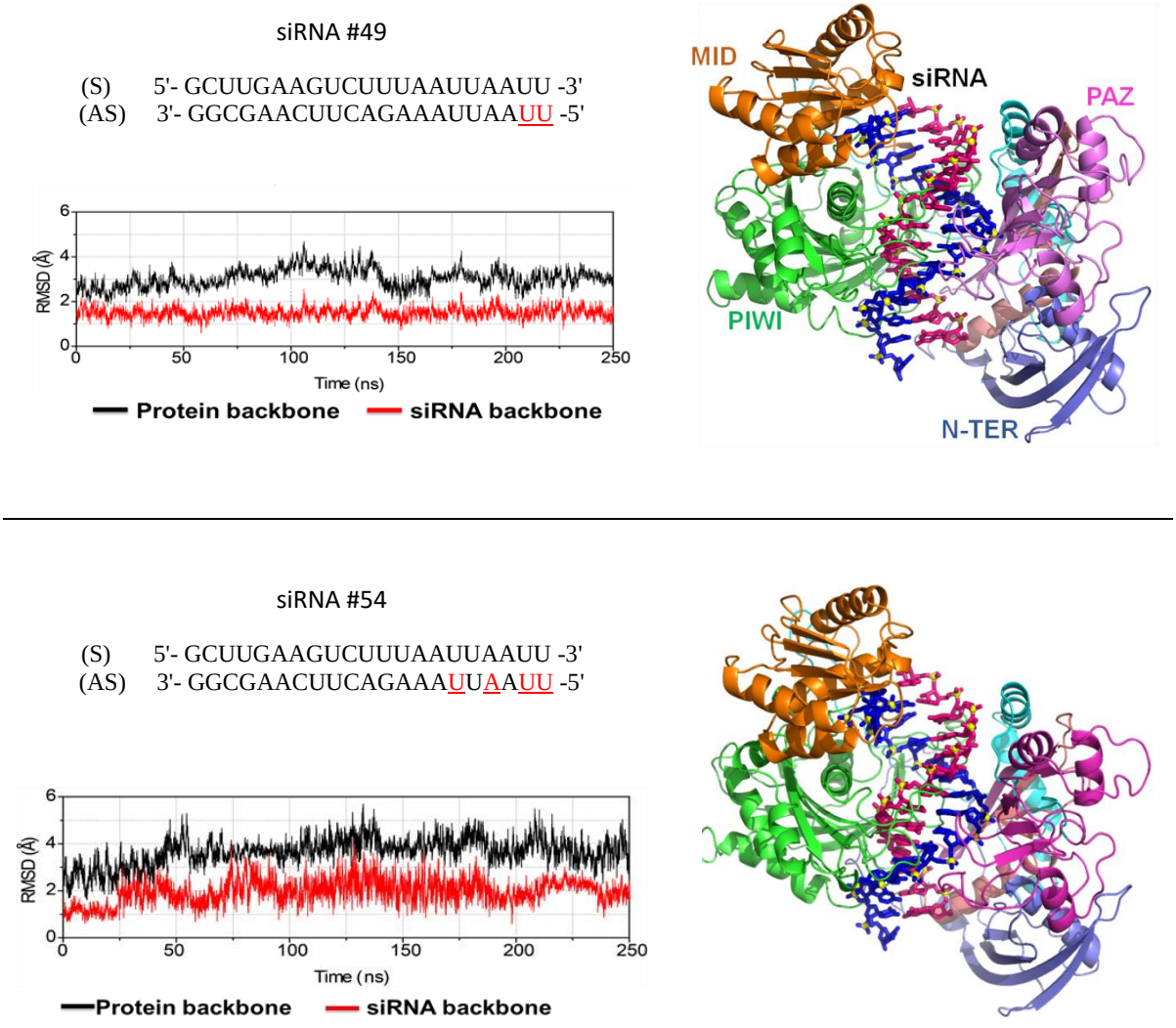

Figure 3.11 Docked structures and root-mean-square deviation (RMSD) graphs from the MD simulations of the 2'-5' linked siRNAs#49 (top) and #54 (bottom) and hAGO2. hAGO2 in the docked structures in presented in cartoon, each domain of the protein is labelled in a different colour; siRNA backbone is presented in ball and stick with AS strand in magenta and passenger strand in blue. RMSD graphs were calculated over 250 ns using equilibrated structures as the reference with hAGO2 displayed in black and siRNA displayed in red. Legend: 3'-5' linked RNA, 2'-5' linked RNA.

accelerated version of AMBER 14.[41] One of the highest quality reported crystal structures of hAGO2 contains a miRNA: target mRNA duplex engaged via eight nucleotide base pairs (PDB entry: 4W5O).[15, 42]

However, in our study, an open conformation of hAGO2 was required to investigate the binding interactions of hAGO2 and an siRNA with nucleotides 2-19 base paired. Once the open hAGO2 was developed (details in experimental section), it was used to dock with the unmodified siRNA, as well as siRNAs 49 and 54. The final MD snapshot of the siRNAs and hAGO2 after 250 ns of MD simulation is shown in **Figure 3.11**.

The RMSD graph of the siRNA 49/hAGO2 complex (**Figure 3.11**, top) shows that the complex was quite stable during the simulations. However, siRNA 54/hAGO2 complex, as shown in the corresponding RMSD graph (**Figure 3.11**, bottom), was found to be highly flexible, especially around the 2'-5' modified region. This was attributed to the high flexibility of the siRNA #54 due to the structural changes of the RNA duplex upon 2'-5' modification.

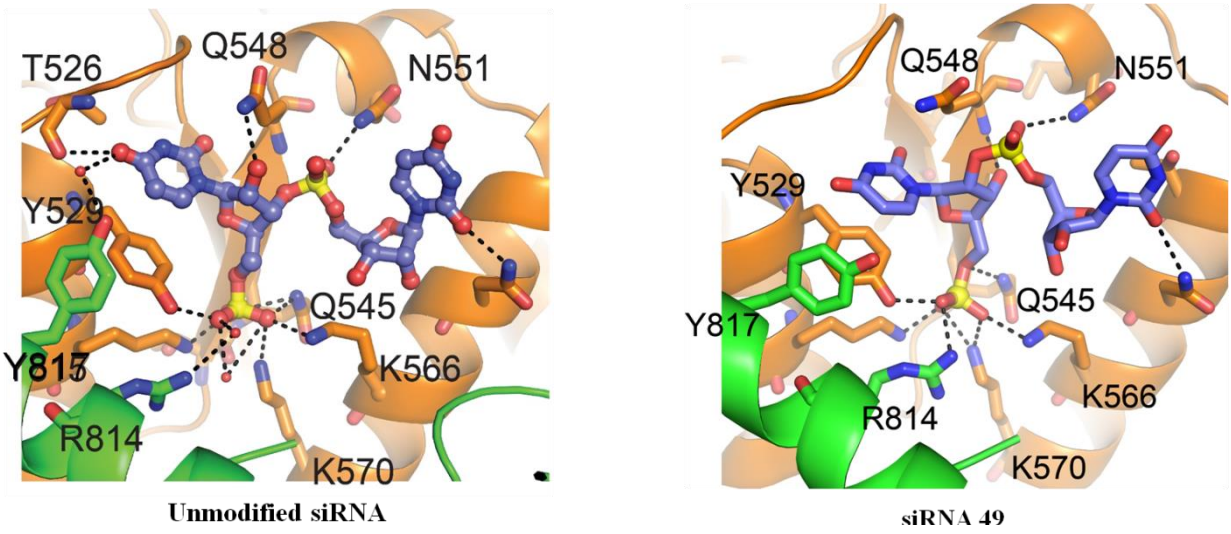

Figure 3.12 Non-covalent interactions between hAGO2 and 5' terminal of unmodified siRNA (left) and siRNA 49 (right). Key interacting amino acid residues of hAGO2 are labelled in both siRNAs. Most of non-covalent interactions between hAGO2 and siRNA 49 are retained.

Next, we compared the non-covalent interactions of hAGO2/unmodified siRNA complex with the interactions of the hAGO2 with the modified siRNAs 49 and 54. Averaged structures from the last 50 ns of the 250 ns MD simulations between hAGO2/ unmodified siRNA and hAGO2/siRNA 49 complexes were compared. siRNA 49, in comparison with the unmodified siRNA, only lost a very few non-covalent interactions at the 5'-binding pocket of hAGO2 (**Figure 3.12**).

Remarkably, the 2'-5' linkage between g1 and g2 did not affect the phosphate backbone bent

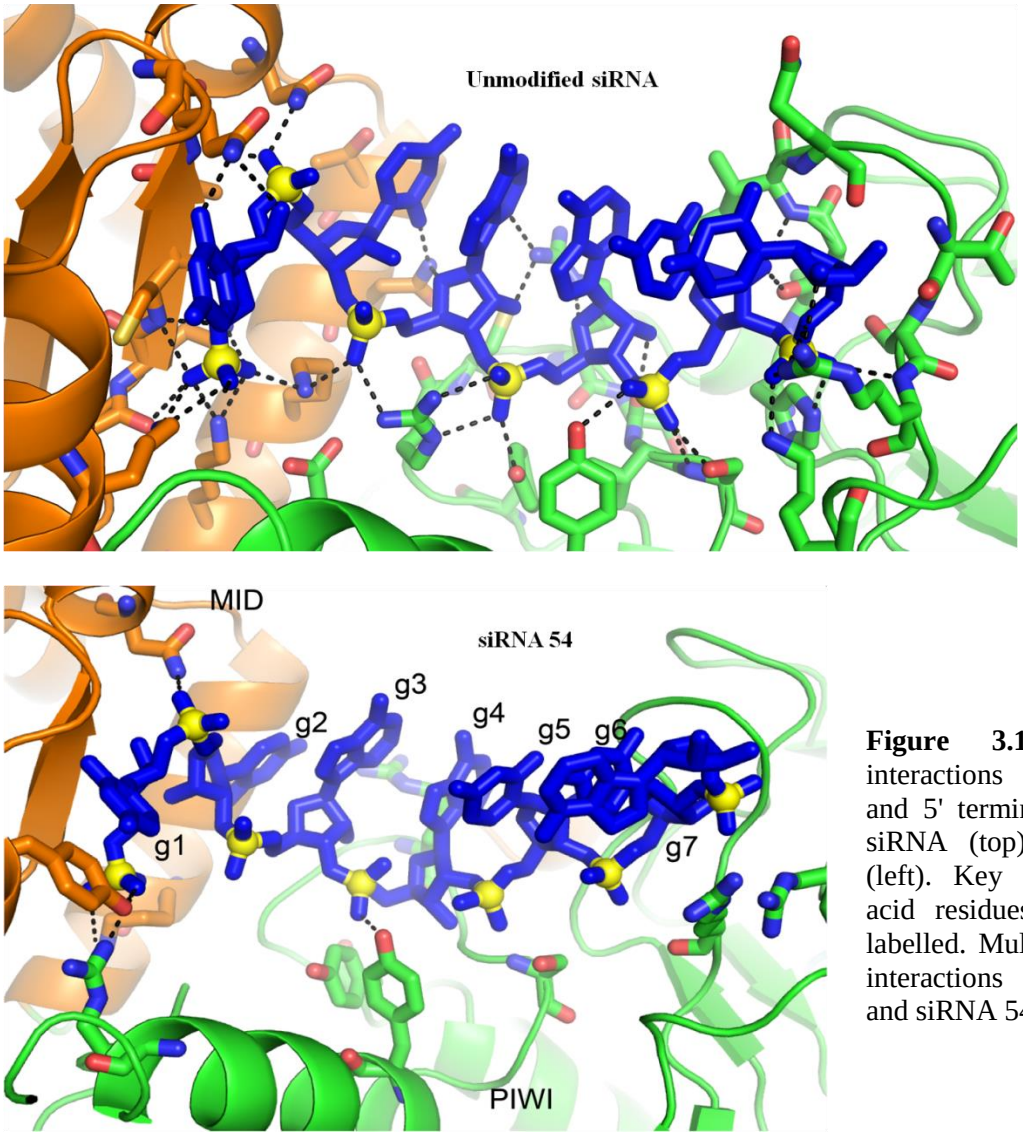

Figure 3.13 Non-covalent interactions between hAGO2 and 5' terminal of unmodified siRNA (top) and siRNA 54 (left). Key interacting amino acid residues of hAGO2 are labelled. Multiple non-covalent interactions between hAGO2 and siRNA 54 are lost.

previously characterized for native RNA (clover leaf structure), however T526, Y529, Q548 interactions with the hAGO2 were lost. These results are in agreement with the retained gene silencing activity of siRNA 49 (**Figure 3.7**).

Similar comparison, however, between hAGO2/unmodified siRNA and hAGO2/siRNA 54 complexes showed that, in this case, many non-covalent interactions between the protein and the modified siRNA are lost during the molecular dynamics, i.e., interactions between Q545, K570, K566, N551, K550, R792, R795, H753, Q757 and Y790 amino acid residues in hAGO2 and the RNA AS strand (**Figure 3.13**). This likely accounts for the inactivity observed for siRNA 54 (**Figure 3.7**).

As mentioned above, the 5' nucleotide in siRNAs has a crucial bend in the backbone referred to as the clover leaf junction (**Figure 3.14**). Deviation from this structure due to modification of the g1 and g2 nucleotides can be linked to loss of non-covalent interactions between hAGO2 and RNA.[15, 43] As shown in **Figure 3.14**, this structure comprises of eight sugar-phosphate backbone dihedral angles. To probe how the 2'-5' linkage is accommodated in the clover leaf into the MID domain of hAGO2, the backbone dihedral angle values at the junction of two nucleotides were calculated from the structure which is averaged from the last 50 ns of 250 ns MD simulations.

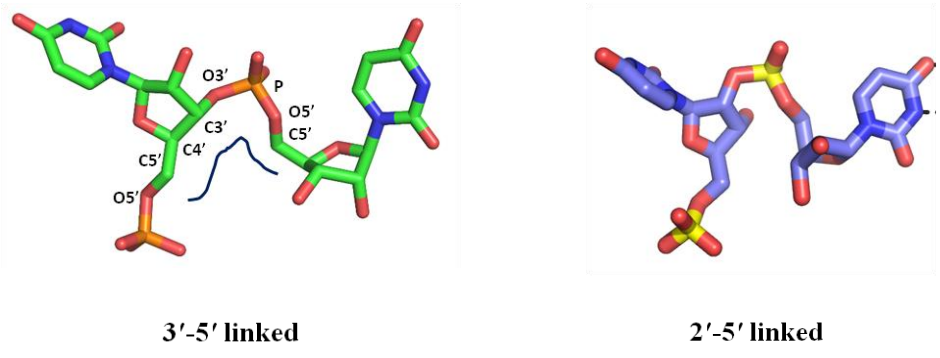

Figure 3.14 Clover leaf junction in an unmodified 3'-5' linked (left) versus a 2'-5' linked (right) siRNA. Atoms comprising the dihedral angels are labelled. Clover leaf junction is illustrated by a dark line.

Table 3.5 Dihedral angle adopted by the unmodified and modified siRNAs at the junction of g1 and g2 (clover leaf model).[a]

Unmodified	Dihedral angle values	Modified	Dihedral angle values (49)	Dihedral angle values (54)
O5'-C5'-C4'-C3'	-173.5	O5'-C5'-C4'-C3'	-179.8	-172.3
C5'-C4'-C3'-O3'	-143.8	C4'-C3'-C2'-O2'	-150.7	-155.5
C4'-C3'-O3'-P	-146.7	C3'-C2'-O2'-P	-45.6	-43.9
C3'-O3'-P-O5'	53.6	C2'-O2'-P-O5'	-38.3	-41.2
O3'-P-C5'-O5'	65.8	O2'-P-C5'-O5'	120.5	127.6
P-O5'-C5'-C4'	154.7	P-O5'-C5'-C4'	-160.6	-156.4
C5'-C4'-C3'-O3'	41.6	C5'-C4'-C3'-O3'	-33.9	-41.7

[a]All the values are mentioned in degree and computed using X3DNA package.

The deviation of these angles for siRNAs 49 and 54 from the unmodified siRNA torsion angles is presented in **Table 3.5**. In both modified siRNAs, the dihedral angles varied largely only at the linked sites; however, the structure and nature of the whole bent was not affected. This suggests that 2'-5' modified siRNAs were flexible enough to adjust themselves to the clover leaf structure.

3.10.2 The effect of 2'-5' linkage on the nucleotide conformation

Sugar conformation of nucleotides is a key factor affecting backbone angles, and final duplex conformation. Variations in the sugar conformation may lead to the disturbance in the geometry of the RNA duplex from the favoured A-form.

We studied the effect of 2'-5' linkage on the siRNA conformation by investigating the sugar conformation of the seed region nucleotides. The percentage of sugar conformation in these nucleotides was calculated from the 250 ns MD trajectory using Altona and Sundaralingam sugar

conformation pseudorotation wheel of nucleotides.[44, 45] Generally, in an unmodified siRNA, the ribose sugar in the g1 nucleotide adopts a *C2'-endo* (South) conformation, and the rest of the nucleotides, from the g2 position onwards, adopt a *C3'-endo* (North) conformation.

In both siRNAs 49 and 54, the sugar conformation of the 2'-5' linked nucleotides were found to be flexible between the *C3'-endo* and *C2'-endo* (**Figure 3.15**). Our results were in agreement with previous X-ray crystallographic studies and molecular dynamics (MD) simulations by the

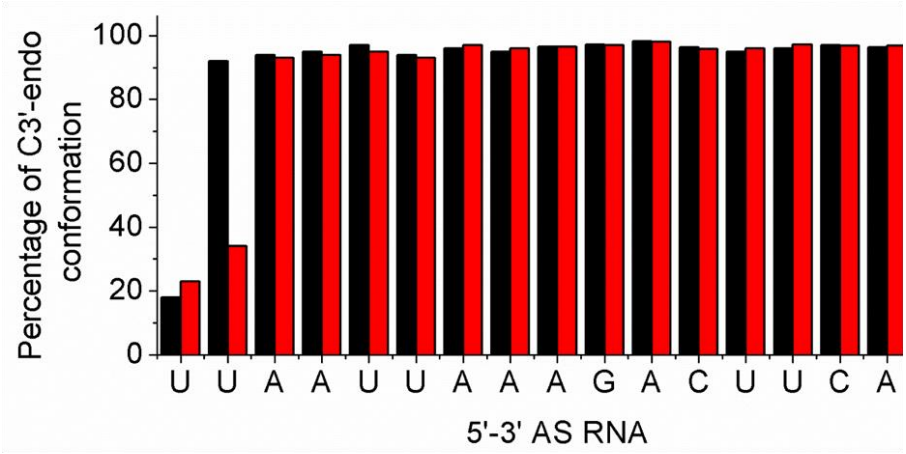

Unmodified siRNA vs. siRNA 49

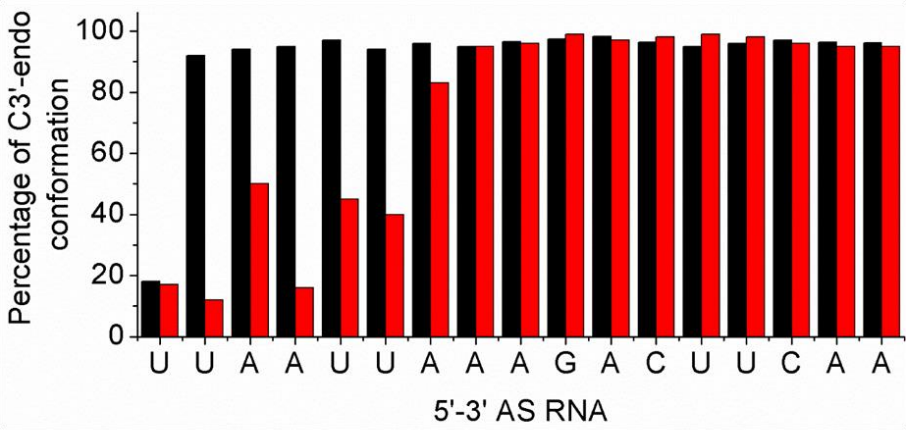

Unmodified siRNA vs. siRNA 54

Figure 3.15 Sugar conformation of AS strand nucleotides in unmodified (black bars) versus 2'-5' modified (red bars) siRNAs 49 (top graph) and 54 (bottom graph).

Szostak group, showing that in RNA duplexes modified with some 2'-5' linkages, the modified nucleotides can adopt either the *C3'-endo* or *C2'-endo* conformation, with a preference for the latter.[13]

Furthermore, they reported that the structural perturbations caused by 2'-5' linkages mainly affected the two nearest base pairs and had minimal effects on the rest of the duplex.[13] Our observations with the 2'-5' modified siRNAs 49 and 54 in complex with hAGO2 protein (**Figure 3.15**) was in agreement with their findings; also suggesting that the siRNA binding to hAGO2 does not affect largely the sugar conformations of the bound nucleotides. In our modeling experiments, unmodified nucleotides, flanked by 2'-5' linked nucleotides, showed varied percentages of *C3'-endo* conformations (40-100%) (**Figure 3.15**). These results are consistent with previously reported X-ray crystallographic data by Szostak and co-workers on 2'-5' modified RNA duplexes, accounting the buffering role of 3'-5' linked nucleotides to reduce the perturbations of the duplex structure, hence pertaining the A-form duplex.

3.10.3 The effect of 2'-5' linkage on RNA duplex properties

We next focused our attention on studying the structural impact of 2'-5' linkage on RNA duplex properties. Previous studies by our laboratory and other groups had shown that an RNA:2'-5' duplex adopts a compact A-form duplex.[16, 18, 46] Crystallographic data as well as molecular dynamic studies from Szostak group provided insight into the diminished thermal and chemical stability of the 2'-5' modified RNA duplexes associated with the perturbed overall base stacking and base pairing due to the presence of 2'-5' linkages.[13]

We investigated the effect of 2'-5' linkage on duplex properties of an siRNA loaded in the hAGO2. To define the orientation and position of each base pair with another in an RNA double helix, structural parameters such as rise, buckle and slide are required. These parameters show

the stacking geometry between neighboring base pairs. A simplified illustration of some of these parameters is given in **Figure 3.16**. Full description of all duplex structural parameters can be found elsewhere.[47, 48] These parameters were calculated using X3DNA package.[48] Theses studies showed that extensive 2'-5' linkage modification, as in siRNA 54, resulted in significantly deviated buckle, slide and rise parameters in comparison with the unmodified siRNA (**Figure 3.16**). Our calculations are in agreement with previous reports[13] by Szostack group, suggesting that the increase in the buckle amplitude upon 2'-5' modification, results in lower base overlap and stacking and hence destabilize the duplex.

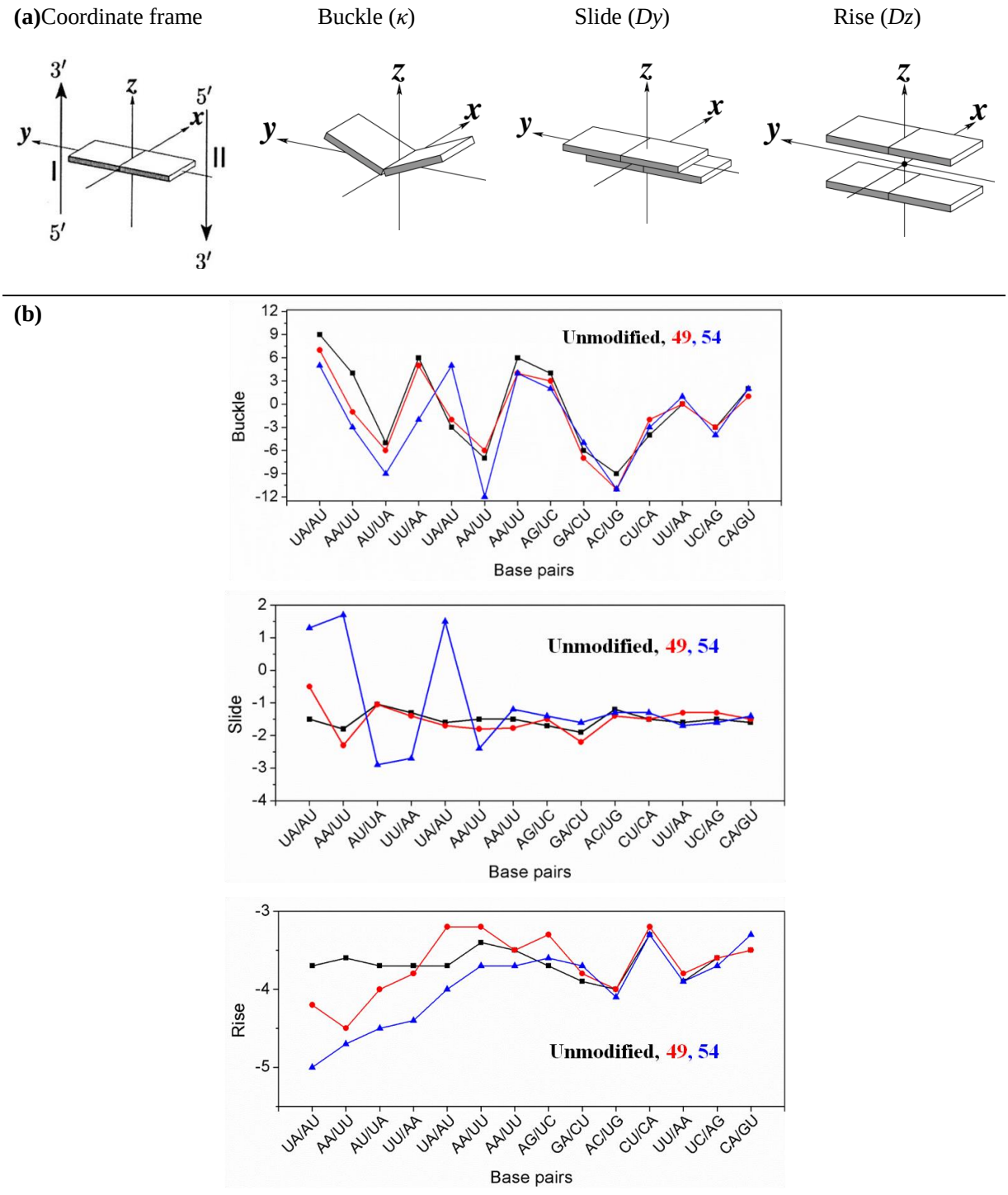

Figure 3.16 (a) Pictorial representation of base pair parameters of nucleic acid duplexes. Each rectangle represents a base and the shaded region represents the minor groove edge of the base pair. Pictures were adapted from [47] (b) Base pair step parameters of the unmodified and modified siRNA duplexes from the averaged structure obtained from the last 50 ns of the 250 ns MD simulations.

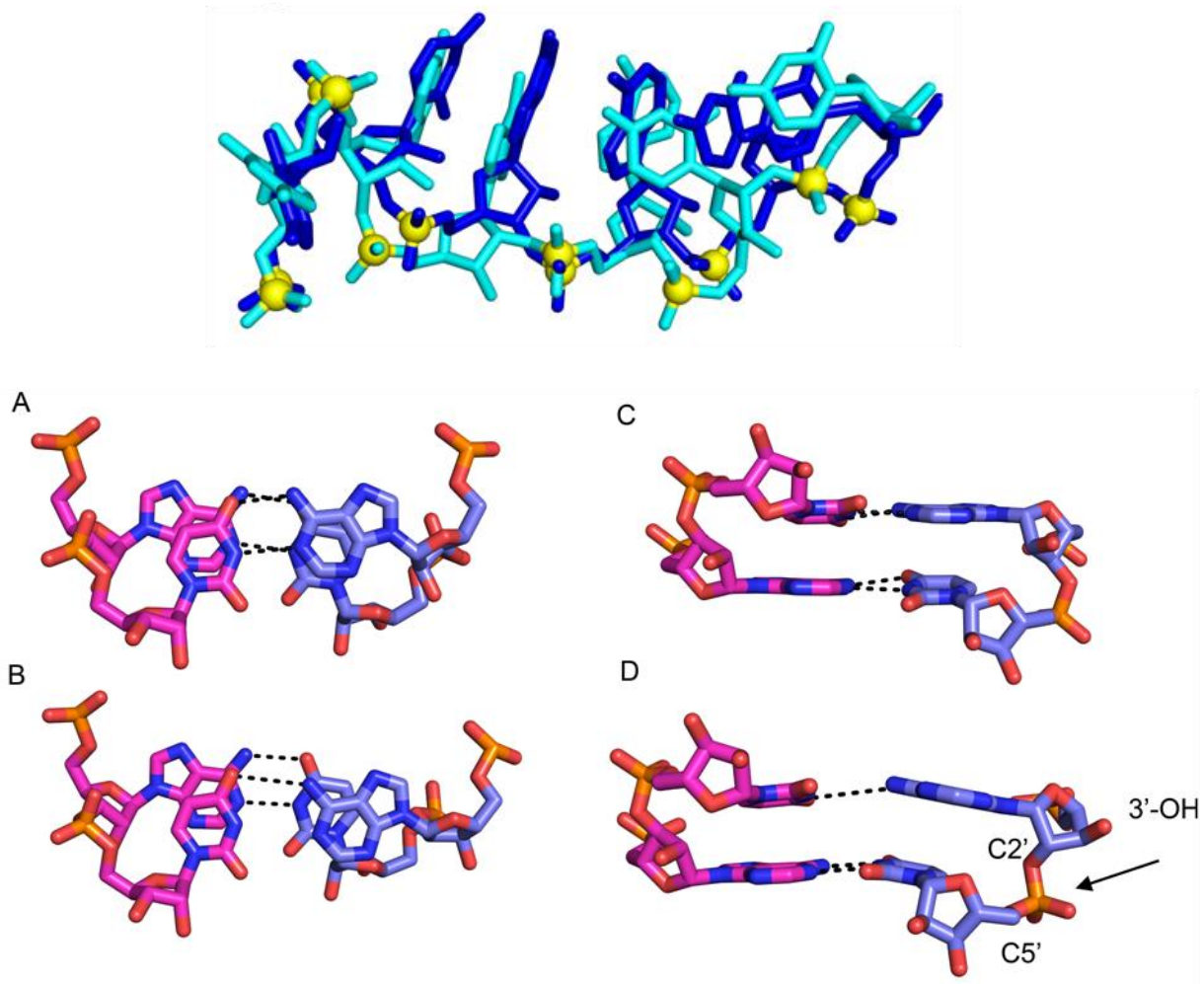

Figure 3.17 (Top) Superimposed snapshot of unmodified (blue) and modified siRNA 54 (cyan) AS strands (sense strand is not shown for clarity), illustrating the deviations in the backbone conformation an suboptimal intrastrand base stacking. RNA is represented as sticks and the phosphate atoms is shows as yellow spheres. (Bottom) MD snapshot depicting the base pair and base stacking architecture of g4-g5 step in unmodified and modified siRNA 54. Base pairing of the (A) unmodified and (B) modified siRNA duplex. Base stacking of the successive base pair steps in the (C) unmodified and (D) modified siRNA duplex. The black dashed lines indicate the WC H-bond between the bases. The modified linkage is highlighted using an arrow.

Moreover, we demonstrated that deviations from the optimal rise distances in the modified duplexes resulted in further destabilization by disturbing the WC base pairs. The percentage of H-bond occupancy was calculated from the 250 ns MD trajectory, using distance and angle cut-off as 3.2 and 150, and CPPTRAJ module to calculate. Hydrogen bond occupancy in linkage

Table 3.6 Percentage occupancy of W-C H-bond in the unmodified and modified siRNAs.[a]

Base pairs	Unmodified	Modified siRNA (49)	Modified siRNA (64)
U-A	99.8%	46.8%	43.5%
A-U	99.9%	97.8%	86.9%
A-U	99.6%	98.7%	39.7%
U-A	99.8%	99.8%	76.3%
U-A	98.9%	99.6%	35.4%
A-U	99.3%	99.3%	78.3%

[a] Calculations were carried out using CPPTRAJ module in AMBER 14 package.

modified sites was greatly affected, indicating that the duplex is deviating from optimal structure and is unstable. Seed region base pairing is critical for target mRNA recognition and a functional RNAi. These results, in line with previous studies, explain the observed experimental RNAi activity of siRNAs 49 and 54.

3.10.4 MM-PBSA estimated binding energy of 2'-5'-linked siRNAs (49) and (54) and hAGO2

The free energies of molecular systems describe the tendency of two or more systems to associate with each other via various noncovalent interactions. A fast and simple computational method to evaluate the binding affinity of a receptor-ligand system based on estimating the relative free energy differences (ΔG) between two equilibrium states is "Molecular Mechanics Poisson-Boltzmann surface area (MM-PBSA) method. It is important to note that MM-PBSA is an approximation method, not an absolute or accurate free energy prediction method. Therefore, values obtained from this method can only be relatively compared.

Table 3.7 Binding free energy components for siRNA-hAGO2 complexes calculated from the last 500 ns of the 1 μs MD simulations. [a]

Calculated value	Unmodified	siRNA49	siRNA64
ΔE_{ELEC}	−2444 ± 25	−2356± 21	−2210 ± 23
ΔE_{VDW}	−313 ± 9	−285 ± 11	−208 ± 9
ΔE_{MM}	−2757± 23	−2641± 26	−2418± 29
ΔG_{PB}	2463± 25	2389± 25	2492± 22
ΔG_{NP}	−13± 0.5	−13 ± 0.5	−13 ± 0.6
ΔG_{SOLV}	2450 ± 21	2376 ± 21	2589 ± 21
ΔH_{PB}	−307± 8	−265± 9	−171± 9
$T\Delta S$	−58 ± 3	−54 ± 3	−46 ± 3
ΔG ($\Delta\Delta G$)	−249 ± 7	−211 ± 11 (38 ± 9)	−125 ± 12 (124 ± 9)

[a]All the values are mentioned in kcal/mol. $\Delta E_{ELEC,}$ electrostatic energy; $\Delta E_{VDW,}$ van der Waals energy; ΔE_{INT} internal energy is negligible in all the cases; $\Delta E_{MM} = \Delta E_{ELEC} + \Delta E_{VDW} + \Delta E_{INT}$; ΔG_{PB}, polar solvation free energy; ΔG_{NP}, non-polar solvation free energy; $\Delta G_{SOLV} = \Delta G_{PB} + \Delta G_{NP}$; $\Delta H_{PB} = \Delta E_{MM} + \Delta G_{SOLV}$; $T\Delta S$, total entropy contribution; $\Delta G = \Delta H_{PB} - T\Delta S$, total binding free energy; $\Delta\Delta G = \Delta G_{modified} - \Delta G_{unmodified}$, difference in the binding free energy. Averaged over 1000 snapshots. All these values are determined using MM-PBSA approach,[49] entropy contributions using normal mode analysis.

Table 3.7 presents the MM-PBSA calculated values for estimated binding energy of unmodified as well as modified (49 and 54) siRNAs. These values were calculated using the last 50 ns of the 250 ns MD simulations trajectories. The $\Delta\Delta G$ values indicate that the non-covalent interactions responsible for the complex formation are significantly affected due to extensive presence of 2'-5' linkages in siRNA 54 (**Table 3.7**). The difference in phosphate orientation, presence of C2′-endo sugar conformation in RNA, loss of W-C H-bonds, and relative deviation in A-form geometry are collectively responsible for the deleterious effect on RNAi activity by siRNA 54.

3.11 Conclusion

In conclusion, our results show that introduction of 2'-5' linkages can afford (depending on the position and extent of modification) a potent class of modified siRNAs with diminished immunostimulatory response. Screening of a large number of siRNAs with modifications in the sense or antisense strands show that 2'-5' linkages are tolerated all over the sense strand and, to some extent, in the antisense strand. 2'-5' modified siRNAs are also found to abrogate the immunostimulatory response in comparison with their native siRNAs. Extensive 2'-5' modification of the antisense strand was only found to minimally affect the siRNA phosphorylation by kinases but was detrimental to its hAGO2 loading. MD simulations studies on modified siRNA-hAGO2 complexes gave significant structural insights and helped explained our observed experimental results.

3.12 Experimental methods

3.12.1 Oligonucleotide synthesis and siRNA preparation

Standard phosphoramidite solid-phase synthesis conditions were used for the synthesis of all modified and unmodified oligonucleotides.[49] Syntheses were performed on an Applied Biosystems 3400 DNA Synthesizer at a 1 μmole scale using Unylinker CPG support (ChemGenes). All phosphoramidites, including the 2'-5' phosphoramidites, were prepared as 0.15 M solutions in acetonitrile(ACN), except DNA, which was prepared as 0.1 M. 5-ethylthiotetrazole (0.25 M in ACN) was used to activate phosphoramidites for coupling. Detritylations were performed using 3% trichloroacetic acid in CH_2Cl_2 for 110 sec. Failure sequences were capped using acetic anhydride in THF and 16% *N*-methylimidazole in THF. A 0.1 M solution of I_2 in 1:2:10 pyridine:water:THF was used for oxidation. Coupling times were 600 sec for all RNA and 2'-5' phosphoramidites, except for their guanosine phosphoramidites

which had 900 sec of coupling time. Chemical 5'-phosphorylation of selected modified AS strands was done at the synthesizer instrument using bis-cyanoethyl-N,N-diisopropyl-2-cyanoethyl phosphoramidite at 0.15 M (600 sec coupling time). Deprotection and cleavage from the solid support for was accomplished with 3:1NH_4OH:EtOH for 48 hours at room temperature (for 2'-5' modified samples), and with 40% methylamine for 10 minutes at 65°C (for unmodified RNA samples).[50] Oligonucleotides containing either 3'-5' or 2'-5' RNAs were both synthesized with standard 2'-TBDMS and 3'-TBDMS phosphoramidites respectively. Desilylation of all samples was achieved with triethylamine trihydrofluoride/N-methyl pyrrolidone/triethylamine (1.5:0.75:1 by volume) for 2.5 hours at 65°C.[50, 51]

Purification of crude oligonucleotides was done by HPLC using an anion exchange column (Protein PAK DEAE 5PW 21.5 mm × 15 cm). The buffer system consisted of water (solution A) and 1 M lithium perchlorate solution in water (solution B), at a flow rate of 4 mL/min. The gradient was 0−40% B over 40 min at 60 °C. Under these conditions, the desired peaks eluted at 20−30 minutes. The collected samples were then lyophilized to dryness and were desalted with Nap-25 Sephadex columns from GE Healthcare. Sequences were verified by high resolution ESI-LCMS. Note that since 2'-5' linked RNAis a regioisomer of RNA, all 2'-5' modified samples had exactly the same mass as their unmodified control (**Table 3.8**).

Table 3.8 MS characterization of S and AS strands comprising the siRNAs targeting firefly luciferase, P53, and 728UU

Sample Name	Sequence	Exact Mass
Luciferase S	5'- GCUUGAAGUCUUUAAUUAAUU -3'	6617.8352
Luciferase AS	3'- GGCGAACUUCAGAAAUUAAUU-5'	6701.9292
Luciferase AS-P	3'- GGCGAACUUCAGAAAUUAAUU-5' (PO_4)	6780.8877
P53 S	3'-CCAAUGUGUACAUGAACAUCA-5'	6660.9392
P53 AS	5'-UUACACAUGUACUUGUAGUGG-3'	6671.8672
728UU S	5'- AAAUCGCUGAUUUGUGUAGUU-3'	6672.8512
728UU AS	3'-UUUUUAGCGACUAAACACAUC-5'	6598.8892

siRNAs were prepared by annealing equimolar quantities of complementary oligonucleotides in siRNA buffer (100 mM KOAc, 30 mM HEPES-KOH, 2 mM $Mg(OAc)_2$, pH 7.4) by slowly cooling from 96 °C to room temperature, and then keeping them at 4 °C overnight.

3.12.2 Thermal denaturation studies

Complementary sequences from siRNA libraries (1.5 nmol) were combined, dried, and rediluted in 1 mL of T_m buffer containing 140 mM KCl, 1 mM $MgCl_2$ and 5 mM Na_2HPO_4 (pH 7.2). Samples were then transferred into UV cuvettes in a Varian Cary 300 UV spectrophotometer and heated up to 90 °C. They were cooled down to 5 °C (ramped at 1°C/min), followed by heating up from 5 °C to 95°C. The change in their absorbance at 260 nm was monitored upon cooling and heating steps. Melting temperatures were determined using the heating ramp and via baseline method, as implemented in the Cary software. Tm curves of siRNAs targeting firefly luciferase are shown in **Figure 3.18**, as example.

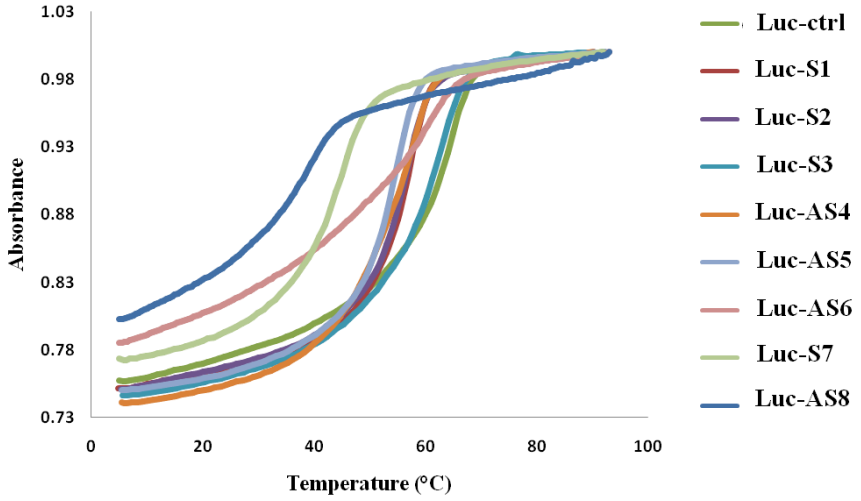

Figure 3.18 Melting profiles of siRNAs targeting firefly luciferase with 2'-5' modification placed in the sense or antisense strands were followed by observing the change in absorbance at 260 nm (A260) of duplex samples upon heating from 5°C to 90°C. Duplexes were 1.5µM (3µM total concentration of strands) in phosphate buffer (140mM KCl, 5mM Na2HPO4, 1mM MgCl2, pH 7.2). siRNA sequences are shown in **Table 3.1**.

3.12.3 Luciferase siRNA assay

Luciferase knockdown assays were performed as described in Deleavey et al.[52] with a few modifications. Typically, HeLa cells were counted and seeded at a density of 10,000 cells/well in a 96-well plate. Cells were allowed to recover for 24 hours at 37°C with 5% CO_2. Subsequently, cells were washed once with serum-free DMEM media and then 80 µl of serum-free DMEM media was added. siRNA and control nucleic acid preparations were diluted up to 20 µl with serum-free media and transfection reagent (Oligofectamine, Invitrogen) and added to the appropriate well (for a total of 100 uL) at increasing concentrations (0.16, 0.8, 4, 20, and 100 nM). Cells were incubated overnight (for a total of 24 hours post-DNA addition). Then 50 µL of ONE-Glo luciferase reagent (Promega, USA) was added to each well and luminescence was measured and normalized to protein levels using a Biotek Synergy HT plate reader. Data was

acquired with the Gen5 software suite and data was manipulated and plotted using Graphpad Prism software suite.

3.12.4 P53 siRNA reporter assay

Cloning of P53 reporter was performed following the instructions reported in literature.[26] Briefly, a G-block was ordered from IDT Technologies containing the p53 target side flanked by restrictions sides for *XhoI* and *NotI* at the 5' and 3' of the sequence, respectively, to clone the sequence into the 3' UTR of the Renilla gene of the plasmid PsiCheck2 (Promega). Following the cloning, the plasmid was sequence verified

Sequence:

"atccgtttcaagccg**CTCGAG**agcgtggtggtaccttatgagccacccgaggccggctctgagtataccaccatccactacaagtac atgtgtaatagctcctgcatgggggggcatgaaccgccgacctatccttaccatc**GCGGCCGC**gttcataggcttatg"

The plasmid and siRNAs were then, transfected into 293T cells using $CaPO_4$, following the procure explained here. 293T cells were seeded with 5000 cells/well in a 96 well plate. After 12 hours, they were transfected with the siRNAs using Oligofectamine (Invitrogen). 24 hours after siRNA transfection, cells were transfected with 20 ng/well of the DNA plasmid, using calcium phosphate. 48 hours after the plasmid transfection, cells were harvested in 100uL PLB (Passive Lysis Buffer, Promega) and 5ul was used to read FF/Ren using a Fluorostar Optima.

3.12.5 Immunostimulation assays in human peripheral blood mononuclear cells (PBMCs)

Peripheral blood mononuclear cells (PBMCs) were obtained from healthy donors at City of Hope National Medical Center using discarded anonymous blood unit leukocyte filters (Pall). PBMCs were plated in 24-well plate ($2.5x10^6$ cells/well) and transfected using DOTAP transfection reagent (Sigma-Aldrich) according to the manufacture's protocol at a final RNA concentration of

80 nM. Cells were incubated at 37 °C for 24 hours. Supernatants from each well were collected, and IFN-a and IL-6 levels were quantified by enzyme-linked immunosorbent assay (ELISA) using 96-well ELISA plates coated with a human IFN-a or IL-6 antibody (Thermo Fisher Scientific), respectively.

During this experiment, discarded peripheral blood from anonymous adult donors from the City of Hope Apheresis Center (Duarte, CA) was used. The proposed research involved blood specimens from anonymous human subjects with no identifiers to age, race, ethnicity, or gender. The information provided for the above submission was evaluated and determined not to involve human subjects research (45 CFR 46.102 (d)(f)). Therefore, it does not need to be approved nor does it need to undergo continuing review by the Institutional Review Board (IRB) in the City of Hope.

3.12.6 RNA Radiolabelling

RNA radiolabelling was performed by Dr. Keith Gagnon, from Southern Illinois University, following a published protocol.[53] All the work was performed behind a shield, and following the safety regulations when handling radioactivity. The assay was performed using the following material:

1. RNase-free distilled and deionized water (dd H_2O).

2. siRNA strands dissolved in dd H_2O at 100 μM:

3. [γ]- ^{32}P-ATP (7000 Ci/mmol) (Purchased from MP Biomedicals).

4. SUPERase-In RNase inhibitor (Purchased from Ambion).

5. T4 polynucleotide kinase (PNK) and 10× PNK buffer: 0.7 M, Tris–HCl, pH 7.6, 100 mM $MgCl_2$, 50 mM dithiothreitol.

6. Redistilled phenol, water-saturated.

7. Chloroform:isoamyl alcohol (24:1).

8. Acetone.

9. Yeast transfer RNA (tRNA) at 10 mg/mL in dd H_2O.

10. Lithium perchlorate ($LiClO_4$).

11. Urea, molecular biology grade.

12. 10 % ammonium persulfate (APS), prepared fresh.

13. *N*,*N*,*N*,*N*′ -Tetramethyl-ethylenediamine (TEMED).

14. 10× TBE: 0.89 M Tris base, 0.89 M boric acid, 20 mM EDTA.

15. 4× Native loading buffer: 4× TBE, 40 % glycerol (v/v), 0.2 mg/mL xylene cyanol, 0.2 mg/mL bromophenol blue.

Radiolabelling was performed by mixing the reaction components below in a 1.5 mL microcentrifuge tube:

(a) 1 μL of siLuc_as (guide strand) (100 μM stock).

(b) 2 μL 10× PNK buffer.

(c) 2.5 μL [γ]- 32 P-ATP (~0.3 mCi).

(d) 2 μL PNK (10 U/μL).

(e) 1 μL SUPERase-In (40 U/μL).

(f) dd H_2O to 20 μL.

The above mixture was incubated at 37 °C for 2.5 h, and then labelled RNA was extracted using Phenol/chloroform mixture (Keep on ice or store at -20 °C until ready to proceed.). After the extraction, radiolabeled RNA strands were purified using standard denaturing gel procedures.

3.12.7 hAGO2 loading assay

This assay was designed to evaluate the *in vitro* binding affinity of hAGO2 for siRNA single strand AS. RNA strands were radioactively labeled and used at very low concentrations (25 nM or less) while titrated by hAGO2 protein. Radioactive RNA will only bind the membrane if it is associated with protein. Radioactive intensity of spots on the membrane should increase as [hAGO2] increases. hAGO2 protein was purchased from Active Motif. 100 µL of 10% glycerol was added to 20 µg of lyophilized hAGO2. 5x Ago Binding Buffer (ABB) was prepared using 100 mM Tris, 500 mM KCl, 250 mM NaCl, and 25 mM $MgCl_2$ and pH was adjusted to 7.5. Final solution contained 0.2 µg/µL (~ 2 µM) hAGO2, in 16 mM Tris, pH 7.4, 400 mM NaCl, 4% trehalose, 4% mannitol, 0.008% Tween-80. It is noteworthy that hAGO2 samples purchased from the Sino Biologicals did not give satisfactory results when used. hAGO2 was serially diluted following the bellow procedure:

1. Serially dilute 2-fold using 1x ABB. Start with 200 nM (1/10 stock). Make 12.5 µL (final) of each: (600, 300, 150, 75, 37.5, 18.75, 9.37, 4.6, 2.3 and 0 nM)
2. Keep hAGO2 samples on ice until ready for use.
3. Prepare 10 µL reactions (multiply by the number of samples needed):

5.75 µL	ddH_2O
2 µL	5x ABB
0.5 µL	BSA (acetylated) (10 mg/mL)
0.5 µL	tRNA (10 mg/mL)
0.25 µL	SUPERase-In (20 U/µL)
1 µL	5' radiolabled single strand or duplex (50 nM final) (2,000 cpm/uL)

---

10 L total volume

4. Add 10 μL of each serially diluted hAGO2 to appropriate tubes. Final volume will be 20 μL, final [siRNA] will be 25 nM, and final [hAGO2] will be 1/2 of serially diluted concentration for all reactions. Incubate at 37°C for 10 min.
5. Spin down reaction and spot into dot blot (reinforced nitrocellulose membrane). Turn vacuum on low to pull sample through during spotting.
6. As each row of wells is loaded, wash each 2x with 200 μL of 1x ABB. After spotting and washing all samples, turn vacuum on high for 30 sec. Turn off vacuum, remove membrane and wash membrane 1x ABB. Remove from wash tank, pat dry with kimwipe, then allow to air dry completely for 15 min.
7. Cover membrane in Saran Wrap and expose to phosphorimager overnight. Scan with Typhoon imager. Quantify spots by using ImageQuant software and fit data to a one-site binding curve in Prism3.

3.12.8 Molecular dynamic studies and calculations

The hAGO2 protein and siRNA (17 base pairs) complex utilized for MD studies was obtained from the model developed by the research group of Dr. Pradeepkumar (unpublished results). The topology and coordinate inputs of protein and RNA complex were prepared using the xleap module in AMBER 14.[54] The protonation state of the amino acids were assigned using PDBPQR program at pH 7.0 in AMBER force field. The system was neutralized using KCl ions and excess ions (100mM) were added to mimic the physiological conditions. Mg^{2+} ions at the cleavage site were parameterized using a reported procedure.[55, 56]

The partial charges for the 2′-5′linked modifications was calculated at the nucleotide level using Gaussian 09 (HF/6-31G*) package.[57] The calculated charges were then fitted using the RESP

algorithm.[58] The force field parameters for 2′-5′ -linkage were derived from the previously reported crystal structure and MD studies.[13] The force fields used for the RNA and the protein are bsc0χ_{OL3}[59-62] and ff12SB,[54] respectively. Using TIP3P water molecules, the system was solvated up to 8 Å from any of the solute atoms. The equilibration and MD simulations were performed as reported earlier.[63, 64] An unrestrained production MD simulations were performed for 250 ns using CUDA version of pmemd[65] in a GPU accelerated version[41, 66] of AMBER 14.[54] Particle mesh ewald method was utilized for calculating the contributions from the non-bonded interactions with a cut-off of 10 Å. SHAKE was used to treat the bonds involving hydrogen atoms. The unrestrained MD simulations were performed in NPT ensemble of 2 fs time step. One atmospheric constant pressure was maintained using Bendersen weak-coupling barostat in a time constant of 1 ps.[67] The MD simulations temperature (300 K) was maintained by Bendersen thermostat of 4 ps. MD trajectories were saved for every ps and then extracted at every 5ps time interval for further analysis.

Root mean square deviations(RMSDs) were calculated for the backbone heavy atoms of protein (CA, C, and N) and RNA (P, O5', C5', C4', C3', and O3') using CPPTRAJ module in AMBER 14.[68]The X3DNA package was utilized to compute the RNA helical parameters and backbone dihedral angles.[48]Hydrogen bonds were considered based upon the heavy atom distance (donor-acceptor) cut-off of ≤ 3.3 Å and an angle cut-off of ≥ 135°. The distance between the two heavy atoms were calculated using PTRAJ module. MD trajectories were visualized using UCSF Chimera.[69] The free energy of siRNA-hAGO2 complex binding was computed using Molecular Mechanics/Poisson-Boltzmann Surface Area (MM/PBSA) method using an earlier report.[70]

3.13 References

1. Joyce, G. F., RNA evolution and the origins of life. *Nature* **1989,** *338*, 217-24.
2. Usher, D. A.; McHale, A. H., Nonenzymic joining of oligoadenylates on a polyuridylic acid template. *Science* **1976,** *192*, 53-54.
3. Engelhart, A. E.; Powner, M. W.; Szostak, J. W., Functional RNAs exhibit tolerance for non-heritable 2′–5′ versus 3′–5′ backbone heterogeneity. *Nat Chem* **2013,** *5*, 390-394.
4. Xu, L.; Wang, W.; Zhang, L.; Chong, J.; Huang, X.; Wang, D., Impact of template backbone heterogeneity on RNA polymerase II transcription. *Nucleic Acids Res* **2015,** *43*, 2232-41.
5. Horowitz, E. D.; Lilavivat, S.; Holladay, B. W.; Germann, M. W.; Hud, N. V., Solution Structure and Thermodynamics of 2′,5′ RNA Intercalation. *J Am Chem Soc* **2009,** *131*, 5831-5838.
6. Premraj, B. J.; Raja, S.; Bhavesh, N. S.; Shi, K.; Hosur, R. V.; Sundaralingam, M.; Yathindra, N., Solution structure of 2',5' d(G4C4). Relevance to topological restrictions and nature's choice of phosphodiester links. *European journal of biochemistry* **2004,** *271*, 2956-66.
7. Plevnik, M.; Gdaniec, Z.; Plavec, J., Solution structure of a modified 2',5'-linked RNA hairpin involved in an equilibrium with duplex. *Nucleic Acids Res* **2005,** *33*, 1749-59.
8. Premraj, B. J.; Patel, P. K.; Kandimalla, E. R.; Agrawal, S.; Hosur, R. V.; Yathindra, N., NMR structure of a 2',5' RNA favors A type duplex with compact C2'endo nucleotide repeat. *Biochem Biophys Res Commun* **2001,** *283*, 537-43.
9. Kirshnan, R.; Seshadri, T. P.; Viswamitra, M. A., Visualisation of a 2'-5' parallel stranded double helix at atomic resolution: crystal structure of cytidylyl-2',5'-adenosine. *Nucleic Acids Research* **1991,** *19*, 379-384.
10. Dhingra, M. M.; Sarma, R. H., Why do nucleic acids have 3'5' phosphodiester bonds? *Nature* **1978,** *272*, 798-801.
11. Robinson, H.; Jung, K.-E.; Switzer, C.; Wang, A. H. J., DNA with 2'-5' Phosphodiester Bonds Forms a Duplex Structure in the A-type Conformation. *J Am Chem Soc* **1995,** *117*, 837-838.
12. Parthasarathy, R.; Malik, M.; Fridey, S. M., X-ray structure of a dinucleoside monophosphate A2'p5'C that contains a 2'-5' link found in (2'-5')oligo(A)s induced by interferons: single-stranded helical conformation of 2'-5'-linked oligonucleotides. *Proceedings of the National Academy of Sciences of the United States of America* **1982,** *79*, 7292-7296.
13. Sheng, J.; Li, L.; Engelhart, A. E.; Gan, J.; Wang, J.; Szostak, J. W., Structural insights into the effects of 2′-5′ linkages on the RNA duplex. *Proceedings of the National Academy of Sciences* **2014,** *111*, 3050-3055.
14. Wasner, M.; Arion, D.; Borkow, G.; Noronha, A.; Uddin, A. H.; Parniak, M. A.; Damha, M. J., Physicochemical and Biochemical Properties of 2‘,5‘-Linked RNA and 2‘,5‘-RNA:3‘,5‘-RNA “Hybrid” Duplexes. *Biochemistry* **1998,** *37*, 7478-7486.
15. Schirle, N. T.; Sheu-Gruttadauria, J.; MacRae, I. J., Structural basis for microRNA targeting. *Science* **2014,** *346*, 608-13.
16. Giannaris, P. A.; Damha, M. J., Oligoribonucleotides containing 2',5'-phosphodiester linkages exhibit binding selectivity for 3',5'-RNA over 3',5'-ssDNA. *Nucleic Acids Research* **1993,** *21*, 4742-4749.

17. Damha, M. J.; Giannaris, P. A.; Zabarylo, S. V., An improved procedure for derivatization of controlled-pore glass beads for solid-phase oligonucleotide synthesis. *Nucleic Acids Research* **1990,** *18*, 3813-3821.
18. Damha, M. J.; Giannaris, P. A.; Khan, N., 2'-5'-linked oligonucleotides form stable complexes with complementary RNA and DNA. *Nucleic acids symposium series* **1991**, 290.
19. Prakash, T. P.; Jung, K.-E.; Switzer, C., RNA recognition by the 2'-structural isomer of DNA. *Chemical Communications* **1996**, 1793-1794.
20. Hashimoto, H.; Switzer, C., Self-Association of 2',5'-linked deoxynucleotides: meta-DNA. *J Am Chem Soc* **1992,** *114*, 6255-6256.
21. Kandimalla, E. R.; Manning, A.; Zhao, Q.; Shaw, D. R.; Byrn, R. A.; Sasisekharan, V.; Agrawal, S., Mixed backbone antisense oligonucleotides: design, biochemical and biological properties of oligonucleotides containing 2′–5′-ribo- and 3′–5′-deoxyribonucleotide segments. *Nucleic Acids Research* **1997,** *25*, 370-378.
22. Torrence, P. F.; Maitra, R. K.; Lesiak, K.; Khamnei, S.; Zhou, A.; Silverman, R. H., Targeting RNA for degradation with a (2'-5')oligoadenylate-antisense chimera. *Proceedings of the National Academy of Sciences of the United States of America* **1993,** *90*, 1300-1304.
23. Prakash, T. P.; Kraynack, B.; Baker, B. F.; Swayze, E. E.; Bhat, B., RNA interference by 2′,5′-linked nucleic acid duplexes in mammalian cells. *Bioorganic & Medicinal Chemistry Letters* **2006,** *16*, 3238-3240.
24. Deleavey, G. F.; Frank, F.; Hassler, M.; Wisnovsky, S.; Nagar, B.; Damha, M. J., The 5′ Binding MID Domain of Human Argonaute2 Tolerates Chemically Modified Nucleotide Analogues. *Nucleic acid therapeutics* **2013,** *23*, 81-87.
25. Hemann, M. T.; Fridman, J. S.; Zilfou, J. T.; Hernando, E.; Paddison, P. J.; Cordon-Cardo, C.; Hannon, G. J.; Lowe, S. W., An epi-allelic series of p53 hypomorphs created by stable RNAi produces distinct tumor phenotypes in vivo. *Nature genetics* **2003,** *33*, 396-400.
26. Jahns, H.; Roos, M.; Imig, J.; Baumann, F.; Wang, Y.; Gilmour, R.; Hall, J., Stereochemical bias introduced during RNA synthesis modulates the activity of phosphorothioate siRNAs. *Nature communications* **2015,** *6*.
27. Tuschl, T.; Zamore, P. D.; Lehmann, R.; Bartel, D. P.; Sharp, P. A., Targeted mRNA degradation by double-stranded RNA in vitro. *Genes & development* **1999,** *13*, 3191-7.
28. Guennewig, B.; Roos, M.; Dogar, A. M.; Gebert, L. F.; Zagalak, J. A.; Vongrad, V.; Metzner, K. J.; Hall, J., Synthetic pre-microRNAs reveal dual-strand activity of miR-34a on TNF-alpha. *RNA (New York, N.Y.)* **2014,** *20*, 61-75.
29. Judge, A. D.; Sood, V.; Shaw, J. R.; Fang, D.; McClintock, K.; MacLachlan, I., Sequence-dependent stimulation of the mammalian innate immune response by synthetic siRNA. *Nat Biotech* **2005,** *23*, 457-462.
30. Hornung, V.; Guenthner-Biller, M.; Bourquin, C.; Ablasser, A.; Schlee, M.; Uematsu, S.; Noronha, A.; Manoharan, M.; Akira, S.; de Fougerolles, A.; Endres, S.; Hartmann, G., Sequence-specific potent induction of IFN-[alpha] by short interfering RNA in plasmacytoid dendritic cells through TLR7. *Nature medicine* **2005,** *11*, 263-270.
31. Deleavey, Glen F.; Damha, Masad J., Designing Chemically Modified Oligonucleotides for Targeted Gene Silencing. *Chemistry & Biology* **2012,** *19*, 937-954.
32. Frank, F.; Sonenberg, N.; Nagar, B., Structural basis for 5'-nucleotide base-specific recognition of guide RNA by human AGO2. *Nature* **2010,** *465*, 818-22.
33. Gaynor, J. W.; Campbell, B. J.; Cosstick, R., RNA interference: a chemist's perspective. *Chemical Society reviews* **2010,** *39*, 4169-84.

34. Humphreys, D. T.; Westman, B. J.; Martin, D. I. K.; Preiss, T., MicroRNAs control translation initiation by inhibiting eukaryotic initiation factor 4E/cap and poly(A) tail function. *Proceedings of the National Academy of Sciences of the United States of America* **2005,** *102*, 16961-16966.
35. Ross C. Wilson, J. A. D., Molecular Mechanisms of RNA Interference. *Annual Review of Biophysics* **2013,** *42*, 217-239.
36. Parker, J. S.; Parizotto, E. A.; Wang, M.; Roe, S. M.; Barford, D., Enhancement of the seed-target recognition step in RNA silencing by a PIWI/MID domain protein. *Molecular cell* **2009,** *33*, 204-14.
37. Wang, Y.; Juranek, S.; Li, H.; Sheng, G.; Tuschl, T.; Patel, D. J., Structure of an argonaute silencing complex with a seed-containing guide DNA and target RNA duplex. *Nature* **2008,** *456*, 921-926.
38. Prakash, T. P.; Allerson, C. R.; Dande, P.; Vickers, T. A.; Sioufi, N.; Jarres, R.; Baker, B. F.; Swayze, E. E.; Griffey, R. H.; Bhat, B., Positional Effect of Chemical Modifications on Short Interference RNA Activity in Mammalian Cells. *Journal of Medicinal Chemistry* **2005,** *48*, 4247-4253.
39. Shukla, S.; Sumaria, C. S.; Pradeepkumar, P. I., Exploring Chemical Modifications for siRNA Therapeutics: A Structural and Functional Outlook. *ChemMedChem* **2010,** *5*, 328-349.
40. Bramsen, J. B.; Pakula, M. M.; Hansen, T. B.; Bus, C.; Langkjaer, N.; Odadzic, D.; Smicius, R.; Wengel, S. L.; Chattopadhyaya, J.; Engels, J. W.; Herdewijn, P.; Wengel, J.; Kjems, J., A screen of chemical modifications identifies position-specific modification by UNA to most potently reduce siRNA off-target effects. *Nucleic Acids Res* **2010,** *38*, 5761-73.
41. Salomon-Ferrer, R.; Götz, A. W.; Poole, D.; Le Grand, S.; Walker, R. C., Routine Microsecond Molecular Dynamics Simulations with AMBER on GPUs. 2. Explicit Solvent Particle Mesh Ewald. *J. Chem. Theory Comput.* **2013,** *9*, 3878-3888.
42. Schirle, N. T.; Sheu-Gruttadauria, J.; Chandradoss, S. D.; Joo, C.; MacRae, I. J., Water-mediated recognition of t1-adenosine anchors Argonaute2 to microRNA targets. *eLife* **2015,** *4*, e07646.
43. Schirle, N. T.; MacRae, I. J., The Crystal Structure of Human Argonaute2. *Science* **2012,** *336*, 1037-1040.
44. Altona, C.; Sundaralingam, M., Conformational analysis of the sugar ring in nucleosides and nucleotides. Improved method for the interpretation of proton magnetic resonance coupling constants. *J Am Chem Soc* **1973,** *95*, 2333-2344.
45. Altona, C.; Sundaralingam, M., Conformational analysis of the sugar ring in nucleosides and nucleotides. New description using the concept of pseudorotation. *J Am Chem Soc* **1972,** *94*, 8205-8212.
46. Li, L.; Szostak, J. W., The Free Energy Landscape of Pseudorotation in 3′–5′ and 2′–5′ Linked Nucleic Acids. *J Am Chem Soc* **2014,** *136*, 2858-2865.
47. Lu, X. J.; Olson, W. K., 3DNA: a software package for the analysis, rebuilding and visualization of three-dimensional nucleic acid structures. *Nucleic Acids Research* **2003,** *31*, 5108-5121.
48. Lu, X.-J.; Olson, W. K., 3DNA: a versatile, integrated software system for the analysis, rebuilding and visualization of three-dimensional nucleic-acid structures. *Nat. Protocols* **2008,** *3*, 1213-1227.
49. Damha, M. J.; Ogilvie, K. K., Oligoribonucleotide synthesis. The silyl-phosphoramidite method. *Methods in molecular biology (Clifton, N.J.)* **1993,** *20*, 81-114.

50. Bellon, L., Oligoribonucleotides with 2'-O-(tert-butyldimethylsilyl) groups. *Current protocols in nucleic acid chemistry* **2001,** *Chapter 3*, Unit 3.6.
51. Wincott, F.; DiRenzo, A.; Shaffer, C.; Grimm, S.; Tracz, D.; Workman, C.; Sweedler, D.; Gonzalez, C.; Scaringe, S.; Usman, N., Synthesis, deprotection, analysis and purification of RNA and ribozymes. *Nucleic Acids Res* **1995,** *23*, 2677-84.
52. Deleavey, G. F.; Watts, J. K.; Alain, T.; Robert, F.; Kalota, A.; Aishwarya, V.; Pelletier, J.; Gewirtz, A. M.; Sonenberg, N.; Damha, M. J., Synergistic effects between analogs of DNA and RNA improve the potency of siRNA-mediated gene silencing. *Nucleic Acids Res* **2010,** *38*, 4547-57.
53. Gagnon, K. T., Loading of Argonaute Protein with Small Duplex RNA in Cellular Extracts. *Methods in molecular biology (Clifton, N.J.)* **2016,** *1421*, 53-67.
54. Case, D. A., Darden, T. A., Cheatham, T. E., III, Simmerling, C. L., Wang, J., Duke, R. E., Luo, R., Walker, R. C., Zhang, W., Merz, K. M., Roberts, B., Wang, B., Hayik, S., Roitberg, A., Seabra, G., Kolossváry, I., Wong, K. F., Paesani, F., Vanicek, J., Liu, J., Wu, X., Brozell, S. R., Steinbrecher, T., Gohlke, H., Cai, Q., Ye, X., Wang, J., Hsieh, M. J., Cui, G., Roe, D. R., Mathews, D. H., Seetin, M. G., Sagui, C., Babin, V., Gusarov, S., Kovalenko, A., and Kollman, P. A. , *AMBER 14, University of Californai, San Francisco* **2014**.
55. Allnér, O.; Nilsson, L.; Villa, A., Magnesium Ion–Water Coordination and Exchange in Biomolecular Simulations. *J. Chem. Theory Comput.* **2012,** *8*, 1493-1502.
56. Meagher, K. L.; Redman, L. T.; Carlson, H. A., Development of polyphosphate parameters for use with the AMBER force field. *J. Comput. Chem.* **2003,** *24*, 1016-1025.
57. Frisch, M. J., Trucks, G. W., Schlegel, H. B., Scuseria, G. E., Robb, M. A., Cheeseman, J. R., Scalmani, G., Barone, V., Mennucci, B., Petersson, G. A., Nakatsuji, H., Caricato, M., Li, X., Hratchian, H. P., Izmaylov, A. F., Bloino, J., Zheng, G., Sonnenberg, J. L., Hada, M., Ehara, M., Toyota, K., Fukuda, R., Hasegawa, J., Ishida, M., Nakajima, T., Honda, Y., Kitao, O., Nakai, H., Vreven, T., Montgomery, J. A., Jr., Peralta, J. E., Ogliaro, F., Bearpark, M. J., Heyd, J., Brothers, E. N., Kudin, K. N., Staroverov, V. N., Kobayashi, R., Normand, J., Raghavachari, K., Rendell, A. P., Burant, J. C., Iyengar, S. S., Tomasi, J., Cossi, M., Rega, N., Millam, N. J., Klene, M., Knox, J. E., Cross, J. B., Bakken, V., Adamo, C., Jaramillo, J., Gomperts, R., Stratmann, R. E., Yazyev, O., Austin, A. J., Cammi, R., Pomelli, C., Ochterski, J. W., Martin, R. L., Morokuma, K., Zakrzewski, V. G., Voth, G. A., Salvador, P., Dannenberg, J. J., Dapprich, S., Daniels, A. D., Farkas, Ö., Foresman, J. B., Ortiz, J. V., Cioslowski, J., Fox, D. J., , *Gaussian09, Revision D.01, Gaussian, Inc.: Wallingford, CT* **2013**.
58. Aduri, R.; Psciuk, B. T.; Saro, P.; Taniga, H.; Schlegel, H. B.; SantaLucia, J., AMBER Force Field Parameters for the Naturally Occurring Modified Nucleosides in RNA. *J. Chem. Theory Comput.* **2007,** *3*, 1464-1475.
59. Pérez, A.; Marchán, I.; Svozil, D.; Sponer, J.; Cheatham Iii, T. E.; Laughton, C. A.; Orozco, M., Refinement of the AMBER Force Field for Nucleic Acids: Improving the Description of α/γ Conformers. *Biophys. J.* **2007,** *92*, 3817-3829.
60. Zgarbová, M.; Otyepka, M.; Šponer, J.; Mládek, A.; Banáš, P.; Cheatham, T. E.; Jurečka, P., Refinement of the Cornell et al. Nucleic Acids Force Field Based on Reference Quantum Chemical Calculations of Glycosidic Torsion Profiles. *J. Chem. Theory Comput.* **2011,** *7*, 2886-2902.
61. Cornell, W. D.; Cieplak, P.; Bayly, C. I.; Gould, I. R.; Merz, K. M.; Ferguson, D. M.; Spellmeyer, D. C.; Fox, T.; Caldwell, J. W.; Kollman, P. A., A Second Generation Force Field

for the Simulation of Proteins, Nucleic Acids, and Organic Molecules. *J. Am. Chem. Soc.* **1995,** *117*, 5179-5197.
62. Wang, J.; Cieplak, P.; Kollman, P. A., How well does a restrained electrostatic potential (RESP) model perform in calculating conformational energies of organic and biological molecules? *J. Comput. Chem.* **2000,** *21*, 1049-1074.
63. Krepl, M.; Havrila, M.; Stadlbauer, P.; Banas, P.; Otyepka, M.; Pasulka, J.; Stefl, R.; Sponer, J., Can We Execute Stable Microsecond-Scale Atomistic Simulations of Protein–RNA Complexes? *J. Chem. Theory Comput.* **2015,** *11*, 1220-1243.
64. Krepl, M.; Réblová, K.; Koča, J.; Šponer, J., Bioinformatics and Molecular Dynamics Simulation Study of L1 Stalk Non-Canonical rRNA Elements: Kink-Turns, Loops, and Tetraloops. *J. Phy. Chem. B* **2013,** *117*, 5540-5555.
65. Darden, T.; York, D.; Pedersen, L., Particle mesh Ewald: An N·log(N) method for Ewald sums in large systems. *J. Chem. Phys.* **1993,** *98*, 10089-10092.
66. Le Grand, S.; Götz, A. W.; Walker, R. C., SPFP: Speed without compromise—A mixed precision model for GPU accelerated molecular dynamics simulations. *Comput. Phys. Commun.* **2013,** *184*, 374-380.
67. Berendsen, H. J. C.; Postma, J. P. M.; van Gunsteren, W. F.; DiNola, A.; Haak, J. R., Molecular dynamics with coupling to an external bath. *J. Chem. Phys.* **1984,** *81*, 3684-3690.
68. Roe, D. R.; Cheatham, T. E., PTRAJ and CPPTRAJ: Software for Processing and Analysis of Molecular Dynamics Trajectory Data. *J. Chem. Theory Comput.* **2013,** *9*, 3084-3095.
69. Pettersen, E. F.; Goddard, T. D.; Huang, C. C.; Couch, G. S.; Greenblatt, D. M.; Meng, E. C.; Ferrin, T. E., UCSF Chimera—A visualization system for exploratory research and analysis. *J. Comput. Chem.* **2004,** *25*, 1605-1612.
70. Hou, T.; Wang, J.; Li, Y.; Wang, W., Assessing the Performance of the MM/PBSA and MM/GBSA Methods. 1. The Accuracy of Binding Free Energy Calculations Based on Molecular Dynamics Simulations. *J. Chem. Inf. Model.* **2011,** *51*, 69-82.

CHAPTER 4: SYNTHESIS AND PROPERTIES OF SHORT INTERFERING RNA MIXMERS

4.1 Introduction

siRNAs, as previously described in Chapter 1, are synthetic oligonucleotide duplexes that can mimic the miRNAs in mammalian cells to knock down the expression of a target gene. An obstacle in the development of siRNAs as therapeutic agents, among others, has been the inherent poor drug-like properties of siRNAs. A general approach taken towards solving this shortcoming is introducing chemical modifications to siRNAs, a focus of the research in the presented thesis.

In Chapter 3, we studied the gene silencing and immunostimulatory properties of 2'-5'-modified siRNA in comparison with native siRNAs and found that the 2'-5' linkage modification can afford potent siRNAs that avoid an immune response. The extent of gene silencing largely depended on the number and location of the 2'-5' linkages along the sense and AS strands. 2'-5' Linkages were tolerated all over the sense strand and, to some extent, in the antisense strand. These findings are consistent with the notion that 2'-5'/3'-5' backbone heterogeneity does not affect, to some extent, RNA recognition and function.[1-4] While the studies described in Chapter 3 laid the grounds for elucidating the relation between 2'-5' modification patterns and siRNA potency, they required the synthesis of a large pool of siRNAs, and screening each duplex separately. In an attempt to develop a *universally applicable* 2'-5'/3'-5' siRNA design, we turned our attention to the synthesis of RNA "mixmers", i.e., a regioisomeric mixture of siRNAs, of the same base sequence, containing all possible combinations of 2′-5'/3'-5' linkages along the backbone. As described below, these siRNA "mixmers" are readily prepared via solid-phase

synthesis by delivering a mixture of ribonucleosides 2'P+3'P amidites to the insoluble solid-support during chain growth.

Our motivation to develop and test mixmer siRNAs was inspired, in part, by the natural process by which some RNAs are produced, where Dicer cleaves long dsRNAs into a mixture of discrete siRNA duplexes, although in this case, they are of different base sequence for targeting multiple RNAs.[5, 6] Based on this system, commercially available siNRA pools (siPools)[7] were developed, which consist of a mixture of up to 30 discrete siRNAs, each targeting a different location of the mRNA target. The advantage of siPools is that while the pool of siRNAs is able to synergistically silence one single on-target mRNA gene, off-target effects are "diluted" out given the low concentration of each duplex. Despite this advantage, regulatory authorities often hesitate to adopt such an approach in a clinical setting.[7] Phosphorothioate (PS) linked DNA is a classical example of an ON pool, containing mixed Rp/Sp internucleotide linkages. The isomeric Sp linkage provides increased nuclease resistance (but reduced mRNA binding), whereas the Rp isomer provides appropriate mRNA binding affinity.[8] Given the difficulty in synthesizing stereoisomerically pure PS-linkages,[9] PS-ONs are generally used as diastereomeric Rp/Sp-mixtures.[10, 11] In fact, Spinraza, a newly FDA-approved drug for the treatment of spinal muscular atrophy (SMA), is a fully 2′-O-methoxyethyl modified antisense oligonucleotide with phosphorothioate (PS) backbone.[12]

Herein, we show that the 2′-5'/3'-5'-mixmer strategy can afford modified siRNA mixtures, with potencies comparable to unmodified counterparts, when knocking down firefly luciferase and P53 mRNA *in vitro.* It is also evident that siRNAs with a 2′-5'/3'-5'-mixmer AS strand lead to potent gene silencing, whereas full 2′-5'-modification arrests RNAi activity.

4.2 2'-5'/3'-5' RNA mixmers

4.2.1 Synthesis and product characterization

In our preliminary studies, siRNA targeting luciferase were synthesized from 2′P + 3′P (1:1) phosphoramidite mixtures using 5-ethylthio-tetrazole (ETT) as activator. The result was a mixed population of 21mer oligomers, all of the same sequence, but containing a statistical mix of 2'-5'/3'-5' linkages at each position (**Figure 4.1**).

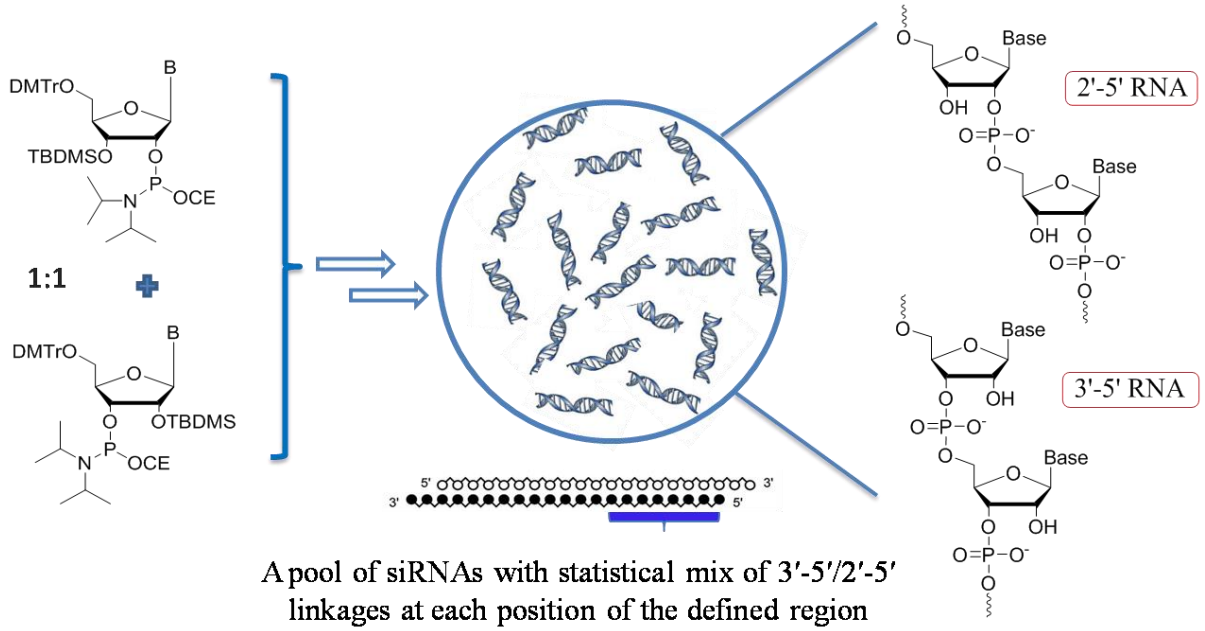

Figure 4.1 Schematic illustration of the mixmer strategy in the preparation of an siRNA duplex with six linkage modified nucleotides in the AS strand. 2'-5' phosphoramidite and 3'-5' phosphoramidites are mixed in a 1:1 ratio. The mixture is used in the synthesis of the siRNA AS strand. The synthesized mixture of strands is then treated as an RNA oligomer and is complexed with the corresponding sense strand to form the siRNA mixmer.

For example, a mixmer with six linkage modification positions in the siRNA AS strand consists of a mixture of 2^7 = 128 sequence-specific siRNAs (**Figure 4.1**). After the synthesis, the mixmer was deprotected and purified by IE-HPLC (**Figure 4.2**). The mass and HPLC profile of the mixmer matched that of the unmodified control RNA strand (**Figure 4.2**).

3'- GGCGAAC UUCAGAA AUUAAUU -5'

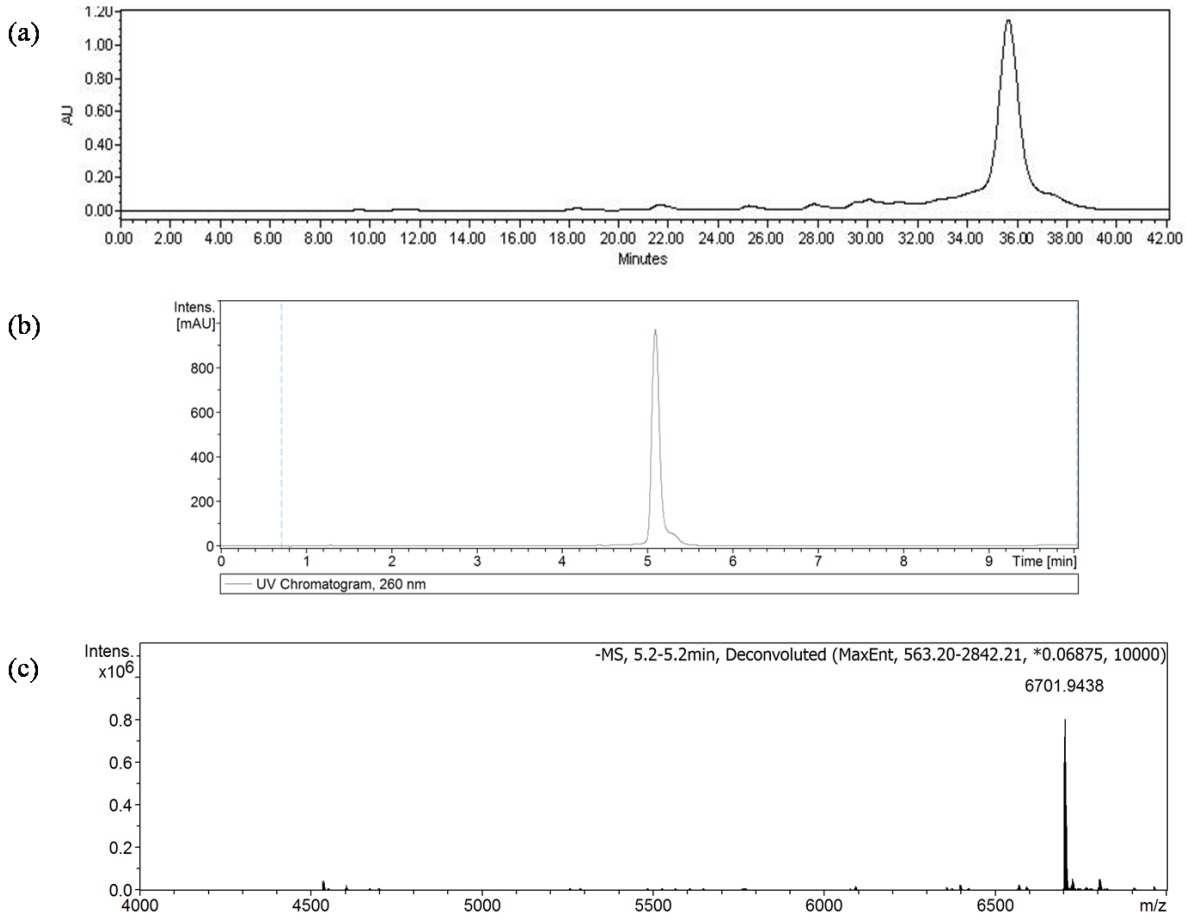

Figure 4.2 HPLC and LCMS chromatograms of a 2'-5'/3'-5' mixmer RNA strand (shown above) illustrating that different species within a 2'-5'/3'-5' mixmer cannot be separated or characterized by HPLC or HRMS. (a) IE-HPLC chromatogram of the crude mixmer product (b) RP-HPLC chromatogram of the IE-HPLC purified mixmer sample (c) HRMS trace of the purified 2'-5'/3'-5' RNA mixmer product showing only a single species corresponding to the unmodified RNA control exact mass.

4.2.2 Coupling efficiency of 2'- versus 3'-phosphoramidite RNA monomers

As explained previously, none of the separation or characterization methods used for unmodified RNA (e.g., MS, HPLC, PAGE) were helpful in determining the presence and extent of 2'-5' linkage modification in a mixmer sample. An indirect method to achieve this would be to determine the relative coupling efficiency of 2'P versus 3'P phosphoramidites during a mixer synthesis set up. We picked an RNA sequence with seven mixmer linkages located at the center of the strand (**Figure 4.3**).

To differentiate between 2'P versus 3'P coupling efficiency, a 1:1 mixture of rU 2'P and rT 3'P phosphoramidites (14 m.u. mass difference) were used during the synthesis (**Figure 4.3**; "U" represents the rU2'-5'/rT3'-5' mixmer position). We assumed that the base [5-methyluracil (thymine) vs uracil] has minimal, if any, effects on coupling during solid phase synthesis. Furthermore, we hypothesized that both rU and rT containing ONs have very similar ionization abilities and would fly very similarly in the MS chamber.

The strand was synthesized in triplicate and purified by IE-HPLC, affording the desired mixmer as a single peak. HRMS analysis provided the trace shown in **Figure 4.3**. Under these conditions, the peak areas in the HRMS trace provide the relative coupling efficiencies of 2'P rU and 3'P rT amidites. To yield a more accurate comparison, all the Salt adducts, isotope abundances and different charge states and for each mixmer were taken into account in these calculations (see experimental section for full details).

Based on this analysis, the relative efficiency of 3'P' coupling versus 2'P coupling was 4:3, in favor of rT 3'P. Therefore, 43% of the linkages in the 7-nt segment are 2'-5' linked, while the rest (57%) are 3'-5' linked. This is consistent with the slightly lower coupling efficiency of 2'P versus

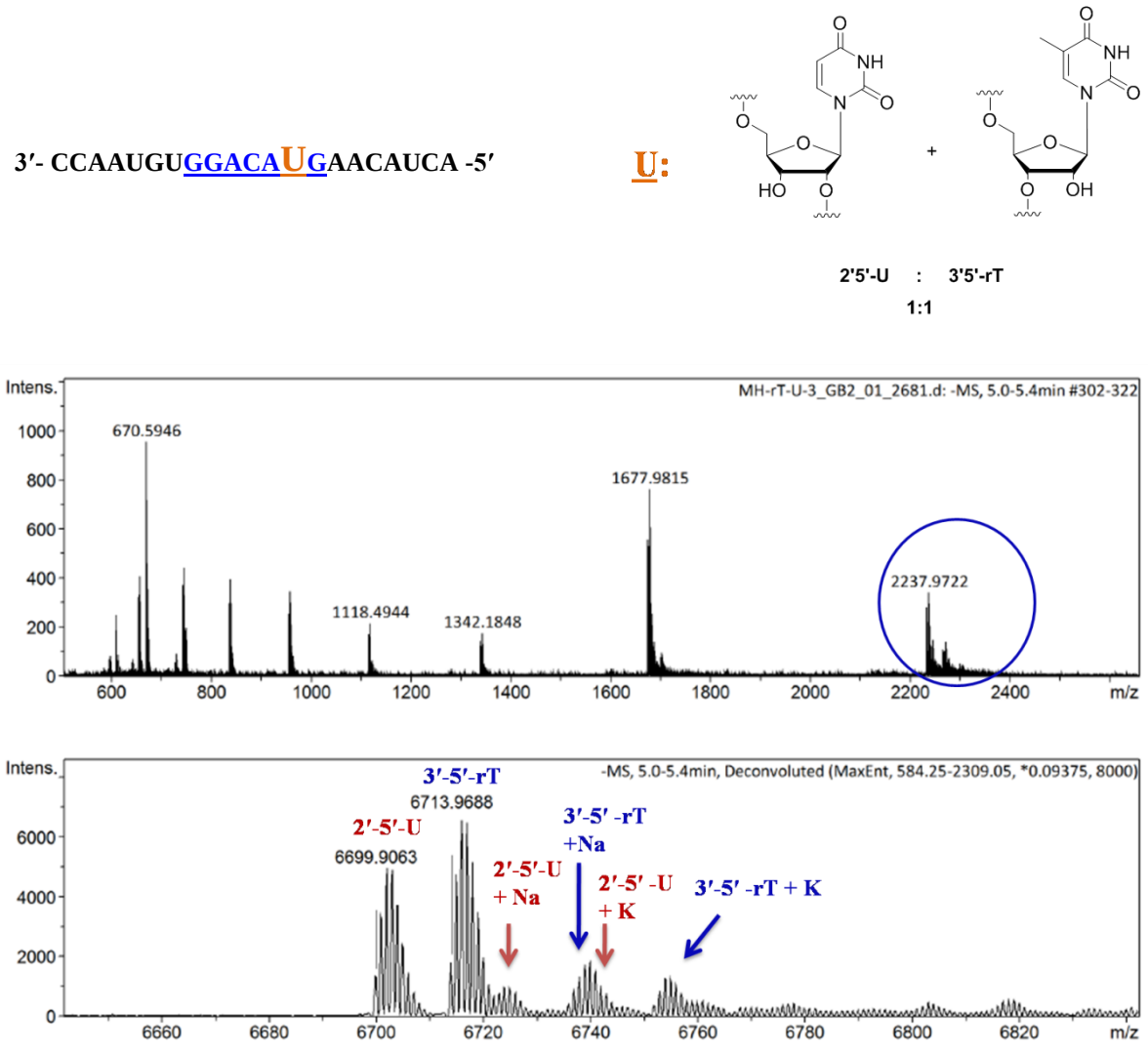

Figure 4.3 Assessing the binding efficiency of 2'P amidites versus 3'P amidites during a mixmer synthesis using ETT as activator. The sequence (top) shows the position of the mixmer segment (mixmer) and the rU/rT mixmer (U). HRMS profile of a test mixmer is shown. The circled peak envelope represents the (-3) charge state, which is deconvoluted to the peaks shown in the bottom spectrogram. Each peak envelope is assigned with the species it corresponds to within the mixmer product. Assessment of the areas under the peaks show the relative coupling efficiency of 0.77:1 for 2'-5':3'-5' RNA amidites while using ETT as an activator.

3'P amidites reported earlier by our group when ETT activator was used.[13]

4.2.3 2'-5'/3'-5' siRNA mixmers targeting firefly luciferase

The mixmer strategy was then applied to the synthesis of siRNAs targeting firefly luciferase. The AS and sense modified mixmers prepared are listed in **Table 4.1**. Gene knockdown data (**Figure 4.4**) show that mixmers with a sense-modified strand generally performed better than mixmers with modified AS strands. IC_{50} values of sense modified siRNAs were in the same range or slightly higher, compared to the unmodified siRNA control (**Figure 4.4**).

Thermal denaturation curves of mixmer siRNA duplexes exhibited sigmoidal melting profile. Furthermore, mixmers had similar or higher T_m values, in comparison with their 2′-5′ modified

Table 4.1 siRNAs targeting firefly luciferase mRNA, modified with 2'-5'/3'-5' mixmer linkages at various positions of sense or antisense strands. Sequence, thermal denaturation, and IC_{50} values of these siRNAs are provided. Legend: 2'-5'/3'-5' mixmer linked RNA, 3'-5' linked RNA.

Sample		Sequence	T_m value (°C)	IC_{50} (nM)
M-Luc-S1	(S) (AS)	5'- GCUUGAA GUCUUUA AUUAAUU -3' 3'- GGCGAAC UUCAGAA AUUAAUU -5'	56.0	77
M-Luc-S2	(S) (AS)	5'- GCUUGAA GUCUUUA AUUAAUU -3' 3'- GGCGAAC UUCAGAA AUUAAUU -5'	54.6	79
M-Luc-S3	(S) (AS)	5'- GCUUGAA GUCUUUA AUUAAUU -3' 3'- GGCGAAC UUCAGAA AUUAAUU -5'	59.5	56
M-Luc-AS4	(S) (AS)	5'- GCUUGAA GUCUUUA AUUAAUU -3' 3'- GGCGAAC UUCAGAA AUUAAUU -5'	56.2	44
M-Luc-AS5	(S) (AS)	5'- GCUUGAA GUCUUUA AUUAAUU -3' 3'- GGCGAAC UUCAGAA AUUAAUU -5'	54.2	106
M-Luc-AS6	(S) (AS)	5'- GCUUGAA GUCUUUA AUUAAUU -3' 3'- GGCGAAC UUCAGAA AUUAAUU -5'	58.8	83
M-Luc-S7	(S) (AS)	5'- GCUUGAA GUCUUUA AUUAAUU -3' 3'- GGCGAAC UUCAGAA AUUAAUU -5'	47.9	22
M-Luc-AS8	(S) (AS)	5'- GCUUGAA GUCUUUA AUUAAUU -3' 3'- GGCGAAC UUCAGAA AUUAAUU -5'	44.4	>300
Luc-CTRL	(S) (AS)	5'- GCUUGAA GUCUUUA AUUAAUU -3' 3'- GGCGAAC UUCAGAA AUUAAUU -5'	65.0	11

counterparts. Stability differences were more pronounced for siRNAs containing a fully modified sense or AS strand. Next, a selected number of mixmer modified siRNAs were studied by circular dichroism (CD). Similar to 2'-5' RNAs and 3'-5' RNAs, CD spectra of 2'-5'/3'-5' mixmer siRNAs show the characteristic signature and peaks for right handed A-form duplexes (**Figure 4.5**).

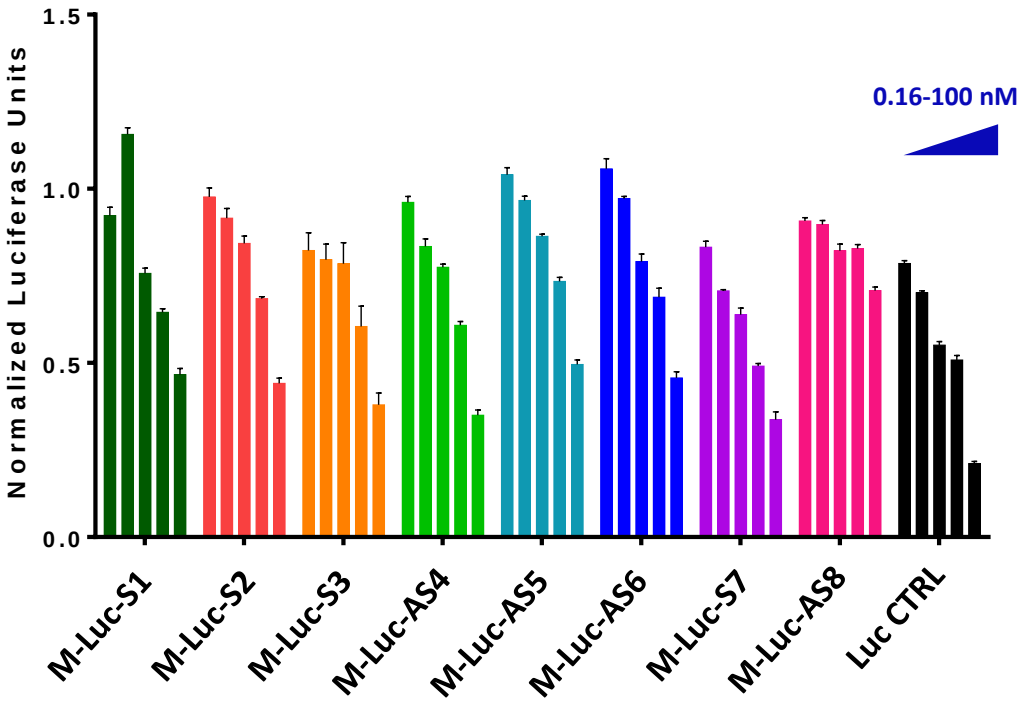

Figure 4.4 Assay demonstrating activity of 2'-5'/3'-5' mixmer siRNAs (n=2) at a range of 0.16, 0.8, 4, 20, 100 nM siRNA concentrations; Firefly luciferase levels were normalized to total cellular protein and luciferase counts of cells treated with scrambled non targeting siRNA. Comparison of mixmer AS-modified (shown here) with 2′-5′ AS-modified siRNAs (shown in **Figure 3.3**) proves that while 2′-5′ modification in the siRNA AS alleviates the siRNA activity, mixmer modification in the siRNAs AS is very well tolerated.

(a) (b)

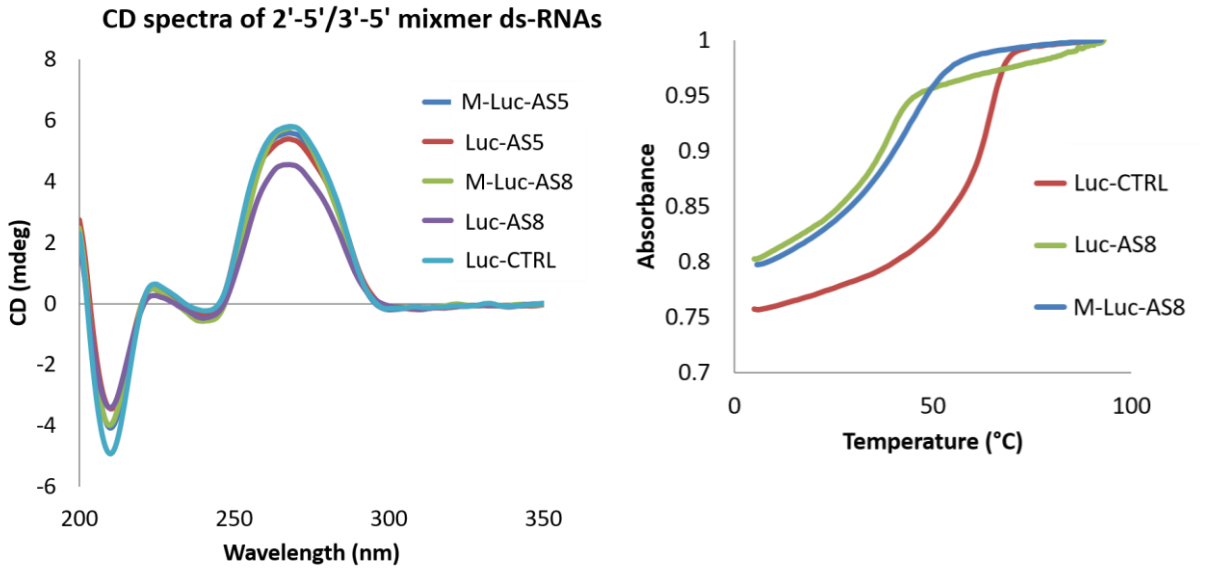

M-Luc-AS5	5'- GCUUGAA GUCUUUA AUUAAUU -3' 3'- GGCGAAC UUCAGAA AUUAAUU -5'
Luc-AS5	5'- GCUUGAA GUCUUUA AUUAAUU -3' 3'- GGCGAAC UUCAGAA AUUAAUU -5'
M-Luc-AS8	5'- GCUUGAAGUCUUUAAUUAAUU -3' 3'- GGCGAAC UUCAGAA AUUAAUU -5'
Luc-AS8	5'- GCUUGAA GUCUUUA AUUAAUU -3' 3'- GGCGAACUUCAGAAAUUAAUU -5'
Luc- ctrl	5'- GCUUGAA GUCUUUA AUUAAUU -3 3'- GGCGAAC UUCAGAA AUUAAUU -5'

Figure 4.5 Normalized CD spectra and UV melting profiles of selected 2'-5'/3'-5' mixmer and 2'-5' modified siRNAs targeting firefly luciferase. Sample sequences and modification patterns are presented above. Legend: 2'-5'/3'-5' mixmer linked RNA, 2'-5' linked RNA, 3'-5' linked RNA.

4.2.4 2'-5'/3'-5' siRNA mixmers targeting P53

An important feature of mixmers is that they improve the potency of AS-modified siRNAs, which are otherwise inactive (e.g., compare 2'-5'-siRNA modified Luc-AS4, **Figure 3.3**, versus 2'-5'/3'-5' mixmer siRNA M-luc-AS4, **Figure 4.4**). To assess the generality of this approach, we applied the 2'-5'/3'-5' mixmer design to a library of siRNAs targeting P53 mRNA.

Here again, we focused on AS-modified siRNAs, comparing the activity of 2'-5'/3'-5' mixmers to their corresponding 2'-5'-modified siRNAs. In this case, we used a dual reporter assay containing a renilla luciferase reporter gene and a cloned target site for P53 siRNA (more details in Chapter 3, Section 3.6). These assays were conducted by Dr. Regina Cencic from the Pelletier research group (McGill). It is noteworthy that while siRNAs with pure 2'-5'-AS strand exhibited poor activity (Chapter 3), siRNAs with mixmer AS strands were quite active (**Figure 4.6**). As seen

Table 4.2 siRNAs targeting P53 mRNA, modified with 2'-5' or 2'-5'/3'-5' mixmer linkages at various positions of antisense strands. Sequences and thermal denaturation values of these siRNAs are shown below. Legend: 2'-5' linked RNA, 2'-5'/3'-5' mixmer linked RNA, 3'-5' linked RNA.

Sample		Sequence	T_m value (°C)
P53-AS4	(S) (AS)	3'-CCAAUGU GUACAUG AACAUCA-5' 5'-UUACACA UGUACUU GUAGUGG-3'	61.6
P53-AS5	(S) (AS)	3'-CCAAUGU GUACAUG AACAUCA-5' 5'-UUACACA UGUACUU GUAGUGG-3'	59.8
P53-AS6	(S) (AS)	3'-CCAAUGU GUACAUG AACAUCA-5' 5'-UUACACA UGUACUU GUAGUGG-3'	63.9
M-P53-AS4	(S) (AS)	3'-CCAAUGU GUACAUG AACAUCA-5' 5'-UUACACA UGUACUU GUAGUGG-3'	64.0
M-P53-AS5	(S) (AS)	3'-CCAAUGU GUACAUG AACAUCA-5' 5'-UUACACA UGUACUU GUAGUGG-3'	62.3
M-P53-AS6	(S) (AS)	3'-CCAAUGU GUACAUG AACAUCA-5' 5'-UUACACA UGUACUU GUAGUGG-3'	65.5
M-P53-ctrl	(S) (AS)	3'-CCAAUGU GUACAUG AACAUCA-5' 5'-UUACACA UGUACUU GUAGUGG-3'	69.7

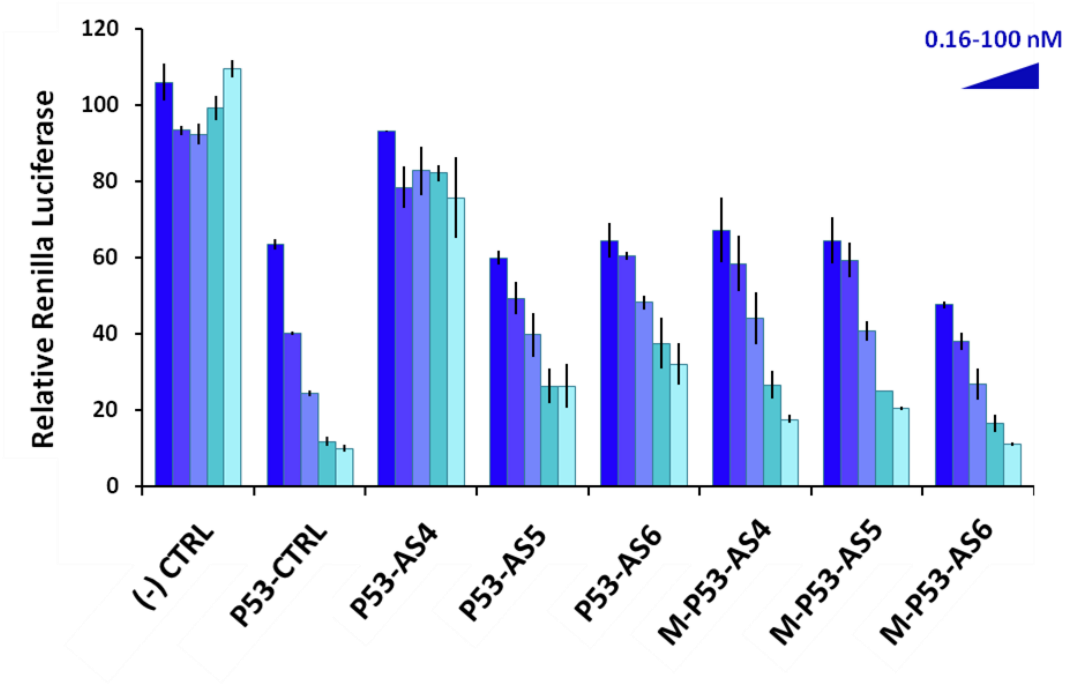

Figure 4.6 P53 assay comparing the activity of 2'-5'/3'-5' mixmer siRNAs (n=2); Renilla luciferase levels were measured relative to the unmodified renilla reporter, Following the treatment of the cells with mixmer siRNAs at a range of concentrations (0.16, 0.8, 4, 20, 100 nM).

with the luciferase library, the lower content of 2'-5' linkages in mixmer duplexes, in comparison with the 2'-5'-only siRNAs, resulted in a modest increase (+2-3 degrees) in the T_m values.

siRNAs with mixmer-modified AS strands exhibited similar (M-P53-AS 5), or significantly higher activity (M-P53-AS 4 and 6) than the 2'-5'-only modified siRNAs (**Figure 4.6**). Therefore, here again, the mixmer configuration restores the activity of an otherwise inactive 2'-5'-siRNAs. As shown in the following sections, this observation also applies to other mixmer modification combinations (Section 4.4).

4.2.5 Immunostimulatory effects of 2'-5'/3'-5' siRNA mixmers

siRNA treatment, as previously explained, can elicit strong interferon-α (IFN-α) responses in human peripherial blood mononuclear cells (PBMCs).[14, 15] In Chapter 3, we demonstrated that the 2'-5'-modified siRNA have immune evading effects, and wonder if the same is true for 2'-5'/3'-5' siRNA mixmers.

To address this question, IFN-α and IL6 production levels were evaluated in PBMC cells treated

Table 4.3 Sequences of single stranded RNAs and siRNAs modified with 2'-5' linkages targeting 728UU gene. Legend: 2'-5' linked RNA, 2'-5'/3'-5' mixmer RNA, 3'-5' linked RNA. The highlighted UGUGU sequence was reported to be the highly immunostimulatory motif and is incorporated in the sense strand of the siRNA targeting 728UU.

Sample	Sequence
728UU ctrl	5'- AAAUCGCUGAUUUGUGUAGUU-3' 3'-UUUUUAGCGACUAAACACAUC-5'
728UU-25S	5'-AAAUCGCUGAUUUGUGUAGUU-3' 3'-UUUUUAGCGACUAAACACAUC-5'
728UU-25AS	5'-AAAUCGCUGAUUUGUGUAGUU-3' 3'-UUUUUAGCGACUAAACACAUC-5'
728UU-MixS	5'-AAAUCGCUGAUUUGUGUAGUU-3' 3'-UUUUUAGCGACUAAACACAUC-5'
728UU-MixAS	5'-AAAUCGCUGAUUUGUGUAGUU-3' 3'-UUUUUAGCGACUAAACACAUC-5'
RNA-S	5'-AAAUCGCUGAUUUGUGUAGUU-3'
RNA-AS	3'-UUUUUAGCGACUAAACACAUC-5'
25-S	5'-AAAUCGCUGAUUUGUGUAGUU-3'
25-AS	3'-UUUUUAGCGACUAAACACAUC-5'
Mixmer-S	5'-AAAUCGCUGAUUUGUGUAGUU-3'
Mixmer-AS	3'-UUUUUAGCGACUAAACACAUC-5'

with the unmodified or mixmer modified siRNAs listed in **Table 4.3**. These studies were performed at Beckman Research Institute at City of Hope, in the laboratory of Dr. John Rossi. PBMC cells were treated with unmodified or modified siRNAs using DOTAP as the transfecting agent. IFN-α and IL6 production levels were measured 24 hours later by ELISA. siRNA sequence 728UU was chosen for this study, as it has been reported to have strong immunostimulatory activity in PBMCs, caused by a "UGUGU" motif in its sense strand.[14]

PBMCs treated with the unmodified control siRNAs (728UU ctrl) and single stranded RNAs (RNA-S and RNA-AS), showed significantly increased IFN production compared to the mock treatments (**Figure 4.7**). Fully modifying the immunostimulatory sense strand of 728UU siRNA with 2'-5' linkages almost completely abolished the immune response. This was also true for the

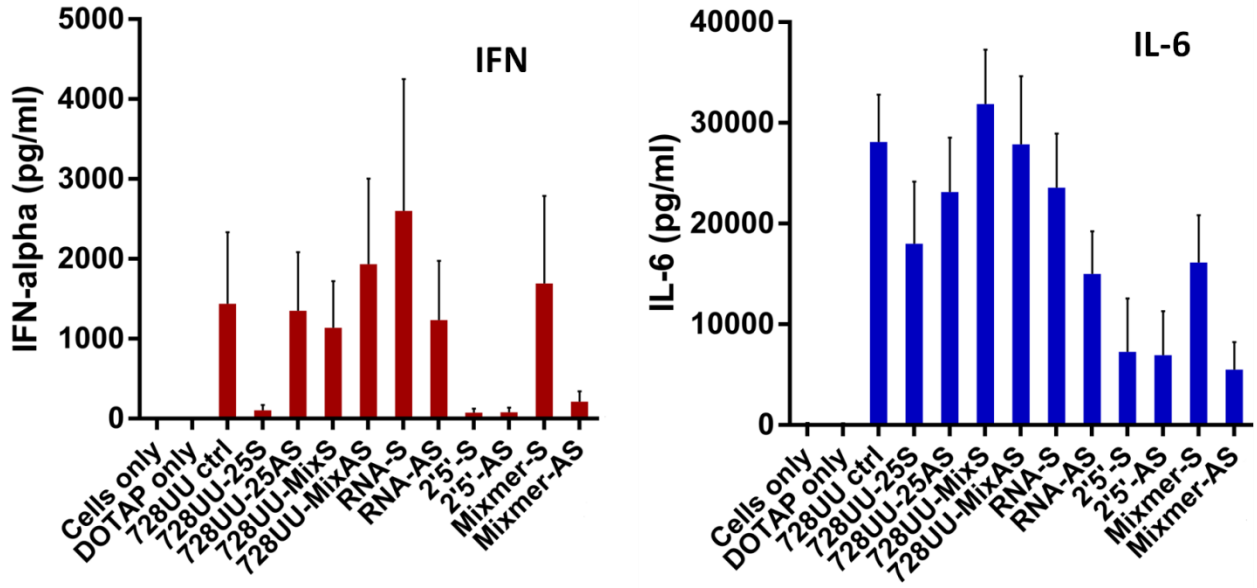

Figure 4.7 Comparison of immunostimulation prior to treatment with the siRNAs targeting 728UU. IFN levels were measured in PBMC cells 24 hours after siRNAs were transfected in duplicate using DOTAP. IFN-α levels (left graph) and IL-6 levels (right graph) in response to unmodified control siRNAs (728UU ctrl) and control single stranded RNAs (RNA-S and RNA-AS), is compared to 2'-5'- or mixmer- modified siRNAs (728UU-25S and 728UU-25AS) and single stranded 2'-5'- or mixmer- modified ssRNAs (S and AS). Cells only was the negative control with no reagents. DOTAP only treatment was transfection without siRNA. Data was collected in duplicate for each of six donors. Bars indicate standard deviation.

2'-5' S and AS single strands. In contrast, both the 2'-5'/3'-5' siRNA mixmer (728UU mixS) and mixmer-S single strand induced IFN and IL-6 secretions to a significant extent. Interestingly, the immunostimulatory activity of the mixmer-AS single strand was much more reduced, as was the case for the 2'-5'-S and AS strand. IL-6 levels followed the same trend in all cases, although IL6 levels were not reduced as IFN levels. The change in IFN levels upon 2'-5' or mixmer modifications were more pronounced in the case of single stranded RNAs, compared to the siRNA duplexes (**Figure 4.7**).

4.3 2'-5'/3'-5' RNA mixmers: Averaging or synergistic effects? Preparation of a 64-member library

To determine whether the observed gene knockdown activity of a mixmer siRNA is simply an average of the activities of all components in the mixture, we evaluated the activity of a mixmer and an artificial mixture prepared by manually combining all possible members found in the mixmer ("pseudo-mixmer"). To accomplish this, each member of the mixmer was prepared separately. Once purified and characterized, each member was combined to afford the "pseudo"-mixmer. If the mixmer were as active as the pseudo-mixmer, then the activity observed for the mixmer is likely the average activity of the members in these mixtures.

In this experiment, we used the 64 member library targeting firefly luciferase described in Chapter 3. Equal stoichiometric amounts from each member of this library were mixed to generate the "64 Mix" pseudo-mixmer sample. First, we compared the gene knockdown activity of the "64 Mix" pseudo-mixmer with the activity of each member in the siRNA library (**Figure 4.8** (a)). Given the large number of samples in the library (64), the IC_{50} values of each member was not determined (this would require over 1500 transfection experiments!). Rather, inhibition of luciferase protein expression was determined for each sample at a fixed duplex concentration

(20 nM). From this, the average of normalized luciferase activity levels for each sample in the library was calculated (ave.: 59% inhibition), and compared it with the luciferase activity level of the "64 Mix" sample (76% inhibition). The significantly higher activity of the artificially prepared "64 Mix" pseudo-mixmer (over the activity obtained by averaging the activity of each member) suggest a synergistic effect may be operating in the "64 Mix" pseudo-mixmer.

To assess the activity of the 2'-5'/3'-5'-siRNA mixmer under the same conditions, we synthesized mixmer samples obtained from two different 3'P/2'P amidite compositions, i.e., 1:1 and 1:1.3. The latter ratio takes into account the better coupling efficiency of 3′P vs 2′P amidites (Section 4.2.2). By using higher equivalents of 2'-5' phosphoramidites (1.3 eq. of 2'P vs. 1 eq. of 3'P amidites) during mixmer siRNA solid-phase synthesis, incorporation of 2'-5' and 3'-5' linkages would proceed with equal efficiency. This would provide theoretically a mixture of 64 siRNA oligomers in approximately equal amounts, as in the artificially prepared "64 Mix" pseudo-mixmer sample.

The dose response and inhibition data shown in **Figure 4.8**b indicates that the activities of the mixmer-1:1 and mixmer-1:1.3 are similar to the native siRNA control (ca. 30 nM), and slightly more active than the "64-Mix"-pseudo mixmer (ca. 60 nM). We estimate that the activity of the siRNA members (averaged over all 64 members) is >100 nM.

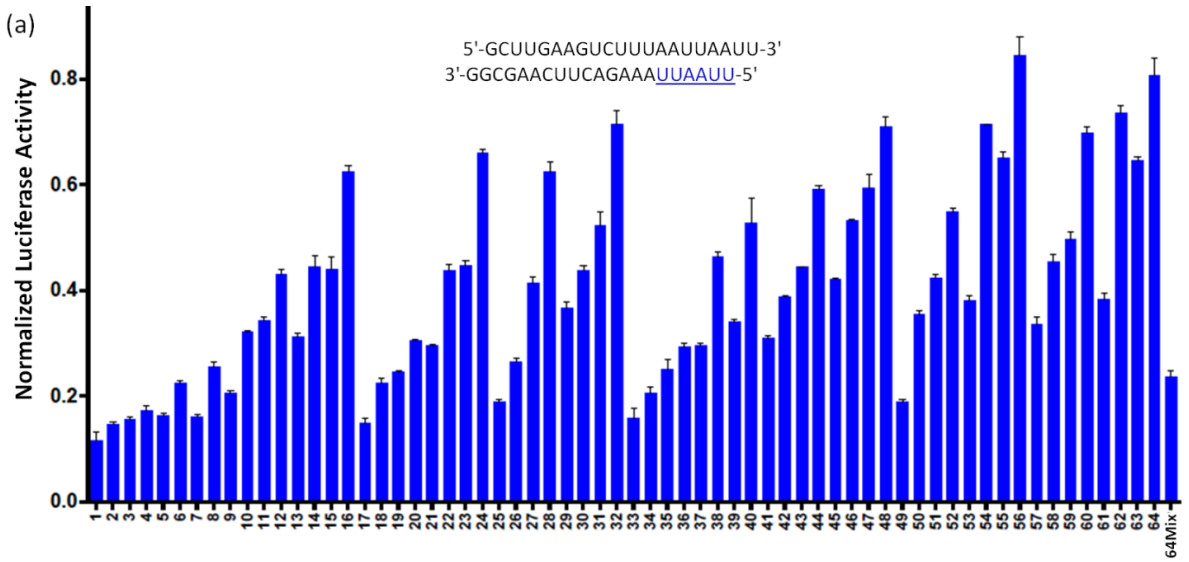

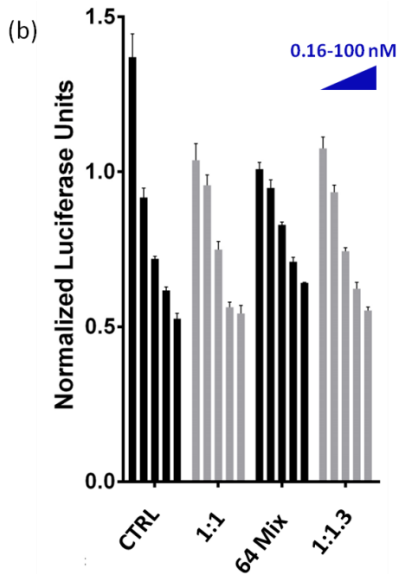

Sample	IC_{50} value
CTRL	29
1:1 mixmer	25
64 Mix	64
1:1.3 mixmer	32

Figure 4.8 (a) Positional screening of 2'-5' linked siRNAs targeting firefly luciferase in 64 library. siRNAs are modified on the six nucleotides on the 5'- terminal of guide strand and are represented by the number corresponding to their guide strand shown in **Table 3.4**. Comparison of the average of normalized luciferase activity levels for samples 1 to 64 (41%) with the luciferase activity level of 64 Mix sample (24%) shows that the observed knockdown potency in the 64 Mix sample is not due to a simple average of the potencies of all the 64 siRNAs. (b) Comparison of the activity of mixmer siRNAs with 1:1 and 1:1.3 ratios of 3'P: 2'P amidites with 64 Mix siRNA. Mixmer siRNAs show similar potency to the native siRNA duplex. siRNA activity was tested at a range of concentrations (0.16, 0.8, 4, 20, 100 nM).

4.4 Beyond the 2'-5'/3'-5' siRNA mixmers: Can other chemical modifications exhibit similar mixmer siRNA properties?

We wondered if mixmers prepared using other nucleotide analogs would also provide active siRNAs. Those considered in this study are various combinations of RNA, 2'-*O*Me RNA, 2'-5'RNA, FANA, and ANA modifications, shown in **Table 4.4**. All samples were purified as a single peak by IE-HPLC following the same protocol used for 2'-5'/3'-5' mixmers. LCMS profile for 2'-*O*Me/ANA and RNA/FANA mixmers (details in experimental section) are provided in **Figure 4.9**. As expected, product distribution within a mixmer sample follows a Boltzmann distribution pattern, with the highest population of products at the center of the peak pocket belonging to the group of products with the highest positional variation of modifications.

Table 4.4 SiRNAs targeting firefly luciferase were modified with either mixmer (X/Y) or pure modifications (X or Y) according to the table below. Modified nucleotides were at the central region of the AS strand.

(S) 5'-GCUUGAA GUCUUUA AUUAAUU-3'
(AS) 3'-GGCGAAC UUCAGAA AUUAAUU-5'

Control siRNA (X)	(X/Y) mixmer siRNA	Control siRNA (Y)
Luc-2'-*O*Me	Luc-2'-*O*Me/RNA	Luc-RNA
Luc-2'-*O*Me	Luc-2'-*O*Me/2'-5'	Luc-2'-5'
Luc-FANA	Luc-FANA/ANA	Luc-ANA
Luc-FANA	Luc-FANA/RNA	Luc-RNA
Luc-ANA	Luc-ANA/RNA	Luc-RNA
Luc-ANA	Luc-ANA/2'-*O*Me	Luc-2'-*O*Me

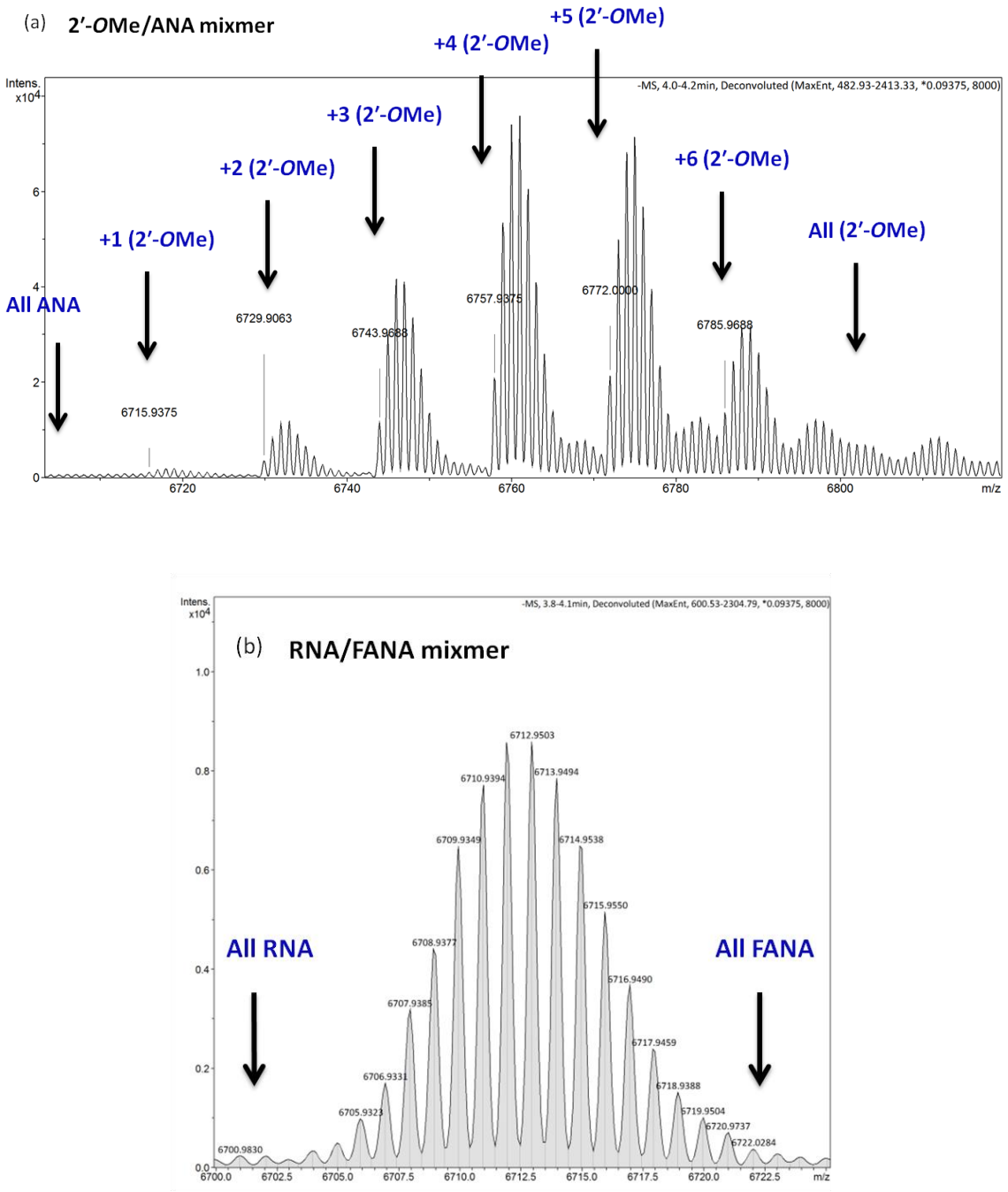

Figure 4.9 ESI-MS profile for 2'-*O*Me/ANA (a) and RNA/FANA (b) mixmers. Distribution of the peaks between the two margins represent the population of the modified species within a mixmer sample.

The lowest and highest margins of the peak pockets for 2'-*O*Me/ANA and RNA/FANA mixmers (**Figure 4.9**) represent a strand with only the lighter or the heavier modification used in the modification segment. In 2'-*O*Me/ANA mixmer, there is 14 mass units difference between 2'-*O*Me and ANA modified nucleotide of the same base, which separates each subgroup of strands with similar number of 2'-*O*Me and ANA. In the case of an RNA/FANA mixmer, the mass unit difference between RNA and FANA is 2 units, which does not allow much separation in between each peak sub-groups, as in 2'-*O*Me/ANA mixmers.

4.4.1 Beyond the 2'-5'/3'-5 mixmers: luciferase assay results

Following the synthesis of the modified AS strands listed in **Table 4.4**, the corresponding siRNA for each X/Y mixmer, as well as their X and Y control siRNAs were prepared and tested against firefly luciferase mRNA. As expected, other than 2'-*O*Me modification, the rest of the modifications used here in the mixmers preparation (2'-5', FANA, ANA) were not much tolerated in the AS strand and resulted in siRNAs with diminished activity. However, when a mixmer siRNA was prepared from RNA or an AS-tolerated modification (such as 2'-*O*Me) mixed with an AS-non-tolerated modification (2'-5', FANA, ANA), the resulting siRNA gained significant activity (**Figure 4.10**). These results are in complete agreement with previous findings, indicating that 2'-5'/3'-5' mixmers can enhance the tolerance of 2'-5' modifications in the siRNA AS strand. An exception to these results were in mixmers prepared from FANA/RNA or FANA/ANA. The latter assay confirmed that mixmers prepared from two inactive AS modifications are less likely to show more activity than any of the parent modified (X or Y) siRNAs.

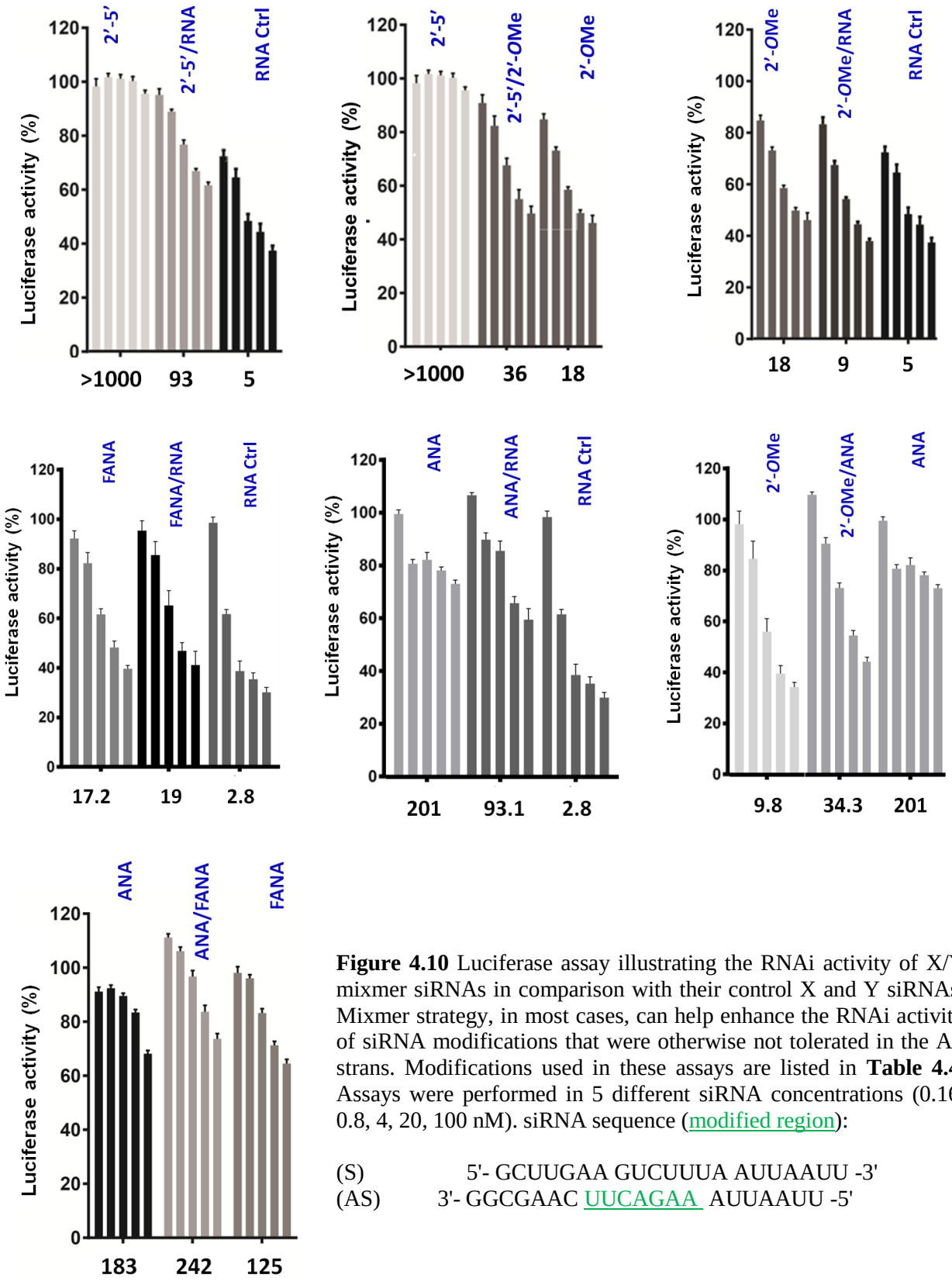

Figure 4.10 Luciferase assay illustrating the RNAi activity of X/Y mixmer siRNAs in comparison with their control X and Y siRNAs. Mixmer strategy, in most cases, can help enhance the RNAi activity of siRNA modifications that were otherwise not tolerated in the AS strans. Modifications used in these assays are listed in **Table 4.4**. Assays were performed in 5 different siRNA concentrations (0.16, 0.8, 4, 20, 100 nM). siRNA sequence (modified region):

(S) 5'- GCUUGAA GUCUUUA AUUAAUU -3'
(AS) 3'- GGCGAAC UUCAGAA AUUAAUU -5'

4.5 Conclusion and future work

The mixmer strategy takes advantage of vast variety of siRNA modifications that are, otherwise, not tolerated in the AS strand. For example, the 2'-5'/3'-5' mixmer strategy produces an active mixture while avoiding the lengthy and labour intensive process of synthesis and screening of dozens-to-hundred of 2'-5'-modified siRNAs. Our results suggest that siRNA mixmers prepared from different modifications can enhance RNAi activity to various degrees. Detailed structural investigations are needed to elucidate why some modifications are more compatible with each other to yield active siRNAs. We speculate the flexibility of modifications, and the ability of mixmer X/Y nucleotides to adjust themselves to the duplex structure is a key factor that modulate the activity of these X/Y siRNA mixmers.

Our strategy can significantly contribute to the design of a new class of AS-modified siRNAs, adding to the handful of modifications that are currently known to be accepted in the AS strand.[16] Our results demonstrate that mixmer strategy can particularly be useful in a smart design of siRNAs, utilizing a variety of chemical modifications to introduce nuclease stability and abrogate immunostimulatory effects.

4.6 Experimental methods

4.6.1 Oligonucleotide synthesis and siRNA preparation

Standard phosphoramidite solid-phase synthesis conditions were used for the synthesis of all modified and unmodified oligonucleotides.[17] Syntheses were performed on an Applied Biosystems 3400 DNA Synthesizer at a 1 μmole scale using Unylinker CPG support (ChemGenes). All phosphoramidites, including the 2'-5' phosphoramidites, were prepared as 0.15 M solutions in acetonitrile (ACN). Mixmer amidites were generally prepared from 1:1 amidite mixtures of the two modification phosphoramidite, unless stated otherwise. 5-

ethylthiotetrazole (0.25 M in ACN) was used to activate phosphoramidites for coupling. Detritylations were performed using 3% trichloroacetic acid in CH_2Cl_2 for 110 sec. Failure sequences were capped using acetic anhydride in THF and 16% *N*-methylimidazole in THF. A 0.1 M solution of I_2 in 1:2:10 pyridine:water:THF was used for oxidation. Coupling times were 600 seconds for all RNA, 2'-5', 2'-*O*Me, 2'-FRNA, ANA, and FANA phosphoramidites as well as their mixmers, except for their guanosine phosphoramidites which had 900 seconds of coupling time. When a mixmer of two modifications with different coupling times were prepared, settings were adjusted based on the modification with higher coupling time. Chemical 5'-phosphorylation of selected modified guide strands was done at the synthesizer instrument using bis-cyanoethyl-N,N-diisopropyl-2-cyanoethyl phosphoramidite at 0.15 M (600 sec coupling time). Deprotection and cleavage from the solid support for was accomplished with 3:1 NH_4OH:EtOH for 48 hours at room temperature (for 2'-5' modified samples, as well as other modifications), and with 40% methylamine for 10 minutes at 65° C (for unmodified RNA samples).[18] Oligonucleotides containing either 3'-5' or 2'-5' RNAs were both synthesized with standard 2'-TBDMS and 3'-TBDMS phosphoramidites respectively. Desilylation of all samples was achieved with triethylamine trihydrofluoride/N-methyl pyrrolidone/triethylamine (1.5:0.75:1 by volume) for 2.5 hours at 65 °C.[18, 19]

Purification of crude oligonucleotides was done by HPLC using an anion exchange column (Protein PAK DEAE 5PW 21.5 mm × 15 cm). The buffer system consisted of water (solution A) and 1 M lithium perchlorate solution in water (solution B), at a flow rate of 4 mL/min. The gradient was 0−40% B over 40 min at 60 °C. Under these conditions, the desired peaks eluted at 20−30 minutes. The collected samples were then lyophilized to dryness and were desalted with Nap-25 Sephadex columns from GE Healthcare.

Table 4.5 MS characterization of S and AS strands comprising the siRNAs targeting firefly luciferase, P53, and 728UU

Sample Name	Sequence	Exact Mass (Calc)	Exact Mass (Exp)
Luciferase S	5'- GCUUGAAGUCUUUAAUUAAUU -3'	6617.8352	6617.8352
Luciferase AS	3'- GGCGAACUUCAGAAAUUAAUU -5'	6701.9292	6701.9292
P53 S	3'-CCAAUGUGUACAUGAACAUCA-5'	6660.9392	6660.9392
P53 AS	5'-UUACACAUGUACUUGUAGUGG-3'	6671.8672	6671.8672
728UU S	5'- AAAUCGCUGAUUUGUGUAGUU-3'	6672.8512	6672.8512
728UU AS	3'-UUUUUAGCGACUAAACACAUC-5'	6598.8892	6598.8892
Luc-2'-*O*Me	3'- GGCGAACUUCAGAAAUUAAUU -5'	6800.0692	6800.0313
Luc-FANA	3'- GGCGAACUUCAGAAAUUAAUU -5'	6715.9331	6715.8438
Luc-ANA	3'- GGCGAACUUCAGAAAUUAAUU -5'	6701.9292	6701.8750
Luc-2'-*O*Me/RNA	3'- GGCGAACUUCAGAAAUUAAUU -5'	6701.9292-6800.0692	6743.9688-6799.9376 (detected range)
Luc-2'-*O*Me/2'-5'	3'- GGCGAACUUCAGAAAUUAAUU -5'	6701.9292-6800.0692	6757.9375-6800.0313 (detected range)
Luc-FANA/ANA	3'- GGCGAACUUCAGAAAUUAAUU -5'	6701.9292-6715.9331	6704.8607-6716.8691 (detected range)
Luc-FANA/RNA	3'- GGCGAACUUCAGAAAUUAAUU -5'	6701.9292-6715.9331	6701.9830-6715.9550 (detected range)
Luc-ANA/RNA	3'- GGCGAACUUCAGAAAUUAAUU -5'	6701.9292	6701.8750
Luc-ANA/2'-*O*Me	3'- GGCGAACUUCAGAAAUUAAUU -5'	6701.9292-6800.0692	6715.9375-6785.9688 (detected range)

Sequences were verified by high resolution ESI-LCMS. Note that since 2'-5' linked RNA is a regioisomer of RNA, all 2'-5' modified samples had exactly the same mass as their unmodified control. The observed mass range for some of the mixmer oligos was shifted more towards one range, due to the differences in coupling efficiency of the modifications used in the mixmer

preparation, as well as different ionization abilities of the modified species in the mixmer (**Table 4.5**). The oligonucleotides were analyzed by LC-MS using a Dionex Ultimate 3000 UHPLC coupled to a Bruker Maxis Impact QTOF mass spectrometer in negative ESI mode. Samples were run through a Phenemonex Luna C18(2)-HST column (2.5 uM 100A 2.0 x 50 mm) using a gradient of 95% mobile phase A (100 mM HFIP and 5 mM TEA in H2O) and 5 % mobile phase B (MeOH) to 40 % mobile phase A and 60% mobile phase B in 8 minutes. The data was processed and deconvoluted using the Bruker Data Analysis software version 4.2.

4.6.2 Thermal denaturation experiments and circular dichroism studies

Complementary sequences from siRNA libraries (1.5 nmol) were combined, dried, and rediluted in 1 mL of T_m buffer containing 140 mM KCl, 1 mM $MgCl_2$ and 5 mM Na_2HPO_4 (pH 7.2). Samples were then transferred into UV cuvettes in a Varian Cary 300 UV spectrophotometer and heated up to 90 °C. They were cooled down to 5 °C (ramped at 1°C/min), followed by heating up from 5 °C to 95 °C. The change in their absorbance at 260 nm was monitored upon cooling and heating steps. Melting temperatures were determined using the heating ramp and via baseline method, as implemented in the Cary software.

CD spectra were obtained on a JASCO J-810 circular dichroism spectrometer equipped with a Peltier temperature controller at the Biochemistry Department at McGill. Samples were annealed at a final concentration of 10 nM prior to the experiment in the same buffer as for the thermal denaturation studies. Spectra were recorded at 25 °C under constant flow of nitrogen gas, and was baseline-corrected with respect to a blank containing the buffer only Smoothing and adjustment for duplex concentration were performed using the Spectra-Manager program (Jasco)

4.6.3 Luciferase siRNA assay

Luciferase knockdown assays were performed as described in Deleavey et al.[20] with a few modifications. Typically, HeLa cells were counted and seeded at a density of 10,000 cells/well in a 96-well plate. Cells were allowed to recover for 24 hours at 37°C with 5% CO_2. Subsequently, cells were washed once with serum-free DMEM media and then 80 µl of serum-free DMEM media was added. siRNA and control nucleic acid preparations were diluted up to 20 µl with serum-free media and transfection reagent (Oligofectamine, Invitrogen) and added to the appropriate well (for a total of 100 uL) at increasing concentrations (0.16, 0.8, 4, 20, and 100 nM). Cells were incubated overnight (for a total of 24 hours post-DNA addition). Then 50 uL of ONE-Glo luciferase reagent (Promega, USA) was added to each well and luminescence was measured and normalized to protein levels using a Biotek Synergy HT plate reader. Data was acquired with the Gen5 software suite and data was manipulated and plotted using Graphpad Prism software suite.

4.6.4 P53 siRNA reporter assay

Cloning of P53 reporter was performed following the instructions reported in literature.[21] Briefly, a G-block was ordered from IDT Technologies containing the p53 target side flanked by restrictions sides for *XhoI* and *NotI* at the 5' and 3' of the sequence, respectively, to clone the sequence into the 3' UTR of the Renilla gene of the plasmid PsiCheck2 (Promega). Following the cloning, the plasmid was sequence verified.

Sequence:

"atccgtttcaagccg**CTCGAG**agcgtggtggtaccttatgagccacccgaggccggctctgagtataccaccatccactacaagtac atgtgtaatagctcctgcatgggggcatgaaccgccgacctatccttaccatc**GCGGCCGC**gttcataggcttatg"

The plasmid was then, transfected into 293T cells using $CaPO_4$, followed by siRNA transfection, following the procure explained here. 293T cells were seeded with 5000 cells/well in a 96 well plate. After 12 hours, they were transfected with the siRNAs using Oligofectamine (Invitrogen). 24 hours after siRNA transfection, cells were transfected with 20 ng/well of the DNA plasmid, using calcium phosphate. 48 hours after the plasmid transfection, cells were harvested in 100uL PLB (Passive Lysis Buffer, Promega) and 5ul was used to read FF/Ren using a Fluorostar Optima.

4.6.5 Immunostimulation assays in human peripheral blood mononuclear cells (PBMCs)

Peripheral blood mononuclear cells (PBMCs) were obtained from healthy donors at City of Hope National Medical Center using discarded anonymous blood unit leukocyte filters (Pall). PBMCs were plated in 24-well plate ($2.5x10^6$ cells/well) and transfected using DOTAP transfection reagent (Sigma-Aldrich) according to the manufacture's protocol at a final RNA concentration of 80 nM. Cells were incubated at 37 °C for 24 hours. Supernatants from each well were collected, and IFN-a and IL-6 levels were quantified by enzyme-linked immunosorbent assay (ELISA) using 96-well ELISA plates coated with a human IFN-a or IL-6 antibody (ThermoFisher Scientific), respectively. During this experiment, discarded peripheral blood from anonymous adult donors from the City of Hope Apheresis Center (Duarte, CA) was used. The proposed research involved blood specimens from anonymous human subjects with no identifiers to age, race, ethnicity, or gender. The information provided for the above submission was evaluated and determined not to involve human subjects research (45 CFR 46.102 (d)(f)). Therefore, it does not need to be approved nor does it need to undergo continuing review by the Institutional Review Board (IRB) in the City of Hope.

4.7 References

1. Trevino, S. G.; Zhang, N.; Elenko, M. P.; Luptak, A.; Szostak, J. W., Evolution of functional nucleic acids in the presence of nonheritable backbone heterogeneity. *Proceedings of the National Academy of Sciences of the United States of America* **2011,** *108*, 13492-7.
2. Engelhart, A. E.; Powner, M. W.; Szostak, J. W., Functional RNAs exhibit tolerance for non-heritable 2′–5′ versus 3′–5′ backbone heterogeneity. *Nat Chem* **2013,** *5*, 390-394.
3. Adamala, K.; Engelhart, A. E.; Szostak, J. W., Generation of Functional RNAs from Inactive Oligonucleotide Complexes by Non-enzymatic Primer Extension. *J Am Chem Soc* **2015,** *137*, 483-489.
4. Sheng, J.; Li, L.; Engelhart, A. E.; Gan, J.; Wang, J.; Szostak, J. W., Structural insights into the effects of 2′-5′ linkages on the RNA duplex. *Proceedings of the National Academy of Sciences* **2014,** *111*, 3050-3055.
5. Myers, J. W.; Jones, J. T.; Meyer, T.; Ferrell, J. E., Recombinant Dicer efficiently converts large dsRNAs into siRNAs suitable for gene silencing. *Nat Biotech* **2003,** *21*, 324-328.
6. Kittler, R.; Surendranath, V.; Heninger, A. K.; Slabicki, M.; Theis, M.; Putz, G.; Franke, K.; Caldarelli, A.; Grabner, H.; Kozak, K.; Wagner, J.; Rees, E.; Korn, B.; Frenzel, C.; Sachse, C.; Sonnichsen, B.; Guo, J.; Schelter, J.; Burchard, J.; Linsley, P. S.; Jackson, A. L.; Habermann, B.; Buchholz, F., Genome-wide resources of endoribonuclease-prepared short interfering RNAs for specific loss-of-function studies. *Nature methods* **2007,** *4*, 337-44.
7. Hannus, M.; Beitzinger, M.; Engelmann, J. C.; Weickert, M.-T.; Spang, R.; Hannus, S.; Meister, G., siPools: highly complex but accurately defined siRNA pools eliminate off-target effects. *Nucleic Acids Research* **2014**.
8. Eckstein, F., Developments in RNA chemistry, a personal view. *Biochimie* **2002,** *84*, 841-8.
9. Guga, P.; Stec, W. J., Synthesis of Phosphorothioate Oligonucleotides with Stereodefined Phosphorothioate Linkages. In *Current protocols in nucleic acid chemistry*, John Wiley & Sons, Inc.2001.
10. Sanghvi, Y. S., A Status Update of Modified Oligonucleotides for Chemotherapeutics Applications. In *Current protocols in nucleic acid chemistry*, John Wiley & Sons, Inc.2001.
11. Bennett, C. F.; Swayze, E. E., RNA targeting therapeutics: molecular mechanisms of antisense oligonucleotides as a therapeutic platform. *Annual review of pharmacology and toxicology* **2010,** *50*, 259-93.
12. Zanetta, C.; Nizzardo, M.; Simone, C.; Monguzzi, E.; Bresolin, N.; Comi, G. P.; Corti, S., Molecular therapeutic strategies for spinal muscular atrophies: current and future clinical trials. *Clinical therapeutics* **2014,** *36*, 128-40.
13. Wasner, M.; Arion, D.; Borkow, G.; Noronha, A.; Uddin, A. H.; Parniak, M. A.; Damha, M. J., Physicochemical and Biochemical Properties of 2‘,5‘-Linked RNA and 2‘,5‘-RNA:3‘,5‘-RNA “Hybrid” Duplexes. *Biochemistry* **1998,** *37*, 7478-7486.
14. Judge, A. D.; Sood, V.; Shaw, J. R.; Fang, D.; McClintock, K.; MacLachlan, I., Sequence-dependent stimulation of the mammalian innate immune response by synthetic siRNA. *Nat Biotech* **2005,** *23*, 457-462.
15. Hornung, V.; Guenthner-Biller, M.; Bourquin, C.; Ablasser, A.; Schlee, M.; Uematsu, S.; Noronha, A.; Manoharan, M.; Akira, S.; de Fougerolles, A.; Endres, S.; Hartmann, G., Sequence-

specific potent induction of IFN-[alpha] by short interfering RNA in plasmacytoid dendritic cells through TLR7. *Nature medicine* **2005,** *11*, 263-270.
16. Martínez-Montero, S.; Deleavey, G. F.; Martín-Pintado, N.; Fakhoury, J. F.; González, C.; Damha, M. J., Locked 2′-Deoxy-2′,4′-Difluororibo Modified Nucleic Acids: Thermal Stability, Structural Studies, and siRNA Activity. *ACS Chemical Biology* **2015,** *10*, 2016-2023.
17. Damha, M. J.; Ogilvie, K. K., Oligoribonucleotide synthesis. The silyl-phosphoramidite method. *Methods in molecular biology (Clifton, N.J.)* **1993,** *20*, 81-114.
18. Bellon, L., Oligoribonucleotides with 2'-O-(tert-butyldimethylsilyl) groups. *Current protocols in nucleic acid chemistry* **2001,** *Chapter 3*, Unit 3.6.
19. Wincott, F.; DiRenzo, A.; Shaffer, C.; Grimm, S.; Tracz, D.; Workman, C.; Sweedler, D.; Gonzalez, C.; Scaringe, S.; Usman, N., Synthesis, deprotection, analysis and purification of RNA and ribozymes. *Nucleic Acids Res* **1995,** *23*, 2677-84.
20. Deleavey, G. F.; Watts, J. K.; Alain, T.; Robert, F.; Kalota, A.; Aishwarya, V.; Pelletier, J.; Gewirtz, A. M.; Sonenberg, N.; Damha, M. J., Synergistic effects between analogs of DNA and RNA improve the potency of siRNA-mediated gene silencing. *Nucleic Acids Res* **2010,** *38*, 4547-57.
21. Jahns, H.; Roos, M.; Imig, J.; Baumann, F.; Wang, Y.; Gilmour, R.; Hall, J., Stereochemical bias introduced during RNA synthesis modulates the activity of phosphorothioate siRNAs. *Nature communications* **2015,** *6*.

CHAPTER 5: PARALLEL HYBRIDS AS TRIGGERS OF RNAi

5.1 Introduction

5.1.1 Parallel duplexes: History and synthesis

Canonical nucleic acid duplexes, as explained in Chapter 1, have their strands arranged in an antiparallel orientation with one strand in 5'-to-3' and the other in 3'-to-5' orientation.[1] However, under certain conditions[2], nucleic acids are capable of forming parallel duplexes (Chapter 1, **Figure 1.5**).[3-8] This noncanonical structure can also be seen as constituents of DNA triplexes,[9-12] G-quadruplexes,[13-15] and i-motifs[16, 17] (Chapter 1, **Figure 1.5**).

Parallel duplex hybridization was not considered feasible until, for the first time, in 1986 Pattabiraman through quantum mechanics calculations demonstrated that a parallel stranded (*ps*) DNA duplex (dA6:dT6) is possible.[18] Triggered by this model, the first structural and thermodynamic study on a parallel DNA duplex was performed at the University of Calgary by Van de Sande and co-workers in 1988.[6] This study investigated hairpin sequences containing either a 3'-p-3' or a 5'-p-5' internucleotide linkage on the loop region, which as a result, forced two DNA strands to hybridize parallel to one another.[6] Much progress has been made ever since in the structural investigations of parallel double helical structures.[19-29] Parallel duplexes are generally difficult to build, as it requires perfect sequence complementarity of the strands in the parallel orientation that is not complementary in the antiparallel orientation. Essentially, special conditions should be maintained in order to avoid the formation of other competing secondary structures such as an antiparallel duplex, G-quadruplex, or triplex, and instead, form a parallel duplex. Other conditions that are required for the formation of parallel duplexes are application of certain chemical modifications, or unnatural environmental conditions. For example, chemical

modification of nucleobases have been demonstrated to help establish the parallel orientation of the strands.[30-34] isoG:C and isoC:G base pairs (chapter 1, section 1.7.2), for instance, have been demonstrated to improve the hydrogen bonding and duplex stability of parallel oriented duplexes.[35, 36] Other chemical modifications establish parallel strand orientation by introducing strand polarity reversal as a consequence of 3′/3′ or 5′/5′ linkages,[6, 37, 38] or by changing the stereochemistry of the glycosidic bonds as in parallel hybrids formed with α-anomeric oligodeoxynucleotides and complementary β-oligodeoxynucleotides.[39, 40] Parallel hybridization can also be attained in acidic pHs, mainly through formation of $C:C^+$ Hoogsteen base pairs.[8, 41-43] The following section focuses on binding patterns in parallel duplexes in more detail.

5.1.2 Base pairing patterns in parallel duplexes

As explained in Chapter 1, nucleobases have different edges for base pairing.[44] These base pairing edges are (i) Watson- Crick (WC) edge, (ii) Hoogsteen (H) edge (purines)/ C-H edge (pyrimidines), and (iii) Sugar edge (SE), where the 2'-hydroxyl group of ribose in RNA is capable of forming efficient H-bonds (Chapter 1, **Figure 1.4**). Unlike the canonical base-pairing motif, which is WC edge-to-WC edge interaction, with relative cis orientation of glycosidic bonds, the major hetero-base pairing pattern (purine-pyrimidine hydrogen bonding) in parallel duplexes of mixed base composition is the reverse Watson Crick (rWC) base pairing (**Figure 5.1**). Similar to WC base pairs, the nucleobases interaction in rWC base pairs is also through their Watson-Crick edges. In rWC base pairing, however, the glycosidic bonds of the nucleotides relative to the axis of interaction are trans to each other.[5]

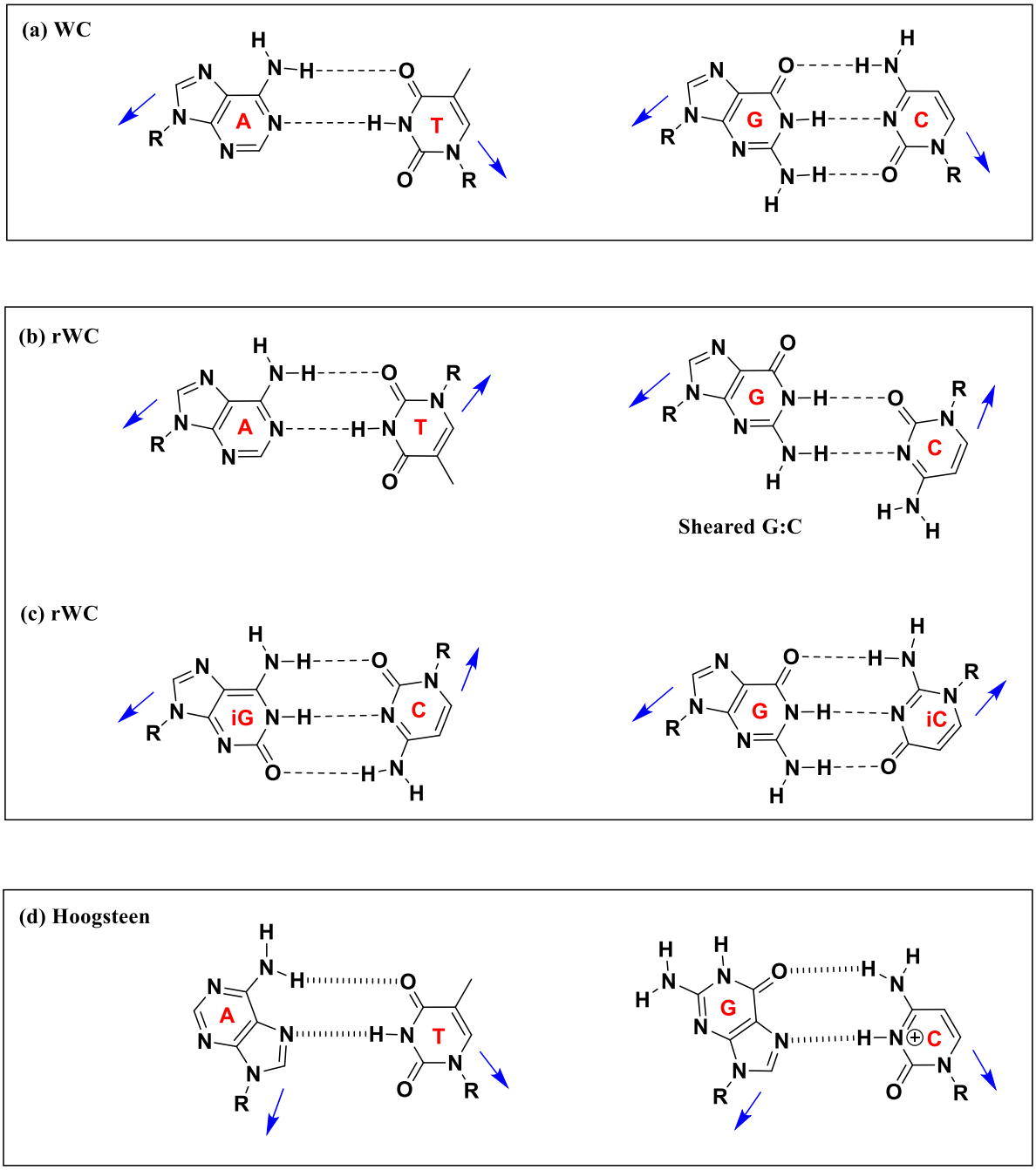

Figure 5.1 Canonical and noncanonical base pairing patterns in antiparallel (a) and parallel (b,c,d) ds DNA. Arrows represent the geometry of the glycosidic bonds in WC, rWC, and Hoogsteen base pairing modes. Purines in WC (a) and rWC (b,c) modes adopt the anti conformation, whereas the Hoogsteen mode (d) adopts a syn conformation. Note that in isoG:C and isoC:G base pairs (c) all three hydrogen bondings in the rWC mode are retained. WC and rWC base pairings are shown with dashed bonds, and Hoogsteen base pairing is shown with hashed bonds.

Thymine (and uracil), as presented in **Figure 5.1**, is symmetrical about the central thymine-N3-adenine-N1 axis of an A:T pair. This means that upon reversal of the strand orientation from antiparallel to parallel, the A:T pair can still form two hydrogen bonds. Therefore, A/T rich oligonucleotides can form stable rWC parallel-stranded duplexes.[3, 23] However, cytosine is not symmetrical in relation to the axis of interaction. As a result, G:C pairing in the rWC arrangement requires the bases to shift relative to one another, causing some stability loss in comparison with canonical G:C pair ("sheared" rWC G:C pair, **Figure 5.1**b). For this reason, rWC parallel sequences can still tolerate the presence of G:C pairs, although with reduced stability, which manifests itself in the low cooperative melting profiles of such duplexes.[5, 29, 45, 46] This energy loss is believed to be due to the sugar-phosphate backbone distortion at the A:T/G:C stacking contact, since the sheared trans G:C pair is not isomorphous to the trans AT pair. With this regard, isoG:C and isoC:G base pairs have been demonstrated to improve the hybridization properties of trans G:C base pairs and compensate for some of the energy loss.[5, 47] The twisted base structures of isoG and isoC (**Figure 5.1**) are able to retain all the three hydrogen bonds within isoG:C or isoC:G rWC base pairs in a mixed base parallel duplex, and hence stabilize the otherwise unstable parallel double helix.[32-35, 48] Parallel duplexes with rWC base pairing are also different with canonical B-DNA duplexes in that they contain grooves of about equal size.[6, 19]

Another class of hetero-base pairs observed for parallel hybridization is the Hoogsteen base pair, which occurs between the Hoogsteen edge of "syn" purines and the Watson-Crick edge of "anti" pyrimidines (**Figure 5.1**). This class of base pairing occurs in acidic environments, where the cytosine N3 is protonated to afford additional duplex stabilization via a C^+:G Hoogsteen pair (**Figure 5.1**).[8, 49, 50] Such acidic conditions can also help stabilize pyrimidine-pyrimidine and purine-purine pairing in the parallel orientation.[41, 51-56]

5.2 Background and objectives

Noncanonical parallel duplexes, as expected, present very different properties e.g. spectroscopic properties,[23, 28, 47] enzymatic recognition, and ligand-binding (drug or protein) properties,[57-59] in comparison to canonical antiparallel duplexes. Much research has been done recently on the structure and function of nucleic acid parallel double helices, mainly due their possible roles in nature,[60, 61] and the development of novel DNA nanostructures,[62] hybridization probes in synthetic biology,[63] and oligonucleotide-based therapeutics.[55, 64] It is important to note that most of these studies have been limited to parallel DNA duplexes.[6, 18-29] Reports of possible parallel stranded (ps) DNA:RNA or RNA:RNA duplexes are rare and remain mostly at the level of T_m characterization/measurements.[32, 34, 42, 65-67] In addition, the biological significance of ps-DNA:RNA or ps-RNA:RNA parallel duplexes, if any, remains to be established.

To expand upon our current knowledge of parallel-stranded duplexes, as well as following our ongoing interest in designing novel chemically modified siRNAs with enhanced drug-like properties, we aimed to study parallel-stranded (ps) duplexes, namely ps-DNA:RNA hybrids and ps-RNA:RNA, as triggers of RNA interference. Previous research from our lab conducted by Dr. Maryam Yahyaee (Ph.D. Thesis, 2015, McGill University)[68] and the Seela group[67] had shown that utilizing isoC and isoG can ensure formation of stable 12mer and 21mer ps-DNA:RNA hybrids under physiological-like conditions. In addition to isoC and isoG modifications, Dr. Yahyaee investigated the impact of 2'-fluorinated sugar modifications (2'F-RNA and 2'F-ANA) on parallel duplex strength, in order to assess whether similar stabilizing effects as in 2'-fluorinated antiparallel duplexes, were observed.[69-74] Remarkably, she observed that chemically modified ps-DNA:RNA duplexes were able to inhibit the expression of the oncoprotein protein Bcl-2. This suggested that the RNAi machinery is not limited to the antiparallel configuration for

recognition of siRNAs. All attempts to form ps-RNA:RNA failed to generate any stable duplex structures and hence could not be tested in the same *in-vitro* silencing assay.

The work in this chapter is in continuation of this line of research, focusing on ps-DNA:RNA hybrids to a) determine whether other mRNA targets can be silenced, b) inquire about the mechanism of action (is it RNAi?), and c) establish guidelines for the selection of effective ps-DNA:RNA for RNAi. In doing so, most of our efforts focused on ps-DNA:RNA duplexes targeting P53, CCND1, and renilla luciferase mRNAs. Results of these studies are described in the following sections.

5.3 Design of parallel stranded DNA:RNA duplexes

In the classical antiparallel siRNAs, the AS strand has full WC complementarity with the target mRNA, while the sense strand has the same sequence as the intended region on the target mRNA (**Figure 5.2**). In our study, we aimed to investigate rWC parallel hybridization as an alternative to the classical antiparallel WC hybridization. As in previous work, the ps-DNA:RNA duplex was designed in such a way that the RNA strand is parallel to the iso-C/G modified DNA strand (**Figure 5.2**); once the duplex is loaded into RISC and the iso-C/G modified DNA sense strand is discarded, the remaining AS RNA strand will hybridize to the target mRNA in the antiparallel orientation. Hence, whether one starts with a parallel stranded or antiparallel stranded duplex, the cleavage of the mRNA is triggered in both cases by an RNA strand bound to the mRNA in the antiparallel orientation (**Figure 5.2**). Thus any difference in activity between a ps-DNA:RNA and the canonical siRNA (antiparallel) duplex would presumably be due to differences in the rate of loading of these duplexes by RISC.

All parallel duplexes were designed as previously. The iso-dG and iso-dC modified DNA strand was hybridized to either a complementary RNA or 2'F-RNA strand. The resulting parallel duplexes were compared to the corresponding DNA:RNA and DNA: 2'F-RNA antiparallel duplexes. The choice for 2'F-RNA as antisense strand stems from previous reports indicating that the catalytic ribonuclease activity (AGO2) of RISC does not require the 2′-OH of guide antisense RNA.[75-78] Furthermore, we hoped to gain duplex stability as duplexes containing the 2'F-RNA modification are generally more stable. Lastly, it was anticipated that having a heavily modified DNA sense strand in our design may decrease the likelihood of this strand to act as an antisense strand, and therefore, minimize the off-target effects.

(a)

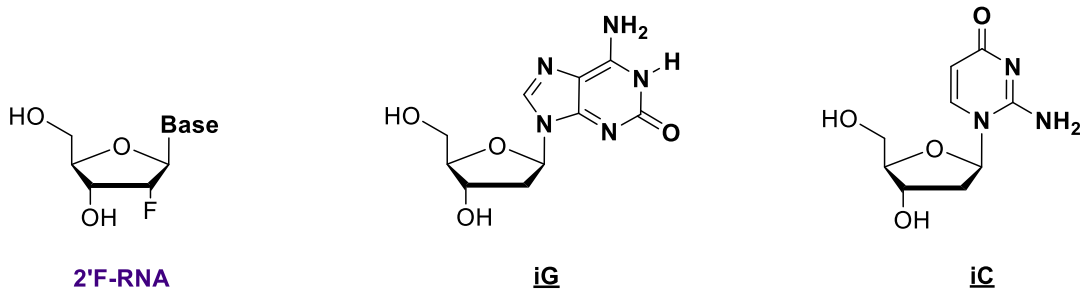

(b)

Parallel duplex	3'-iGiCATiGiCiGiGiCiCTiCTiGTTTiGATT-5'	Sense strand
Antiparallel duplex	3'-UUCGUACGCCGGAGACAAACU-5'	AS strand
	5'-GCAUGCGGCCUCUGUUUGA-3'	mRNA

(c)

Antiparallel duplex	5'-GCAUGCGGCCUCUGUUUGAUU-3'	Sense strand
Antiparallel duplex	3'-UUCGUACGCCGGAGACAAACU-5'	AS strand
	5'-GCAUGCGGCCUCUGUUUGA-3'	mRNA

Figure 5.2 Strategy used in the design of parallel stranded duplexes targeting Bcl2 (see (b)) in comparison with canonical antiparallel Bcl-2 siRNA duplex (see (c)). rWC ps-duplex was stabilized through incorporation of isoG and isoC in the sense strand (represented as iG and iC respectively). In both cases (b) and (c), the RISC is loaded with an identical AS strand which is antiparallel to the target mRNA and can elicit mRNA cleavage. AS strand was either all RNA, or modified with 2'F-RNA (shown here). Legend: DNA, iso-DNA, 2'-F-RNA, RNA.

Based on the above considerations, libraries of parallel duplexes targeting P53, CCND1, and renilla luciferase were synthesized, characterized (Tm, CD, PAGE), and assessed in RNAi gene knockdown experiments. Results of these experiments are presented below.

5.4 P53 library

5.4.1 Synthesis, thermal stability, and native gel electrophoretic analysis

A library of parallel and antiparallel siRNAs targeting P53 mRNA was synthesized (**Table 5.1**) based on the sequence design described before. Thermal stabilities of all duplexes were evaluated in T_m buffer containing 140mM KCl, 1mM $MgCl_2$, and 5mM Na_2HPO_4, at pH 7.2, which is a good representative for physiological conditions. Several parallel and antiparallel control duplexes were incorporated into this library, to compare the thermal stability and biological activity of parallel vs antiparallel duplexes.

Table 5.1 Sequence and melting temperatures of 21-nt parallel and antiparallel siRNA duplexes targeting P53 mRNA. Legend: iso-DNA, DNA, RNA, 2′-FRNA.

Code	Sequence	T_m (°C)
iDD:R3	3'-AiCT AiCA AiGT AiCA TiGT iGTA AiCiC-5' 3'-GGU GAU GUU CAU GUA CAC AUU-5'	-
iDD:rF3	3'-AiCT AiCA AiGT AiCA TiGT iGTA AiCiC-5' 3′-GGU GAU GUU CAU GUA CAC AUU-5'	-
D1:R3	3'-ACT ACA AGT ACA TGT GTA ACC-5' 3′-GGU GAU GUU CAU GUA CAC AUU-5'	-
D1:rF3	3'-ACT ACA AGT ACA TGT GTA ACC-5' 3'-GGU GAU GUU CAU GUA CAC AUU-5'	-
D2:R3	5'-ACT ACA AGT ACA TGT GTA ACC-3' 3'-GGU GAU GUU CAU GUA CAC AUU-5'	48.9
D2:rF3	5'-ACT ACA AGT ACA TGT GTA ACC-3' 3'-GGU GAU GUU CAU GUA CAC AUU-5'	58.4
R2:R3	5'-ACU ACA AGU ACA UGU GUA ACC-3' 3'-GGU GAU GUU CAU GUA CAC AUU-5'	69.7
R2:rF3	5'-ACU ACA AGU ACA UGU GUA ACC-3' 3'-GGU GAU GUU CAU GUA CAC AUU-5'	75.1

(a)

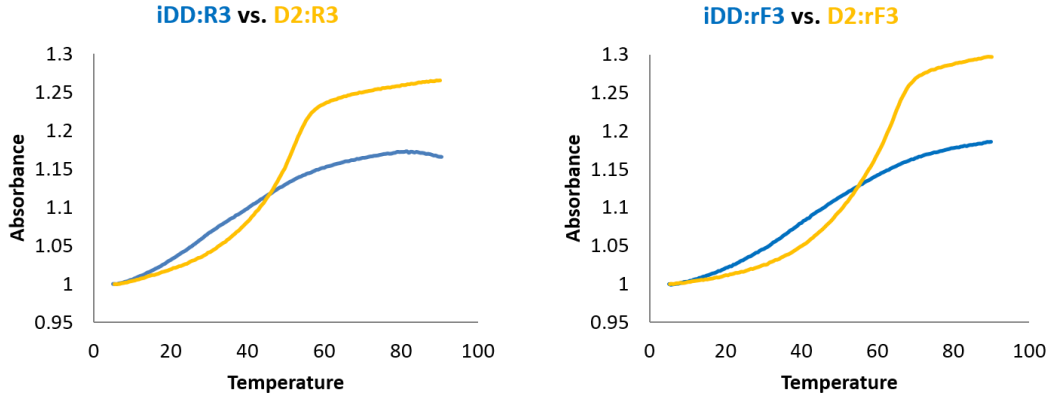

(b)

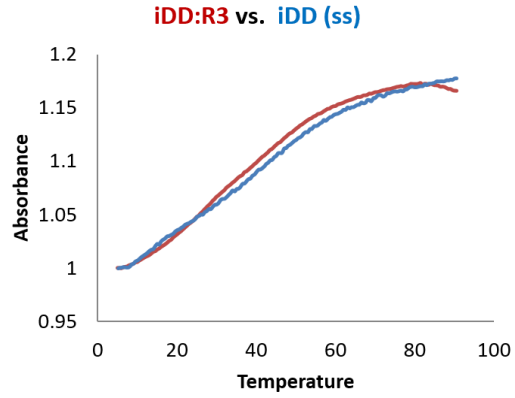

(c)

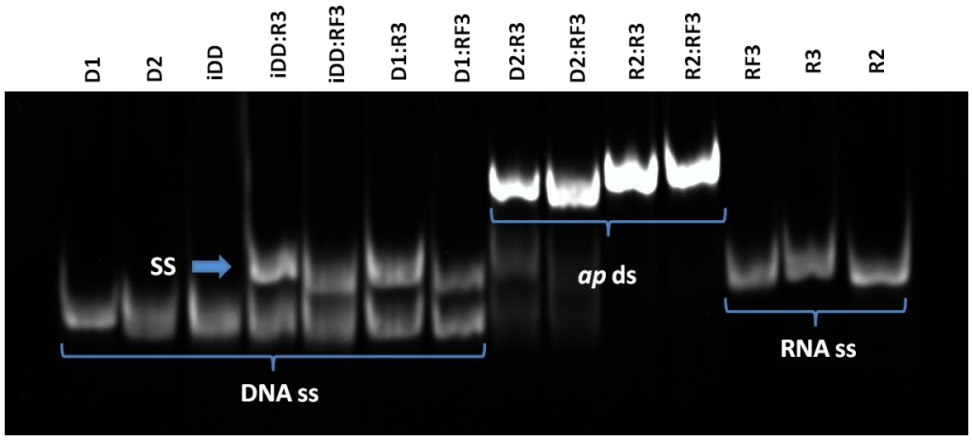

Figure 5.3 UV melting profiles (5-95 °C) of parallel oriented samples iDD:R3 and iDD:rF3 targeting P53 versus their antiparallel counterparts, D2:R3 and D2:rF3 (a). Comparison of melting curves of iDD:R3 with iDD (ss) shows similar curves and hyperchromicity, suggesting iDD:R3 has not formed a parallel duplex (b). In agreement with previous evidences, native gel electrophoretic analysis of the library members, as well as the single stranded components prove that parallel duplexes were not formed under native gel conditions (see experimental methods for details) (c).

Melting profile analysis of all parallel samples (iDD:R3, iDD:rF3, D1:R3, D1:rF3) revealed that these samples did not exhibit sharp cooperative transitions that are typically observed when stable duplexes are formed (**Figure 5.3**). While we noticed a 15-20% hyperchromic change in the "melting" curve of iDD:R3, the curve obtained was clearly different from the antiparallel duplex profile (**Figure 5.3** a), and was almost superimposable to the curve of the single strand alone (iDD) (**Figure 5.3** b) suggesting that no interaction between iDD and R3 occurred. To confirm this, the duplexes were next analyzed by gel electrophoresis at 4 °C in a buffer containing 40mM Tris, 20mM acetic acid and 1mM EDTA (pH =8) (**Figure 5.3** c). In agreement with our results from melting profile analysis, none of the samples designed to form ps-duplexes eluted as a slow moving single band; instead, these samples displayed bands corresponding to their single stranded species. Moreover, no bands with unexpected higher mobilities (e.g., due to high order secondary structures) were detected.

Our failed efforts in forming stable ps-duplexes targeting p53 mRNA highlights the importance of sequence selection. We hypothesized that increasing the number of isoG and isoC

Table 5.2 Sequence comparison of iDD:R3 siRNAs targeting different genes. Number of isoC/G and isoC/G base pairs within each duplex indicates the possible stability increase in a parallel duplex. Legend: iso-DNA, DNA, RNA, 2′-FRNA.

Target	iDD:R3 sequence	G/C base pairs
Bcl-2	3′ -iGiCATiGiCiGiGiCiCTiCTiGTTTiGATT-5′ 3′-UUCGUACGCCGGAGACAAACU-5′	11
P53	3′-AiCTAiCAAiGTAiCATiGTiGTAAiCiC-5′ 3′-GGUGAUGUUCAUGUACACAUU-5′	6
CCND1	3′-iGiGiCiCUiGAAiCiCUiGAiGiGAiGiCiCiCA-5′ 3′-UUCCGGACUUGGACUCCUCGG-5′	13
Renilla firefly	3'-iGAiGiCiGAAiGAiGiGiGiCiGAiGAAATT-5' 3'-CUCGCUUCUCCCGCUCUUUAA-5'	11

modification sites within a duplex from six to at least eleven isoG/isoC base pairs, as for the Bcl-2 ps-siRNA, are required to induce parallel duplex formation. Hence, we moved on to investigate sequences containing a higher G/C content (**Table 5.2**).

5.5 CCND1 library

5.5.1 Synthesis, thermal stability, and native gel electrophoretic analysis

To test our hypothesis, we attempted the synthesis of a ps-siRNAs targeting the Cell-cycle regulator cyclin D1 (CCND1) protein,[79] containing 13 G/C base pairs throughout the siRNA sequence (**Table 5.3**). Thermal stabilities of all duplexes, as well as their single strands, were evaluated in T_m buffer at pH 7.2.

Table 5.3 Sequence and melting temperatures of 21-nt parallel and antiparallel siRNA duplexes targeting CCND1 mRNA. Legend: iso-DNA, DNA, RNA, 2′-FRNA.

Code	Sequence	T_m (°C)
iDD:R3	3'-iGiGiC iCTiG AAiC iCTiG AiGiG AiGiC iCiCA-5′ 3'-UUC CGG ACU UGG ACU CCU CGG-5'	-
iDD:rF3	3'-iGiGiC iCTiG AAiC iCTiG AiGiG AiGiC iCiCA-5′ 3'-UUC CGG ACU UGG ACU CCU CGG-5'	-
D1:R3	3'-GGC CTG AAC CTG AGG AGC CCA-5′ 3'-UUC CGG ACU UGG ACU CCU CGG-5'	-
D1:rF3	3'-GGC CTG AAC CTG AGG AGC CCA-5′ 3'-UUC CGG ACU UGG ACU CCU CGG-5'	-
D2:R3	5'-GGC CTG AAC CTG AGG AGC CCA-3' 3'-UUC CGG ACU UGG ACU CCU CGG-5'	70.0
D2:rF3	5'-GGC CTG AAC CTG AGG AGC CCA-3' 3'-UUC CGG ACU UGG ACU CCU CGG-5'	84.5
R2:R3	5'-GGC CUG AAC CUG AGG AGC CCA-3' 3'-UUC CGG ACU UGG ACU CCU CGG-5'	58.4
R2:rF3	5'-GGC CUG AAC CUG AGG AGC CCA-3' 3'-UUC CGG ACU UGG ACU CCU CGG-5'	66.7

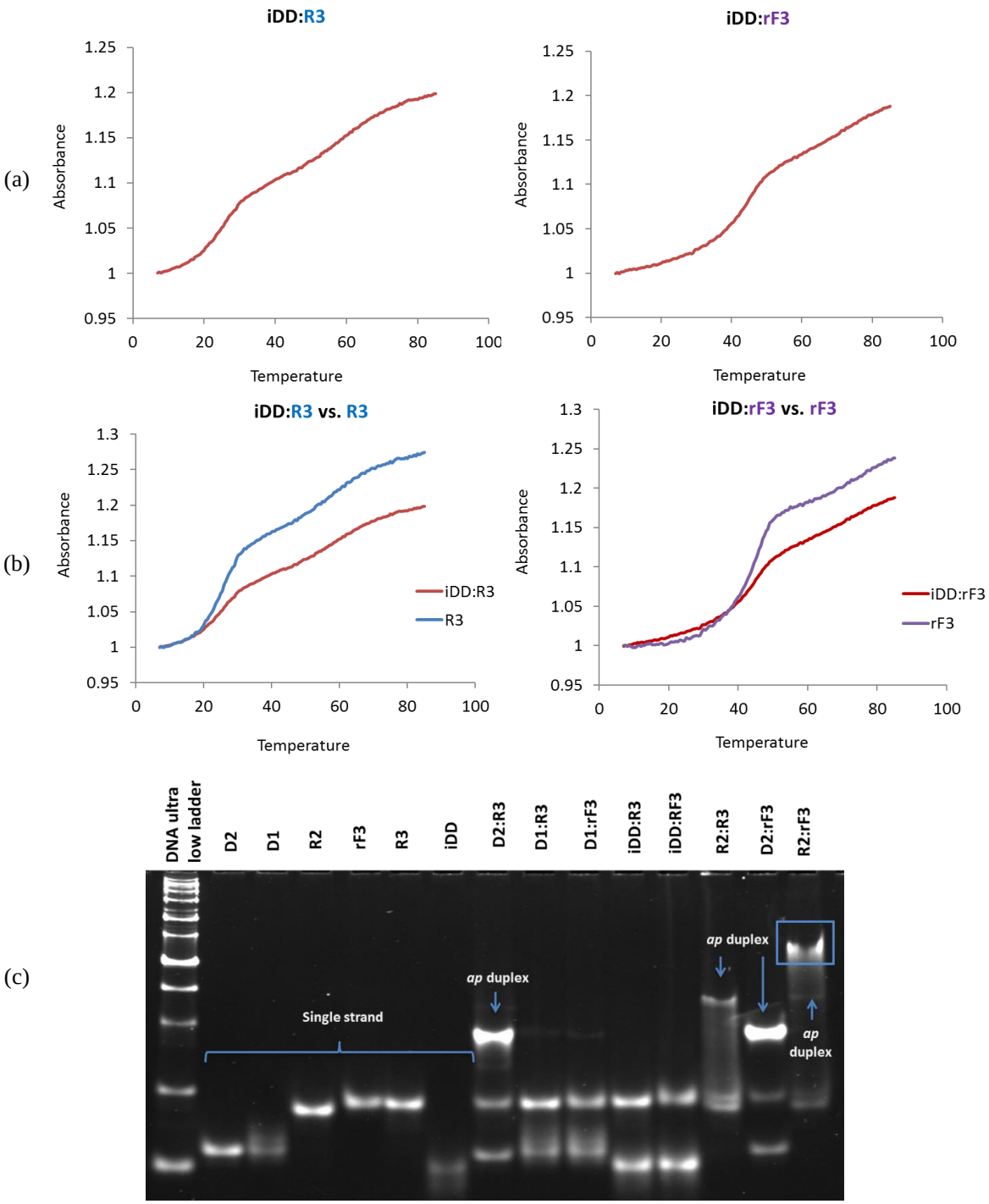

Figure 5.4 UV melting profiles (5-95 °C) of parallel oriented samples iDD:R3 and iDD:rF3 targeting CCND1 (a). Comparison of melting curves of iDD:R3 and iDD:rF3 with R3 and rF3 (ss) shows similar curve patterns, suggesting that parallel duplexes were not formed (b). In agreement with previous evidences, native gel electrophoretic analysis of the library members, as well as the single stranded components prove that parallel duplexes were not formed under native gel conditions (see experimental methods for details) Blue rectangle shows a band representing a higher order secondary structure (c).

Many of the samples within the CCND1 library did not exhibit clear sigmoidal curves (**Figure 5.4**). Instead, most samples presented melting profiles consisting of multiple transitions, likely due to the presence of two or more complexes (**Figure 5.4**). These complexes are derived from the single strands alone, namely R3 and rF3, since the melting curves of these oligomers matched those of the mixtures (iDD + R3 and iDD + rF3). Thus, the secondary structures formed by R3 and rF3 must be far more stable than the desired iDD:R3 and iDD:rF3 parallel duplexes. Given the high G-rich content of R3 and rF3, it is conceivable that the structures formed under these conditions are G-quadruplexes,[80-84] but no attempts were made to verify this hypothesis.

Analysis by PAGE (**Figure 5.4**) confirmed the lack of association between iDD and the complementary sequences (R3 and rF3). Furthermore, the R3 and rF3 bands exhibited slower electrophoretic mobility compared to the single stranded controls (D1, D2 and iDD), consistent with the formation of higher order structures. Based on analogy with previously reported GG- and GU-rich sequences forming G-quadruplexes,[85, 86] we suspected that the three "GG" units (dispersed throughout the 21-nt R3 and rF3 sequences) were responsible for inducing G-quadruplex formation. As such, we applied a new criteria for designing ps-DNA:RNA duplexes: >50% G/C base pairs, but avoiding multiple "GG" repeats within the sequence. It is noteworthy that many other sequence motifs involved in the formation of G-quadruplexes have been reviewed in databases, and should be discussed prior to the design of a parallel DNA:RNA duplex.[87, 88]

5.6 siRNAs targeting renilla luciferase

Our next efforts were directed towards the synthesis of parallel siRNAs targeting Renilla luciferase mRNA. The reported[89] sequence for this target contained 11 G/C base pairs and no repeating "GG" motifs in either the sense and AS sequences (**Table 5.2**).

5.6.1 Design and thermal stability evaluation

A library of parallel and antiparallel siRNAs targeting renilla luciferase mRNA was synthesized (**Table 5.4**). This time the duplexes contained "blunt ends" to maximize the number of possible isoG/isoC base pairs. For comparison purposes, iDD:R4 and R2:R4 regular parallel and antiparallel siRNA controls were also added to the library. Thermal melting profiles of duplexes and single strands were evaluated at pH 7.2. Fortunately, none of the single strands showed any transition indicative of competing higher order structures (**Figure 5.5**). However, both iDD:R3 and iDD:rF3 parallel duplexes, as well as the rest of antiparallel control duplexes showed clear

Table 5.4 Sequence and melting temperatures of 21-nt parallel and antiparallel siRNA duplexes targeting renilla luciferase mRNA. Legend: iso-DNA, DNA, RNA, 2′-FRNA.

Code	Sequence	T_m (°C)
iDD:R3	3'-iGAiG iCiGA AiGA iGiGiG iCiGA iGAA ATT-5' 3'-CUC GCU UCU CCC GCU CUU UAA-5'	63.5
iDD:rF3	3'-iGAiG iCiGA AiGA iGiGiG iCiGA iGAA ATT-5' 3'-CUC GCU UCU CCC GCU CUU UAA-5'	64.5
D1:R3	3'-GAG CGA AGA GGG CGA GAA ATT-5' 3'-CUC GCU UCU CCC GCU CUU UAA-5'	-
D1:rF3	3'-GAG CGA AGA GGG CGA GAA ATT-5' 3'-CUC GCU UCU CCC GCU CUU UAA-5'	-
D2:R3	5'-GAG CGA AGA GGG CGA GAA ATT-3' 3'-CUC GCU UCU CCC GCU CUU UAA-5'	54.5
D2:rF3	5'-GAG CGA AGA GGG CGA GAA ATT-3' 3'-CUC GCU UCU CCC GCU CUU UAA-5'	58.7
R2:R3	5'-GAG CGA AGA GGG CGA GAA AUU-3' 3'-CUC GCU UCU CCC GCU CUU UAA-5'	82.5
R2:rF3	5'-GAG CGA AGA GGG CGA GAA AUU-3' 3'-CUC GCU UCU CCC GCU CUU UAA-5'	>95
iDD:R4	3'-iGAiG iCiGA AiGA iGiGiG iCiGA iGAA ATT-5' 3'-UUC UCG CUU CUC CCG CUC UUU-5'	
R2:R4	5'-GAG CGA AGA GGG CGA GAA AUU-3' 3'-UUC UCG CUU CUC CCG CUC UUU-5'	80.3

sigmoidal melting profiles indicative of the desired parallel and antiparallel duplex structures (**Figure 5.6**). Duplex formation in both cases was confirmed by PAGE (**Figure 5.7**). In agreement with our results from melting profile analysis, parallel (iDD:R3 and iDD:rF3) and antiparallel duplexes migrated more slowly on the gel relative to the single stranded controls. Interestingly, both iso-modified parallel duplexes iDD:R3 and iDD:rF3 showed higher melting temperatures, but lower hyperchromicity, in comparison with D2:R3 and D2:rF3 antiparallel control duplexes, respectively (**Figure 5.6**a). Consistent with this, in research published by Seela and co-workers,[34] it was reported that ps-isoG/C base pairs can stabilize ps-DNA:DNA duplexes significantly more than ps-isoC/G and antiparallel (Watson-Crick) G/C base pairs.

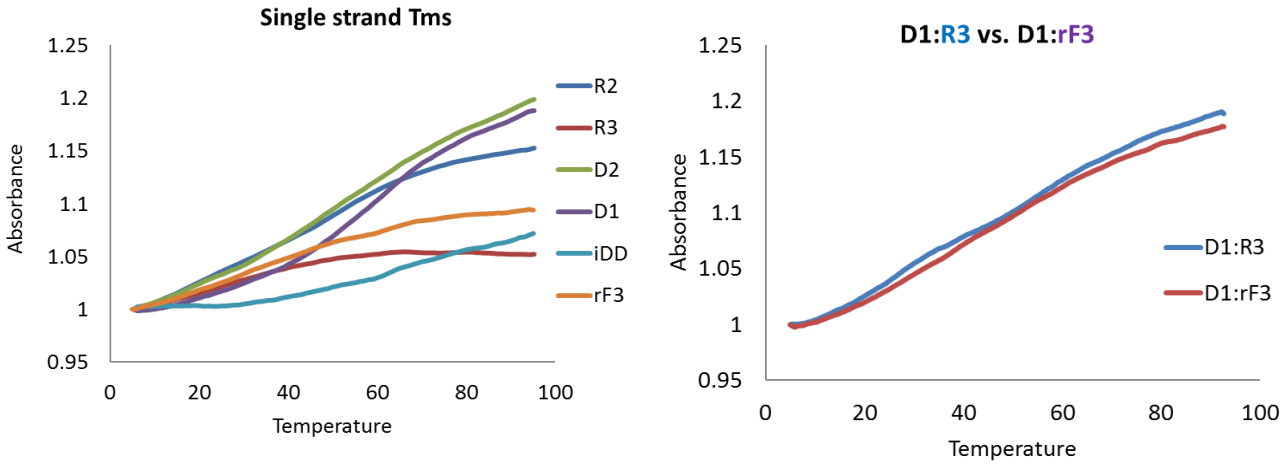

Figure 5.5 UV melting profiles of the single strand samples (left), as well as the parallel controls D1:R3 and D1:rF3 (right), do not exhibit formation of any secondary structures. The A_{260} was monitored from 5- 95 °C with a heating rate of 0.5 °C/min.

(a)

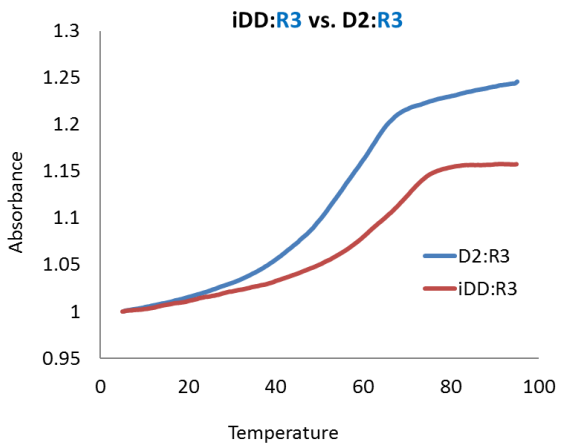

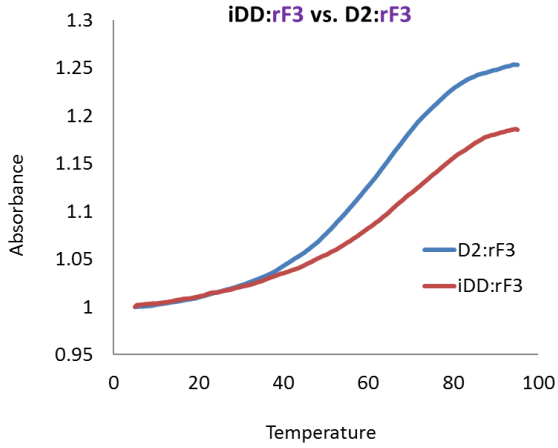

(b)

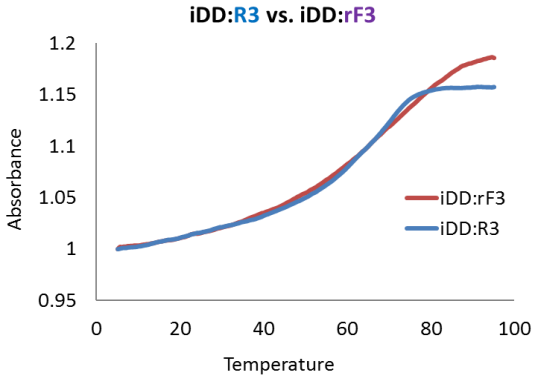

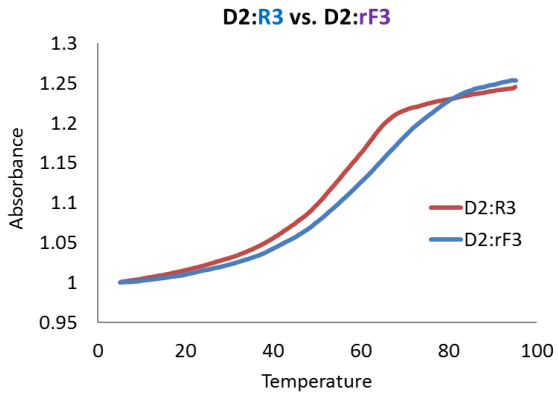

(c)

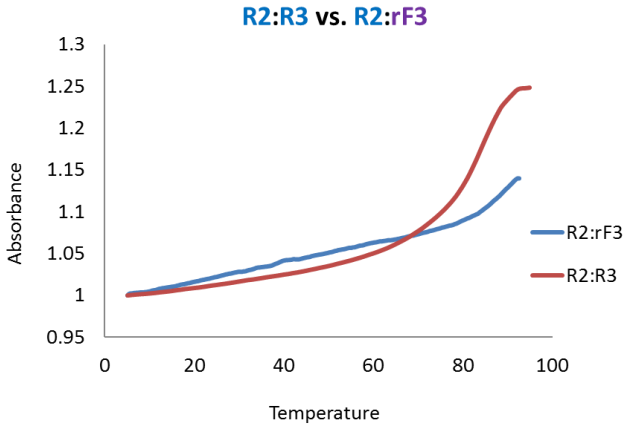

Figure 5.6 UV melting profiles (5-95 °C) of siRNA duplexes targeting renilla firefly. Comparison of melting profiles of parallel with antiparallel duplexes (a), DNA:RNA with DNA:2′-FRNA hybrids (b), and RNA:RNA with RNA:2′-FRNA hybrids (c).

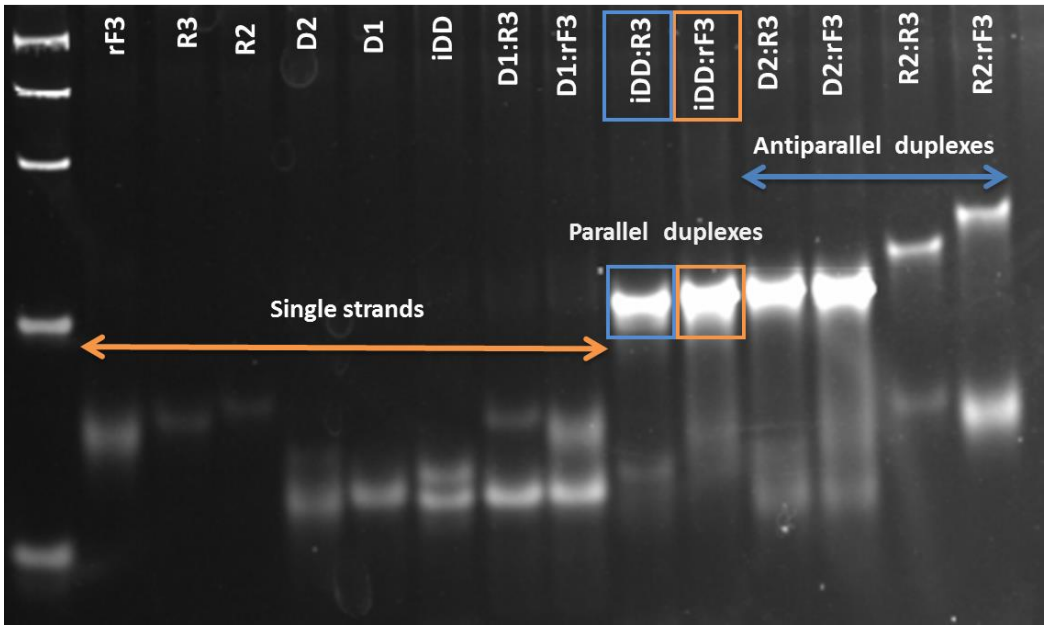

Figure 5.7 Native gel electrophoretic analysis of parallel and antiparallel blunt ended siRNA duplexes targeting renilla luciferase (details in experimental section). Sequences of these samples are shown in **Table 5.4**.

Hence, the higher T_m value of the ps-iDD:R3 duplex in comparison to the antiparallel DNA:RNA duplex, likely results from the stability gain by multiple isoG/C base pairs, which are clearly desirable when stabilizing ps-hybrids. Accordingly, the requirement (rules) were refined as follows: have > 50% G/C content, avoid GG repeats, and maximize isoG/C base pairs.

5.6.2 Circular Dichroism studies

Circular dichroism (CD) is a powerful tool in studying the global structure of nucleic acids, and particularly elucidating the helical arrangement of double helices.[90-93] Antiparallel DNA duplexes present a CD spectrum characteristic of a B-form helix, with a positive band centered near 275-280 nm, a negative band near 245-250nm, and a crossover signature at around 260nm. CD spectrum of canonical RNA duplexes exhibit a strong positive band centered at around 260nm and a weak negative band centered at around 240nm, representative of A-form double

helix. Canonical DNA/RNA duplexes adopt a helical structure that is more sequence-dependent and generally resembles the A-helical structure.[90, 92, 93] Previous CD studies by our group[68] and others[34, 67] on 12-bp parallel iso-modified and antiparallel DNA:RNA hybrids suggested they adopt a right-handed helical structure in both cases. The 12-bp parallel duplexes exhibit positive and negative peaks (and crossover points) that were red-shifted relative to the antiparallel duplexes. Also, CD spectra of 12mer parallel duplexes showed an increase in the magnitude of their positive CD upon raising the temperature, whereas an opposite (hypochromic) effect was seen for the corresponding antiparallel duplexes.

The CD spectra of 21-mer isoC and isoG modified ps-DNA:RNA and ps-DNA:2′-FRNA hybrids were investigated for the first time during the course of our study (**Figure 5.8**). Both parallel duplexes presented similar CD profiles, which were different from that of typical A- or B-form helices. Parallel iDD:R3 and iDD:rF3 duplexes presented three positive CD bands at around 275, 250 and 220 nm, as well as two negative bands at around 210 and 305 nm, with CD profiles resembling the traces of left-handed helical structures (**Figure 5.8**). An interesting feature in the CD spectra of our parallel duplexes (iDD:R3 and iDD:rF3) was that the magnitude of the negative band at 305 nm and the positive band at 250 nm decreased upon raising the temperature. Antiparallel duplexes D2:R3 and D2:rF3, also, presented a hypochromic effect, with the magnitude of the positive band at 270 nm and the negative band at 210 nm decreasing upon raising the temperature (**Figure 5.8**). The differences in CD profiles of our isoG- and isoC-modified parallel duplexes with antiparallel DNA:RNA and DNA:2′-FRNA duplexes are not only due to the change of the strand orientation, but likely also due to the altered spectroscopic properties of the isoG and isoC modified bases.

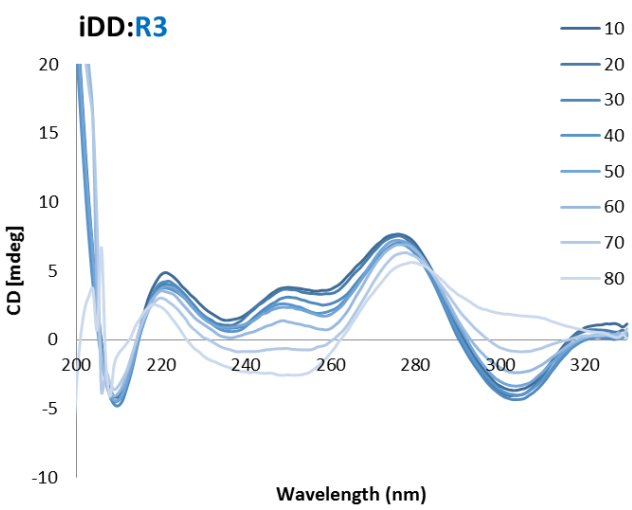

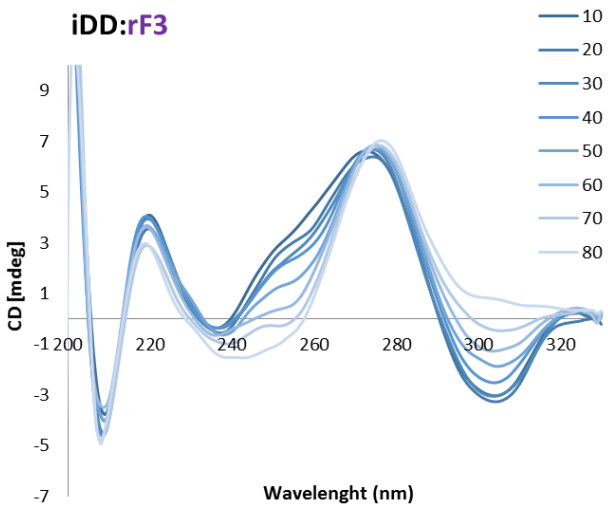

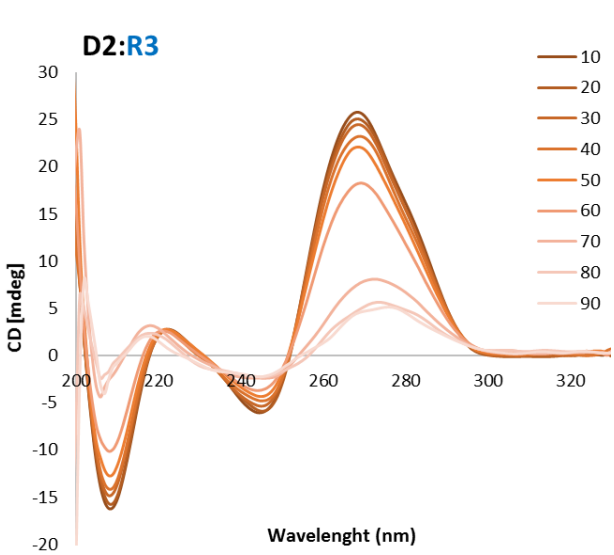

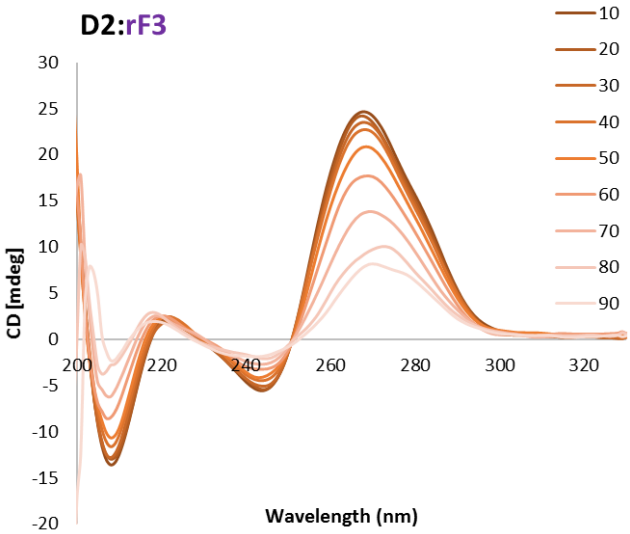

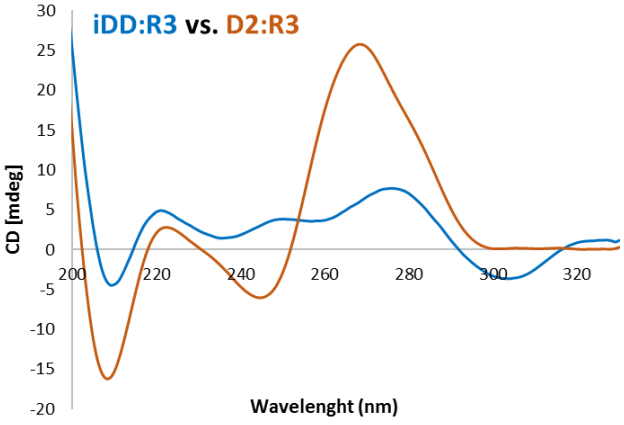

Figure 5.8 (Up) CD spectra of 21-bp parallel (iDD:R3 and iDD:rF3) and antiparallel (D2:R3 and D2:rF3) siRNAs targeting renilla. CD Spectra was collected every 10 degrees from 10-90 °C in buffer containing 140 mM KCl, 1 mM $MgCl_2$, and 5 mM Na_2HPO_4, at pH 7.2 with single strand concentration of 10 µM + 10 µM. (Left) Comparison of CD spectra iDD:R3 parallel duplex vs. D2:R3 antiparallel duplex at 10 °C.

5.6.3 ^{1}H-NMR analysis of parallel siRNA hybrids

NMR is a valuable tool in studying the structure and dynamics of nucleic acids.[94] In our study, we used ^{1}H-NMR to look at the formation of a parallel duplex based on the observation of the imino signals of the paired bases. The ^{1}H-NMR imino region of parallel and antiparallel duplexes, located between 12-14 ppm, is a region with resolved peaks, that is used to investigate the hybridization of paired bases.[95] Previous NMR studies by us[68] and others[96] showed that imino proton resonances of parallel DNA duplexes with rWC base pairing and antiparallel DNA duplexes fall roughly in the same region. A similar observation was made in our experiments with the chemical shifts of the imino exchangeable protons in parallel iDD:R3 duplex being comparable to those observed in antiparallel D2:R3 control duplex (**Figure 5.9**). This finding suggests the base pairing pattern in parallel iDD:R3 duplex to be rWC.

^{1}H-NMR experiments were performed by Dr. Carlos Gonzalez at the Instituto de Química Física Rocasolano in Madrid. Temperature dependent 1D ^{1}H-NMR experiments were performed in a buffer containing 25 mM sodium phosphate, 100 mM NaCl at pH 7, and spectra were collected with 10 degrees increments from 5 °C to 45 °C. Upon the duplex melting, imino protons gradually disappear (**Figure 5.9**). ^{1}H-NMR experiments also confirmed that other secondary structures are not formed, since no signals were detected in the spectra region between 11-12 ppm where G-quadruplex protons appear.[95]

Full assignment of imino proton peaks, as well as a complete structural determination for this parallel duplex can be attained by performing high resolution 2D-NMR spectroscopy experiments, something that can now be pursued given the high stability exhibited of our ps-duplexes.

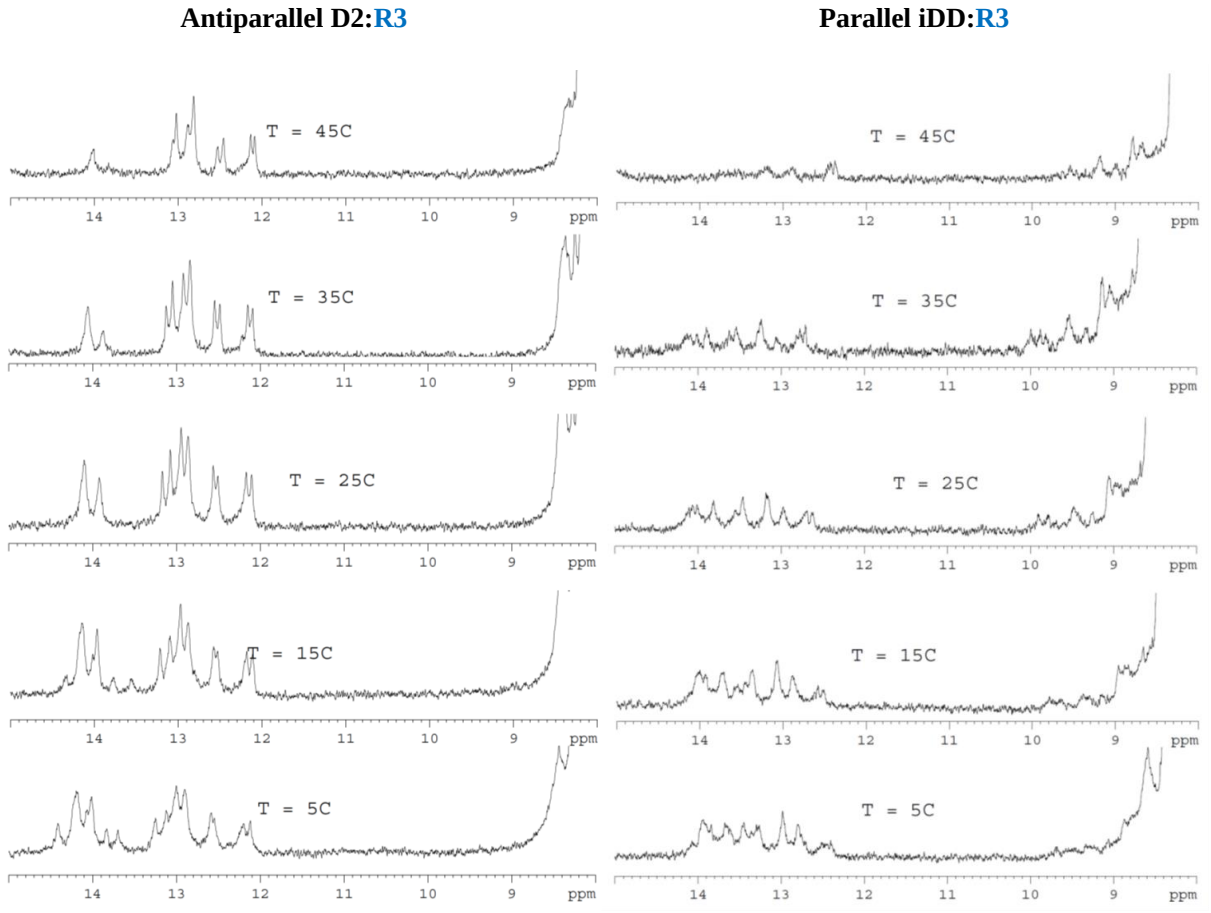

Figure 5.9 Imino region of the 1D ^{1}H-NMR spectra of parallel iDD:R3 vs. antiparallel D2:R3 duplexes at different temperatures. Buffer condition: 25 mM sodium phosphate, 100 mM NaCl at pH 7.

5.6.4 Induction of RNAi activity by parallel siRNA hybrids

To investigate the ability of iso-modified ps-DNA:RNA duplexes, a library comprising the parallel and antiparallel duplexes, along with the single stranded AS strands were tested for RNAi activity in HEK293T cells using a renilla dual reporter assay. This assay was performed by Matije Lucic, in the laboratory of Dr. Jonathan Hall at the Swiss Federal Institute of Technology Zurich (ETH Zurich). All samples were transfected at 0, 2.25, 10 and 40 nM using lipofectamine 2000.

Following the transfection of dual-luciferase reporter plasmid, luminescence was measured and normalized against the firefly luciferase (details in experimental section). Dose response diagrams of all the tested samples targeting renilla luciferase are presented in **Figure 5.10**.

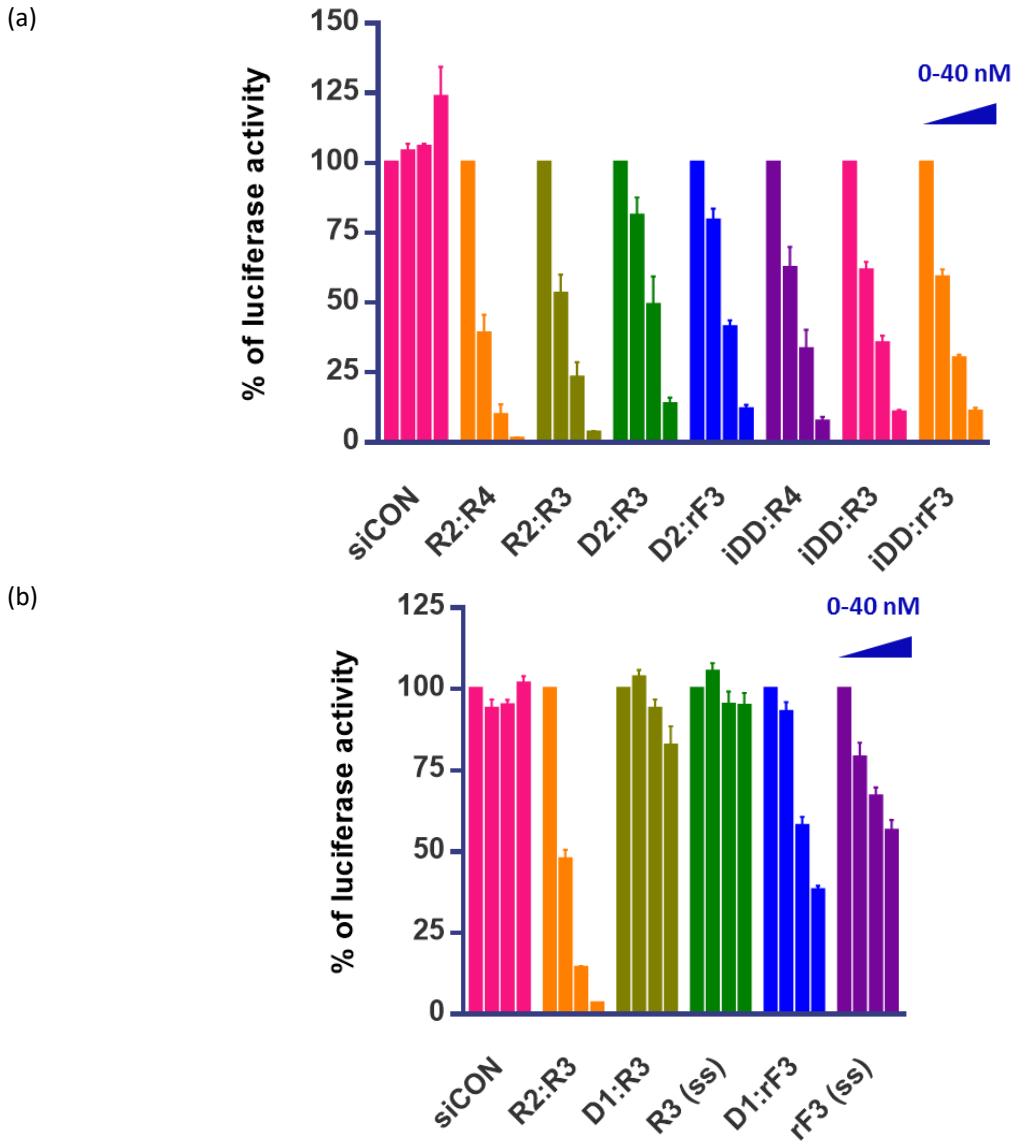

Figure 5.10 Knockdown of renilla luciferase in HEK293T cells by parallel and antiparallel siRNAs targeting renilla (a). Unmodified parallel samples, as well as single stranded AS strands were separately tested against renilla luciferase as negative controls (b). Sequence of samples are available in **Table 5.4**. All samples were tested at 0, 2.5, 10, and 40 nM concentrations.

The native antiparallel classical R2:R4 and to a lesser extent the blunt ended R2:R3 siRNAs were both able to greatly reduce the renilla mRNA levels in HEK293T cells. While the antiparallel D2:R3 and D2:rF3 duplexes showed some activity, the parallel iDD:R3, iDD:R4, and iDD:rF3 duplexes were significantly better in lowering the renilla mRNA levels (**Figure 5.10**). However, none of the samples could exceed the activity of the antiparallel R2:R3 and R2:R4 RNA:RNA control siRNAs. Also, none of the unmodified parallel negative controls (D1:R3 and D1:rF3), as well as the AS single strands (R3 and rF3) could induce gene knockdown, which was inferred from their inability to form duplexes.

The lower activity observed with the ps-duplexes, in comparison with classical and blunt ended siRNA controls, may be attributed, at least in part, to the lower thermal stability of the former (e.g. ps-iDD:R3 T_m: 65.5 °C vs. ap-R2:R3 T_m: 82.5 °C). This means that at the assay temperature (37 °C) slightly less parallel duplexes could take part in the gene silencing pathway, compared to the classical antiparallel siRNAs. More likely, however, local structural changes, helical conformation and strand orientation play a more significant role. Nevertheless, it is remarkable that ps-duplexes are able to modulate gene expression and demonstrate that the substrate specificity of RISC is not too stringent. This assumes, of course, that the ps-duplexes operate via the RNAi pathway, a hypothesis that was tested (and supported) in the experiments described below.

Next, the activity of the parallel iDD:rF3 duplex with a fully modified 2'F-RNA AS strand was assessed. Previous studies[75, 97] have demonstrated that classical antiparallel siRNAs with fully 2'F-RNA modified AS strands function well in RNAi. In line with that, our ps-iDD:rF3 duplex was also quite active in reducing renilla gene expression; its potency was comparable to that of the ps-iDD:R3 duplex. Similar to antiparallel siRNAs, non-blunt ended ps-duplexes were slightly more potent than the corresponding blunt ended ps-duplexes. These results are entirely consistent with previous reports[78, 98] suggesting that the 3′-overhangs have a possible contribution to the

siRNA activity. This is specially the case with the 3′-overhang of the guide strand which interacts with the PAZ domain of AGO2, taking part in the strand selection.[99, 100]

Our results support the notion that the same regulations governing the activity of antiparallel siRNAs are also applicable to the ps-duplexes studied here. Taken together, we concluded that iso-modified ps-duplexes can be utilized as modified siRNAs with effective gene knockdown abilities.

5.6.5 Mechanistic investigations: siAGO knockdown experiments

To this end, we showed that parallel siRNA duplexes are able to express gene knockdown activities. To verify if this gene knockdown was happening via RNAi pathway, a control experiment was designed through which the effect of AGO2 mRNA knockdown on the potency of renilla target siRNAs was investigated. An siRNA pool targeting the 3′-UTR (siAGO2) of AGO2 mRNA was employed to knockdown AGO2 mRNA levels in HEK293T cells.[101] To confirm AGO2 knockdown, we used western blot analysis to determine the levels of AGO2 following siAGO2 transfection.

To analyze the influence of AGO2 knockdown on the potency of our siRNAs, following the addition of 50 and 100 nM of siAGO2, R2:R3 and iDD:R3 siRNAs were transfected in HEK293T cells, and renilla luciferase expression levels were measured. With both parallel and antiparallel siRNAs, a significant reduction in luciferase expression was observed in cells upon AGO2 knockdown (siRNA + siAGO2), compared to the control siRNA (siRNA without siAGO2). Moreover, higher concentrations of siAGO2 resulted in more reduction in siRNA potency. These findings confirm that AGO2 was required for an efficient knockdown of renilla mRNA by R2:R3 and iDD:R3 siRNAs. It can, therefore, be inferred that parallel siRNAs, like antiparallel classic siRNAs, employ the RNAi machinery for gene silencing. Partial inhibition of

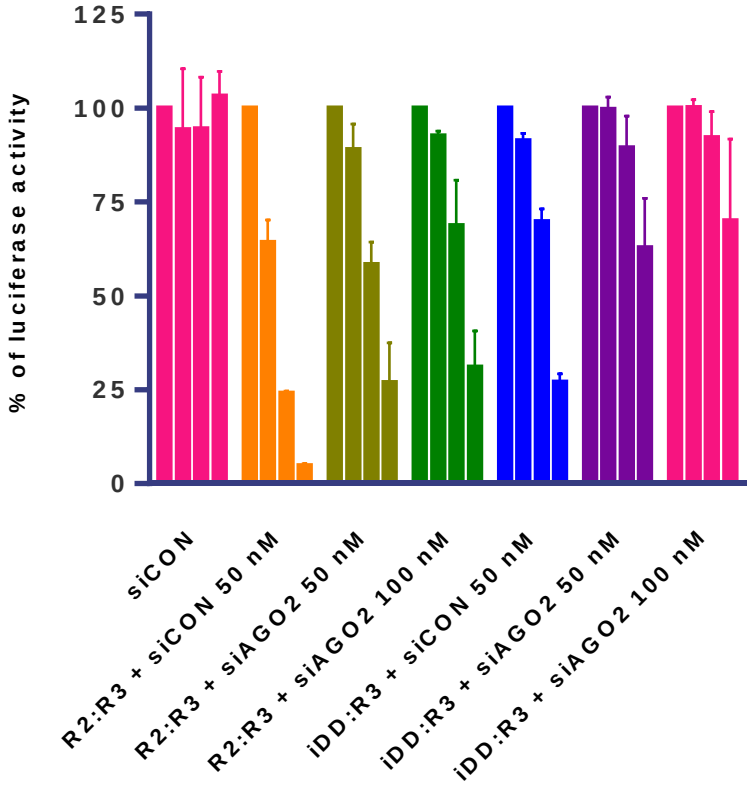

Figure 5.11 Renilla luciferase dual reporter assay demonstrating the effect of AGO2 knockdown on the potency of parallel and antiparallel siRNAs iDD:R3 and R2:R3 against renilla mRNA knockdown. siCON represents the nontargeting negative control. The experiment is run in duplicates, with statistical tests for R;R3 and iDD:R3 run separately against "R2:R3 +siCON" and "iDD:R3 +siCON"-treatments respectively. Error bars represent standard error of the mean (SEM). The potency of both parallel and antiparallel siRNAs is significantly decreased by siAGO2 combo-treatment, supporting the claim that antiparallel duplexes are working through canonical RNAi pathway.

renilla luciferase expression was likely due to incomplete knockdown of AGO2, or the possible effects of other Argonaute proteins, such as AGO-1, -3, or -4.

More experiments are currently underway to quantitate the AGO2 knockdown efficiency by western blot and complete these sets of biological assays.

5.6.6 Can parallel hybridization enhance the therapeutic properties of siRNAs?

As previously explained (Chapter 1), the immense therapeutic potentials of siRNAs are hampered by their disadvantages, namely poor nuclease stability, poor cellular uptake, off-target effects arising from partial complementarities to unintended genes, and nonspecific immune responses.[102, 103] The strategies used so far, to overcome the siRNAs shortcomings, as well as to enhance their gene silencing properties, have been mainly focused on the use of ribose sugar or phosphate backbone alternatives in antiparallel siRNAs.[104-106] Our results demonstrated, for the first time, that parallel hybridization of siRNAs can be utilized as an attractive alternative to classical modification approaches. Moreover, our study questioned whether such a "global" modification of the siRNA structure could improve the siRNA properties.

An advantage to our presented siRNAs with parallel strand hybridization is minimized off-target effects. Since the sense strands in such parallel duplexes are heavily modified, there is less chance that the sense strand act as the AS strand and target the wrong genes. Even though parallel siRNAs were recognized and were functional with the RNAi machinery proteins, we expect that the interactions of parallel siRNAs with other intercalating molecules and proteins be affected. Different helical structure of rWC parallel duplexes, compared to WC antiparallel duplexes also causes the major and minor grooves to differ in size and nature. Antiparallel duplexes, as previously described, have major and minor grooves that differ in polarity, hydrogen bonding, steric effects, and hydration. Based on these differences, various proteins and small molecules recognize and bind specifically either to the minor or the major groove. Since rWC parallel duplexes have grooves of equal size,[6] the nature of molecular recognition by intercalating molecules and proteins, such as nucleases is expected to be different.[59] This theory is supported by previous findings, demonstrating that parallel DNA duplexes are more resistant

against certain nucleases and restriction endonucleases, compared to antiparallel DNA duplexes.[28] It is, therefore, very plausible that the parallel DNA:RNA siRNAs studied here can also have lowered nuclease recognition and therefore, benefit from improved nuclease stability.

Based on the same argument, we can assume that the structural differences of parallel siRNAs might modulate their interactions with off-target proteins. An example of such proteins is the RNA-dependent protein kinase (PKR), which is a cellular double stranded RNA binding protein that participates in sequence-independent binding to siRNAs and off-target effects.[107, 108] As this protein can only interacts with siRNAs through their minor groove, it is likely that parallel duplexes with grooves of equal size cannot be recognized as PKR substrates, and hence, have reduced off-target effects, while they are still substrates to RNAi machinery. Further investigations need to be conducted to evaluate these hypotheses regarding the interactions of parallel siRNA duplexes with proteins of biological interest.

5.7 Conclusion and future works

In conclusion, we presented here a step by step strategy to successfully design and synthesize chemically modified parallel hybrids. We also demonstrated that these parallel hybrids could act as potent siRNAs, and provided evidence for their RNAi mechanism of action via AGO2 knockdown experiments.

Our attempts to synthesize parallel siRNAs targeting P53, CCND1, and renilla luciferase led us to a set of strategies for the successful design of parallel siRNA hybrids, namely: (i) Choosing sequences with high GC content (50% or more); (ii) Avoiding sequences with motifs favouring unwanted secondary structures (e.g. “GG” repeats, favouring G-quadruplexes); (ii) Benefiting from extra duplex stability gain through using blunt ended siRNAs; (iv) Choosing sequences with higher G content in the sense strand, rather than C; and (v) Benefiting from duplex stability

gain via incorporating 2′-FRNA in the AS strand. Structures of selected parallel and antiparallel siRNA duplexes targeting Renilla were thoroughly investigated for the first time, using UV thermal denaturation, CD, gel electrophoresis, and 1D ^{1}H-NMR.

The results obtained from gene silencing assays against the expression of renilla luciferase mRNA indicated that a parallel siRNA is capable of RNA activation and eliciting gene silencing activity. These results, as well as the results obtained from AGO2 knockdown experiment provides evidence that the helical conformation of the si-duplex and its groove dimensions are not critical determinants in activation of RNAi. Therefore, duplexes that do not closely resemble the A-form standard siRNAs can still be recognized by RNAi machinery.

Our findings bring light to novel opportunities in designing a new class of potent chemically modified parallel siRNAs at physiological conditions with improved drug-like properties.

5.8 Experimental methods

5.8.1 Oligonucleotide synthesis and purification and siRNA preparation

Isoguanosine and isocytidine phosphoramidites (deoxy ribose) were purchased from ChemeGenes Inc. (Wilmington, MA). The oligonucleotide synthesis was performed on an Applied Biosystems 3400 DNA Synthesizer at a 1-μmol scale using Unylink CPG support (ChemeGenes, Wilmington, MA).[109] Iso-phosphoramidites were prepared as 0.15M solutions in acetonitrile (ACN). 5-ethylthiotetrazole (0.25M in ACN) was used to activate phosphoramidites for coupling. For detritylation 3% dichloroacetic acid (DCA) in toluene was used. Oxidation was done using 0.1M I_2 in 1:2:10 pyridine: water: THF. Coupling times were 600 seconds for deoxyisocytidine phosphoramidites (isoC) and 900 seconds for the deoxyisoguanosine phosphoramidites (isoG). The removal of CPG support, base protecting groups and the cyanoethyl protecting groups occurred with ammonium hydroxide (1mL) added to the CPG

containing bound oligo and the tightly sealed solution was shaken at 25 °C for 72 hours (for renilla library). The duration of this deprotection step was proportional to the number of isoC and isoG modifications in the strand, and was determined by following the reaction with IE-HPLC (conditions below). All iso-modified oligonucleotides were purified using polyacrylamide gel electrophoresis (PAGE).

Standard phosphoramidite solid-phase synthesis conditions were used for the synthesis of all DNA, RNA, and 2′-FRNA oligonucleotides.[110] Syntheses were performed on an Applied Biosystems 3400 DNA Synthesizer at a 1 μmole scale using Unylinker CPG support (ChemGenes). All phosphoramidites, were prepared as 0.15 M solutions in acetonitrile (ACN), except DNA, which was prepared as 0.1 M. ETT (0.25 M in ACN) was used to activate phosphoramidites for coupling. Detritylations were performed using 3% TCA in CH_2Cl_2 for 110 seconds. Failure sequences were capped using acetic anhydride in THF and 16% *N*-methylimidazole in THF. A 0.1 M solution of I_2 in 1:2:10 pyridine: water: THF was used for oxidation. Coupling times were 600 sec for all RNA and 2'-FRNA phosphoramidites, except for their guanosine phosphoramidites which had 900 seconds of coupling time. Deprotection and cleavage from the solid support for 2′-FRNA was accomplished with 3:1 NH_4OH: EtOH for 48 hours at room temperature, and with 40% methylamine for 10 minutes at 65° C for unmodified DNA and RNA samples.[111] Oligonucleotides containing RNA were synthesized with standard 2'-TBDMS phosphoramidites, and were desylilated with triethylamine trihydrofluoride/N-methyl pyrrolidone/triethylamine (1.5:0.75:1 by volume) for 2.5 hours at 65 °C.[111, 112]

Purification of crude oligonucleotides was done by HPLC using an anion exchange column (Protein PAK DEAE 5PW 21.5 mm × 15 cm). The buffer system consisted of water (solution A) and 1 M lithium perchlorate solution in water (solution B), at a flow rate of 4 mL/min. The

Table 5.5 MS characterization of oligonucleotide used in constructing the siRNAs targeting Renilla luciferase. Legend: iso-DNA, DNA, RNA, 2′-FRNA.

Sample Name	Sequence	Exact Mass (Calc)	Exact Mass (Exp)
iDD	3'-iGAiG iCiGA AiGA iGiGiG iCiGA iGAA ATT-5'	6590.1692	6589.9375
D1	3'-GAG CGA AGA GGG CGA GAA ATT-5'	6590.1692	6590.2188
D2	5'-GAG CGA AGA GGG CGA GAA ATT-3'	6590.1692	6590.2188
R2	5'-GAG CGA AGA GGG CGA GAA AUU-3'	6898.0232	6898.0000
R3	3'-CUC GCU UCU CCC GCU CUU UAA-5'	6479.8132	6479.5938
R4	3'-UUC UCG CUU CUC CCG CUC UUU-5'	6344.7572	6344.5862
rF3	3'-CUC GCU UCU CCC GCU CUU UAA-5'	6521.8618	6521.5938

gradient was 0−40% B over 40 min at 60 °C. Under these conditions, the desired peaks eluted at 20−30 minutes. The collected samples were then lyophilized to dryness and were desalted with Nap-25 Sephadex columns from GE Healthcare. Sequences were verified by high resolution ESI-LCMS. Corresponding masses for all oligonucleotides from renilla library are listed in **Table 5.5**. All siRNAs were prepared by annealing equimolar quantities of complementary oligonucleotides in siRNA buffer (100 mM KOAc, 30 mM HEPES-KOH, 2 mM $Mg(OAc)_2$, pH 7.4) by slowly cooling from 96 °C to room temperature, and then keeping them at 4 °C overnight.

5.8.2 Thermal denaturation experiments and circular dichroism studies

Complementary sequences from siRNA libraries (1.5 nmol) were combined, dried, and rediluted in 1 mL of T_m buffer containing 140 mM KCl, 1 mM $MgCl_2$ and 5 mM Na_2HPO_4 (pH 7.2). Samples were then transferred into UV cuvettes in a Varian Cary 300 UV spectrophotometer and

heated up to 90 °C. They were cooled down to 5 °C (ramped at 0.5 °C/min), followed by heating up from 5 °C to 95 °C. The change in their absorbance at 260 nm was monitored upon cooling and heating steps. Melting temperatures were determined using the heating ramp and via baseline method, as implemented in the Cary software. T_m curves are shown in **Figure 5.5** and **Figure 5.6**.

CD spectra were obtained on a JASCO J-810 circular dichroism spectrometer equipped with a Peltier temperature controller at the Biochemistry Department at McGill. Samples were annealed at a final concentration of 15 nM prior to the experiment in the same buffer as for the thermal denaturation studies. Spectra were recorded in triplet from 10-90 °C (ramped at 0.5 °C/min) under constant flow of nitrogen gas, and was baseline-corrected with respect to a blank containing the buffer only. Smoothing and adjustment for duplex concentration were performed using the Spectra-Manager program (Jasco). CD spectra are shown in **Figure 5.8**.

5.8.3 Characterization of parallel and antiparallel siRNA duplex formation by native gel electrophoresis

Formation of parallel and antiparallel siRNAs was investigated through acrylamide gel electrophoresis of duplexes and single strands under native conditions. Samples were prepared to contain 8 µL of 1 µM oligonucleotides in siRNA buffer (100 mM KOAc, 30 mM HEPES-KOH, 2 mM $Mg(OAc)_2$, pH 7.4) and were mixed with 2 µL of glycerol. Samples were then loaded onto 20% (w/v) acrylamide running gel prepared in a Tris-acetate-EDTA buffer (TAE buffer: 40 mM Tris-acetate, 1 mM EDTA, pH 8.0). Gel was then immersed in TAE buffer and electrophoresed at constant voltage of 60V for 15 minutes, followed by 3 hours at 250V at 10 °C. Oligonucleotides were revealed following manufacture's protocol for SYBR Gold nucleic acid

gel stain (Invitrogen, Carlsbad, CA) and fluorescence was recorded on a ChemiDoc XRS (Bio-Rad, Gladesville NSW) (see **Figure 5.3**, **Figure 5.4**, and **Figure 5.7**).

5.8.4 Characterization of parallel and antiparallel duplex formation by 1D ^{1}H-NMR experiment

Selected parallel and antiparallel duplexes (40 μM samples) were suspended in 300 μL of H_2O/D_2O 9:1 in sodium buffer, 250 mM Na_2HPO_4, 1 M NaCl and 1 mM EDTA (pH 7). NMR spectra were acquired in a Bruker Avance spectrometers operating at 700 MHz and processed with Topspin software (**Figure 5.9**).

5.8.5 Renilla luciferase siRNA assay

Cell culture: HEK293T cells (ATCC, #CRL-3216) were maintained in Dulbecco's Modified Eagle's medium (Gibco, 31966021) supplemented with 10% FBS (Gibco, #10270106) and kept at 37 °C in a 5% CO_2 incubator.

siRNA transfection: siRNAs targeting renilla (listed in **Table 5.4**) were transfected at 0, 2.25, 10 and 40 nM concentrations using Lipofectamine 2000 (Invitrogen, #11668027) according to the manufacturer's instructions. siCON (**Table 5.6**) was used as negative control.

Luciferase reporter plasmid cloning and transfection: PsiCHECK-2 dual-luciferase reporter

Table 5.6 Sequences of the non-targeting negative control (siCON) and the siRNA pool used for AGO2 knockdown experiment.

Name	Sequence (5′-3′)
siCON	GUGUGUGUUGUUUAUGCACTT (as) GUGNNUAANNAACNCANACTT (s)
siAGO2 (siRNA pool)	CAGACUCCCGUGUGUCCUATT (as) UAGGACACACGGGAGUCUGTT (s) CGGACAAUCAGACCUCCACTT(as) GUGGAGGUCUGAUUGUCCGTT(s)

Table 5.7 Target sites for siRenilla. Three fully complementary target sites for renilla are underlined. Restriction sites are marked in red.

Sequence (5′-3′)
*CTCGAG*CCCTGATCAAGAGCGAAGAGGGCGAGAAATTGGTGCTTGAGCCCTGATCAAGAGCGAAGAG GGCGAGAAATTGGTGCTTGAGCCCTGATCAAGAGCGAAGAGGGCGAGAAATTGGTGCTTGAG*GCGGC CGC*

plasmid (Promega, #C8021) was digested with NotI and XhoI and the insert bearing three fully-complementary target sites for siRenilla (**Table 5.7**) was cloned in the 3′-untranslated region (3′-UTR) of the Renilla gene. The plasmid was confirmed by sequencing and transfected at 20 ng/well using jetPEI (Polyplus, #101-10) according to the manufacturer's instructions.

Renilla luciferase assay: HEK293T cells were seeded in white 96-well plates at 10'000 viable cells/well and siRNAs were transfected after ca. 12-16 h, whereas the reporter plasmid ca. 24 h post-seeding. 48 h later, supernatants were removed and luminescence was measured on a microtiter plate reader (Mithras LB940, Berthold Technologies) using the Dual-Glo Luciferase Assay System (Promega, #E2940) according to the manufacturer's instructions. Values were normalized against firefly luminescence and the corresponding mock control whose relative luciferase activity was set to 100%. The experiment was repeated in three biological replicates.

Statistical analysis: Statistical analysis was performed with GraphPad Prism. An independent student's t test was used to compare the statistical significance of two groups, whereas two-way ANOVA was applied to compare more than two groups.

AGO2 knockdown experiment: siAGO2 siRNA pool was transfected at 50 and 100 nM using Lipofectamine 2000 (Invitrogen, #11668027) according to the manufacturer's instructions in HEK293T cells. Following the siAGO2 transfection, siRNAs targeting renilla were transfected

and renilla assay was conducted according to the instructions above. The experiment was repeated in two biological replicates.

5.9 References

1. Watson, J. D.; Crick, F. H. C., Molecular Structure of Nucleic Acids: A Structure for Deoxyribose Nucleic Acid. *Nature* **1953,** *171*, 737-738.
2. Kamiya, H.; Kasai, H., Mutations Induced by 2-Hydroxyadenine on a Shuttle Vector during Leading and Lagging Strand Syntheses in Mammalian Cells. *Biochemistry* **1997,** *36*, 11125-11130.
3. Ramsing, N. B.; Jovin, T. M., Parallel stranded duplex DNA. *Nucleic Acids Res* **1988,** *16*, 6659-76.
4. Ramsing, N. B.; Rippe, K.; Jovin, T. M., Helix-coil transition of parallel-stranded DNA. Thermodynamics of hairpin and linear duplex oligonucleotides. *Biochemistry* **1989,** *28*, 9528-35.
5. Rippe, K.; Ramsing, N. B.; Klement, R.; Jovin, T. M., A parallel stranded linear DNA duplex incorporating dG.dC base pairs. *Journal of biomolecular structure & dynamics* **1990,** *7*, 1199-209.
6. van de Sande, J. H.; Ramsing, N. B.; Germann, M. W.; Elhorst, W.; Kalisch, B. W.; et al., Parallel Stranded DNA. *Science* **1988,** *241*, 551.
7. Shchyolkina, A. K.; Lysov, Y. P.; Il'ichova, I. A.; Chernyi, A. A.; Golova, Y. B.; Chernov, B. K.; Gottikh, B. P.; Florentiev, V. L., Parallel stranded DNA with AT base pairing. *FEBS Letters* **1989,** *244*, 39-42.
8. Raghunathan, G.; Miles, H. T.; Sasisekharan, V., Parallel nucleic acid helices with hoogsteen base pairing: Symmetry and structure. *Biopolymers* **1994,** *34*, 1573-1581.
9. Frank-Kamenetskii, M. D.; Mirkin, S. M., Triplex DNA Structures. *Annual Review of Biochemistry* **1995,** *64*, 65-95.
10. Lavelle, L.; Fresco, J. R., UV spectroscopic identification and thermodynamic analysis of protonated third strand deoxycytidine residues at neutrality in the triplex d(C+-T)6:[d(A-G)6d(C−-T)6]; evidence for a proton switch. *Nucleic Acids Research* **1995,** *23*, 2692-2705.
11. Marfurt, J.; Parel, S. P.; Leumann, C. J., Strong, specific, monodentate G-C base pair recognition by N7-inosine derivatives in the pyrimidine.purine-pyrimidine triple-helical binding motif. *Nucleic Acids Res* **1997,** *25*, 1875-82.
12. Sun, J.-S.; Hélène, C., Oligonucleotide-directed triple-helix formation. *Current Opinion in Structural Biology* **1993,** *3*, 345-356.
13. Burge, S.; Parkinson, G. N.; Hazel, P.; Todd, A. K.; Neidle, S., Quadruplex DNA: sequence, topology and structure. *Nucleic Acids Research* **2006,** *34*, 5402-5415.
14. Phan, A. T., Human telomeric G-quadruplex: structures of DNA and RNA sequences. *The FEBS journal* **2010,** *277*, 1107-17.
15. Collie, G. W.; Parkinson, G. N., The application of DNA and RNA G-quadruplexes to therapeutic medicines. *Chemical Society reviews* **2011,** *40*, 5867-92.
16. Gueron, M.; Leroy, J. L., The i-motif in nucleic acids. *Curr Opin Struct Biol* **2000,** *10*, 326-31.
17. Volker, J.; Klump, H. H.; Breslauer, K. J., The energetics of i-DNA tetraplex structures formed intermolecularly by d(TC5) and intramolecularly by d[(C5T3)3C5]. *Biopolymers* **2007,** *86*, 136-47.

18. Pattabiraman, N., Can the double helix be parallel? *Biopolymers* **1986,** *25*, 1603-1606.
19. Shchyolkina, A. K.; Borisova, O. F.; Jovin, T. M., Parallel-Stranded Oligonucleotides with Alternating d(A-isoG)/d(T·C) and d(A·G)/d(T·m5isoC) Sequences. *Nucleosides and Nucleotides* **1999,** *18*, 1555-1562.
20. Parvathy, V. R.; Bhaumik, S. R.; Chary, K. V.; Govil, G.; Liu, K.; Howard, F. B.; Miles, H. T., NMR structure of a parallel-stranded DNA duplex at atomic resolution. *Nucleic Acids Res* **2002,** *30*, 1500-11.
21. Germann, M. W.; Zhou, N.; van de Sande, J. H.; Vogel, H. J., [9] Parallel-stranded duplex DNA: An NMR perspective. In *Methods in enzymology*, Academic Press1995; Vol. Volume 261, pp 207-225.
22. Germann, M. W.; Kalisch, B. W.; van de Sande, J. H., Structure of d(GT)n.d(GA)n sequences: formation of parallel stranded duplex DNA. *Biochemistry* **1998,** *37*, 12962-70.
23. Germann, M. W.; Kalisch, B. W.; van de Sande, J. H., Relative stability of parallel- and antiparallel-stranded duplex DNA. *Biochemistry* **1988,** *27*, 8302-6.
24. Barsky, D.; Colvin, M. E., Guanine−Cytosine Base Pairs in Parallel-Stranded DNA: An ab Initio Study of the Keto−Amino Wobble Pair versus the Enol−Imino Minor Tautomer Pair. *The Journal of Physical Chemistry A* **2000,** *104*, 8570-8576.
25. Sunami, T.; Kondo, J.; Kobuna, T.; Hirao, I.; Watanabe, K.; Miura, K.; Takenaka, A., Crystal structure of d(GCGAAAGCT) containing a parallel-stranded duplex with homo base pairs and an anti-parallel duplex with Watson-Crick base pairs. *Nucleic Acids Res* **2002,** *30*, 5253-60.
26. Cubero, E.; Avino, A.; de la Torre, B. G.; Frieden, M.; Eritja, R.; Luque, F. J.; Gonzalez, C.; Orozco, M., Hoogsteen-based parallel-stranded duplexes of DNA. Effect of 8-amino-purine derivatives. *J Am Chem Soc* **2002,** *124*, 3133-42.
27. Garcia, A. E.; Soumpasis, D. M.; Jovin, T. M., Dynamics and relative stabilities of parallel- and antiparallel-stranded DNA duplexes. *Biophysical journal* **1994,** *66*, 1742-55.
28. Rippe, K.; Ramsing, N. B.; Jovin, T. M., Spectroscopic properties and helical stabilities of 25-nt parallel-stranded linear DNA duplexes. *Biochemistry* **1989,** *28*, 9536-41.
29. Rentzeperis, D.; Rippe, K.; Jovin, T. M.; Marky, L. A., Calorimetric characterization of parallel-stranded DNA: stability, conformational flexibility, and ion binding. *J Am Chem Soc* **1992,** *114*, 5926-5928.
30. Ishikawa, F.; Frazier, J.; Howard, F. B.; Miles, H. T., Polyadenylate polyuridylate helices with non-Watson-Crick hydrogen bonding. *Journal of molecular biology* **1972,** *70*, 475-90.
31. Seela, F.; Melenewski, A.; Wei, C., Parallel-stranded duplex DNA formed by a new base pair between guanine and 5-aza-7-deazaguanine. *Bioorganic & Medicinal Chemistry Letters* **1997,** *7*, 2173-2176.
32. Sugiyama, H.; Ikeda, S.; Saito, I., Remarkably Stable Parallel-Stranded Oligonucleotides Containing 5-Methylisocytosine and Isoguanine. *J Am Chem Soc* **1996,** *118*, 9994-9995.
33. Seela, F.; Wei, C.; Melenewski, A.; He, Y.; Kröschel, R.; Feiling, E., Parallel-Stranded DNA Formed by New Base Pairs Related to the Isoguanine-Cytosine or Isocytosine-Guanine Motifs. *Nucleosides and Nucleotides* **1999,** *18*, 1543-1548.
34. Seela, F.; He, Y.; Wei, C., Parallel-stranded oligonucleotide duplexes containing 5-methylisocytosine-guanine and isoguanine-cytosine base pairs. *Tetrahedron* **1999,** *55*, 9481-9500.

35. Yang, X. L.; Sugiyama, H.; Ikeda, S.; Saito, I.; Wang, A. H., Structural studies of a stable parallel-stranded DNA duplex incorporating isoguanine:cytosine and isocytosine:guanine basepairs by nuclear magnetic resonance spectroscopy. *Biophysical journal* **1998,** *75*, 1163-71.
36. Seela, F.; Wei, C., Oligonucleotides Containing Consecutive 2′-Deoxyisoguanosine Residues: Synthesis, duplexes with parallel chain orientation, and aggregation. *Helvetica Chimica Acta* **1997,** *80*, 73-85.
37. Lancelot, G.; Guesnet, J. L.; Vovelle, F., Solution structure of the parallel-stranded duplex oligonucleotide alpha-d(TCTAAAC)-beta-d(AGATTTG) via complete relaxation matrix analysis of the NOE effects and molecular mechanics calculations. *Biochemistry* **1989,** *28*, 7871-8.
38. Thuong, N. T.; Asseline, U.; Roig, V.; Takasugi, M.; Helene, C., Oligo(alpha-deoxynucleotide)s covalently linked to intercalating agents: differential binding to ribo- and deoxyribopolynucleotides and stability towards nuclease digestion. *Proceedings of the National Academy of Sciences of the United States of America* **1987,** *84*, 5129-33.
39. Praseuth, D.; Chassignol, M.; Takasugi, M.; Le Doan, T.; Thuong, N. T.; Helene, C., Double helices with parallel strands are formed by nuclease-resistant oligo-[alpha]-deoxynucleotides and oligo-[alpha]-deoxynucleotides covalently linked to an intercalating agent with complementary oligo-[beta]-deoxynucleotides. *Journal of molecular biology* **1987,** *196*, 939-42.
40. Aramini, J. M.; Kalisch, B. W.; Pon, R. T.; van de Sande, J. H.; Germann, M. W., Structure of a DNA Duplex That Contains α-Anomeric Nucleotides and 3‘−3‘ and 5‘−5‘ Phosphodiester Linkages: Coexistence of Parallel and Antiparallel DNA. *Biochemistry* **1996,** *35*, 9355-9365.
41. Luo, J.; Sarma, M. H.; Yuan, R. D.; Sarma, R. H., NMR study of self-paired parallel duplex of d(AAAAACCCCC) in solution. *FEBS Lett* **1992,** *306*, 223-8.
42. Rich, A.; Davies, D. R.; Crick, F. H. C.; Watson, J. D., The molecular structure of polyadenylic acid. *Journal of molecular biology* **1961,** *3*, 71-IN19.
43. Coll, M.; Solans, X.; Font-Altaba, M.; Subirana, J. A., Crystal and molecular structure of the sodium salt of the dinucleotide duplex d(CpG). *Journal of biomolecular structure & dynamics* **1987,** *4*, 797-811.
44. Leontis, N. B.; Stombaugh, J.; Westhof, E., The non-Watson-Crick base pairs and their associated isostericity matrices. *Nucleic Acids Res* **2002,** *30*, 3497-531.
45. Tchurikov, N. A.; Chernov, B. K.; Golova, Y. B.; Nechipurenko, Y. D., Parallel DNA: generation of a duplex between two Drosophila sequences in vitro. *FEBS Lett* **1989,** *257*, 415-8.
46. Borisova, O. F.; Shchyolkina, A. K.; Chernov, B. K.; Tchurikov, N. A., Relative stability of AT and GC pairs in parallel DNA duplex formed by a natural sequence. *FEBS Letters* **1993,** *322*, 304-306.
47. Mohammadi, S.; Klement, R.; Shchyolkina, A. K.; Liquier, J.; Jovin, T. M.; Taillandier, E., FTIR and UV Spectroscopy of Parallel-Stranded DNAs with Mixed A•T/G•C Sequences and Their A•T/I•C Analogues. *Biochemistry* **1998,** *37*, 16529-16537.
48. Geinguenaud, F.; Mondragon-Sanchez, J. A.; Liquier, J.; Shchyolkina, A. K.; Klement, R.; Arndt-Jovin, D. J.; Jovin, T. M.; Taillandier, E., Parallel DNA double helices incorporating isoG or m5isoC bases studied by FTIR, CD and molecular modeling. *Spectrochimica acta. Part A, Molecular and biomolecular spectroscopy* **2005,** *61*, 579-87.
49. Liu, K.; Miles, H. T.; Frazier, J.; Sasisekharan, V., A novel DNA duplex. A parallel-stranded DNA helix with Hoogsteen base pairing. *Biochemistry* **1993,** *32*, 11802-11809.

50. Escudé, C.; Mohammadi, S.; Sun, J.-S.; Nguyen, C.-H.; Bisagni, E.; Liquier, J.; Taillandier, E.; Garestier, T.; Hélène, C., Ligand-induced formation of Hoogsteen-paired parallel DNA. *Chemistry & Biology* **1996,** *3*, 57-65.
51. Suda, T.; Mishima, Y.; Asakura, H.; Kominami, R., Formation of a parallel-stranded DNA homoduplex by d(GGA) repeat oligonucleotides. *Nucleic Acids Res* **1995,** *23*, 3771-7.
52. Wang, Y.; Patel, D. J., Solution Stucture of the d(T-C-G-A) Duplex at Acidic pH: A Parallel-Stranded Helix Containing C+ · C, G · G and A · A Pairs. *Journal of molecular biology* **1994,** *242*, 508-526.
53. Robinson, H.; Wang, A. H., 5'-CGA sequence is a strong motif for homo base-paired parallel-stranded DNA duplex as revealed by NMR analysis. *Proceedings of the National Academy of Sciences of the United States of America* **1993,** *90*, 5224-5228.
54. Robinson, H.; Van der Marel, G. A.; Van Boom, J. H.; Wang, A. H. J., Unusual DNA conformation at low pH revealed by NMR: parallel-stranded DNA duplex with homo base pairs. *Biochemistry* **1992,** *31*, 10510-10517.
55. Rippe, K.; Fritsch, V.; Westhof, E.; Jovin, T. M., Alternating d(G-A) sequences form a parallel-stranded DNA homoduplex. *The EMBO journal* **1992,** *11*, 3777-86.
56. Dolinnaya, N. G.; Ulku, A.; Fresco, J. R., Parallel-stranded linear homoduplexes of d(A+-G)n > 10 and d(A-G)n > 10 manifesting the contrasting ionic strength sensitivities of poly(A+.A+) and DNA. *Nucleic Acids Research* **1997,** *25*, 1100-1107.
57. Förtsch, I.; Birch-Hirschfeld, E.; Jovin, T. M.; Stelzner, A.; Zimmer, C., Studies on the Interaction of Dna-Ligands with Modified Parallel-Stranded Duplex-Dna Oligomers. *Nucleosides and Nucleotides* **1998,** *17*, 1539-1545.
58. Jain, A. K.; Bhattacharya, S., Groove Binding Ligands for the Interaction with Parallel-Stranded ps-Duplex DNA and Triplex DNA. *Bioconjugate chemistry* **2010,** *21*, 1389-1403.
59. Li, H.; Peng, X.; Leonard, P.; Seela, F., Binding of actinomycin C1 (D) and actinomin to base-modified oligonucleotide duplexes with parallel chain orientation. *Bioorg Med Chem* **2006,** *14*, 4089-100.
60. Tchurikov, N. A.; Chistyakova, L. G.; Zavilgelsky, G. B.; Manukhov, I. V.; Chernov, B. K.; Golova, Y. B., Gene-specific Silencing by Expression of Parallel Complementary RNA in Escherichia coli. *Journal of Biological Chemistry* **2000,** *275*, 26523-26529.
61. Liu, Y. S.; Zhang, Y. Q.; Yang, L. X.; Yao, T. J.; Xiao, C. L., Gene-specific silencing induced by parallel complementary RNA in Pseudomonas aeruginosa. *Biotechnology letters* **2009,** *31*, 1571-5.
62. Soyfer, V. N.; Potaman, V. N., *Triple-Helical Nucleic Acids*. Springer New York2012.
63. Tchurikov, N. A., Natural DNA sequences complementary in the same direction: evidence for parallel biosynthesis? *Genetica* **1992,** *87*, 113-7.
64. Fritzsche, H.; Akhebat, A.; Taillandier, E.; Rippe, K.; Jovin, T. M., Structure and drug interactions of parallel-stranded DNA studied by infrared spectroscopy and fluorescence. *Nucleic Acids Research* **1993,** *21*, 5085-5091.
65. Tchurikov, N. A.; Ponomarenko, N. A.; Golova, Y. B.; Chernov, B. K., The formation of parallel RNA-RNA duplexes in vitro. *Journal of biomolecular structure & dynamics* **1995,** *13*, 507-13.
66. Safaee, N.; Noronha, A. M.; Rodionov, D.; Kozlov, G.; Wilds, C. J.; Sheldrick, G. M.; Gehring, K., Structure of the Parallel Duplex of Poly(A) RNA: Evaluation of a 50 Year-Old Prediction. *Angewandte Chemie International Edition* **2013,** *52*, 10370-10373.

67. Ingale, S. A.; Leonard, P.; Tran, Q. N.; Seela, F., Duplex DNA and DNA–RNA Hybrids with Parallel Strand Orientation: 2′-Deoxy-2′-fluoroisocytidine, 2′-Deoxy-2′-fluoroisoguanosine, and Canonical Nucleosides with 2′-Fluoro Substituents Cause Unexpected Changes on the Double Helix Stability. *The Journal of Organic Chemistry* **2015,** *80*, 3124-3138.
68. Anzahaee, M. Y., Structural studies and gene silencing activities of chemically modified nucleic acids: Effect of C2 'sugar modifications and iso-nucleobases on the stability and polarity of duplex and tetraplex structures. **2015**.
69. Watts, J. K.; Martín-Pintado, N.; Gómez-Pinto, I.; Schwartzentruber, J.; Portella, G.; Orozco, M.; González, C.; Damha, M. J., Differential stability of 2′F-ANA•RNA and ANA•RNA hybrid duplexes: roles of structure, pseudohydrogen bonding, hydration, ion uptake and flexibility. *Nucleic Acids Research* **2010,** *38*, 2498-2511.
70. Anzahaee, M. Y.; Watts, J. K.; Alla, N. R.; Nicholson, A. W.; Damha, M. J., Energetically important C-H...F-C pseudohydrogen bonding in water: evidence and application to rational design of oligonucleotides with high binding affinity. *J Am Chem Soc* **2011,** *133*, 728-31.
71. Pallan, P. S.; Greene, E. M.; Jicman, P. A.; Pandey, R. K.; Manoharan, M.; Rozners, E.; Egli, M., Unexpected origins of the enhanced pairing affinity of 2'-fluoro-modified RNA. *Nucleic Acids Res* **2011,** *39*, 3482-95.
72. Patra, A.; Paolillo, M.; Charisse, K.; Manoharan, M.; Rozners, E.; Egli, M., 2′-Fluoro RNA Shows Increased Watson–Crick H-Bonding Strength and Stacking Relative to RNA: Evidence from NMR and Thermodynamic Data. *Angewandte Chemie International Edition* **2012,** *51*, 11863-11866.
73. Seela, F.; Wei, C.; Becher, G.; Zulauf, M.; Leonard, P., The influence of modified purine bases on the stability of parallel DNA. *Bioorg Med Chem Lett* **2000,** *10*, 289-92.
74. Seela, F.; Peng, X.; Li, H., Base-Pairing, Tautomerism, and Mismatch Discrimination of 7-Halogenated 7-Deaza-2‘-deoxyisoguanosine: Oligonucleotide Duplexes with Parallel and Antiparallel Chain Orientation. *J Am Chem Soc* **2005,** *127*, 7739-7751.
75. Deleavey, G. F.; Watts, J. K.; Alain, T.; Robert, F.; Kalota, A.; Aishwarya, V.; Pelletier, J.; Gewirtz, A. M.; Sonenberg, N.; Damha, M. J., Synergistic effects between analogs of DNA and RNA improve the potency of siRNA-mediated gene silencing. *Nucleic Acids Res* **2010,** *38*, 4547-57.
76. Manoharan, M.; Akinc, A.; Pandey, R. K.; Qin, J.; Hadwiger, P.; John, M.; Mills, K.; Charisse, K.; Maier, M. A.; Nechev, L.; Greene, E. M.; Pallan, P. S.; Rozners, E.; Rajeev, K. G.; Egli, M., Unique Gene-Silencing and Structural Properties of 2′-Fluoro-Modified siRNAs. *Angewandte Chemie International Edition* **2011,** *50*, 2284-2288.
77. Anzahaee, M. Y.; Deleavey, G. F.; Le, P. U.; Fakhoury, J.; Petrecca, K.; Damha, M. J., Arabinonucleic acids: 2'-stereoisomeric modulators of siRNA activity. *Nucleic acid therapeutics* **2014,** *24*, 336-43.
78. Elbashir, S. M.; Martinez, J.; Patkaniowska, A.; Lendeckel, W.; Tuschl, T., Functional anatomy of siRNAs for mediating efficient RNAi in Drosophila melanogaster embryo lysate. *The EMBO journal* **2001,** *20*, 6877-88.
79. Oridate, N.; Kim, H. J.; Xu, X.; Lotan, R., Growth inhibition of head and neck squamous carcinoma cells by small interfering RNAs targeting eIF4E or cyclin D1 alone or combined with cisplatin. *Cancer biology & therapy* **2005,** *4*, 318-23.

80. Biffi, G.; Di Antonio, M.; Tannahill, D.; Balasubramanian, S., Visualization and selective chemical targeting of RNA G-quadruplex structures in the cytoplasm of human cells. *Nature chemistry* **2014,** *6*, 75-80.
81. Cammas, A.; Millevoi, S., RNA G-quadruplexes: emerging mechanisms in disease. *Nucleic Acids Research* **2016**.
82. Zhang, A. Y.; Bugaut, A.; Balasubramanian, S., A sequence-independent analysis of the loop length dependence of intramolecular RNA G-quadruplex stability and topology. *Biochemistry* **2011,** *50*, 7251-8.
83. Sacca, B.; Lacroix, L.; Mergny, J. L., The effect of chemical modifications on the thermal stability of different G-quadruplex-forming oligonucleotides. *Nucleic Acids Res* **2005,** *33*, 1182-92.
84. Stegle, O.; Payet, L.; Mergny, J.-L.; MacKay, D. J. C.; Huppert, J. L., Predicting and understanding the stability of G-quadruplexes. *Bioinformatics* **2009,** *25*, i374-i1382.
85. Zarudnaya, M. I.; Kolomiets, I. M.; Potyahaylo, A. L.; Hovorun, D. M., Downstream elements of mammalian pre-mRNA polyadenylation signals: primary, secondary and higher-order structures. *Nucleic Acids Res* **2003,** *31*, 1375-86.
86. Kankia, B. I.; Barany, G.; Musier-Forsyth, K., Unfolding of DNA quadruplexes induced by HIV-1 nucleocapsid protein. *Nucleic Acids Research* **2005,** *33*, 4395-4403.
87. Chen, Y.; Yang, D., Sequence, Stability, Structure of G-Quadruplexes and Their Drug Interactions. *Current protocols in nucleic acid chemistry / edited by Serge L. Beaucage ... [et al.]* **2012,** *CHAPTER*, Unit17.5-Unit17.5.
88. Kostadinov, R.; Malhotra, N.; Viotti, M.; Shine, R.; D'Antonio, L.; Bagga, P., GRSDB: a database of quadruplex forming G-rich sequences in alternatively processed mammalian pre-mRNA sequences. *Nucleic Acids Research* **2006,** *34*, D119-D124.
89. Jahns, H.; Roos, M.; Imig, J.; Baumann, F.; Wang, Y.; Gilmour, R.; Hall, J., Stereochemical bias introduced during RNA synthesis modulates the activity of phosphorothioate siRNAs. *Nature communications* **2015,** *6*.
90. Gray, D. M.; Ratliff, R. L.; Vaughan, M. R., Circular dichroism spectroscopy of DNA. *Methods in enzymology* **1992,** *211*, 389-406.
91. Vorlickova, M.; Kejnovska, I.; Bednarova, K.; Renciuk, D.; Kypr, J., Circular dichroism spectroscopy of DNA: from duplexes to quadruplexes. *Chirality* **2012,** *24*, 691-8.
92. Ratmeyer, L.; Vinayak, R.; Zhong, Y. Y.; Zon, G.; Wilson, W. D., Sequence Specific Thermodynamic and Structural Properties for DNA.cntdot.RNA Duplexes. *Biochemistry* **1994,** *33*, 5298-5304.
93. Hung, S. H.; Yu, Q.; Gray, D. M.; Ratliff, R. L., Evidence from CD spectra that d(purine).r(pyrimidine) and r(purine).d(pyrimidine) hybrids are in different structural classes. *Nucleic Acids Res* **1994,** *22*, 4326-34.
94. Wijmenga, S. S.; van Buuren, B. N. M., The use of NMR methods for conformational studies of nucleic acids. *Progress in Nuclear Magnetic Resonance Spectroscopy* **1998,** *32*, 287-387.
95. Phan, A. T.; Mergny, J.-L., Human telomeric DNA: G-quadruplex, i-motif and Watson–Crick double helix. *Nucleic Acids Research* **2002,** *30*, 4618-4625.
96. Zhou, N.; Germann, M. W.; van de Sande, J. H.; Pattabiraman, N.; Vogel, H. J., Solution structure of the parallel-stranded hairpin d(T8.ltbbrac..rtbbrac.C4A8) as determined by two-dimensional NMR. *Biochemistry* **1993,** *32*, 646-656.

97. Ui-Tei, K.; Naito, Y.; Zenno, S.; Nishi, K.; Yamato, K.; Takahashi, F.; Juni, A.; Saigo, K., Functional dissection of siRNA sequence by systematic DNA substitution: modified siRNA with a DNA seed arm is a powerful tool for mammalian gene silencing with significantly reduced off-target effect. *Nucleic Acids Res* **2008,** *36*, 2136-51.
98. Elbashir, S. M.; Harborth, J.; Lendeckel, W.; Yalcin, A.; Weber, K.; Tuschl, T., Duplexes of 21-nucleotide RNAs mediate RNA interference in cultured mammalian cells. *Nature* **2001,** *411*, 494-498.
99. Lee, H. S.; Lee, S. N.; Joo, C. H.; Lee, H.; Lee, H. S.; Yoon, S. Y.; Kim, Y. K.; Choe, H., Contributions of 3'-overhang to the dissociation of small interfering RNAs from the PAZ domain: molecular dynamics simulation study. *Journal of molecular graphics & modelling* **2007,** *25*, 784-93.
100. Sano, M.; Sierant, M.; Miyagishi, M.; Nakanishi, M.; Takagi, Y.; Sutou, S., Effect of asymmetric terminal structures of short RNA duplexes on the RNA interference activity and strand selection. *Nucleic Acids Research* **2008,** *36*, 5812-5821.
101. Wilson, J. A.; Zhang, C.; Huys, A.; Richardson, C. D., Human Ago2 is required for efficient microRNA 122 regulation of hepatitis C virus RNA accumulation and translation. *Journal of virology* **2011,** *85*, 2342-50.
102. Jackson, A. L.; Burchard, J.; Leake, D.; Reynolds, A.; Schelter, J.; Guo, J.; Johnson, J. M.; Lim, L.; Karpilow, J.; Nichols, K.; Marshall, W.; Khvorova, A.; Linsley, P. S., Position-specific chemical modification of siRNAs reduces "off-target" transcript silencing. *RNA (New York, N.Y.)* **2006,** *12*, 1197-1205.
103. Whitehead, K. A.; Dahlman, J. E.; Langer, R. S.; Anderson, D. G., Silencing or stimulation? siRNA delivery and the immune system. *Annual review of chemical and biomolecular engineering* **2011,** *2*, 77-96.
104. Deleavey, Glen F.; Damha, Masad J., Designing Chemically Modified Oligonucleotides for Targeted Gene Silencing. *Chemistry & Biology* **2012,** *19*, 937-954.
105. Watts, J. K.; Corey, D. R., Silencing disease genes in the laboratory and the clinic. *The Journal of Pathology* **2012,** *226*, 365-379.
106. Peacock, H.; Kannan, A.; Beal, P. A.; Burrows, C. J., Chemical Modification of siRNA Bases To Probe and Enhance RNA Interference. *The Journal of Organic Chemistry* **2011,** *76*, 7295-7300.
107. Der, S. D.; Yang, Y.-L.; Weissmann, C.; Williams, B. R. G., A double-stranded RNA-activated protein kinase-dependent pathway mediating stress-induced apoptosis. *Proceedings of the National Academy of Sciences* **1997,** *94*, 3279-3283.
108. Clemens, M. J.; Elia, A., The double-stranded RNA-dependent protein kinase PKR: structure and function. *Journal of interferon & cytokine research : the official journal of the International Society for Interferon and Cytokine Research* **1997,** *17*, 503-24.
109. Christodoulou, C., Oligonucleotide Synthesis. In *Protocols for Oligonucleotides and Analogs: Synthesis and Properties*, Agrawal, S., Ed. Humana Press: Totowa, NJ, 1993; pp 19-31.
110. Damha, M. J.; Ogilvie, K. K., Oligoribonucleotide synthesis. The silyl-phosphoramidite method. *Methods in molecular biology (Clifton, N.J.)* **1993,** *20*, 81-114.
111. Bellon, L., Oligoribonucleotides with 2'-O-(tert-butyldimethylsilyl) groups. *Current protocols in nucleic acid chemistry* **2001,** *Chapter 3*, Unit 3.6.
112. Wincott, F.; DiRenzo, A.; Shaffer, C.; Grimm, S.; Tracz, D.; Workman, C.; Sweedler, D.; Gonzalez, C.; Scaringe, S.; Usman, N., Synthesis, deprotection, analysis and purification of RNA and ribozymes. *Nucleic Acids Res* **1995,** *23*, 2677-84.

CHAPTER 6: CONTRIBUTIONS TO KNOWLEDGE AND FUTURE WORKS

6.1 Summary of research and future directions

6.1.1 Stereoselective synthesis of oxepane nucleoside analogs and studies on their conformation

This work describes the synthesis of a novel series of seven-membered ring nucleoside (oxepane) analogs as candidates for biological screening and gene silencing applications. The conformational landscape and preferred ring-puckering of selected oxepane nucleosides were investigated by means of NMR, X-ray crystallography, and quantum mechanical calculations. These nucleoside analogs are valuable compounds for both antiviral and anticancer applications. Also, our results build the grounds for designing novel sugar-expanded oligonucleotides for gene silencing purposes.

The ongoing research in our lab focuses on optimizing the synthesis of the obtained nucleoside library, as well as other oxepane analogs, in larger quantities for incorporation into oligonucleotides. Molecular modeling experiments can shed light on the duplex structure of the incorporated oxepane analogs, within DNA and RNA duplexes. Also, oxepane nucleoside triphosphates can be synthesized for further screening of these analogs as anticancer and antiviral agents, and as precursors of xenonucleic acids.[1, 2]

6.1.2 2′-5′ modification of siRNA creates potent siRNAs with enhanced drug-like abilities

During the course of this work, we investigated the effect of 2'-5' linkage modification on siRNA efficiency. siRNA libraries targeting firefly luciferase and P53 mRNAs were prepared with different positional variations of 2'-5' linkages throughout the sense or antisense strands of the duplexes. Screening of these libraries against their corresponding mRNA target revealed that 2'-

5' linkages are tolerated in the sense strand and, to some extent, the antisense strand of siRNAs. 2'-5' Linked siRNAs were also found to abrogate the immunostimulatory response in comparison with their native siRNAs. In conclusion, we demonstrated, for the first time, that introduction of 2'-5' linkages can afford a potent class of modified siRNAs with improved nuclease stability and diminished immunostimulatory response.

Future directions for this project can involve more detailed structural investigations to further elucidate the degree which an siRNA duplex is destabilized by 2'-5' linkages, considering factors such as the sequence and arrangement of the linkage modifications. X-ray crystallography is a powerful tool that can help study the siRNAs structure upon linkage modification, both in the form of duplex, as well as once bound to AGO2. Such studies can provide evidence on why siRNAs with alternating 2'-5' linkages exhibit higher potencies in comparison with the siRNAs with consecutive 2'-5' linkages.

6.1.3 Protein interactions and structural investigations of 2′-5′ modified siRNAs

Following our previous findings with 2'-5' modified siRNAs, we studied the interactions of such siRNAs with the proteins involved in the RNAi pathway. Interactions of 2'-5' linked siRNAs with the kinase and hAGO2 proteins were investigated by radiolabelling and gel shift assays. Our experiments revealed that extensive 2'-5' modification of the antisense strand was only minimally affecting the siRNA phosphorylation by kinases, but was detrimental to its hAGO2 loading. We also performed extensive structural studies on 2'-5' linked siRNAs in the active site of hAGO2, using molecular modelling and MD simulations. Our results indicate 2'-5' linkages do not significantly affect hAGO2-siRNA interactions, except when a large number of these linkages are introduced; in this case, destabilization arises from the structural changes in the RNA duplex induced by the linkage modification. Our study contributes to the ongoing research

on the origin of life, proving that 2'-5'/3'-5' backbone heterogeneity could, to some extent, be compatible with RNA structure and its interaction with some proteins. While interactions of polymerases with 2′-5′ has been investigated, our work is the first to demonstrate that 2′-5′ liked siRNAs can retain molecular recognition and catalytic properties with regard to proteins involved in gene regulation.

During the evaluation of this thesis, more experiments were performed to investigate the binding affinity of 2'-5' modified siRNAs to hAGO2 using immunoprecipitation techniques.[3] These experiments further confirmed that extensive 2'-5' modification in the AS strand reduce the siRNA loading in AGO2, as well as decrease the preference of AGO2 for selecting the modified strand as the AS strand (**Figure 6.1)**.

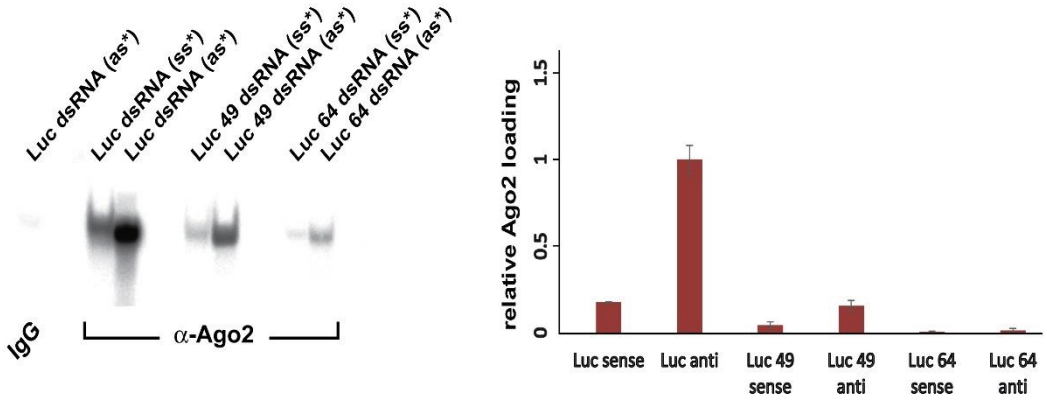

Sample #	Sequence
Luc 49 anti	(S) Ⓟ GCUUGAA GUCUUUA AUUAAUU -3′ (AS) 3′- GGCGAAC UUCAGAA AUUAAUU Ⓟ
Luc 49 sense	(S) Ⓟ GCUUGAA GUCUUUA AUUAAUU -3′ (AS) 3′- GGCGAAC UUCAGAA AUUAAUU Ⓟ
Luc 64 anti	(S) Ⓟ GCUUGAA GUCUUUA AUUAAUU -3′ (AS) 3′- GGCGAAC UUCAGAA AUUAAUU Ⓟ
Luc 64 sense	(S) Ⓟ GCUUGAA GUCUUUA AUUAAUU -3′ (AS) 3′- GGCGAAC UUCAGAA AUUAAUU Ⓟ
Luc anti	(S) Ⓟ GCUUGAA GUCUUUA AUUAAUU -3′ (AS) 3′- GGCGAAC UUCAGAA AUUAAUU Ⓟ
Luc sense	(S) Ⓟ GCUUGAA GUCUUUA AUUAAUU -3′ (AS) 3′- GGCGAAC UUCAGAA AUUAAUU Ⓟ

Legend: 2′,5′ modifications, RNA
Ⓟ Hot phosphate group Ⓟ Cold phosphate group

Figure 6.1 In vitro hAGO2 siRNA loading assay using immunoprecipitation on Hela cells extract. siRNAs (left) were radiolabelled either on their sense or antisense strands and their loading into hAGO2 was separately assessed (top). siRNA linkage modification in the AS strand was found to reduce the siRNA loading (sense + AS) in hAGO2.

6.1.4 Synthesis and properties of siRNA mixmers

We introduced, for the first time, the “mixmer” strategy as a novel approach in preparing active mixtures of chemically modified siRNAs. siRNA libraries targeting firefly luciferase and P53 mRNAs were prepared with 2'-5' linkages and various 2'-5'/3'-5' (mixmer) modification patterns present in the sense or antisense (AS) strands. These libraries were screened against their corresponding mRNA target, showing that siRNAs with 2'-5' or 2'-5'/3'-5' mixmer modifications in the sense strand are as potent as 3'-5' siRNAs. While 2'-5' modification in the antisense strand was found to be detrimental to the siRNA activity, the siRNA activity was restored by introducing a 2'-5'/3'-5' mixmer stretch in the same region. These results are in line with previous findings suggesting that mixed 2'-5'/3'-5' linkages in nucleic acids could be an important alternative functional backbone during early evolution.

Future directions for this project can focus on expanding the mixmer strategy from 2′-5′/ 3′-5′ to other X/Y modification combinations. Our results, as discussed briefly in chapter 4, suggest that siRNA mixmers prepared from different modifications can enhance RNAi activity to various degrees. Detailed structural investigations, utilizing techniques such as X-ray crystallography or NMR, can help elucidate why some modifications are more compatible with each other to yield active siRNAs.

6.1.5 Synthesis, characterization, and biological investigations of parallel duplexes as triggers of RNA interference

We have investigated the impact of several sugar and nucleobase modifications on the formation of parallel-stranded duplexes at neutral pH. Our study focused on the synthesis and full structural analysis of isoC- and isoG- modified parallel stranded DNA:RNA and DNA:2′-FRNA hybrids as active siRNAs under physiological conditions. This study also revealed the benefits and

challenges to the design of parallel stranded siRNAs and explained the underlying rules to a successful parallel stranded siRNA design and synthesis. Further mechanistic investigations through AGO2 knockdown experiments confirmed that gene silencing by these parallel siRNAs is, indeed, happening via RNAi mechanism. Our findings suggest that helical conformation and groove dimensions of parallel stranded duplexes are not critical determinants in activation of RNAi, thus offering new opportunities in designing a new class of potent chemically modified siRNAs at physiological conditions.

Our results for this project open many opportunities to future work. Our fundamental interest would be to elucidate the structure of the synthesized parallel siRNAs using X-ray crystallography or NMR studies. Immunostimulation studies on parallel siRNAs can support our hypothesis that their different helical structure can render them unrecognized by the immune system machinery. Off-target effect studies are important experiments that are required to demonstrate that our specific parallel siRNA design with DNA sense strand can prevent the off-targets caused by wrongly choosing the sense strand for AS by AGO2. These can also be verified by AGO2 pull down loading assays showing the AGO2's preference for the sense and AS strands, as well the general AGO2 loading ability of parallel siRNAs. Finally, it would be of great interest to investigate whether our parallel DNA:RNA hybrids can trigger RNase H dependent mRNA degradation. This assay, will suggest if the reduced activity of parallel siRNAs is due to their partial degradation by RNase H enzyme, or is a result of their inherent lower activity.

6.2 Papers and conference presentations

6.2.1 Papers published

- M. Habibian, S. Martínez-Montero, G. Portella, Z. Chua, D. S. Bohle, M. Orozco, and M. J. Damha "Seven-Membered Ring Nucleoside Analogues: Stereoselective Synthesis and Studies on Their Conformational Properties", *Org. Lett.* **2015**, *17* (21), 5416-5419.

- K. Yamada, A. S. Wahba, J. Bernatchez, T. Ilina, S. Martínez-Montero, M. Habibian, M. Götte, M. A. Parniak, M. J. Damha, "Nucleotide Sugar Pucker Preference Mitigates excision by HIV-1 RT", *ACS Chem. Bio*. **2015**, *(10)* 2024-2033.

6.2.2 Patent applications

- Z. Kartje, C. Barkau, K. Rohilla, M. Habibian, E. Malek-Adamian, D. O'Reilly, M. J. Damha, and K. T. Gagnon, "Chemical Substitution of CRISPR RNA Nucleotides for Enhanced Assembly, Specificity, and Enzyme Activity of Cas9 Ribonucleoprotein Complexes", **2016**, US provisional patent application #62/398,775.

6.2.3 Manuscripts in preparation

- M. Yahyaee Anzahaee, **M. Habibian**, E. Moroz, N. Martın-Pintado, J. Fakhoury, J. Leroux, C. Gonzales, and M. J. Damha "Structural Properties and Gene Silencing Activity of Parallel-Stranded Duplexes".

- **M. Habibian**, J. Fakhoury, R. Cencic, K. T. Gagnon, S. Harikrishna, F. Robert, P.I. Pradeepkumar, J. Pelletier, Mayumi Takahashi, John Rossi, and M. J. Damha "Effect of 2'-5'/3'-5' phosphodiester linkage heterogeneity on RNA interference efficiency".

- **M. Habibian**, J. Fakhoury, R. Cencic, J. Pelletier, Mayumi Takahashi, John Rossi, and M. J. Damha "Synthesis and properties of mixmer RNA duplexes".

6.2.4 Attended conferences

- "Effect of 2'-5' phosphodiester linkage modification on RNA interference efficiency", **M. Habibian**, J. Fakhoury, R. Cencic, K. T. Gagnon, S. Harikrishna, F. Robert, P.I. Pradeepkumar, J. Pelletier, Mayumi Takahashi, John Rossi, and M. J. Damha, Oral presentation at the 12th Annual Meeting of the Oligonucleotide Therapeutics Society (OTS) September 2016, Montreal.

- "Effect of 2'-5' phosphodiester linkage modification on RNA interference efficiency", **M. Habibian**, J. Fakhoury, R. Cencic, K. T. Gagnon, S. Harikrishna, F. Robert, P.I. Pradeepkumar, J. Pelletier, Mayumi Takahashi, John Rossi, and M. J. Damha, Poster presentation at the 22nd International Round Table on Nucleosides, Nucleotides and Nucleic Acids (IRT), July 2016, Paris- Received best poster award.

- "Studies on Oxepane Based Nucleosides and Oligonucleotides", **M. Habibian**, S. Martínez-Montero, G. Portella, Z. Chua, D. S. Bohle, M. Orozco, and M. J. Damha, Poster presentation

at the 10th Annual Meeting of the Oligonucleotide Therapeutics Society (OTS), October 2014, San Diego.

- "Studies on Oxepane-Based Nucleosides and Oligonucleotides", **M. Habibian**, M. J. Damha, Oral presentation at the 96th Canadian Society of Chemistry Conference (CSC) May 2013, Montreal, Received best oral presentation award.

- "Studies on Oxepane-Based Nucleosides and Oligonucleotides", **M. Habibian**, M. J. Damha, Poster presentation at the McGill CIHR Drug Development and Training Program Retreat, May 2013, Montreal- Received best poster award.

- "Synthesis and Studies on Oxepane Based Nucleosides and Oligonucleotides", **M. Habibian**, P. Gallant, and M. J. Damha, Poster presentation at the 13th International Round Table on Nucleosides, Nucleotides and Nucleic Acids (IRT), August 2012, Montreal- Received best poster award.

6.3 References

1. Peng, C. G.; Damha, M. J., Polymerase-Directed Synthesis of 2'-Deoxy-2'-fluoro-β-D-arabinonucleic Acids. *J Am Chem Soc* **2007,** *129*, 5310-5311.
2. Pinheiro, V. B.; Taylor, A. I.; Cozens, C.; Abramov, M.; Renders, M.; Zhang, S.; Chaput, J. C.; Wengel, J.; Peak-Chew, S.-Y.; McLaughlin, S. H.; Herdewijn, P.; Holliger, P., Synthetic Genetic Polymers Capable of Heredity and Evolution. *Science* **2012,** *336*, 341.
3. Gagnon, K. T., Loading of Argonaute Protein with Small Duplex RNA in Cellular Extracts. *Methods in molecular biology (Clifton, N.J.)* **2016,** *1421*, 53-67.